UNIVERSITAS
Miguel
Hernández

UNIVERSITAS
Miguel
Hernández

Consejo Superior de Investigaciones Científicas
Universidad Miguel Hernández
Instituto de Neurociencias

Cold-sensitive fibers of the mouse tongue: Molecular and functional types and modulatory role on drinking behavior

Presented by:

Bristol Denlinger
For the Degree of Doctor in Neuroscience from the University Miguel Hernández de Elche

Directors: Dr. Carlos Belmonte and Dr. Félix Viana

San Juan de Alicante, Spain
2014

UNIVERSITAS
Miguel
Hernández

Consejo Superior de Investigaciones Científicas
Universidad Miguel Hernández
Instituto de Neurociencias

INSTITUTO DE NEUROCIENCIAS

A QUIEN CORRESPONDA:

Prof. Juan Lerma Gómez, Director del Instituto Neurociencias, centro mixto de la Universidad Miguel Hernández (UMH) y la Agencia Estatal Consejo Superior de Investigaciones Científicas (CSIC)

CERTIFICA,

Que la Tesis Doctoral "*Cold-Sensitive fibers of the mouse tongue. Molecular and functional types and modulatory role on dinking behavior*" ha sido realizada por Dña. **Bristol Layne Delinger** , Licenciada en Biología (Biology Major),bajo la dirección de los Dres. **Carlos Belmonte Martínez** y **Félix Viana de la Iglesia** y da su conformidad para que sea presentada a la Comisión de Doctorado de la Universidad Miguel Hernández.

Para que así conste a los efectos oportunos, firma el presente Certificado, en San Juan de Alicante, a 20 de MAYO de 2014.

Fdo. Juan Lerma
Director

INSTITUTO DE NEUROCIENCIAS CSIC Miguel Hernández

direccion.in@umh.es
director.in@csic.es
www.ina.umh.es

Tel: +34 965-919221 (d)
+34 965-919220 (s)
Fax: +34 965 919561

Av Ramón y Cajal s/n
Campus de San Juan
03550 SAN JUAN DE ALICANTE– ESPAÑA

UNIVERSITAS
Miguel
Hernández

Los Dres. CARLOS BELMONTE MARTÍNEZ y FÉLIX VIANA DE LA IGLESIA, en el Instituto de Neurociencias de Alicante, centro mixto CSIC-UMH,

CERTIFICAN,

Que Doña BRISTOL LAYNE DENLINGER, Biology Major (Licenciada en BIOLOGÍA), ha realizado bajo su dirección el trabajo experimental que recoge su Tesis Doctoral "COLD-SENSITIVE FIBERS OF THE MOUSE TONGUE. MOLECULAR AND FUNCTIONAL TYPES AND MODULATORY ROLE ON DRINKING BEHAVIOR".

Que han revisado los contenidos científicos y los aspectos formales del trabajo y dan su conformidad para su presentación y defensa públicas.

Para que así conste, y a los efectos oportunos, firman el presente Certificado en San Juan de Alicante, a 20 de MAYO de 2014.

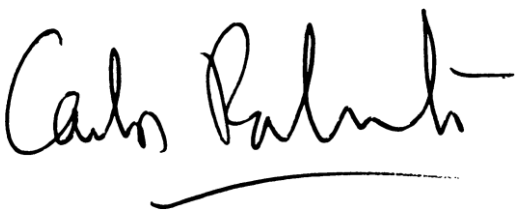

Fdo.: Carlos Belmonte

Fdo.: Félix Viana

Universidad Miguel Hernández. Campus de San Juan
Apartado 18. 03550 San Juan de Alicante. España
Tel. 34 96 591 95 30 Fax: 34 96 591 95 49. e-mail: carlos.belmonte@umh.es

UNIVERSITAS
Miguel
Hernández

INDEX

UNIVERSITAS
Miguel
Hernández

ABBREVIATIONS

$[Ca^{2+}]_i$:	Intracellular calcium concentration
AITC:	Allyl isothiocyanate
ANKTM1:	Ankyrin-like with transmembrane domains protein 1
AP:	Action potential
ASICs:	Acid-sensing ion channel
BCTC:	4-(3-Chloro-2-pyridinyl)-N-[4-(1,1-dimethylethyl)phenyl]-1piperazinecarboxamide
C:	Carboxyl
C57BL/6:	Common strain of wild-type laboratory mice
Ca^{2+}:	Calcium
CO_2:	Carbon dioxide
CGRP:	Calcitonin gene-related peptide
CMR1:	Cold menthol receptor 1
CNS:	Central nervous system
DAB:	3, 3'-diaminobenzidine
DAPI:	4',6-diamidino-2-phenylindole
DiI:	1,1',di-octadecyl-3,3,3'3'-tetramethylindocarbocyanine perchlorate
DRG:	Dorsal root ganglion
F_{340}:	Fluorescence emitted by Fura-2 excited with light at a wavelength of 340 nm
F_{380}:	Fluorescence emitted by Fura-2 excited with light at a wavelength of 380 nm
FBS:	Fetal bovine serum
fMRI:	Functional magnetic resonance imaging
Fura 2-AM:	Fura-2-acetoxymethyl ester
GFP:	Green fluorescent protein
HBSS:	Hank's Balanced Salt Solution
HEPES:	4-(2-hydroxyethyl)-1-piperazineethanesulfonic acid
HT:	High threshold
I_{KD}:	Voltage-gated potassium current
ISI:	Interspike interval
K^+:	Potassium
K_{2P}:	Two-pore domain potassium channel
KCl:	Potassium chloride
K_{ir}:	Inward-rectifier potassium channel
KO:	Knockout
K_v:	Voltage-gated potassium channel

LT:	Low threshold
MCOLN:	Mucolipin
MEM:	Minimal essential medium
MLIV:	Mucolipidosis type IV
mOsm:	Milliosmol
N:	Amino
Na^+:	Sodium
NGF:	Nerve growth factor
nompC:	No mechanoreceptor potential C
NTS:	Solitary nucleus
OVLT:	Organum vasculosum lamina terminalis
pOsm:	Plasma osmolality
PKD:	Polycystic kidney disease
SA:	Slowly adapting
SD:	Standard deviation
SEM:	Standard error of the mean
SpV:	Spinal tract of the trigeminal nerve
TG:	Trigeminal ganglion
TRAAK:	Potassium channel subfamily K member 4
TREK-1:	Potassium channel subfamily K member 2
TROMA-1:	Cytokeratin 8, a monoclonal antibody
TRP:	Transient receptor potential
TRPA:	Transient receptor potential ankyrin
TRPA1:	Transient receptor potential ankyrin 1
TRPC:	Transient receptor potential canonical
TRPM:	Transient receptor potential melastatin
TRPM8:	Transient receptor potential melastatin 8
TRPML:	Transient receptor potential mucolipin
TRPN:	Transient receptor potential no mechanoreceptor potential C
TRPP:	Transient receptor potential polycystic
TRPV:	Transient receptor potential vanilloid
TRPY:	Transient receptor potential yeast
Vm:	Membrane potential
VP:	Vasopressin
VR-1:	Vanilloid receptor 1
WT:	Wild-type
YFP:	Yellow fluorescent protein

SUMMARY

The tongue is richly innervated by cold-sensitive nerve afferents. The molecular basis of cold transduction in sensory fibers is not fully understood; TRP channels and leak K+ channels are thought to play important roles. We developed an 'in vitro' preparation of the superfused mouse tongue to record impulse activity in single sensory fibers of the lingual nerve in wild-type (WT), TRPM8$^{-/-}$, TRPA1$^{-/-}$, and TRPM8$^{-/-}$/TRPA1$^{-/-}$ mice and analyzed the effect of controlled thermal stimuli on this activity. Sustained nerve impulse discharges were evoked in a fraction of sensory fibers when temperature of the perfusing solution was decreased from a basal temperature of 35ºC down to 10ºC. Based on their firing pattern and thermal threshold, cold-sensitive fibers in WT mice were subdivided into groups. Deletion of TRPM8 did not completely abrogate the population of cold-sensitive fibers, however there was a lower incidence of cold-sensitive fibers found, with those still responding to cold exhibiting thresholds in the low and high ranges. The cold-sensitive fibers in TRPA1$^{-/-}$ more closely resembled those of the WT mice, but the overall threshold shifted toward warmer temperatures, supporting the contention that cold transduction in the population of higher threshold fibers depends largely on TRPA1. In TRPM8$^{-/-}$/TRPA1$^{-/-}$ mice, cold-sensitive fibers were still present, however the purely phasic firing pattern response was not found and with the vast majority being low threshold fibers. Inflammation decreases the sensitivity of low threshold cold thermoreceptors. Chloroform (20 mM), an activator of thermosensitive TREK-1 potassium channels, attenuates or eliminates responses of these fibers to cold. Altogether, these results indicate that activation of lingual sensory fibers by cold depends on several transduction mechanisms. TRPM8 appears to be important but not unique for the detection of discrete temperature reductions. Other channels, presumably background potassium channels appear to also be involved, while TRPA1 seems to mediate transduction of more intense cooling.

We also explored the contribution of cold thermoreceptors in the oral mucosa to drinking preference and overall water intake in mice using an experimental cage in which the water temperature of the drinking bottles could be cooled and heated from a control temperature

of 22ºC. After water deprivation during 24 hours, entries to drink, drinking time, and water volume were measured over a one hour period. With only one bottle present, WT mice drank overall the same volume of water despite the different temperatures offered. TRPM8$^{-/-}$ mice, however drank significantly less volume, and TRPA1$^{-/-}$ mice drank significantly more volume than wild-type mice. During preference tests, WT mice drastically preferred water at 22ºC over cooler water, while TRPM8$^{-/-}$ mice had no preference and TRPM8$^{-/-}$/TRPA1$^{-/-}$ mice even preferred the cooler water. TRPA1$^{-/-}$ mice preference closely resembled that of the WT mice. These data suggest that information from cold thermosensitive fibers is an important cue in thirst and in preabsorptive signaling of satiety, with TRPM8 low threshold cold thermoreceptors providing a positive drinking drive and possibly TRPA1 vagal fibers of the stomach signaling the cumulative volume of ingested fluid.

RESUMEN

La lengua está densamente inervada por fibras aferentes nerviosas sensibles al frío. Los mecanismos moleculares de la transducción de la sensación de frío por fibras sensoriales no se entiende completamente pero hay indicios de que tanto los canales TRP como los canales de K+ de fuga pueden desempeñan un papel importante. En esta tesis, hemos desarrollado una preparación "in vitro" de la lengua de ratón perfundida en solución fisiológica para registrar la actividad de impulsos eléctricos en fibras sensoriales individuales del nervio lingual. Esta preparación se ha utilizado para analizar el efecto de estímulos térmicos controlados sobre la actividad de ratones silvestre, TRPM8$^{-/-}$, TRPA1$^{-/-}$ y TRPM8$^{-/-}$/TRPA1$^{-/-}$. El enfriamiento de la solución de perfusión desde una temperatura basal de 35ºC hasta los 10ºC provocó descargas de impulsos nerviosos sostenidas en una fracción de las fibras sensoriales registradas. En base a su patrón de activación y a su umbral térmico, las fibras sensibles a frío registradas en los ratones silvestres se subdividieron en distintos grupos. La eliminación del receptor TRPM8 disminuyó drásticamente, pero no eliminó por completo, la población de fibras sensibles a frío. Las fibras restantes presentaron respuestas al frío similares a las observadas en el ratón silvestre, con umbrales de respuesta en todo el rango de temperatura. Las fibras sensibles a frío en ratones TRPA1$^{-/-}$ se parecían más a las de los ratones silvestres, pero el valor medio del umbral está desplazado hacia temperaturas más cálidas, apoyando la afirmación de que la transducción de frío en la población de fibras de umbral más alto depende en gran medida de TRPA1. En ratones TRPM8$^{-/-}$/TRPA1$^{-/-}$, todavía se registran algunas fibras sensibles a frío, sin embargo, estas fibras no muestran el patrón de disparo puramente fásico y, en su inmensa mayoría, se trata de fibras de bajo umbral.

La inflamación de la lengua disminuyó la sensibilidad de los termoreceptors de frío de bajo umbral y el cloroformo (20 mM), un activador de los canales termosensibles de potasio TREK-1, atenuó o eliminó las respuestas de estas fibras al frío. En conjunto, estos resultados indican que la activación de fibras sensoriales linguales por frío depende de varios mecanismos de transducción. TRPM8 parece ser importante pero no indispensable, para la detección de las reducciones de temperatura discretas en todas las fibras linguale. Otros canales, presumiblemente los canales de potasio fuga también parecen estar

involucrados, mientras que TRPA1 parece mediar la transducción de enfriamiento más intenso.

En la tesis, también hemos explorado la contribución de termoreceptores de frío localizados en la mucosa oral a la preferencia de bebida y al consumo total de agua en ratones, usando para ello una jaula experimental en la que la temperatura del agua de las botellas de bebida podía ser regulada. Tras la privación de agua durante 24 horas, se midió, durante una hora, el número de veces que los ratones bebían, el tiempo que pasaban bebiendo, y el volumen total de agua ingerido. Con sólo una botella disponible, los ratones silvestres bebieron el mismo volumen de agua, independientemente de su temperatura. Sin embargo, los ratones TRPM8$^{-/-}$, bebieron significativamente menos y los ratones TRPA1$^{-/-}$ mucho más volumen que los ratones silvestres. Durante las pruebas de preferencia, los ratones silvestres mostraron una clara preferencia por el agua a 22ºC sobre el agua más fría, mientras que ratones TRPM8$^{-/-}$ no tuvieran ninguna preferencia y los ratones TRPM8$^{-/-}$/TRPA1$^{-/-}$ incluso prefirienron el agua más fría. La preferencia de los ratones TRPA1$^{-/-}$ fue muy similar a la de los ratones silvestres. Estos datos sugieren que la información enviada por las fibras termosensibles de frío de la cavidad bucal juega un papel muy importante en la regulación de la sed y en la señalización preabsorptiva de saciedad y que los termoreceptores de frío de bajo umbral que expresan TRPM8 proporcionan un impulso positivo para la ingesta de agua. Además, muy posiblemente, las fibras vagales del estómago con receptores TRPA1 señalizan el volumen acumulativo de fluido ingerido.

1. INTRODUCTION

1.1. Sensory receptors detecting temperature changes

Peripheral sensory receptors detect the energy changes that occur in the internal and external environment, in particular those relevant for survival and reproduction. They transform stimuli into a discharge of electrical signals that conveys the information about the nature, intensity, time course and location of the stimulus to the brain (Adrian 1926). Such information is processed by a complex network of specialized sensory neurons, circuits, and pathways which altogether constitute the somatosensory division of the nervous system. The operation of the somatosensory system underlies the conscious perceptions of touch, movement, pressure, pain, and temperature as well as a large number of non-conscious motor and autonomic responses, aimed at maintaining the equilibrium of the internal milieu (homeostasis) against continuous environment oscillations (Barlow & Mollon 1982, Mountcastle & Bard 1968).

Sensory receptors can either be peripheral endings of primary sensory neurons or separate, specialized cells that transduce the stimulus and then pass the information to primary sensory neurons. The cell bodies of primary sensory neurons are located in the dorsal root ganglia (DRG) or when the sensations originate in the head and neck, in cephalic ganglia (trigeminal ganglion (TG)), and nodose, petrosal, and geniculate ganglia. The first-order somatosensory afferent neurons are pseudounipolar cells. The cell body gives rise to a single process that divides to form a peripheral axon and a central axon. The peripheral axon travels to and ends in the skin, mucosae, muscle, tendon, bone and joints and the central axon travels to and ends in the central nervous system (e.g. dorsal horn of the spinal cord).

As mentioned above, the different forms of stimuli are transduced by their specific somatosensory receptors into a local depolarization of the plasma membrane, producing the so called ‘receptor potential’, which is in turn transformed into a discharge of action potentials which encodes the spatial and temporal characteristics of the stimulus. This

process is named ‘sensory transduction’ (Belmonte 1996). In mammals, each functional class of receptors responds preferentially to one or few forms of energy (mechanical, thermal, chemical) thus providing the basis for sensory specificity (Block 1992). Thermoreceptors respond to changes in temperature, either hot or cold; mechanoreceptors are activated by mechanical force such as pressure, touch, and vibration; and nociceptors respond to injurious stimuli. Nerve fibers supplying sensory receptors are usually classified based on their conduction velocity for action potentials, i.e. the speed at which action potentials travel to the CNS, determined by measuring the time between an electrical stimulus applied at the receptive field and the appearance of the evoked action potential at a given distance.

The transduction process involves a conformational change of a membrane protein (receptor protein or ion channel) that leads directly or indirectly through intracellular signaling pathways, to the opening and/or closing of the ion channels located on the receptor membrane and thereby to the receptor potential (Widmaier et al 2006).

The encoding characteristics of specific stimuli into a discharge of nerve impulses by the various functional types of sensory receptors (low threshold mechano-receptors, photoreceptors, chemoreceptors, nociceptors, thermal receptors) were essentially defined in the second half of the 20th Century (Kandel 2012). More recently, significant advances were made in the understanding of the molecular mechanisms involved in stimulus transduction by photoreceptors and by chemoreceptors (in particular gustatory and olfactory) (Fain 2003, Lamb 2013). However, these mechanisms were comparatively less understood in somatosensory mechanoreceptors, nociceptors and thermoreceptors (Belmonte 1996). This was due in part to the small size of their peripheral nerve terminals, (where transduction processes take place under normal circumstances) which precluded the application of conventional biophysical recording methods to sensory nerve endings. The use of the cell bodies of cultured DRG or TG neurons has, in part, avoided this problem (Cesare & McNaughton 1996). Moreover, the identification and cloning of ion channel proteins associated to the transduction of stimulating forces by somatosensory receptors, like some members of the TRP superfamily of ion channels, is providing new insights for the understanding of the transduction of temperature changes, noxious chemicals, and

mechanical forces by somatosensory receptors (Bandell et al 2007, Basbaum et al 2009, Belmonte & Viana 2008, Dhaka et al 2006, Gees et al 2012, Montell 2003).

The development of genetically modified mice, where genes associated to the various steps involved in transduction were selectively deleted, also represented an important step toward understanding the molecular basis of sensory transduction (Julius & Nathans 2012). The changes in transducing and encoding capacities resulting from genetic manipulations of the expression of proteins associated to the transduction of innocuous or injurious mechanical, thermal and chemical stimuli have been explored with morphological, biophysical, biochemical, and behavioral techniques. Nonetheless, studies using genetically manipulated animals have mainly been centered in immunocytochemical studies of peripheral sensory structures, calcium imaging, and electrophysiological recordings of cultured primary sensory neurons, and in the analysis of the behavioral responses to specific sensory stimulation. Electrophysiological recordings of sensory axons in the whole animal or in organ preparations of genetically manipulated mice are comparatively scarce.

Hence, in spite of the advances made in recent years, the different molecular mechanisms involved in the transduction and coding of the stimulus into a discharge of nerve impulses for each modality of sensation are still incompletely known, in particular for somatosensory primary sensory neurons involved in the detection of innocuous and noxious thermal, chemical and mechanical stimuli which ultimately lead to sensations of temperature and pain.

In the case of cold detection, specific cold thermosensitive sensory fibers were first identified and described in the tongue (Hensel & Zotterman 1951a) and this tissue was extensively used afterwards as an experimental model to analyze the functional properties of low threshold cold thermoreceptors. Since then, various functional subclasses of cold thermosensitive fibers have been described (Benzing et al 1969, Hensel et al 1960, Hensel & Zotterman 1951a, Hensel & Zotterman 1951b, Lundy & Contreras 1995, Pittman & Contreras 1998). In addition, several classes of ion channels have been implicated in the detection of thermal changes by cold thermoreceptors (Belmonte et al 2009, Belmonte & De la Pena 2013). However, and despite these highly significant findings, the transducing

mechanisms for peripheral cold detection and the distinct functional types of cold sensitive sensory fibers are not fully elucidated.

As mentioned above, the tongue, which is richly innervated by different classes of sensory receptors, including thermoreceptors, mechanoreceptors, and nociceptors, constitutes an advantageous model to investigate the functional characteristics of somatosensory receptors in wild-type mice and in mice in which the expression of channel proteins associated to sensory transduction are selectively deleted. For this reason, we chose this preparation to extend our present knowledge about the contribution of different ion channels, in particular TRPs, to cold transduction.

1.1.1. Thermoreceptors

Peripheral thermoreceptors are defined as receptors that display high sensitivity to thermal stimuli applied to the skin and mucosa within an innocuous range. Neurons that express thermo-sensitive channels usually have peripheral branches in direct contact with tissues exposed to environmental temperature changes. The receptive fields of these axons are distributed in localized sensory spots on the skin (Blix 1882) and mucosa and cover less than 1 mm^2. Thermoreceptors in the skin are thus a source of constant conscious sensory information as well as responsible for providing an important input for behavioral and thermoregulatory responses. Functional characteristics of thermoreceptors vary greatly among species, adapting and evolving to fit specific environmental conditions (Belmonte & De la Pena 2013). In mammals, terminals in the skin and mucosa detect these temperature changes and help to regulate body temperature. Classes have been divided into cold receptors, warm receptors, and thermosensitive nociceptors based on the type of sensations each evoke (Basbaum et al 2009, Belmonte et al 2009, Hensel 1973, Pierau & Wurster 1981, Schepers & Ringkamp 2010). The high sensitivity of these thermoreceptors allows them to respond to small changes in temperature. Characteristic properties include a continuous firing of impulses at a constant temperature with an increase or decrease in firing when the temperature changes. Firing frequency increases in cold thermoreceptors when the temperature falls and in warm thermoreceptors when the temperature rises. Nociceptors respond when high or low temperatures reach the noxious range and evoke pain sensations. In general there are more cold thermoreceptors found in the body surface

than warm thermoreceptors, while the face contains the greatest density of temperature sensitive points.

1.1.1.1. Warm thermoreceptors

Receptors sensitive to moderate heating were characterized by an increase in discharge with a warming of only 3ºC from the baseline temperature, total insensitivity to cooling, and a very low response to mechanical stimulation. This specific population of warm thermoreceptors was initially located in the orofacial mucosa and the skin (Hensel et al 1960, Iggo 1959, Stolwijk & Wexler 1971). The density and distribution of warm thermoreceptors appears to vary markedly between species. They are more frequently recorded in the skin of primates (Darian-Smith et al 1979, LaMotte & Campbell 1978), including man (Hallin & Wiesenfeld 1981, Johnson et al 1979, Konietzny & Hensel 1977) than in rodents being in both cases more abundant in the nose mucosa (Hensel & Kenshalo 1969). In the nasal region of the cat, single warm fibers showed at constant temperatures from 30°C on, a steady discharge with a regular sequence of impulses, the frequency of which rose steeply with temperature and reached a maximum between 45ºC and 47º C. At higher temperatures the frequency fell to zero. Rapid warming caused a dynamic overshoot and rapid cooling a transient inhibition of the warm fiber discharge. The highest dynamic frequency of single fibers was 200 impulses/sec. The average maximum of static activity in a large population of warm fibers was 36 impulses/sec at 46ºC, whereas in a parallel cold fiber population the maximum was 9 impulses/sec at 27º C (Hensel & Kenshalo 1969). Warm thermoreceptor characteristics and transduction mechanisms have not been analyzed in the present study.

1.1.1.2. Cold thermoreceptors

Active within a broad range of temperatures, from 35ºC to close to 0ºC, canonical cold thermoreceptors were characterized by the frequent presence of an ongoing regular impulse discharge at background skin temperatures that increases in frequency often in bursts upon a cooling stimulus, a decrease or inhibition of activity with heating, and no response to mechanical stimuli (Hensel et al 1960). Cold stimuli are thought to be mediated by

unmyelinated C and thinly myelinated Aδ primary afferent fibers (Hensel & Zotterman 1951a) whose terminals lie in or just below the dermis. Cold-sensitive fibers exhibit different thresholds and have been subdivided into low and high threshold groups (Belmonte et al 2009). The low threshold thermoreceptors, which are already activated when temperature is reduced from 34ºC down to 26.5ºC, has previously been found to account for 75% of these cold-sensitive neurons (Madrid et al 2009).

In human skin, it has long been known that cold spots are more densely distributed than warm spots. However, to classify a nerve ending as a thermoreceptor, quantitative measurements of stimuli were needed. The first thermoreceptors identified using electrophysiology were small myelinated cold fibers in the cat tongue (Zotterman 1935, Zotterman 1936). At constant temperatures in the innocuous range, cold thermoreceptors maintain a constant basal firing. This firing can be regular or comprised of periodic burst sequences (Hensel 1973), which has also been found in cold fibers of the lingual nerve of the cat tongue (Hensel & Zotterman 1951a) (Figure 1.1). Cooling to lower temperatures provokes a response with an increase in firing frequency, an adaptation period, a decrease in firing or complete silence with rewarming, and a return to the initial firing frequency value when the temperature returns to baseline (Hensel 1973) (Figure 1.1B). The temperature range to which the fibers respond and the firing pattern can vary between species and target tissues, along with the temperature at peak response (Iggo 1969).

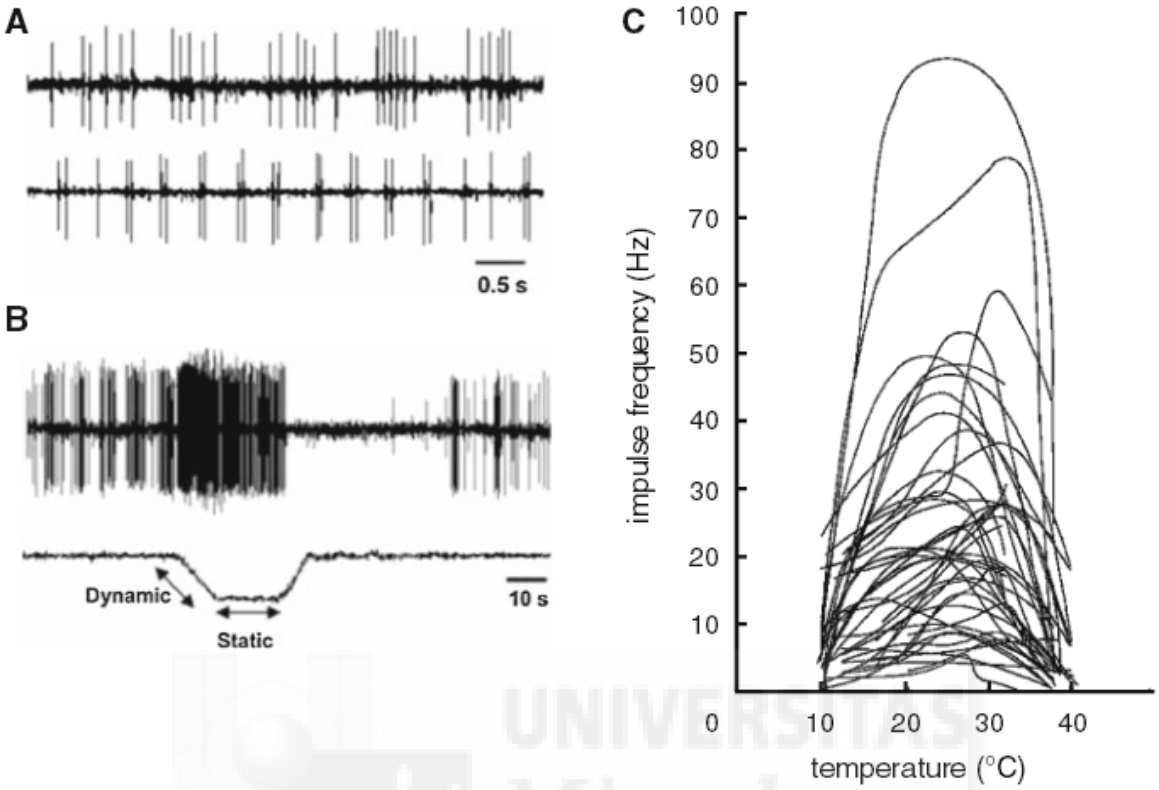

Figure 1.1. Discharge characteristics of cold-sensitive nerve fibers. A. Recording of spontaneous nerve impulse activity at 32ºC in two scleral cold receptor fibers in the cat. **B.** Action potential impulse discharge of a cold-sensitive unit in response to a cooling pulse from a baseline temperature of 35ºC down to 21ºC (Gallar et al 2003). **C.** Representation of the static discharge frequencies of 44 different cold-sensitive fibers in the cat tongue as a function of constant temperatures (Benzing et al 1969). Figure adapted from (Belmonte et al 2009).

Paradoxical responses have also been observed in cold fibers in the lingual nerve of the cat tongue (Dodt & Zotterman 1952), where cold fibers will start firing at temperatures above 45°. This response may be responsible for the reason that hot water provokes cold sensations, as well as the chill reactions when one has a high fever.

Compounds such as menthol, an essential oil found in peppermint and mint, can also evoke cooling sensations when applied to the skin or mucosa through the activation of cold thermoreceptors (Eccles 1994). Menthol enhances the spontaneous discharge of cold sensitive fibers, and potentiates their response to cold temperatures by sensitizing cold thermoreceptors to evoke sensations of intense cooling (Schafer et al 1986).

Several cold-sensitive transducing channels have been identified in mammalian sensory neurons, including TRPM8, a member of the TRP ion channel superfamily that has been revealed as the main transducer channel in specific low threshold cold thermoreceptor fibers (McKemy et al 2002, Peier et al 2002). In addition to this, another TRP ion channel, called TRPA1, has also been proposed to play a role in cold transduction (Story et al 2003), but this is still poorly defined and limited to the population of neurons exhibiting a very high threshold to cold (Julius 2013, Viana & Ferrer-Montiel 2009). Moreover, two-pore domain potassium channels, specifically TREK-1 and TRAAK, which sustain background leak conductances have been reported to be closed by cold (Noel et al 2009, Reid & Flonta 2001, Viana et al 2002). Other classes of potassium channels (Kv1) appear also to be particularly sensitive to cold, acting as a break against depolarizing currents induced by cooling (Madrid et al 2009, Viana et al 2002). However, the relative importance of these different molecular entities in the detection and coding of thermal stimuli by the various classes of cold thermoreceptors is still unclear.

The distribution of cold thermoreceptor endings in the body surface is not homogeneous. The number of cold-sensitive points is comparatively larger in the peripheral territory of mammalian TG than of DRG neurons being particularly abundant in the snout skin, with marked differences between species possibly associated to the use of the snout for exploration (Kenshalo & Hall 1974). Also, the mucosa covering the nasal and oral cavities and the anterior part of the tongue are rich in cold thermoreceptor endings.

1.1.2. Mechanoreceptors

Mechanoreceptors are characterized by their preferential sensitivity to mechanical force. They are often classified based on their adaptation and threshold. Rapidly adapting fibers show a sudden response to the start and/or end of mechanical stimulation with no maintenance of the discharge during a continuous stimulus, while slowly adapting mechanoreceptors fire as long as the stimulus is maintained (Widmaier et al 2006). Readily found in sensory nerves, low threshold mechanoreceptors respond to light mechanical stimuli, such as moderate pressure or vibration. Few low threshold mechanoreceptor nerve fibers have free nerve endings, while most have thick axons with complex encapsulated

endings. Those with encapsulated nerve endings include fast-adapting mechanoreceptors such as Meissner and Pacinian corpuscles, and slow-adapting mechanoreceptors as Merkel and Ruffini corpuscles (Widmaier et al 2006). Low threshold mechanoreceptors give rise to sensations of touch, pressure, movement, and vibration (Cain et al 2001, Widmaier et al 2006).

1.1.2.1. Thermo-mechanoreceptors

A fraction of mechanoreceptors have also been seen to respond to temperature. This observation was first made by what is known as 'Weber's deception' or the silver Thaler (a German coin used in Europe in the 18–19th century) illusion, i.e. the perception that a colder object appears heavier than a warmer one of the same weight. This is explained by the cold sensitivity found in large myelinated afferents which respond vigorously to mechanical stimuli. Thus, about half of the slowly adapting mechanoreceptors (SA fibers), i.e. the Merkel discs in superficial skin layers and the Rufini endings in deeper skin layers, respond to cooling thermal gradients from normal skin temperature to 14.5-8ºC (Cahusac & Noyce 2007, Duclaux & Kenshalo 1972, Hensel & Zotterman 1951b, Iggo & Muir 1969, Tapper 1965). Some of these thermo-mechanoreceptors have also been reported to exhibit a bursting response to cooling, but with a lower frequency than cold receptors (Burton et al 1972). Nevertheless, it is rather unlikely that activity in large myelinated afferents actively contributes to the sensation of cool, since the response to cool is negligible compared to one following mechanical stimulation or in comparison to the response of cold fibers (Johnson et al 1973).

1.1.3. Nociceptors

Nociceptors are a population of receptors that responds only when stimuli reach noxious or near-noxious levels, serving to warn the body from potentially harmful environmental inputs (Belmonte 1996, Kumazawa 1996, Perl 1996). The sensation of pain was first believed to be the summation of responses to excessive stimulation in low threshold sensory receptors, but at the beginning of the 20th century, free nerve ending, described as

being able to detect selectively skin damaging stimuli were discovered. The impulse activity in these fibers may ultimately evoke conscious sensation of pain. The term nociceptors (Sherrington 1903) was coined to emphasize the fact that the specific stimuli for this sensory receptor type is tissue damage, caused by different forms of energy acting at noxious levels. A part of this group of nociceptive high threshold sensory neurons, respond preferentially to high intensity mechanical stimuli such as intense pressure and are very phasic, responding at the start of stimulation. The majority of nociceptors are activated by a variety of stimuli of different natures, and are accordingly known as polymodal nociceptors (Bessou & Perl 1969). The final group, silent nociceptors, does not respond to any stimuli until inflammation occurs (Schaible & Schmidt 1988). This group is important in the study of chronic pain.

The most common type of nociceptor, the polymodal nociceptor responds to high-threshold mechanical stimuli, high temperatures and a large variety of irritant chemicals with classifications based on responses to these stimuli (Basbaum et al 2009, Belmonte & Viana 2008, Viana 2011). Specificity to each of them is determined by the expression of ion channels responsible for the detection of these high-threshold stimuli (Belmonte & De la Pena 2013, Ramsey et al 2006). The discovery of transducing mechanisms for polymodal nociceptors at the molecular level started with the identification of the ion channel TRPV1 (transient receptor potential vailloid 1), whose thermal threshold matches that of heat pain, around 42ºC (Caterina et al 1999). Other ion channels that attribute their sensitivity to noxious stimuli to polymodal nociceptors include TRPA1, TRPM3, TRPV4, ASICS (Belmonte & De la Pena 2013). A prominent feature of polymodal nociceptors is sensitization, developed when inflammation follows tissue injury and characterized by a reduction of threshold and enhanced responsiveness to noxious stimulation, post discharge and development of spontaneous activity (Perl 1996). The molecular mechanisms underlying transduction of noxious stimuli and sensitization in nociceptors have been extensively studied in recent years (Belmonte & De la Pena 2013, Dubin & Patapoutian 2010, Petho & Reeh 2012, Stucky et al 2009, Viana 2011, Zhang & McNaughton 2006).

Nociceptor fibers responding only when noxious low temperatures are reached are known as cold nociceptors (Georgopoulos 1976, Georgopoulos 1977, LaMotte & Thalhammer 1982). The existence of this specific population of cold nociceptors is disputed (Belmonte

et al 2009). Polymodal nociceptors may also respond to extreme temperatures and mechano-cold and mechano-heat nociceptors have been characterized in the mouse skin (Cain et al 2001). Mechano-cold and more commonly mechano-heat nociceptors are often slow-adapting with a continuous response during the mechanical stimulation, often developing spontaneous activity and responding to chemical irritants (Meyer & Campbell 1981, Ringkamp et al 2012, Treede 1995).

Transduction mechanisms for extreme low temperature possibly include TRP ion channels such as TRPM8, the main ion channel involved in cold transduction and TRPA1 (transient receptor potential ankyrin 1) (see below). TRPM8 knockout mice show a reduced percentage of high and low threshold cold-sensitive fibers (Bautista et al 2007, Colburn et al 2007), while TRPA1 knockout mice also showed a reduction in their responses to deep cooling (Karashima et al 2009), suggesting that both channels are involved in noxious cold detection.

1.2. Cold transduction

Thermal transduction is the process by which a temperature change acting on the peripheral nerve terminals of sensory neurons is converted into action potentials which travel along the axon to reach the brain. Thermal, particularly cold, transduction in thermoreceptors is a complex process which involves the participation of several different ion channels (Belmonte & Viana 2008) (Figure 1.2). These have important and distinct functions for transduction and coding of thermal stimuli.

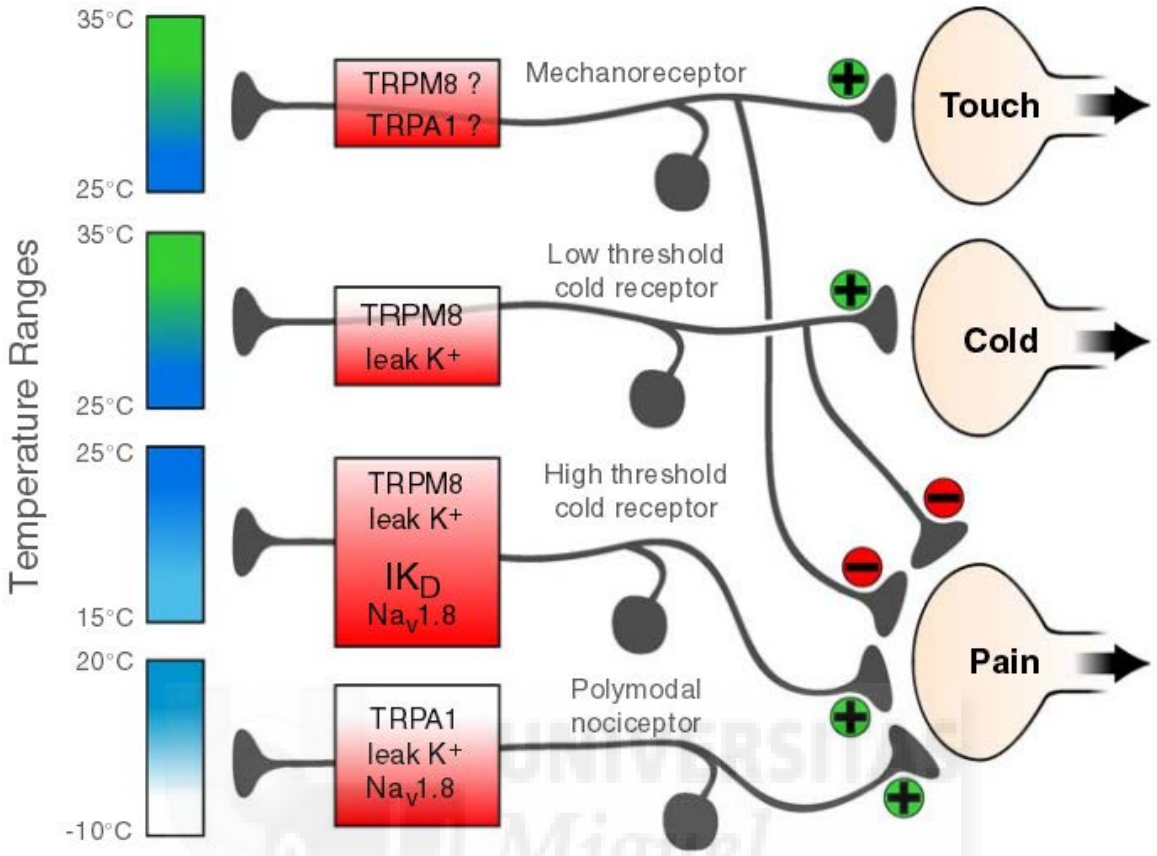

Figure 1.2. Canonical view of cold detection mechanisms in primary sensory neurons. The red boxes refer to the ion channel excited by the various temperature ranges on the left by different types of peripheral sensory neurons. The type of sensation evoked and possible excitatory (+) or inhibitory (-) interactions involved in touch, cold, and pain are represented. (Figure adapted from (Belmonte et al 2009)).

Ion channels are membrane proteins that form a pore which acts as a selective gateway, facilitating the diffusion of ions across a biological membrane. Hundreds of ion channels that regulate the passage of ions across the lipid bilayer are encoded by the human genome (Hille 2001). Ion channel gating is controlled by voltage and external chemical or physical modulators, and the ion flux generates electrical signals in excitable cells. Moreover, in neurons, these signals are coupled to a transient increase in intracellular calcium, controlling different physiological processes. Ion channels are classified based on their sequence, ion selectivity, and gating. Groups include voltage gated channels, ligand gated

channels, second messenger gated channels, and channels opened by physical forces (mechanical stimulation and temperature) (Hille 2001).

1.2.1. TRP ion channels

The transient receptor potential, TRP channels are members of a superfamily of ion channels made of protein subunits with six transmembrane domains and cytoplasmic N- and C-termini, which assemble to form cation-permeable ion channels (Stucky et al 2009). When they open, the sensory cell is depolarized through raised concentrations of intracellular sodium and calcium and the outflow of potassium (Ramsey et al 2006).

The TRP ion channels owe their name to a mutation in the *Drosophila melanogaster* ion channel protein associated with phototransduction. This mutant Drosophila strain is characterized by a transient receptor response to light, while the wild-type shows sustained photoreceptor cell activity in response to continuous light stimulation. The discovery of the blind mutant fly was made in 1969 (Cosens & Manning 1969), but it was not until 1989 that the genetic defect underlying the phenotype was characterized and the trp gene was cloned (Montell & Rubin 1989). Finally in 1992, TRP proteins were identified as ion channels (Hardie & Minke 1992), and since then many other ion channels that belong to the TRP channel family have been identified, making it one of the largest families of ion channels. Since then many other major findings have been made in the field, including the identification of human TRP channels (Wes et al 1995, Zhu et al 1995) and the discovery of "thermoTRPs" (Caterina et al 1997, Dhaka et al 2006).

The discovery of TRP channels has helped redefine sensory physiology. Their presence has been conserved from worms to humans (Wes et al 1995), all of which who's senses depend on TRP channels. Their presence in specialized cells allows for the existence of complex sensory processing, including vision, smell, touch, taste, hearing, temperature detection, and pain. All TRP channels are cation permeable; the channels mediate the passage of cations through the plasma membrane, so Ca^{2+} and Na^{+} pass into the cell by a favorable electrochemical gradient which increases intracellular calcium [Ca^{2+}] and sodium [Na^{+}] concentrations while K^{+} ions flow out. This causes a change in the plasma

membrane potential (Vm) to more positive values, and in excitable cells, such as neurons, this depolarization determines the generation of propagated action potentials.

1.2.1.1. Classification

The TRP superfamily of ion channels are expressed in wide variety of multicellular organisms, including worms, fruit flies, zebrafish, mice, and humans. TRP channels are divided into two groups, which are in turn divided into seven subfamilies. An eighth subfamily, consisting of yeast TRPs, called TRPY is not included in these two groups due to a difference in its primary sequence. Groups 1 and 2 are divided based on the homology of the primary amino acid sequences and topological differences (Clapham 2003). Group 1 is made up of five subfamilies, all of which have a high degree of homology with *Drosophila* TRP (Montell & Rubin 1989). These closest homologs of the Drosophila TRP are known as the TRPC channels, referring to classical or canonical TRPs. Other subfamilies in group 1 include TRPN, TRPV, TRPM, and TRPA. TRPN was first discovered in fruit flies and given the name nompC, no mechanoreceptor potential C (Walker et al 2000). This subfamily is not found in mammals, but is expressed in some vertebrates, like zebrafish. The TRPV subfamily consists of six members and owes its name to the first member identified, which was the vanilloid receptor, VR-1 (Caterina et al 1997) now known as TRPV1. The TRPM subfamily is made up of eight members and was named after the ion channel TRPM1, called melastatin, which was the first of the family to be identified (Duncan et al 1998). The final subfamily in group 1, the TRPA subfamily contains just one member in mammals; originally called ANKTM1 (Jaquemar et al 1999), TRPA1 or ankyrin 1.

In group 2 there are only two subfamilies, TRPP (polycystic) and TRPML (mucolipin). TRPP2, the founding member of the TRPP subfamily, was found to contain two genes, PKD1 and PKD2 (polycystic kidney disease protein), which in their mutant forms, cause autosomal dominant polycystic kidney disease (ADPKD) (Mochizuki et al 1996). The TRPML subfamily is comprised of three proteins (TRPML1-3) which are encoded by the mucolipin (MCOLN1-3) genes. Although this subfamily is not well characterized, it is known that MCOLN1 is implicated in the hereditary disease mucolipidosis type IV (MLIV) (Venkatachalam & Montell 2007).

1.2.1.2. Structure

The TRP channel subunits are proteins with six transmembrane domains and cytoplasmic N- and C-termini (Gaudet 2007, Gaudet 2008, Stucky et al 2009). These channels also contain a pore loop segment between transmembrane domains five and six. This amino acid loop forms an ion selectivity filter at the extracellular channel pore. In the cytoplasmic part of the pore it is believed that domain six forms a gate that regulates the entrance of cations by mediating channel opening and closing. Domain four has arginine residues that give it positive charges, making it involved in the sensitivity to transmembrane voltage changes. Functional channels are believed to form tetrameric structures.

The rest of the channel outside this region provides the subunits the ability to associate, allowing the formation of homotetramers or hetertetramers, or to act as connecting elements to control channel opening. Several members of the TRP family contain additional structural domains at the cytoplasmic termini, one of which is called the TRP box. The TRP box is a well conserved protein sequence of 23 to 25 amino acids found in the TRPC and TRPM subfamily members.

1.2.2. TRPM8

TRPM8 was first identified in the human prostate when an unknown gene, which had a high sequence homology with other TRP ion channels, was sequenced. It was then called TRP-p8 (Tsavaler et al 2001). Shortly thereafter the same gene was identified from a DNA library of rat trigeminal ganglia, as a menthol receptor, also activated by cold (McKemy et al 2002) and called CMR1 (cold menthol receptor 1). This new ion channel proved to be the rat ortholog of TRp-p8. In parallel, the group headed by A. Patapoutian, using a bioinformatic approach, was able to identify the same sequence and clone it in the mouse dorsal root ganglion, identifying its activity as an ion channel sensitive to cold and to chemical compounds like menthol and eucalyptol (Peier et al 2002). In 2002 it was included in the TRPM subfamily as TRPM8 (Montell et al 2002).

The TRPM (melastatin) subfamily consists of eight members, one of which is TRPM8. The TRPM8 subunit is comprised of 1104 amino acids (Tsavaler et al 2001). The functional channel subunits contain six transmembrane domains assembling as a tetramer around a central pore. Three extracellular and two cytoplasmic loops join the subunits, with cytoplasmic amino (N) and carboxyl (C) termini (Figure 1.3). The C-terminal domain has been shown to be vital for channel function while the N-terminal is essential for the correct localization of the channel in the plasma membrane (Phelps & Gaudet 2007).

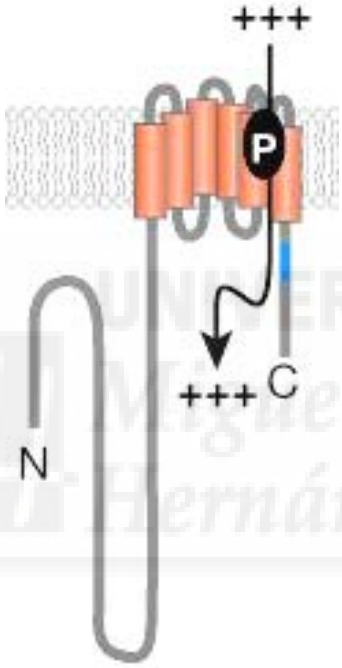

Figure 1.3. General structure of the TRPM8 subunit. Six transmembrane domains are represented by orange cylinders while N and C indicate the intracellular amino and carboxyl regions. The blue segment shows the TRP domain. The pore domain, marked by the letter P, allows the passage of cations, marked by the + sign. (Figure adapted from (Venkatachalam & Montell 2007)).

The TRPM8 channel is expressed in small- and medium-diameter sensory neurons in the trigeminal and dorsal root ganglia (Clapham 2003, Stucky et al 2009), but there is also evidence for its expression in the nodose ganglia (Abe et al 2005, Fajardo et al 2008, Zhang et al 2004) and geniculate ganglia (Katsura et al 2006). There is no clear evidence for the

existence of TRPM8 in the central nervous system. In sensory neurons, TRPM8 is expressed in cutaneous free nerve endings of cold receptors, proven by the development of genetically modified mice that express green fluorescent protein (GFP) controlled by the TRPM8 promoter (Dhaka et al 2008, Parra et al 2010, Takashima et al 2007). TRPM8 is also expressed in a variety of tissues including the taste papillae (Abe et al 2005), cornea (Parra et al 2010), liver (Fonfria et al 2006), testis, and bladder (Stein et al 2004). At the cellular level, TRPM8 partially co-localizes with TRPV1, CGRP, and substance P (Axelsson et al 2009, Babes et al 2004, Dhaka et al 2008, Takashima et al 2007, Viana et al 2002, Xing et al 2006), promoting the hypothesis that TRPM8 could be involved in nociceptive functions.

Activation of TRPM8 in sensory neurons expressing the channel causes depolarization, which in turn elicits action potentials. Additionally, activation allows the inflow of calcium into the neuron. In recombinant systems, TRPM8 can be stimulated when temperature decreases below 25-28ºC (McKemy et al 2002), however *in vivo* threshold values of TRPM8-expressing cold-sensitive neurons are probably much lower since responses are observed after small temperature drops below 34ºC (de la Pena et al 2005, Madrid et al 2006, Malkia et al 2007). The role of TRPM8 in cold detection has been evidenced *in vivo* with the use of knockout mice (Bautista et al 2007, Colburn et al 2007, Dhaka et al 2007). Behavioral temperature preference tests showed the inability of TRPM8 knockout mice to show a preference for warm over cold temperatures (Daniels & McKemy 2007), while other experiments showed clear sensory deficits until temperatures near 10ºC (Bautista et al 2007). However, in other temperature experiments, no avoidance behavior to noxious cold was seen in TRPM8 knockout mice (Knowlton et al 2010).

As well as temperature, several agonists and antagonists have been identified that act on TRPM8. The effect of menthol on cold-evoked neuronal excitation is the most thoroughly studied and dates back to the 1950s when its effects were linked to cold-sensitive fibers, demonstrating how menthol affects action potential firing, shifting it toward warmer temperatures (Hensel & Zotterman 1951a). Several decades later, after the cloning of TRPM8, it was confirmed to be the channel mediating the activity produced by menthol, eucalyptol, and icilin (McKemy et al 2002, Peier et al 2002). Other agonists include the natural odorants linalool, geraniol, and hydroxycitronellal (Almaraz et al 2014, Behrendt et

al 2004). Compounds that have an antagonistic effect on TRPM8 include 4-(3-Chloro-2-pyridinyl)-N-[4-(1,1-dimethylethyl)phenyl]-1piperazinecarboxamide (BCTC) and capsazepine (Behrendt et al 2004, Madrid et al 2006, Malkia et al 2007, Weil et al 2005). Other antagonists include the antifungal agent clotrimazole (Meseguer et al 2008) and the antimycotic agent 1,10-phenanthroline (Malkia et al 2007). However, one of the main problems with pharmacology is the lack of selectivity of many agents. Clotrimazole, for example can also activate TRPA1 and TRPV1 (Meseguer et al 2008), and cinnamaldehyde, an agonist of TRPA1, also inhibits TRPM8 (Macpherson et al 2006). (Macpherson et al 2006).

1.2.3. TRPA1

TRPA1 (transient receptor potential ankyrin 1), another TRP channel also suggested to be involved in cold transduction, has diverse functions as a sensor for irritating and cell damaging signals. The TRPA1 gene was first cloned from cultures of human lung fibroblasts (Jaquemar et al 1999) and later from the mouse dorsal root ganglion, where it was named ANKTM1 and identified as a receptor for noxious cold (Story et al 2003). Shortly after this, TRPA1 was established as the mustard oil receptor (Jordt et al 2004). TRPA1 is the only mammalian member of the TRPA family, and it consists of six transmembrane domains with cytoplasmic N- and C- termini (Figure 1.4). The N-terminal region contains 14 ankyrin repeats, which are proposed to interact with the cytoskeleton (Howard & Bechstedt 2004) or to modulate ligand binding (Lishko et al 2007). TRPA1 is mainly found to be expressed in the neurons of the trigeminal, dorsal root, and nodose ganglia (Fajardo et al 2008, Jordt et al 2004, Story et al 2003), which suggests specific sensory functions. However, it has also been found in the skin, hair, brain, and gastrointestinal mucosa (Atoyan et al 2009, Corey et al 2004, Kwan et al 2009). In sensory neurons, TRPA1 is highly co-expressed with neurons containing calcitonin gene-related peptide (CGRP), substance P, and also with TRPV1 (Kobayashi et al 2005, Story et al 2003), which further suggests its role in nociceptive functions.

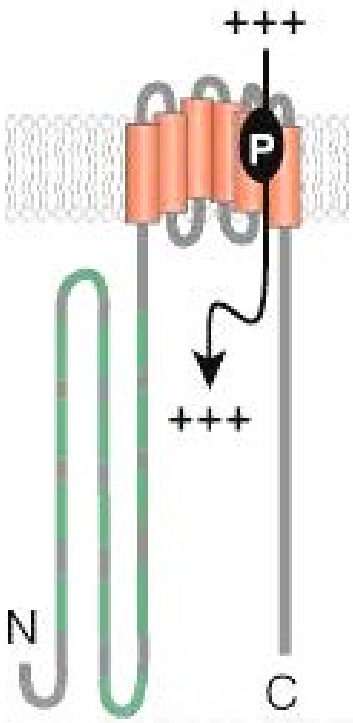

Figure 1.4. General structure of the TRPA1 subunit. Six transmembrane domains are represented by orange cylinders. N and C respectively indicate the intracellular amino and carboxyl regions. The green segments represent ankyrin domains. The pore domain, marked by the letter P, allows the passage of cations, marked by the + sign. (Figure adapted from (Venkatachalam & Montell 2007)).

Temperature dependent gating of TRPA1 is attributed to a shift in voltage dependence of channel activation, which is similar to what has been previously shown for TRPM8 (Voets et al 2004). Even though it was originally identified as a noxious cold sensor with activation to temperatures below that of TRPM8, cold sensitivity of TRPA1 has been a controversial issue (Bautista et al 2006, Jordt et al 2004, Kwan et al 2006). The major cold-sensitive population of sensory neurons respond to cooling and is sensitive to menthol, indicating the involvement of TRPM8, however, a small percentage responds to cold, but not menthol, demonstrating that other mechanisms, such as TRPA1 could be involved (Kobayashi et al 2005). When looking at TRPA1 expression, reports have found that it is expressed in 20-36.5 percent of trigeminal neurons (Bautista et al 2005, Nagata et al 2005), yet no correlation between cold sensitivity and mustard oil responses were found in

cultured neurons (Babes et al 2004, Madrid et al 2009). Altering the cooling protocol to use a more intense and prolonged stimuli, a population of trigeminal neurons that are cold and mustard oil sensitive was observed that was also absent in TRPA1 knockout mice, providing evidence for impaired noxious cold sensation (Karashima et al 2009). TRPA1 also seems to be the main mechanism for cold sensitivity in nodose ganglion neurons innervating the respiratory and gastrointestinal tracts (Fajardo et al 2008).

The role that TRPA1 plays as a chemosensor seems to be quite clear. Since it was first identified to be activated by mustard oil, it has also been found to be activated by a broad variety of natural compounds, including allyl isothiocyanate (AITC, the pungent compound found in mustard oil), horseradish, and wasabi (Bandell et al 2004, Jordt et al 2004). Additionally, it can be activated by cinnamaldehyde (Macpherson et al 2006), allicin (found in garlic) (Macpherson et al 2005), tetrahydrocannabinol (found in marijuana) (Jordt et al 2004), and nicotine (Talavera et al 2009). Other non-natural chemicals can activate it as well, such as isocyanates and acrolein, toxic environmental pollutants (Bandell et al 2004, Bautista et al 2006, Bessac et al 2009). Menthol, in addition to activating TRPM8, has a bimodal effect on TRPA1. Menthol can act as an agonist to TRPA1 at micromolar levels, from 100-300 μM, while it is able to block the channel at much higher submillimolar concentrations (Karashima et al 2007, Macpherson et al 2006).

1.2.4. Potassium Channels

Potassium channels are structurally very diverse and found in almost all types of organisms where they are involved in various biological functions. The formation of a K^+ selective transmembrane aqueous pore is common to them all. There are two main classes defined by these transmembrane proteins, the six-transmembrane-helix voltage-gated (K_v) and the two-transmembrane-helix inward-rectifier K^+ channels (K_{ir}) (Ho et al 1993, Papazian et al 1987, Pongs et al 1988). Two subfamilies of channels include the calcium-activated K^+ channels and the two-pore domain K^+ channels (K_{2P}). The channels TREK-1 and TRAAK are found within one of the six subfamilies of mammalian K_{2P} channels.

1.2.4.1. TREK-1 and TRAAK

K_{2P} channel subunits contain four transmembrane segments and two pore sequences with intracellular N- and C-termini. Found within the TREK subfamily of K_{2P} channels, TREK-1 (also known as KCNK2 or $K_{2P}2$) was the first member discovered (Fink et al 1996), closely followed by TRAAK (KCNK4, $K_{2P}4$) (Fink et al 1998). K_{2P} channels mediate background currents, stabilizing the membrane resting potential, and helping control cell excitability (Enyedi & Czirjak 2010). Both TREK-1 and TRAAK are expressed in the nervous system, TRAAK seems to have specific expression there (Fink et al 1998) while TREK-1 is highly expressed in the brain and DRG (Maingret et al 2000), as well as other tissues like the heart, lung, and kidneys (Fink et al 1996).

Also known as 'leak' channels that open at rest, they were first identified as mechanosensitive K^+ channels, opened by membrane stretch, cell swelling, and shear stress (Maingret et al 1999, Patel et al 1998), TREK-1 and TRAAK were later demonstrated to be temperature-gated channels as well. First, TREK-1 was found to be gradually and reversible opened by heat. When warmed to 42ºC, the opening of the channel hyperpolarized cells, reducing the discharge of action potentials. Cooling was found to close TREK-1, causing cell depolarization and the firing of action potentials, leading to speculation of its involvement as a temperature sensor in cold-sensitive fibers (Maingret et al 2000). Other studies found cold-sensitive neurons that responded to cooling by the closure of K^+ channels in the same manner (Reid & Flonta 2001, Viana et al 2002). Later, similar temperature sensitivity was seen in TRAAK, which is active near physiological body temperatures and its sensitivity ranges from 24ºC to >42ºC. Maximum activity was reached between 37-42ºC and severely decreased at higher temperatures (Kang et al 2005).

More details about their role in cold detection came from the characterization of TREK-1 and TRAAK knockout mice. In studies made in DRG neurons, it was found that in the TREK-1 and TRAAK double knockout mice the population of neurons that responded to cold and menthol or cold and AITC significantly increased, along with the population of cold-sensitive and menthol- and AITC-insensitive neurons, which increased 2.5 fold. This showed clear evidence for the role of both channels together, if not individually to cold detection (Noel et al 2009). More recently, in a study on networks of cultured hippocampal neurons, the closure of K_{2P} channels during mild cooling produced an increase in action

potential firing and synaptic activity, which was then prevented with a K_{2P} channel opener, chloroform (de la Pena et al 2012). This also suggests an important role that TREK-1 and TRAAK channels play in thermosensation.

1.2.4.2. Voltage-gated potassium channels (Kv)

Kv channels represent the largest and most diverse family of genes in the K+ channel family. They are encoded by 40 genes and are represented by 12 families (Kv1-Kv12). Kv1-Kv4 are the ones most widely associated with the nervous system. Functional Kv channels are formed by four α-subunits, each subunit having six transmembrane segments with a membrane reentering P-loop. Four α-subunits from within a family can form tetramers around the central conducting pore. They assemble as channel complexes of homo-tetramers or hetero-tetramers, and include four cytoplasmic auxiliary Kv ß-subunits, creating a diverse array of possible channel combinations. Kv1 channels, assembled cotranslationally in the endoplasmic reticulum, are transported selectively to their subcellular locations and anchored in the plasma membrane by scaffolding molecules (Pongs et al 1999, Rhodes et al 1996). Cell surface expression of Kv1.1 and Kv1.2 is typically concentrated along axons and axon terminals of neurons. Kv1.1- and Kv1.2-containing channels are able to modulate action potential propagation and dampen normal or abnormal repetitive firing (Jan & Jan 2012).

Kv channels are a very large subfamily of potassium channels. They play a vital role in action potential (AP) initiation and propagation, shaping APs, and regulating of AP firing patterns (Bean 2007). The membrane spanning Kv channels allow charged ions to flow rapidly into or out of the cell in response to membrane potential changes, determining the intrinsic excitability of neurons (Llinas 1988). This excitability has been shown to be regulated dynamically through channel composition and expression, differential distribution and localization, as well as additional mechanisms such as phosphorylation that modify channels, thereby influencing neuronal output and leading to experience-dependent plasticity in intrinsic excitability (Schulz et al 2008).

This modulatory role of Kv channels on neuronal electrical activity has important significance in the determination of threshold sensitivity in sensory neurons. For example, Madrid et al (Madrid et al 2009) have shown that a cold-sensitive current dubbed IK_D, and

dependent on Kv1 channels is expressed by a subpopulation of cold thermosensitive neurons, acting as a brake that reduces responsiveness to cooling. In the same vein, it has been recently described as a mechanosensitive K+ current in DRG neurons (I_{Kmech}) carried by Kv1.1-Kv1.2, with mechanosensitivity embedded within the Kv1.1 α-subunit. It has been hypothesized that local membrane distortions induced by applied forces alter interaction between phospholipids and positively charged arginine residues located in the voltage sensor of Kv1.1, i.e. mechanosensitivity would be determined by the inherent stretch sensitive properties of the voltage sensor (Hao et al 2013).

In summary, responsiveness to cooling appears to be present to a variable degree in the different functional classes of peripheral sensory receptors innervating the body surface, depending in each case on the particular expression of various types of thermosensitive ion channels. However, the contribution of each fiber class and thermosensitive channel to the final sensory message under physiological and pathological conditions is unknown.

1.3. Thermoreceptors and water balance

The canonical role ascribed to cold thermoreceptors in mammals is to detect reductions of body surface temperature. This serves to obtain conscious information about the temperature of surrounding objects, food and drinking water, but also to measure the oscillations in environmental temperature. This information is used to regulate metabolic and behavioral responses aimed at keeping the core temperature of the body relatively constant (Belmonte & De la Pena 2013). In recent years, these established functions of cold thermoreceptors have been extended to the detection of potentially injurious cold stimuli and the modulation of pain sensations (Belmonte et al 2009, Belmonte & Viana 2008).

Occasionally, additional roles have been proposed for cold thermoreceptors. For instance, it was reported that acute changes in regional ocular blood flow activate perivascular cold thermoreceptor endings, suggesting an involvement of ocular cold sensory afferents in the regulation of local blood flow (Gallar et al 2003). A contribution of cold thermoreceptors of the respiratory pathway to the detection and regulation of air flow rate has been repeatedly proposed (Sant'Ambrogio et al 1986) an effect mediated by TRPM8 channels

expressed by polymodal vagal afferent fibers innervating the airways (Xing et al 2008). Recently it was shown that sensory inflow from cold thermoreceptors innervating the ocular surface (cornea and bulbar conjunctiva) encodes ocular surface dryness, maintaining basal tear flow (Parra et al 2010). This may also be the case for thermoreceptor fibers innervating the oropharyngeal and respiratory pathways which may detect the moistness level of their target mucosal surfaces evoking conscious sensations of dryness and thirst that would stimulate water intake, as well as reflex autonomic responses including fluid secretion by salivary glands, adjustment of airways surface liquid volume, or defensive reflexes such as cough and increased airways resistance, as seen in asthma (Nadel et al 1979, Xing et al 2008).

1.3.1. Water balance in multicellular organisms

Life initially developed in the ocean and evolved around the unique properties of water molecules. Water is the most abundant substance in living cells, and the majority of intracellular reactions occur in an aqueous environment. The apparition of the plasma membrane represented a crucial step in earliest forms of life, allowing a separation of the cellular content from the external environment. Likewise, the development of epithelial sheets formed by cells bound together in multicellular organisms enhanced their mechanical strength but also acted as a barrier that prevents a free passage of molecules, thereby generating a sheltered internal environment. In complex multicellular animals epithelial sheets of cells line all external and internal surfaces in the body, creating separate sheltered compartments with controlled internal environments where specialized functions are performed by differentiated cells (Alberts 2002).

In water filled compartments, water molecules move down a concentration gradient until equilibrium is reached or movement is prevented. Cell walls of simple multicellular organisms tend to be semi-permeable to water molecules: in hypotonic media, water moves into the cells until osmotic equilibrium is achieved. If the difference in osmolality is large then the cell runs the risk of swelling until bursting. When the liquid environment is slightly hypertonic, water moves out of the organism until equilibrium is established. Once again if the difference is large the organism runs the risk of losing too much intracellular

water and becoming lethally dehydrated. While large, multicellular organisms living in either fresh or sea water have developed mechanisms to deal with the regulation of these movements of water, for land animals the problem is to obtain and maintain enough water inside the body. The maintenance of a constant volume and electrolyte concentration of the intracellular and extracellular fluids is critical for enzymatic activity and maintenance of body functions such as blood circulation or food absorption. Hence, body water content must be kept within quite narrow limits which mean that the intake and loss of water have to be tightly regulated. In mammals, water content of the body (about 70-75% in humans) is lost through urine, sweating, in the feces, and as moisture in expired air (Schmidt 1986), while fluid intake mainly comes from drinking, with a small contribution from metabolism of ingested food. The distribution of water is assured by the cardiovascular system, with all its inherent control mechanisms. The renal system (and to some extent the respiratory system) is the main physiological system responsible in regulating water loss. However, other regulated physiological systems depend on the water ingested. Therefore, various separate control mechanisms interact for the maintenance of body fluid homeostasis (Thornton 2010).

1.3.2. Neural regulation of water intake

Fluid intake is a basic drive for mammals, arising in response to cellular and extracellular dehydration. The drive, experienced as thirst, is a motivational state when one is ready to consume water (Eccles 2000). The neural mechanisms regulating the apparition and satiation of thirst are complex and include central and peripheral components.

1.3.2.1. Central mechanisms

It is well established that important stimulus for water intake are the increases in the extracellular concentration of non-permeable osmolytes that result in the osmotic movement of water from body cells. Therefore, osmolarity changes were envisioned as the main stimulus for thirst, whereas water intake decreasing plasma osmolality (pOsm) back to normal causes satiety by removing the excitatory signal for thirst. There is considerable

experimental support for this model of internal fluid regulation based on a single-loop negative-feedback system where dehydration increases pOsm thereby providing a stimulus for water intake. Cerebral osmoreceptors located in the vascular organ of the lamina terminalis (OVLT) detect increases in effective pOsm; the OVLT is a structure in the basal forebrain that lacks a blood-brain barrier and therefore can readily respond to alterations in pOsm (Johnson et al 1996, Oldfield et al 1994). Actually, increases of only 1-2% in pOsm stimulate thirst in animals and cause proportional increases in water intake (Fitzsimons 1963). When projections from the OVLT activate neurons in the median preoptic area in the lamina terminalis ventral to the anterior commissure, thirst is stimulated, although the consequent neural circuitry that mediates thirst and drinking behavior has not been precisely determined yet. Different projections from the OVLT to the paraventricular and supraoptic nuclei of the hypothalamus stimulate secretion of VP from the posterior lobe of the pituitary gland (McKinley et al 1992, Robertson et al 1976). Destruction of the OVLT surgically, eliminates both water drinking and neurohypophyseal VP secretion as a result of increased pOsm (Buggy & Jonhson 1977, Mangiapane et al 1983).

1.3.2.2. Peripheral mechanisms

A control system of fluid intake based on osmoregulation alone is possibly simplistic. Thirst satiation is obtained through primary or secondary drinking. Primary, also called need-induced drinking, results from a lack of water in the body, while secondary drinking, the most common way satiation occurs, involves drinking without the need to replenish water (Schmidt 1986). Primary drinking is likely produced by cellular dehydration (Fitzsimons 1976). On another hand, secondary drinking is triggered by thirst occurring in the absence of significant body-fluid changes in men that had access to water *ad libitum* (Phillips et al 1984) and anticipates the development of body-fluid deficits (Brunstrom & Macrae 1997).

Indeed, there is a substantial delay between the time when water is ingested and the time when it appears in the circulation affecting pOsm and stimulating the cerebral osmoreceptors. More specifically, it takes 10 to 20 minutes for water that is ingested to produce significant decreases in pOsm, whereas thirst, VP secretion, and water intake end much more rapidly (Huang et al 2000, Thrasher et al 1981). Therefore, an earlier stimulus

has to occur to inform the brain in anticipation of subsequent rehydration. This effect is similar to the feed forward reflexes in the control of several other autonomic functions such as the insulin response evoked by the taste of food before its digestion and assimilation. This anticipatory element in the control of water intake has been also observed in humans (Bellows 1939, Holmes & Gregersen 1950). Immediately after drinking, humans experience a transient reduction in thirst. It is accepted that further liquid ingestion is inhibited by unidentified preabsorptive oropharyngeal and gastrointestinal factors (Figure 1.5). A few minutes later absorption begins and inhibition is sustained.

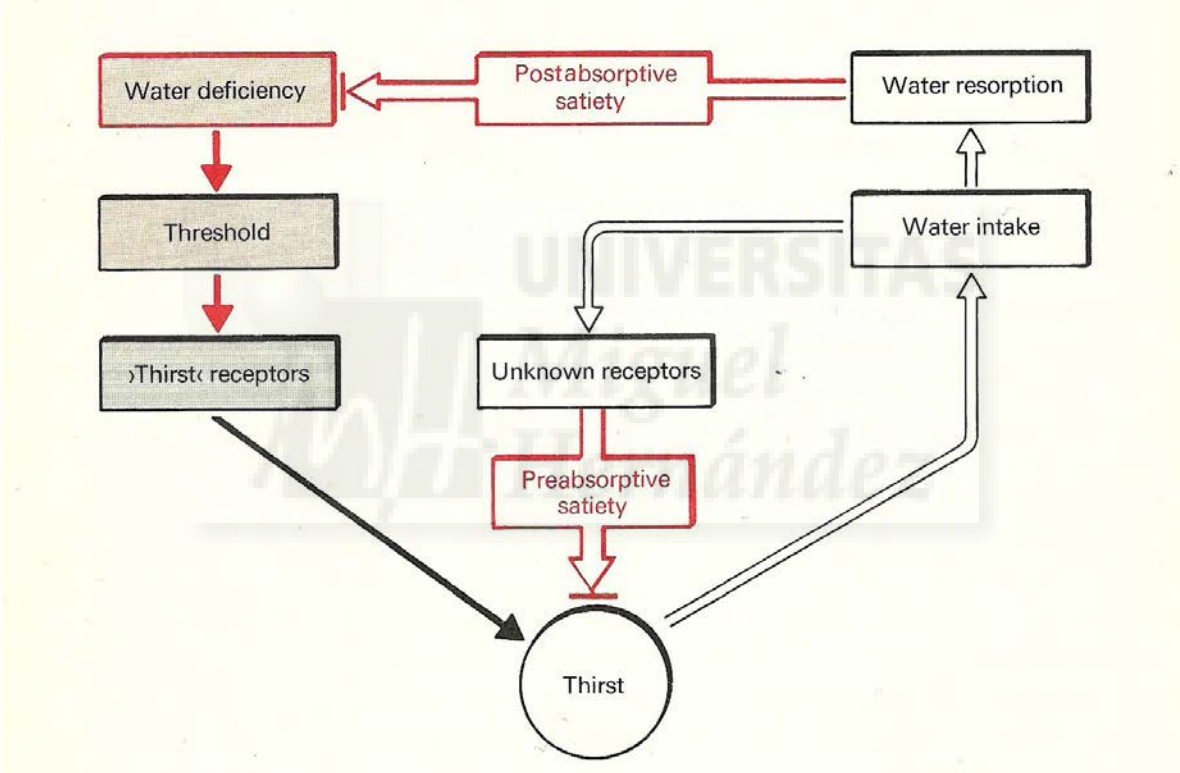

Figure 1.5. Diagram of proposed preabsorptive and postabsorptive satiety mechanisms in the body caused by a water deficiency. (Figure adapted from (Schmidt 1986)

Suppression of the symptom of mouth dryness by drinking is one of these inhibitory factors. In fact, oropharyngeal dryness was considered by Cannon (Cannon 1918) as the main origin of thirst ('dry-mouth theory'). However, thirst defined as 'a motivational state within the nervous system that arouses and maintains the behavior involved in the search for and ingestion of water' (Fitzsimons 1979) or more narrowly, as the sensation aroused

by a need for water also depends on other factors. There is abundant experimental data showing that mouth dryness is not an exclusive and isolated determinant of thirst and drinking behavior as originally proposed by Cannon. For instance, Epstein (Epstein 1960) showed that the direct injection of water into the stomach using a chronic catheter did not stop the drive to drink, thus probing that the sensory information about taste and smell of water, the feeling of water in the mouth or the proprioceptive information about drinking was not critical to maintain the neural regulation of water intake. This confirmed an old observation by C. Bernard (Bernard 1855) showing that animals with an esophagic fistula that prevented the absorption of ingested water continue drinking. Likewise, dehydrated ruminants that have continuous salivary secretion drink avidly (Fitzsimons 1976).

Nevertheless, the drinking behavior displayed in intact animals and in animals where the stomach was directly filled with water were different, suggesting that sensory information from the orogastric area contributes to the definition of the water appetite and the modulation of water volume intake. Moreover, fMRI studies has shown that the genesis of a compelling consciousness of thirst involving a contemporaneous awareness of dryness of the mouth caused striking activation and inhibitory processes in the parahippocampus, amygdala, and thalamus, together with cingulate areas and insula, (Denton et al 1999). The consummatory act of rapid drinking, associated with contemporaneous loss of thirst was accompanied within three minutes of completion by a reduced foci activation not only in parietal sensory areas, but also in the limbic system and particularly the cingulate areas. Characteristically, gratification occurred without any alteration in plasma [Na^+] or osmolality. These results underscore the importance of thirst in abolishing sensory inflow from mouth, esophageal monitoring of volume swallowed, and gastric distension (Denton 1982). Nonetheless, the peripheral sensory mechanisms that measure mouth dryness and thirst and trigger its pre-absorbtive relief following normal daily drinking are still not completely understood.

Sensory receptors innervating the mucous membranes of the mouth possibly provide information on the wetness levels of the oral mucosa but which receptor types are involved is currently unknown. There is no evidence of water-sensitive taste receptors, implying that peripheral detection of water and the metering of water intake must be mediated by other classes of somatosensory receptors (Kapatos & Gold 1972, Schmidt 1986). Some thoughts

are that some of these are sensory receptors of the oral mucosa, acting as osmoreceptors detect the level of mucosal hydration, but no experimental evidence supports this speculation. Mechanoreceptors activated by the sheer forces of tongue movements as the mucosal surfaces dries have also been implicated; saliva lubricates the oral mucosa and would reduce this friction and dryness, helping to prevent thirst (Eccles 2000). Finally, there is indirect evidence involving thermoreceptors in the regulation of water intake (Deaux 1973). After being deprived of water for 24 hours, albino rats prefer drinking water closer to body temperature, 30ºC, than cooler water, 12ºC (Steiner et al 1986). In one study involving a once-a-day drinking schedule in rats, peak water intake occurred at 36ºC with water intake decreasing as the temperature decreased. This suggested that tongue cooling contributed to satiation (Kapatos & Gold 1972).

Even though cold and warm water have the same effects on osmolality, cold water (5ºC) is typically more thirst quenching than room temperature water (22ºC) (Brunstrom & Macrae 1997). One explanation for this is the fact that cold water (0ºC) was shown to evoke more saliva production than water at 22ºC (Pangborn et al 1970). Alternatively, it has been proposed that the increase of satiety by cold water is mediated by the stimulation of sensory cold receptors found in the oral cavity (Eccles 2000).

1.4. Sensory innervation of the oropharyngeal mucosa

The innervation of the oral cavity is provided by cranial nerves, V, VII, IX and X, whose cell bodies are located in the cranial ganglia (Gross et al 2003). Three broad types of sensory neurons are found in these ganglia, i.e., somatosensory, general viscerosensory, and special viscerosensory, which together provide non-gustatory and gustatory innervation to the oral and pharyngeal regions. Non-gustatory neurons include both somatosensory fibers, which terminate as free nerve endings in the non-taste bud-bearing regions of the oropharyngeal epithelia and project centrally to the nucleus of the spinal tract of V (SpV; (Phelan & Falls 1991), and general visceral fibers, which innervate sensory receptors in the cardiovascular and gastric epithelia and project to the caudal solitary nucleus (NTS) (Cechetto 1987). Gustatory neurons, which are also termed special visceral (Finger 1993), innervate the taste buds located in the epithelial surfaces of the mouth and pharynx, and

project to the rostral solitary nucleus within the hindbrain (Harlow & Barlow 2007, Herrick 1944, Martin & Mason 1977, Smith & Davis 2000). The different functional classes of sensory neurons have a different embryological origin. Gustatory neurons in ganglia VII, IX and X are of placode origin, whereas those neurons in these ganglia that innervate general epithelia have, in most cases, a neural crest origin. While gustatory, or special visceral afferents converge into the fasciculus solitary and then synapse on neurons of the rostral nucleus of the solitary tract (NTS), cranial neural crest-derived neurons of ganglia V, VII, IX and X which are entirely non-gustatory in function and contribute only to the general epithelial innervation of the oral and pharyngeal cavity project into the spinal trigeminal tract (SpV) (Harlow & Barlow 2007).

The trigeminal nerve, or fifth (V) cranial nerve, is the largest of the cranial nerves (Soeira et al 1994) whose somatic afferent fibers provide input including tactile sensation, pain, and temperature from the face and mucous membranes of the oral cavity (Carpenter & Sutin 1983). The cell bodies of the sensory fibers of the trigeminal nerve are found in the trigeminal ganglion. It serves as the major path of sensory information from the face while also providing some motor innervation.

The trigeminal nerve has three main branches, the ophthalmic (V1), maxillary (V2), and mandibular (V3) nerves. The ophthalmic branch provides sensory innervation from the eye and forehead, and the maxillary branch provides sensory innervation from the upper lip, cheek, nasal cavity, and nose. The mandibular nerve is the largest of the branches, and provides sensory information from the side of the head and scalp, chin, lower lip, and tongue (Williams et al 2003). It is comprised of a sensory and motor root and then divides into an anterior and posterior trunk (Gray & Lewis 1918). One branch of the mandibular nerve is the lingual nerve.

There is evidence of TRPM8 expression within the trigeminal ganglion in a subset of small diameter neurons, representing 11.8% of TG neurons (Abe et al 2005). Additionally TRPM8 mRNA was observed in 5-10% of TG neurons (Peier et al 2002). In regards to TRPA1 expression in trigeminal neurons, one study observed that 14.9% of neurons from adult mice could be classified as TRPA1+ cold-sensitive. They also showed that TRPM8 and TRPA1 act as the primary, but not only, cold sensors in TG neurons, with TRPA1+

cold-sensitive neurons having a higher thermal threshold, a slower response to cold, and a general sensitivity to capsaicin (Karashima et al 2009).

1.4.1. Sensory innervation of the tongue

The tongue is a mass of skeletal muscle covered by oral mucosa located on the floor of the mouth, richly supplied with nerves and blood vessels (Gray & Lewis 1918). In mammals, the tongue serves various sensory and motor functions, including aiding in chewing, swallowing, and speech. Its sensory innervation is very extensive, serving the sensations of temperature, touch, pain, and taste (Rong et al 2000). The surface of the tongue contains different types of lingual papillae located on the anterior two-thirds of the dorsal side of the tongue which include foliate, circumvallate, filiform, and fungiform papillae. Foliate papillae are located along the lateral edges of the tongue. Circumvallate are large prominent papillae located in the posterior part of the tongue with taste buds lining their grooves (Kandel 2012). Filiform papaillae are the most numerous and located along the dorsum of the tongue, while fungiform papillae are mushroom-shaped and found in the anterior two-thirds of the tongue.

Several nerves innervate the tongue, including the hypoglossal, glossopharyngeal, chorda tympani, and the lingual nerve. The hypoglossal nerve controls tongue motor functions, except for the palatoglossus muscle which is innervated by a branch of the vagus nerve. In the posterior one-third of the tongue, the glossopharyngeal nerve conveys sensory and taste information, while in the anterior two-thirds, taste is mediated by the chorda tympani, a branch of the facial nerve which joins with the lingual nerve (Gray & Lewis 1918). The lingual nerve, a branch of the trigeminal sensory nerve, supplies general sensory information to the anterior two-thirds of the tongue (Rusu et al 2008). Its fibers terminate in the lingual epithelium and in the epithelium that surrounds the taste buds of the fungiform papillae (Dhaka et al 2008, Wang et al 1993). Afferent fibers of the lingual nerve terminate in the dorsal one-third of the spinal nucleus of the trigeminal complex and in the lateral nucleus between the rostral and caudal poles overlapping with the chorda tympani nerve (Whitehead & Frank 1983). The chorda tympani nerve, involved with taste, is responsive

to chemical stimuli, while it also contains fibers sensing cold and heat. The lingual nerve sends information about temperature, touch, and pain (Pittman & Contreras 1998), while having little sensitivity to prototypical tastants.

The lingual nerve contains four functional classes of receptor fibers, including thermoreceptors, mechanoreceptors, nociceptors, and proprioceptors (Kandel 2012). In a pioneering study in the lingual nerve of the cat, abundant specific cold and warm thermoreceptors were identified (Zotterman 1936). These exhibited a consistent response pattern consisting of a steady spontaneous activity at background skin temperature, dynamic responses to sudden temperature changes, and insensitivity to mechanical stimulation (Hensel et al 1960). This basis allowed thermoreceptors to be distinguished from other types of receptors, such as mechanoreceptors and nociceptors.

Sensory nerve fibers can also be categorized based on their conduction velocity. The lingual nerve contains Aδ, Aβ, and C fibers, with mean conduction velocities of 13.3, 32.1, and 1.2 m/s respectively. In a study from the rat lingual nerve the fibers most often recorded from are the Aδ fibers, and when considering chemical responses, Aδ and C fibers most often responded to chemical stimulation, while Aβ did not (Wang et al 1993). Cell bodies of sensory afferent fibers from the lingual nerve were identified in the rear of the trigeminal ganglion, in close proximity to the cell bodies of afferents from around the oral cavity (Wang et al 1993).

2. OBJECTIVES

2.1. General objective

The general objective of this thesis is to analyze the cold-sensitive fibers of the mouse tongue and study their modulatory role on drinking behavior.

2.2. Specific objectives

- The first specific objective of this thesis was to use the sensory innervation of the tongue mucosa as an experimental model to electrophysiologically characterize the responsiveness to cold of different functional classes of sensory fibers and to determine the contribution of the various cold-sensitive channels to their specific thermal sensitivity.

- A second specific objective of this thesis was to explore the possibility that cold thermoreceptors in exposed mucosa measure their level of wetness contributing to the sensory drive that modulates their moistness levels, using tongue's cold thermoreceptors and thirst satiation as an experimental model.

- A third specific objective of this thesis was to determine the contribution of the various classes of cold thermosensitive fibers innervating the tongue and oropharyngeal mucosa to the modulation of water intake.

UNIVERSITAS
Miguel
Hernández

3. MATERIALS AND METHODS

3.1. Animals

Adult male mice were used for all experiments, which included wild-type (C57BL/6, $TRPM8^{+/+}$, $TRPA1^{+/+}$), $TRPM8^{-/-}$ (Dhaka et al 2007), $TRPA1^{-/-}$ (Kwan et al 2006), $TRPM8^{-/-}$/$TRPA1^{-/-}$, and TRPM8-YFP mice (Parra et al 2010). Prior to the experiments all mice were housed in the animal house of the Universidad Miguel Hernández in San Juan de Alicante with free access to food and water. The animals were treated in accordance with institutional animal care guidelines and according to Spanish Royal Decree 1201/2005 and the European Community Council directive 2007/526/EC.

3.2. Electrophysiological recordings in an 'in vitro' tongue preparation

3.2.1. Tissue preparation

Mice were sacrificed with carbon dioxide then decapitated and the tongue, along with the jaw and upper part of the pharynx, was removed from the head. It was placed in a Petri dish filled with cold (4ºC) saline solution (in mM) 133.4 NaCl, 4.7 KCl, 2 $CaCl_2$, 1.2 $MgCl_2$, 1.3 NaH_2PO_4, 16.3 $NaHCO_3$ and 9.8 glucose. Additional dissection of the tissue was performed under a dissection microscope until the lingual nerve, which enters from the posterior border, was isolated. The superior side of the tongue was opened with an incision along the midline so the nerves on each side of the tissue could be accessed and further dissected into the anterior part of the tongue, as shown in Figure 3.1. The tissue was maintained in saline solution, gassed with carbogen (95% O_2, 5% CO_2) to maintain the pH at 7.3.

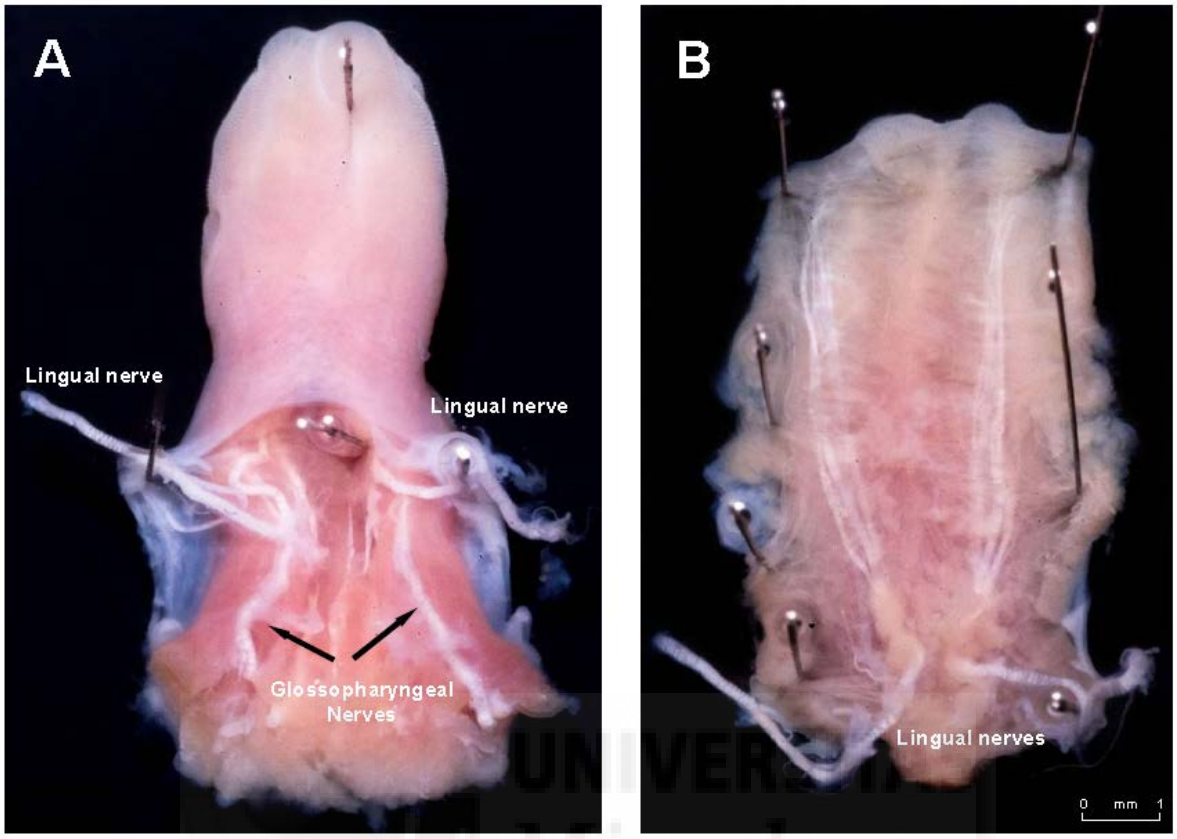

Figure 3.1. Dissection of the tongue in preparation for electrophysiological recordings of the lingual nerve. (A) The superior side of the tongue opened along the midline to expose the lingual and glossopharyngeal nerves. (B) The extended cut along the midline to the tip of the tongue to fully expose the lingual nerves on either side and prepare for recording.

Next the tongue was pinned into a recording chamber with the upper surface down (Figure 3.2). The recording chamber was continuously superfused with saline solution and maintained at a temperature of 35ºC. The temperature of the solution was controlled at the entrance of the chamber with a peltier device that could be cooled or heated to values between 0ºC-50ºC at a cooling rate of 1ºC/s. The temperature of the tongue in the chamber was monitored with a thermistor that was placed in the bath close to the tongue's surface. The distal end of one of the lingual nerves was placed in an adjoining compartment filled with paraffin oil, and under a dissection microscope, the nerve was separated into smaller filaments. Filaments were then placed on a monopolar platinum wire electrode connected to an AC-amplifier to record the electrical activity which was monitored in an oscilloscope and stored on a hard disk for analysis done with Spike 2 software (CED).

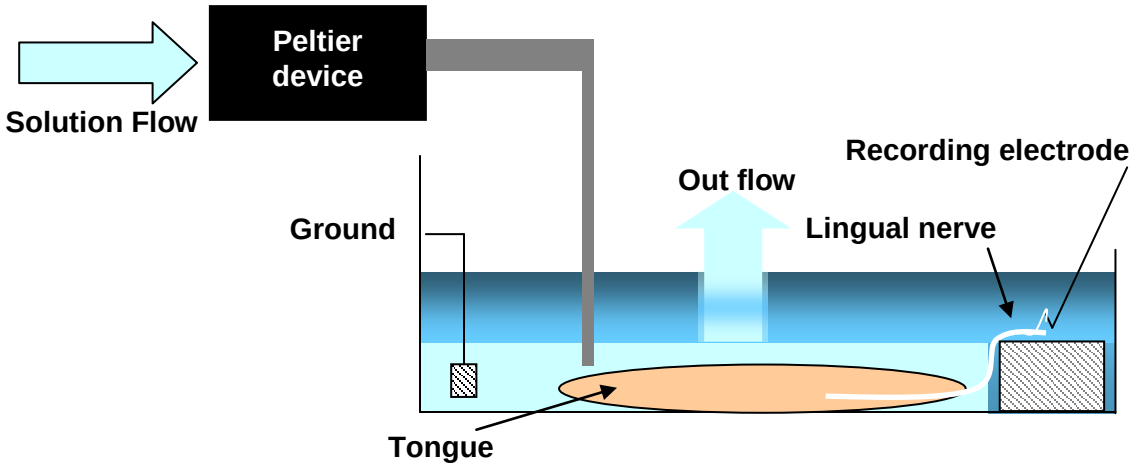

Figure 3.2. Experimental setup, showing the diagram of the recording chamber and dissected tongue.

In a group of animals, an acute inflammation of the tongue was performed prior to recording. To cause the inflammation, mice were anesthetized with an intraperitoneal injection of xylazine (10 mg/kg)/ketamine (70 mg/kg), and then a 5 µL injection of carrageenan (2% in saline) was made down the midline toward the tip of the underside of the tongue. This caused a marked tissue edema (Winter et al 1962) that was fully developed after two hours. The mouse was then sacrificed and the tongue prepared in the same manner as above.

3.2.2. Stimulation

Recordings were first made using the left lingual nerve. Then the tissue was rotated in the chamber so that recordings could be made with the right side nerve. Thermal stimulation was carried out by adjusting the temperature of the peltier device which changed the temperature of the solution flowing into the chamber in contact with the tongue's receptive field. A cooling curve lasted 60 s and temperature was dropped to around 5ºC. During heating pulses, the temperature was raised to 48º-50ºC. Mechanosensitivity was tested by touching the receptive field of the tongue with a von Frey hair (2.65 mN). To test the effect of drugs, they were dissolved in saline solution at the desired concentrations and placed in

separate perfusion containers. Perfusion was shifted to the containers with the test solutions during a given period.

3.2.3. Electrophysiology

The whole lingual nerve was first placed on the electrode to record the spontaneous multiunit activity. To locate the receptive field, mechanical stimulation was performed with a von Frey hair. To test for cold activity, a 60 s cooling pulse was made from the adapting temperature of 35ºC down to 5ºC and back to 35ºC, and then after a resting period of three minutes a heating pulse to 45ºC was applied for ten seconds. The nerve was then separated into smaller filaments and checked for activity. Filaments containing one single unit or few distinguishable units were then subjected to the stimulus protocol designed to characterize the activity. Fibers responsive to mechanical stimulation were further characterized by applying repeated stimulation with the von Frey hair to the receptive field. For cold sensitive units, a 60 s cooling pulse to 5ºC was made, returning to the adapting temperature for three minutes. This was repeated a total of three times. Then successive temperature steps of 2 - 3ºC and 30 s in duration were performed until a temperature of 5ºC was reached. In a number of experiments, cooling pulses were made in the presence of different activators and inhibitor drugs. In these experiments after an initial cooling pulse was applied, the different reagents were perfused in the solution for three minutes before a one minute cooling pulse was administered. A recovery period of at least five minutes was made between each different substance used. The same fiber was tested with menthol (5 μM), chloroform (20 mM), and cinnamaldehyde (100 or 200 μM). Also, heating pulses were applied three times for filaments that were sensitive to heat.

3.2.4. Data Analysis

Fibers obtained from the lingual nerve were characterized based on the response to the stimulus protocol. Responses to mechanical, cold, and heat stimuli were considered; also

the response to different chemical activators was studied. The responses in WT animals were compared to those of different knockout mice to the same protocol.

The parameters analyzed for the cooling curves are as follows: Spontaneous activity was measured, in impulses per second, as the average activity in 30 s prior to the cooling pulse. The firing frequency during a cooling pulse was taken as the average of the impulse activity, in impulses per second, during the whole 60 s of the cooling pulse. The average firing frequency during a cooling pulse was also measured, in impulses per second, in terms of the mean firing frequency reached between the first and last action potential of the complete firing response of each unit. The temperature of peak firing frequency was defined as the temperature (in ºC) during the cooling curve at which the highest firing rate in impulses per second was observed. The peak firing frequency was the maximal firing frequency in impulses per second during a cooling pulse. Thermal threshold, when there was no spontaneous activity, was defined as the first nerve impulse elicited by cooling after the temperature change was applied. When spontaneous activity was present the threshold was defined as the temperature at which the firing frequency was higher than two standard deviations above the mean basal firing. The time to the peak frequency was the time, in seconds, between thermal threshold and peak firing frequency and the discharge to the peak frequency, the number of impulses fired between threshold and peak frequency. The silencing temperature was the temperature at which the impulse discharge silenced, either at the end of the cooling pulse or during reheating to 35ºC. The threshold during reheating to 35ºC, was the temperature at which impulse activity resumed after silencing during reheating.

To measure the nerve impulse activity during the cooling steps, first the temperature (ºC) of each step was recorded. The temperature of the step was expressed as the average temperature (ºC) of the entire cooling step. Within the step the dynamic phase corresponded to the first 30 s after the onset of the temperature change, and the static phase, the last 30 s of the step when the temperature was constant. The average firing frequency, in impulses per second, of the first 30 s of each step (dynamic) and the average frequency, in impulses per second, of the last 30 s (static) were measured. The average firing frequency, in impulses per second, was also taken for each entire cooling step as a whole, measuring the average firing frequency during the entire duration of each step.

The presence of a bursting pattern during cooling pulses and steps was also measured. Bursting was defined when the interspike interval (ISI), or time between each action potential (in ms), was less than 30 ms in duration. Additional bursting parameters measured included the number of bursts fired per cooling pulse; the bursting pattern, percentage of impulses fired in bursts compared to the total number of impulses fired; and the cycle time of bursts, the mean time between the onset of successive bursts. Finally the mean number of impulses per burst, which was the mean number of impulses contained in the bursts produced by each bursting unit during the 60 s cooling pulse was also measured. These parameters were also measured when stepwise cooling was applied during the static phase (the last 30 s of each cooling step) of each cooling step.

All electrophysiological data were recorded and analyzed with Spike 2 data analysis software. Individual fibers in multiunit recordings were sorted based on their impulse amplitude and shape.

Statistical analysis of data was done with Microsoft Office Excel 2003 using Student's t test and one-way Anova. Significance was set at $p < 0.05$ (*), $p < 0.01$ (**), and $p < 0.001$ (***). Data are presented as mean ± standard error of the mean.

3.3. Lingual trigeminal ganglion neurons

3.3.1. Retrograde labeling of lingual trigeminal neurons

Adult male mice, from a mouse line expressing yellow fluorescent protein under the control of the TRPM8 promoter were used (18 - 25 g) and anesthetized with an intraperitonial injection of 100 mg/kg ketamine and 10 mg/kg xylazine. 10 µL of DiI (Invitrogen) 1 mg/20 µL diluted in 60% ethanol was carefully injected into the tip of the tongue to retrogradely label trigeminal sensory cell bodies whose axons innervate the tongue.

3.3.2. Quantification of labeled trigeminal neurons in culture

Retrograde labeling and the primary culture of lingual trigeminal neurons was made in the same way as described below. Figure 3.3 shows the visible TRPM8 YFP+ labeled neurons in the trigeminal ganglia. Once the neurons were in culture on the coverslips, photos were taken of each coverslip under a fluorescent microscope, to analyze the proportion of DiI and YFP marked neurons in each culture. Nine photos were taken per coverslip, in three rows of three photos per row. Photos were taken with transmitted light, to count the total number of neurons present in the photo area. Then in the same area, two more photos were taken, using a GFP filter and a Texas Red filter, to determine the number of YFP and DiI marked neurons, respectively. Total neuron counts were made per animal.

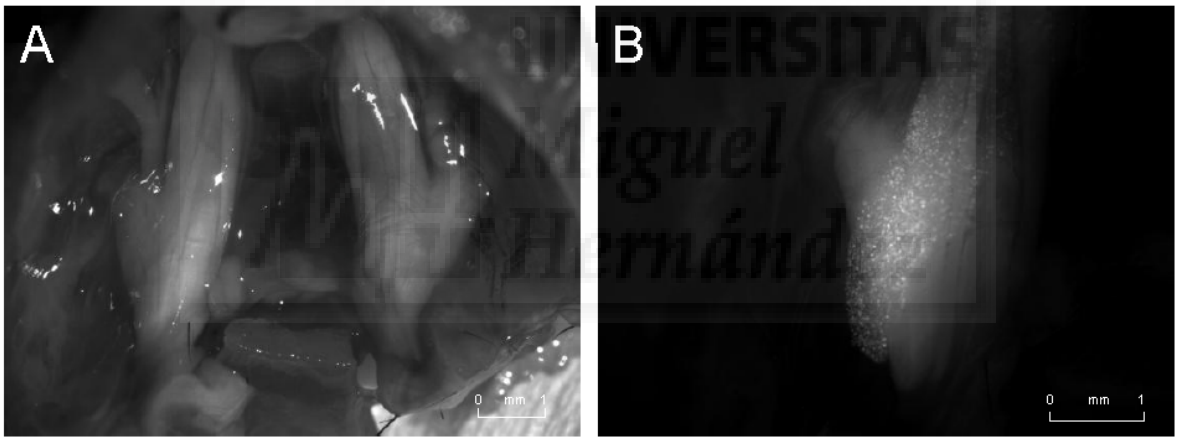

Figure 3.3. Mouse trigeminal ganglia (A) Trigeminal ganglia of the mouse visualized with a binocular scope. (B) Left trigeminal ganglion of a TRPM8-YFP mouse under a fluorescent microscope where TRPM8-expressing neurons can be seen.

3.3.3. TRPM8+ lingual nerve terminal quantification

TRPM8+ nerve endings in the mouse tongue were counted to determine how they are distributed throughout the surface of the tongue. Adult male TRPM8-YFP mice were used since they express yellow fluorescent protein (YFP) wherever TRPM8 channels are

expressed. The mice were sacrificed by cervical dislocation and the tongue excised. The inferior side of the tongue was opened with an incision along the midline and the two lateral sides were opened and spread flat. Excess muscle tissue from the inferior side was removed, taking care not to damage the superior surface of the tongue, to flatten the tissue as much as possible. Pictures were taken under a fluorescent microscope of the whole tissue to easily see the terminals expressing TRPM8. Using the photos, nerve terminals for each animal were counted.

3.3.4. Primary cultures of trigeminal ganglion neurons.

After the three day labeling period described above, mice were sacrificed by cervical dislocation and decapitated. The skin covering the head was removed using scissors, and two longitudinal cuts were made in the cranium to allow the removal of the skull and exposure of the brain. The brain tissue was slowly removed to expose the trigeminal ganglia located at the base of the skull. Then the three peripheral branches were cut and the intact ganglia bodies were extracted and deposited in a P35 Petri dish with HBSS. Each ganglion was then cleaned of connective tissue and nerve branches. Next, the clean ganglia were placed in a concave glass dish containing the enzymes collagenase type XI (0.66 mg/ml) and dispase (3 mg/ml) dissolved in incubation medium consisting of (in mM) 155 sodium chloride (NaCl), 1.5 dipotassium hydrogen phosphate (K_2HPO_4), 10 HEPES, and 5 glucose. This enzymatic digestion was made in a cell culture incubator at 37ºC and 5% CO_2 for 1 hour. The enzymatic solution along with the ganglia was then transferred to a centrifuge tube. One ml of culture medium (89% minimum essential medium (MEM), 10% fetal bovine serum (FBS) with 1% MEM vitamins, 100 µg/ml penicillin/streptomycin, and 100 ng/ml nerve growth factor (NGF)) was added, and a gentle mechanical dissociation was made using a glass Pasteur pipette. Culture medium was added to the tube until the volume reached 5 ml, and then it was centrifuged at 1000 rpm for 5 minutes. The excess medium was removed, and 20 µL of culture medium for each 6 mm coverslip was added to resuspend the precipitate. 20 µL of the suspension was then plated on the surface of every glass coverslip, each of which was previously treated with poly-L-lysine 0.01% for 20 minutes. After 1 hour in the incubator 1 ml of culture medium with 100 ng/ml of NGF was

added to the coverslips. They were then left in the incubator until experimental use, about 24 hours.

3.3.5. Calcium imaging

Trigeminal neurons were incubated with 5 µM fura-2 AM dissolved in standard extracellular solution (in mM); 140 NaCl, 3 KCl, 1.3 $MgCl_2$, 2.4 $CaCl_2$, 10 glucose, and 10 HEPES, pH 7.4 adjusted with NaOH; and 0.02% Pluronic (Invitrogen) for 1 hour in the incubator at 37ºC. Fluorescence measurements were made with a Leica DM IRE2 inverted microscope fitted with a 12-bit cooled CCD camera (Imago QE Sensicam, Till Photonics). Fura-2 was excited at 340 and 380 nm with a Polychrome IV monochromator (Till Photonics), and the emitted fluorescence was filtered with a 510 nm longpass filter. Calibrated ratios (0.5 Hz) were displayed online with TillVision software v4.01 (Till Photonics). The bath temperature was simultaneously recorded. The coverslips with culture neurons were placed in a microchamber and continuously perfused with solution around 34ºC. Temperature was cooled with a water-cooled Peltier device which delivered the solution directly to the cells. Cooling curves down to 10 - 12ºC were administered for 3 minutes before returning to 34ºC. To test the effect of specific ion channel agonists, they were dissolved in saline solution at the desired concentrations and placed in separate perfusion containers. Perfusion was shifted to the containers with the test solutions during a given period.

Threshold temperature values for $[Ca^{2+}]_i$ elevation were estimated by linearly interpolating the temperature at the midpoint between the last baseline point and the first point at which a rise in $[Ca^{2+}]_i$ deviated by at least four time the SD of the baseline.

Experimental protocol

A 6 mm coverslip was placed in the recording chamber, and retrogradely DiI labeled TG neurons were identified by fluorescence microscopy. DiI was excited with light at a wavelength of 560 nm using a Polychrome IV monochromator (Till Photonics), and the emitted fluorescence was filtered with a 590 nm long-pass filter before detection. YFP labeled neurons were identified by exposure to light at a wavelength of 475 nm and the

emitted fluorescence was filtered with a 510 nm long-pass filter. Unlabeled neurons were visualized under transmitted light and pictures were taken to calculate the percentage of labeled neurons. After identifying the neurons as DiI positive (those innervating the tongue) and/or YFP positive (those expressing TRPM8), a calcium imaging protocol was then implemented. After one minute at a control temperature of 34ºC, a cooling curve down to 12 - 10ºC was applied for 3 minutes before returning to 34ºC. The temperature was maintained for 3 minutes for recovery, and then menthol (100 µM) was applied for 2 minutes followed by a one minute cooling curve in the presence of menthol. Temperature was returned to 34ºC and control solution was applied. After at least 3 minutes in control conditions, other ion channel agonists were applied (without administering more cooling curves), with a recovery period of at least 3 minutes between applications. Substances used include AITC (100 µM) and capsaicin (0.5 µM). In addition to this, a hypotonic solution (217 mOsm) was used to evaluate responses to changes in osmolarity and KCl (30 mM) to test neuron excitability.

3.4. Behavior experiments

Adult male mice (C57BL/6, TRPM8$^{-/-}$, TRPA1$^{-/-}$, TRPM8$^{-/-}$/TRPA1$^{-/-}$) weighing around 30 g were used for all the experiments. An experimental cage was designed with two external Peltier devices built into one end, in which water bottles could be inserted for drinking (Figure 3.4). The Peltier devices could be heated or cooled independently thereby maintaining the water temperature in each bottle at the desired value. Graduated homemade bottles were used to accurately measure small changes in water volume. Mice were placed in a cage and were allowed free access to food and water prior to the experiment giving them several days to acclimate to the new placement of the water bottles in this experimental cage. 24 hours prior to the start of each experiment, the water was removed from the cage, but food was still available.

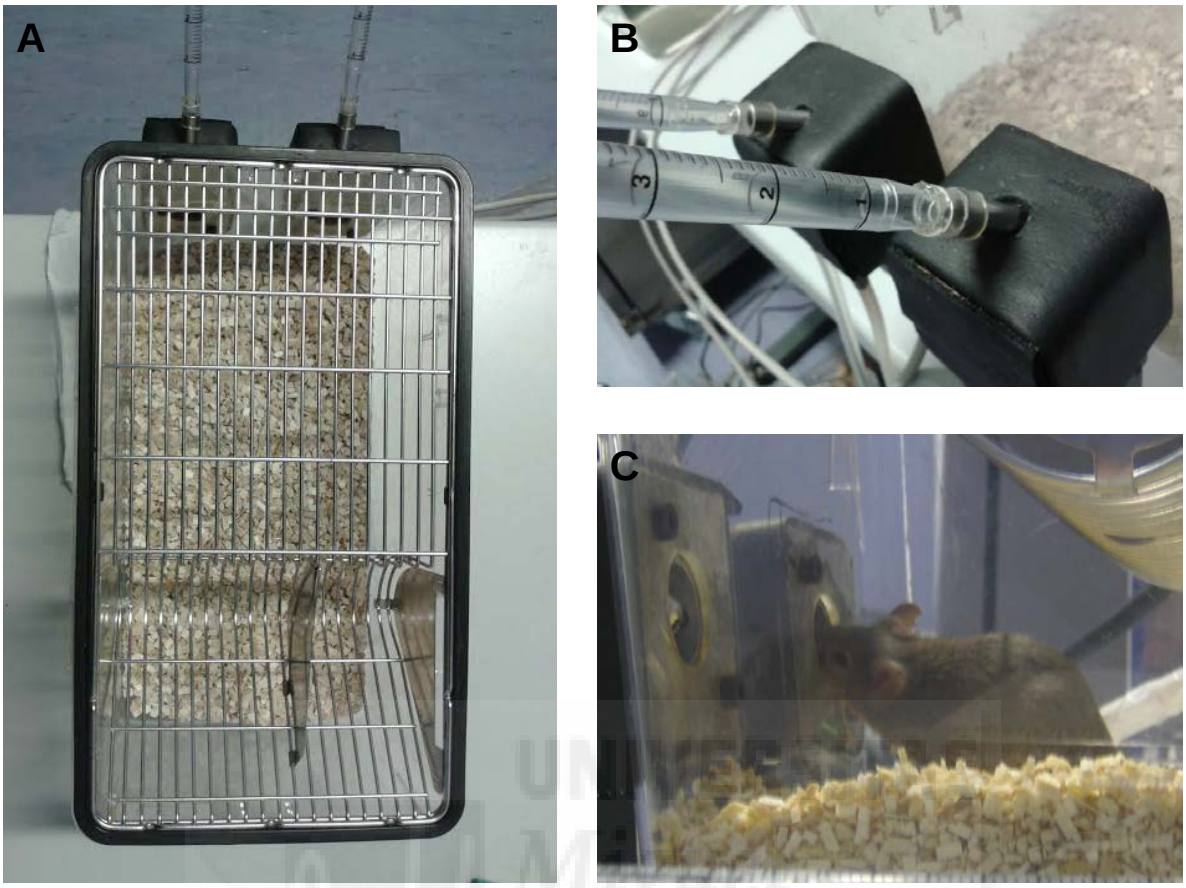

Figure 3.4. Experimental setup used for drinking behavioral experiments. (A) Experimental mouse cage with two external Peltier devices at one end (shown at the top). (B) Homemade graduated drinking bottles inserted into the external Peltier devices for which allows for heating or cooling the drinking water. (C) Trained mouse drinking from a drinking bottle in the experimental cage.

The first water temperature test that was preformed involved only one bottle for drinking, so was a no-choice water temperature test with no preference involved. After being kept without water for 24 hours, mice were temporarily placed in a different cage so that the water temperature could be set in the bottles of the experimental cage. Additionally, the food was removed 30 minutes prior to starting the experiment. Mice were tested at the temperatures, 40, 30, 22, 15, 10, and 5ºC, and room temperature (22ºC) was used as the control. When water temperatures were stable, mice were individually placed in the experimental cage and allowed free access to water for one hour. During the one hour experimental period, the parameters measured for each of the two bottles included the number of entries made to drink, the time spent drinking (in seconds), and the total volume

drunk (in ml). After the one hour experiment, mice were given free access to food and water for at least one full day before starting another water temperature test. With only one bottle being used, there was no option of preference and the mice were obliged to drink the water at the temperature provided.

The second set of experiments involved a water temperature preference test. The same experimental cage, procedure, and temperatures were used as in the no-choice water temperature test, the only difference being that during these experiments there were two water bottles present instead of one, allowing the mice to choose the desired temperature at which to drink. One of the water bottles was always left at room temperature, 22ºC, and a second bottle was set to one of the following experimental temperatures, 40, 30, 15, 10 or 5ºC. The same mice were tested with all the experimental temperatures: 40/22ºC, 30/22ºC, 22/22ºC, 22/15ºC, 22/10ºC, and 22/5ºC. The control experiment was considered as the water temperature preference test when both bottles were set to room temperature (22/22ºC). The same parameters were measured for all temperature preference tests.

All experimental procedures were carried out according to the Spanish Royal Decree 1201/2005 and the European Community Council directive 2007/526/EC. The ethics committee from Universidad Miguel Hernández, Alicante, Spain, approved this study.

3.5. Reagents

- AITC: 100 µM in DMSO, Sigma
- Capsaicin: 0.5 µM in 100% ethanol, Sigma
- Carrageenan: 5 µL, 2% in saline, Sigma
- Chloroform: 20 mM, Merck
- Cinnamaldehyde: 100 µM and 200 µM in DMSO, Sigma
- DiI: 10 µL, 1 mg/20 µL in 60% ethanol, Invitrogen
- Fura 2-AM: 1 mM in DMSO, Invitrogen
- Ketamine: 100 mg/kg, Richter Pharma
- Menthol: 5 µM and 100 µM in DMSO, Scharlau
- Xylacin: 10 mg/kg, Calier

4. RESULTS

4.1. Origin and distribution of putative cold nerve terminals in the mouse tongue

4.1.1. Populations of labeled trigeminal ganglion neurons

Neurons obtained from the trigeminal ganglia of five DiI labeled TRPM8-YFP mice were counted in tissue cultures to determine the proportions of total marked neurons. Of the total number of neurons in culture, 2.2% contained DiI indicating that their axons innervate the anterior tongue through the lingual nerve. There are around 19,000 neurons in the mouse trigeminal ganglion by the time of birth (Davies & Lumsden 1984); therefore, according to the percent of DiI labeled neurons seen in in our tissue culture experiments, there are 420 lingual TG neurons in the mouse. In culture, 6.5% of the total number of TG neurons expressed TRPM8 (YFP+) i.e. around 1240; only 0.2% of these neurons were double-labeled with DiI, which corresponds to 36 lingual nerve axons expressing TRPM8 channels (Figure 4.1).

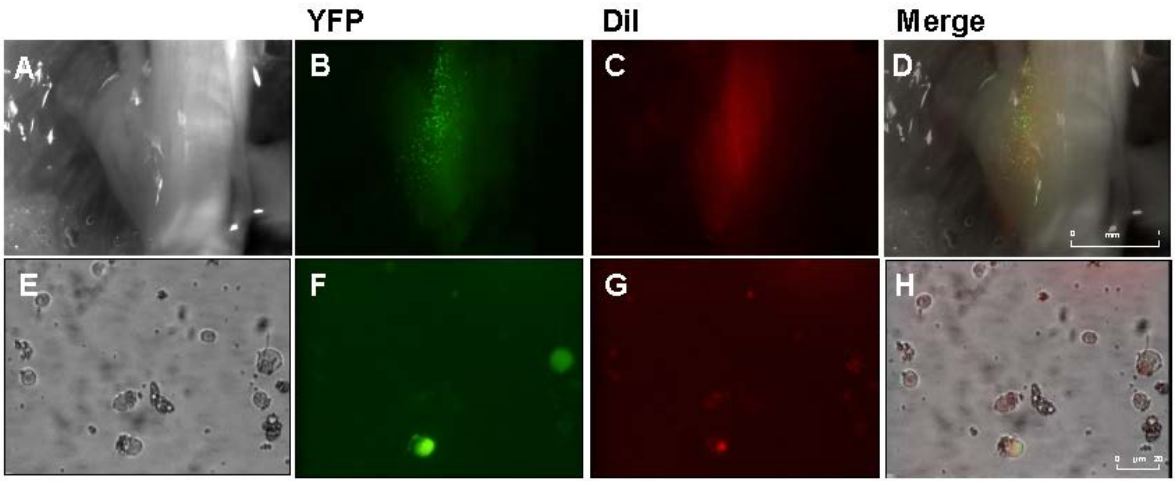

Figure 4.1. TG culture with YFP+ and DiI+ neurons. Neurons labeled in the trigeminal ganglion and in culture that contain TRPM8 (YFP+) and originating from the tongue (DiI+). (A-D) Intact left trigeminal ganglion in a TRPM8-YFP mouse and (E-H) trigeminal neurons in culture. YFP+ neurons (green) contain TRPM8 and DiI+ neurons (red) originate from the lingual nerve in the tongue.

4.1.2. TRPM8+ nerve terminal distribution in the tongue

The analysis of the tongues of ten adult male TRPM8-YFP mice from previous work done in the laboratory showed that lingual nerve terminals expressing TRPM8 channels appear as complex terminals whose parent axons ramified as they approached the epithelial surface, forming a cluster of highly branched fibers with multiple bulbar endings and usually associated to fungiform papillae (Figures 4.2-4). The TRPM8-immunoreactive nerve fiber branches reached the outer epithelial layer in each papilla, without penetrating into taste buds. Each cluster could be identified as a fluorescent point when the tongue surface was examined under low magnification with the fluorescence microscope (Figure 4.5). Clusters of terminals were more densely expressed in the tip and the middle of the tongue compared to the caudal and lateral parts (Figure 4.6). Mice had an average of 81.4 ± 4.8 TRPM8-expressing nerve terminal clusters on the surface of the tongue. Considering that only 36 trigeminal ganglion neurons innervate the lingual nerve in the tongue and express TRPM8 channels, each neuron must serve an average of 2.2 clusters of cold nerve terminals.

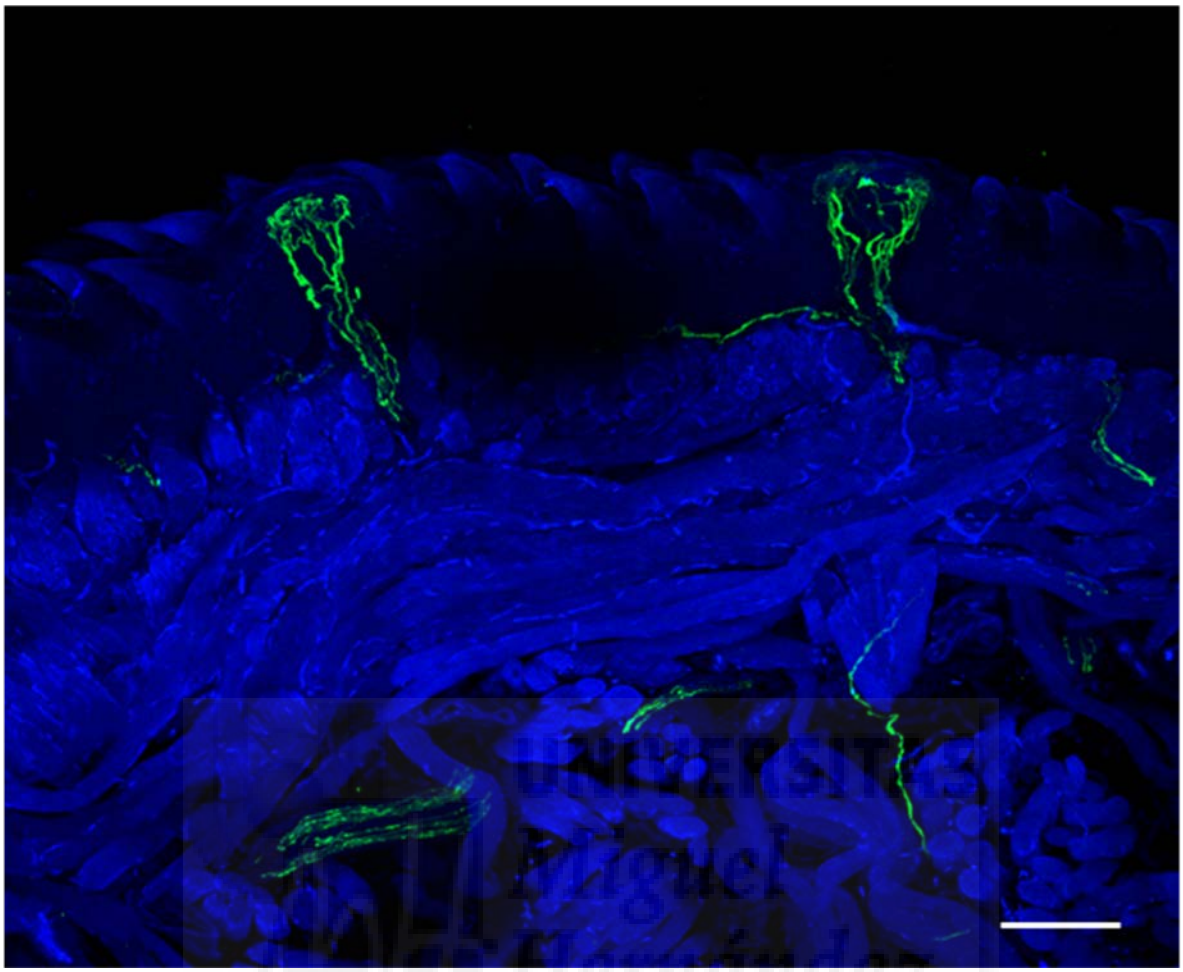

Figure 4.2. Confocal image of TRPM8 GFP+ nerve branches and terminal clusters. Terminal clusters (green) near the epithelial surface of the tongue around fungiform papillae. DAPI (blue) marks the tongue tissue. The error bar represents 50 µm.

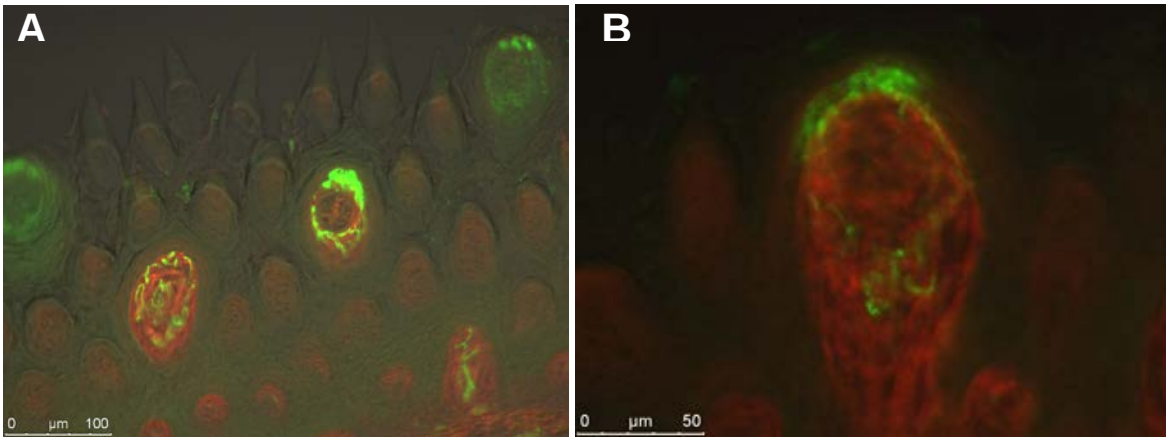

Figure 4.3. Images of taste buds on the epithelial surface of the tongue. Shows fungiform papillae (A) and an enlarged view of a single fungiform papilla (B) showing TRPM8 (green) nerve clusters in a terminal around a taste bud labeled with TROMA-1 (red).

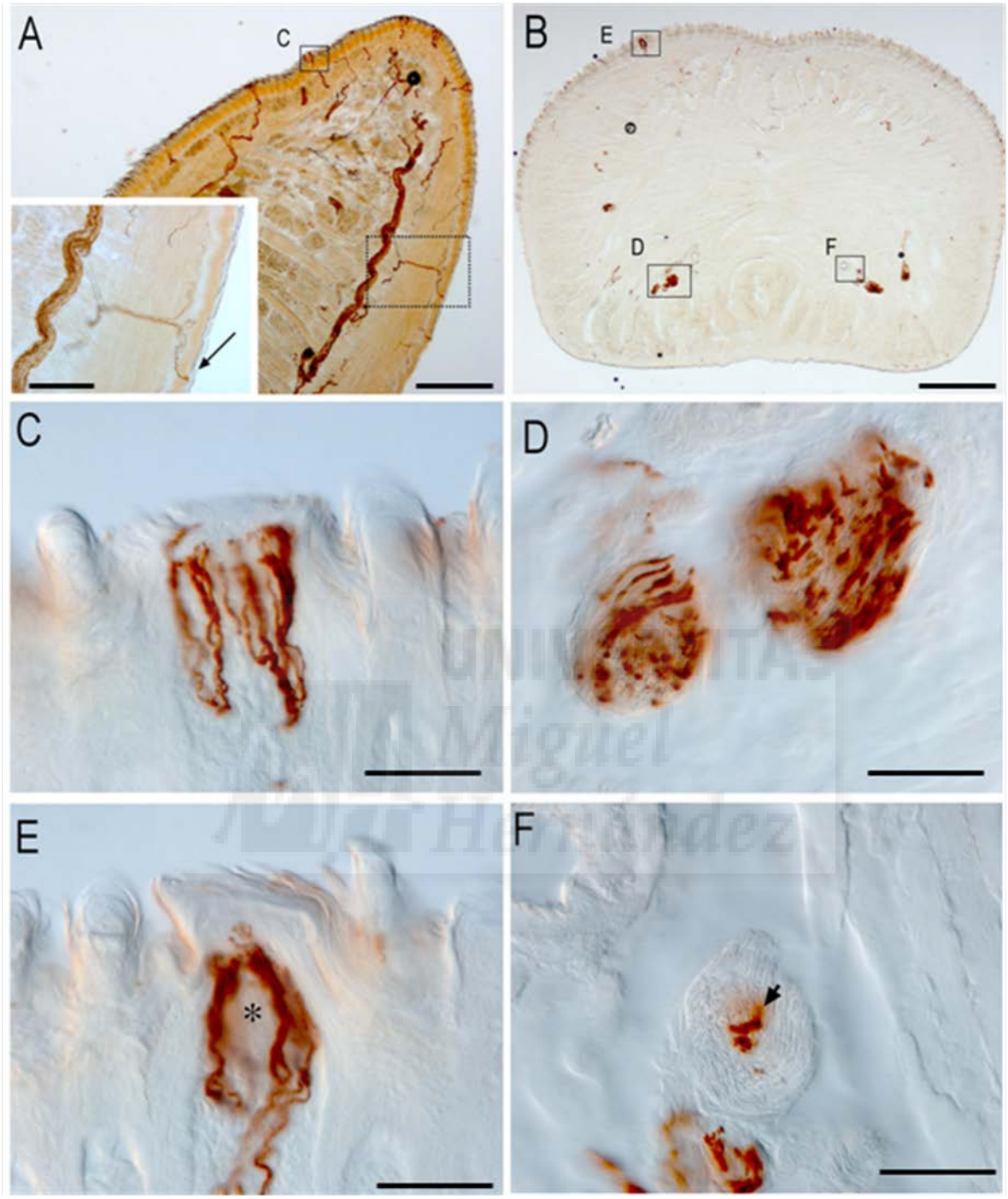

Figure 4.4. TRPM8 lingual nerve terminals labeled with DAB (red). Sagittal slice (A) and transversal slice (B) of the tongue with TRPM8+ nerve fibers. Error bars represent 500 µm. The error bar in the A insert represents 100 µm. (C) Enlarged image of a cluster of TRPM8+ nerve terminals in a cluster in a fungiform papilla in the sagittal slice. (D and F) Enlarged images from the transversal slice of the tongue of TRPM8+ lingual nerve fibers. Arrow designates a transversal slice of a TRPM8+ branch of the lingual nerve (E) Close up view of a fungiform papilla from the transversal slice. Asterisk designates the presence of a nerve terminal cluster innervating the papilla. Error bars in C-F represent 50 µm.

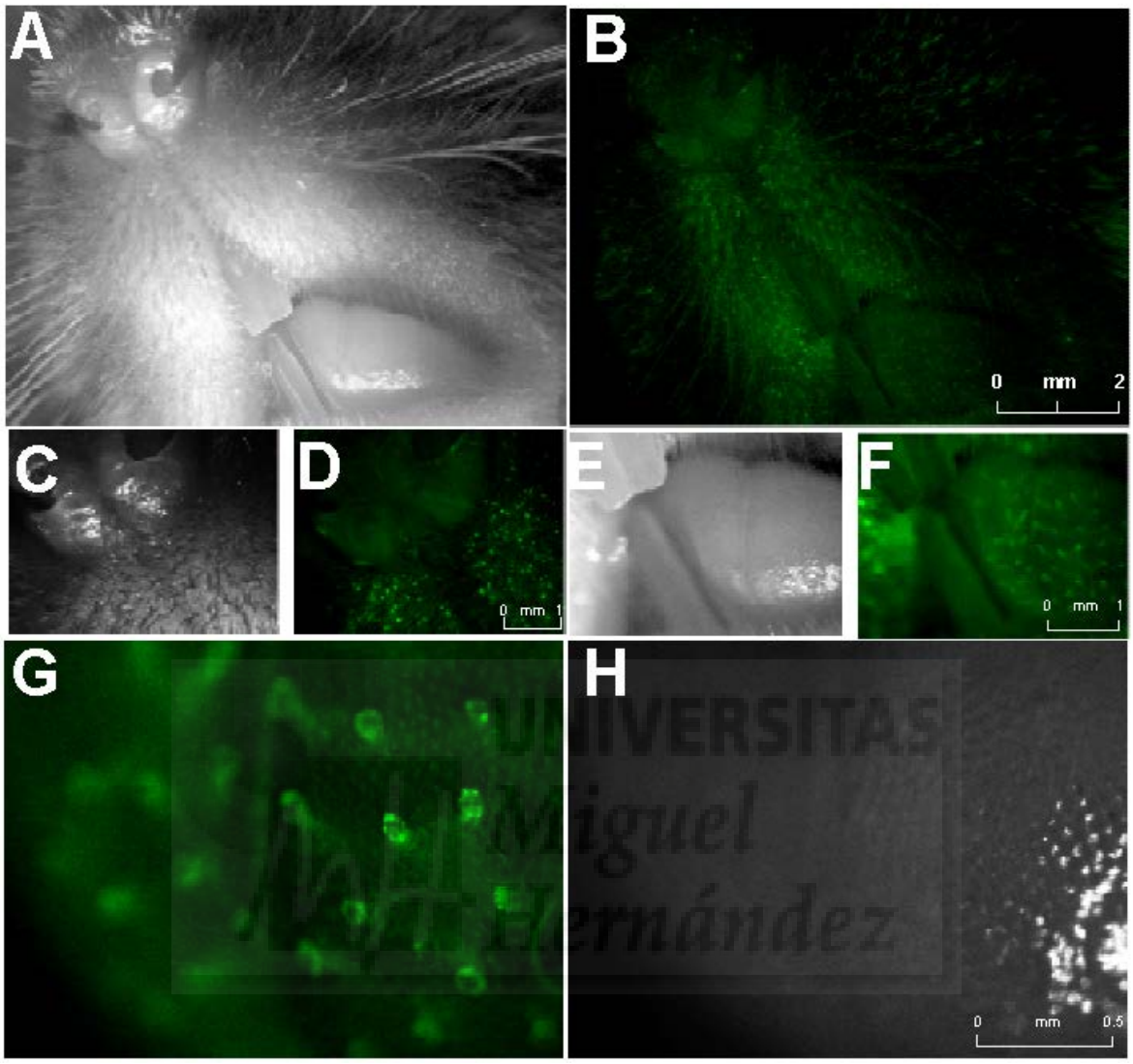

Figure 4.5. TRPM8 epidermal free nerve endings in the snout and tongue of the mouse. Images of the nose and mouth (A, B) of a mouse, with close-up images of the nose (C, D) and mouth where the teeth and tongue surface (E, F) can be seen. (G, H) Tongue surface showing clusters of terminals. Corresponding green images show the location of YFP-labeled TRPM8-containing terminals.

Terminals density was also analyzed as the total number in each mm from the tip of the tongue to the back and from the midline to each lateral side, as observed in Figure 4.6. When measuring from the tip to the back of the tongue (Figure 4.7a), the highest proportion of TRPM8-positive nerve ending clusters was found in the second mm from the tip, with an average of 16.8 ± 2.3 terminals. It was most likely higher there than in the first mm from the tip, for the shape of the tongue with less surface area at the very tip. The next highest

density was found in the third mm from the tip, with 14.9 ± 2.8 clusters of terminals. For each consecutive mm toward the back, the number of clusters of terminals decreased. When considering the number of terminals from the midline to the lateral sides (Figure 4.7b), the highest proportion of TRPM8-positive terminals clusters were found in the first mm to the right and left of the midline, with 19.3 ± 2.1 clusters and 17.3 ± 2.7 clusters of TRPM8-immunoreactive terminals. When looking at the lateral sides, the farther away from the midline, corresponded with a lower number of TRPM8-expressing nerve terminals.

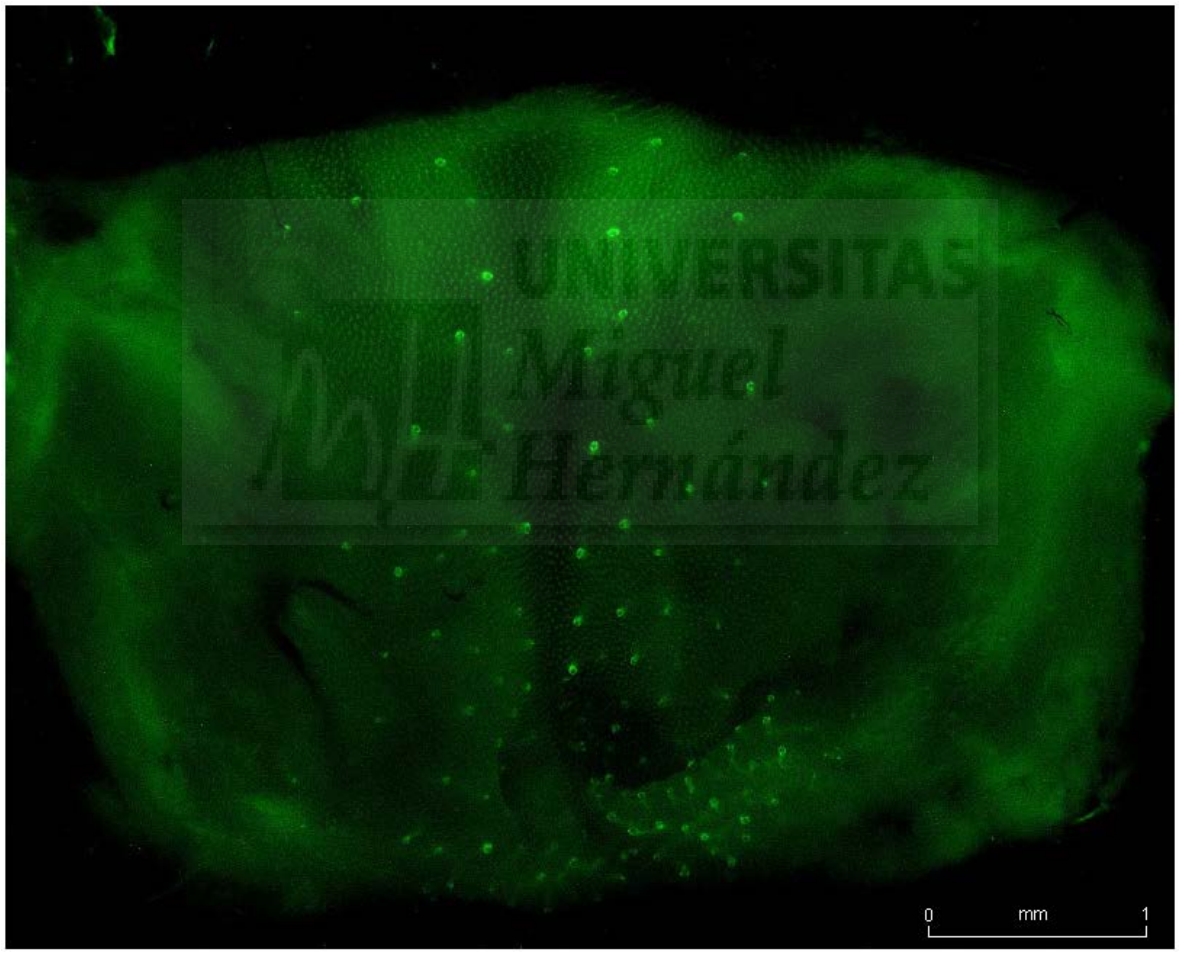

Figure 4.6. TRPM8-expressing nerve terminals on the mouse tongue. Surface of the tongue, cut along the midline of the inferior side, opened, and flattened showing a concentration of nerve terminal clusters at the tip (bottom) and along the superior midline.

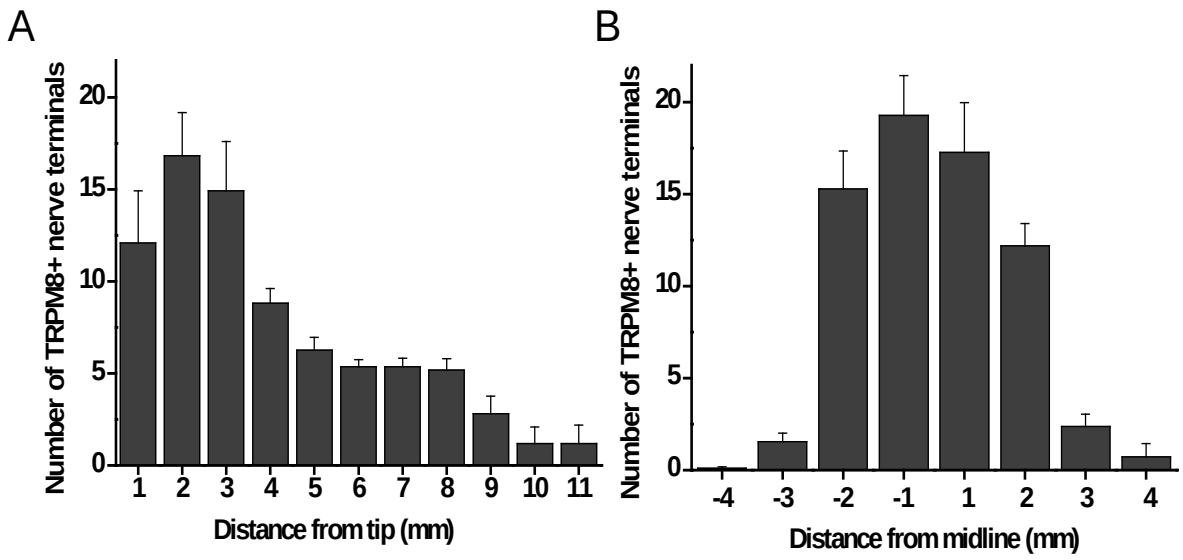

Figure 4.7. Number of TRPM8+ nerve terminals located on the surface of the mouse tongue. Graphs display the distribution of terminals from (A) the tip of the tongue to the back and from (B) the midline to the lateral sides (in mm).

4.2. Functional characteristics of cold-sensitive TG neurons innervating the tongue

4.2.1. Firing properties of cold-sensitive nerve fibers

Whole nerve activity was first recorded from the lingual nerve in wild-type (C57BL/6, TRPM8$^{+/+}$, and TRPA1$^{+/+}$) and knockout (TRPM8$^{-/-}$, TRPA1$^{-/-}$, and TRPM8$^{-/-}$/TRPA1$^{-/-}$) mice. All animal genotypes exhibited a proportion of units displaying spontaneous activity that increased upon, cooling, heating, or mechanical stimulation. Figure 4.8 shows typical responses to these three different stimuli in units recorded from wild type animals.

4.2.1.1. Wild-type mice

In wild-type mice, fibers giving a sustained impulse discharge (≥ 12 impulses) in response to a cooling pulse to 15 - 10ºC, from the adapting temperature of 35ºC were classified as 'cold-sensitive'. A total of 154 cold sensitive multi- and single-unit filaments were recorded; 94 of these units were unambiguously defined as single units. The general pattern of response to cold temperature in these units was variable. Several parameters were measured in an effort to distinguish possible functional subpopulations among cold-sensitive sensory fibers innervating the tongue. These included thermal threshold, discharge, duration, magnitude and firing pattern of the impulse discharge evoked by cooling pulses from 35ºC to 10ºC, presence of spontaneous activity at the resting temperature of 35ºC, and response to stepwise cooling.

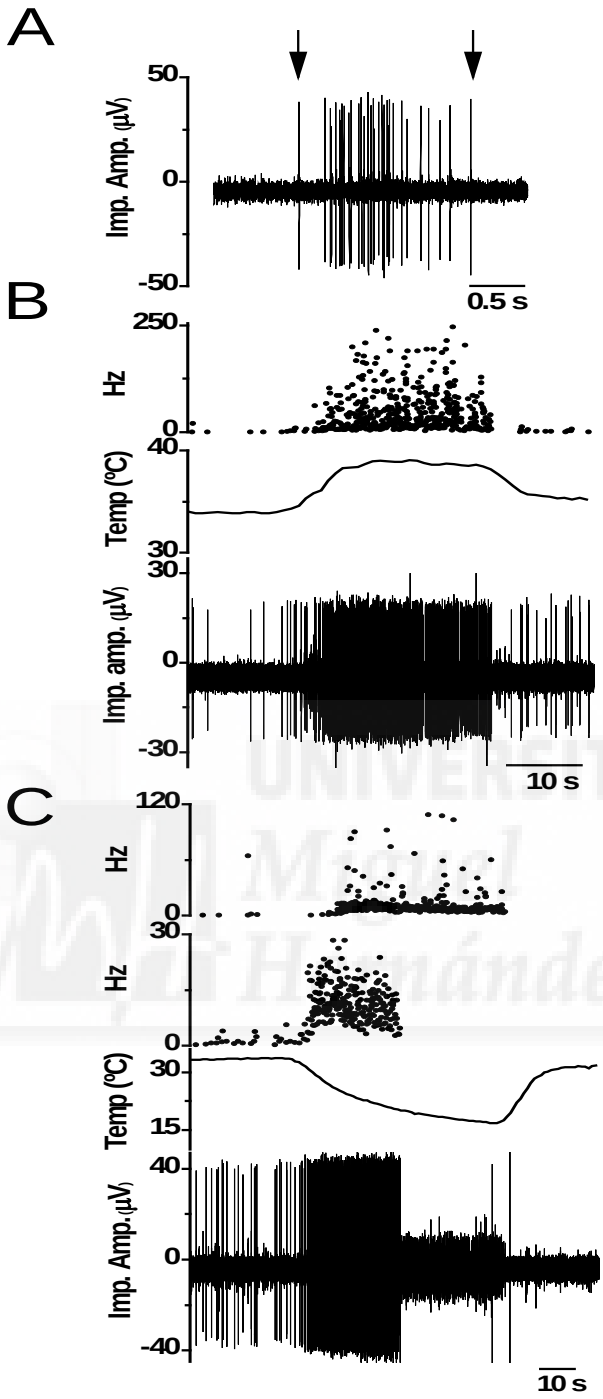

Figure 4.8. Response characteristics of WT lingual nerve fibers in the mouse tongue to stimuli of different modality. (A) Impulse discharge in a fiber sensitive to mechanical stimulation (2.65 mN). Arrows indicate the onset and end of the mechanical stimulus. (B) Impulse activity in a heat-sensitive single-unit fiber in response to a heating pulse. Traces from top to bottom: Instantaneous frequency (Hz); temperature recording of the bath solution; direct recording of impulse activity. (C) Impulse activity in two cold-sensitive single-unit fibers in response to a cooling pulse. Traces from top to bottom: Instantaneous frequency (Hz) of a HT cold-sensitive fiber; Instantaneous frequency (Hz) of a LT cold-sensitive fiber; temperature recording of the bath solution; direct recording of impulse activity.

Temperature threshold

Individual lingual fibers had different temperature activation thresholds. Based on the temperature value at which impulse firing increased significantly (see Methods), fibers were separated into low (> 29ºC) and high (≤ 29ºC) threshold groups. 29ºC was chosen in as the cutoff for the thermal threshold based on a number of common characteristics in the firing pattern of a large majority of fibers. Figure 4.9 offers an example of a recording showing two units that are recruited at different temperature values by the same cooling pulse. Of the 154 wild-type fibers sensitive to cooling that were analyzed in this study 47% were considered low threshold (LT) and 53% high threshold (HT) fibers. Of those unambiguously considered single units (n = 94) mean threshold was 26.4 ± 0.7ºC; 47% of them were LT and had an average thermal threshold of 32.4 ± 0.3ºC; 53% were HT fibers exhibiting an average thermal threshold of 20.8 ± 0.8ºC, ranging from 29.0ºC down to 8.8ºC. Figures 4.10 and 4.11A show the distributions of threshold values in the total population of single-unit fibers included in this study. As described below, the value of cold threshold was clearly associated with the presence of spontaneous activity and with the firing characteristics in response to cooling pulses of the fiber.

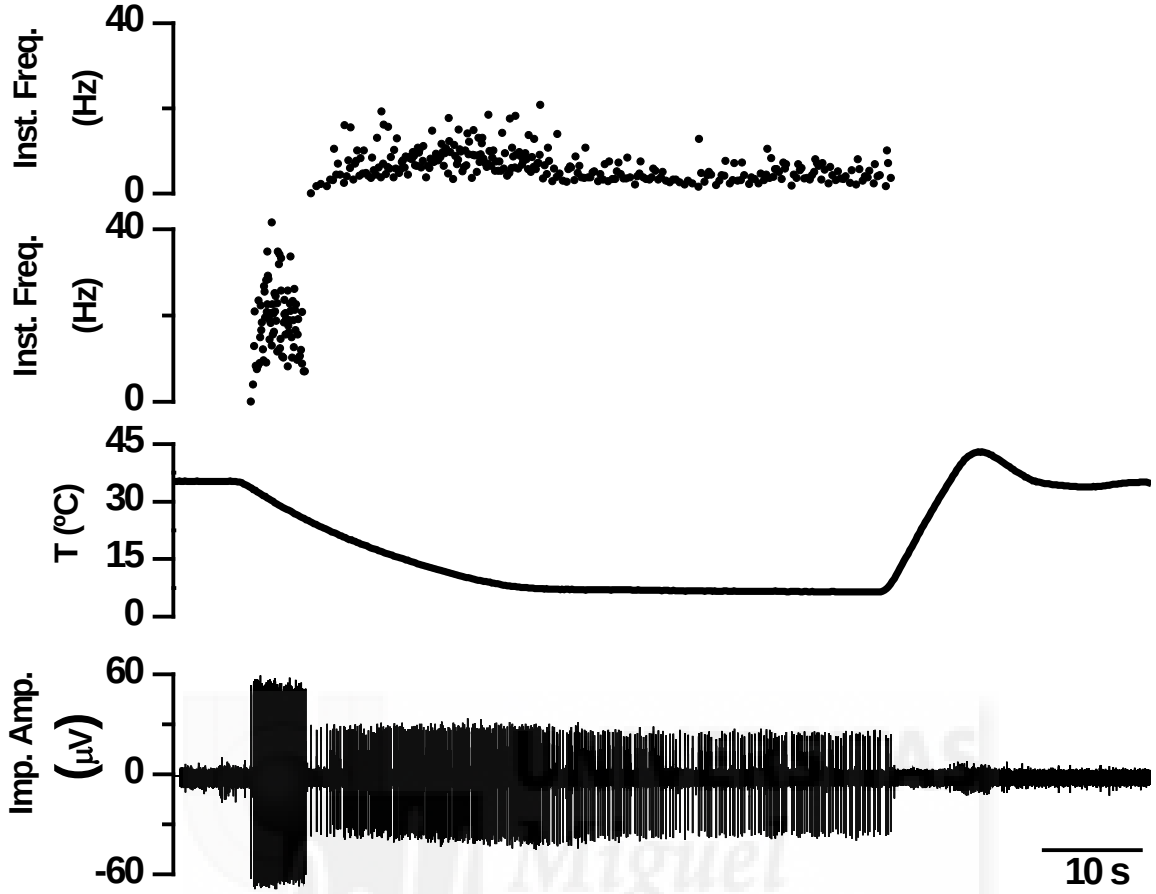

Figure 4.9. Recording of cold-sensitive lingual nerve fibers in the mouse tongue. Impulse activity in two cold-sensitive units recorded from the same filament in response to a cooling pulse. Traces from top to bottom: Instantaneous frequency (Hz) of a HT cold-sensitive fiber; Instantaneous frequency (Hz) of a LT cold-sensitive fiber; temperature recording of the bath solution; direct recording of impulse activity.

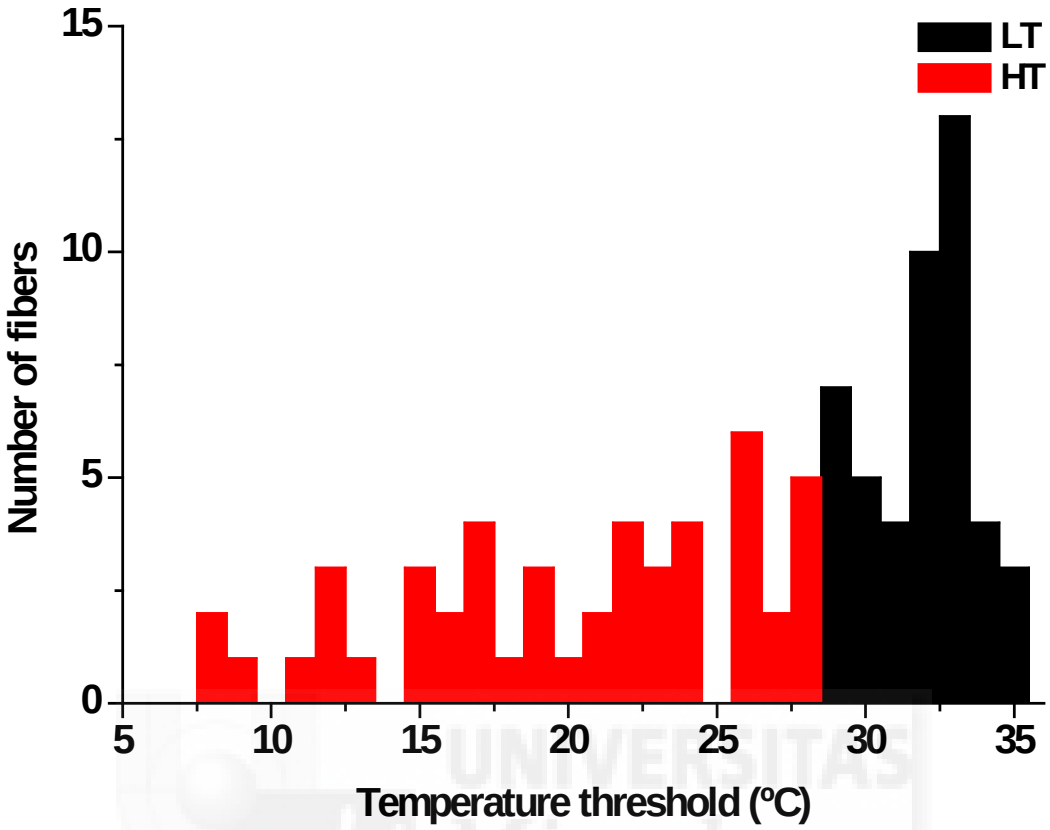

Figure 4.10. Cooling threshold distribution of WT cold-sensitive single-unit fibers. Distribution, shown as the number of fibers whose thermal threshold fell into each one degree temperature range, of the single-unit cold-sensitive fibers (n = 94). Black bars represent LT fibers and red bars represent HT fibers.

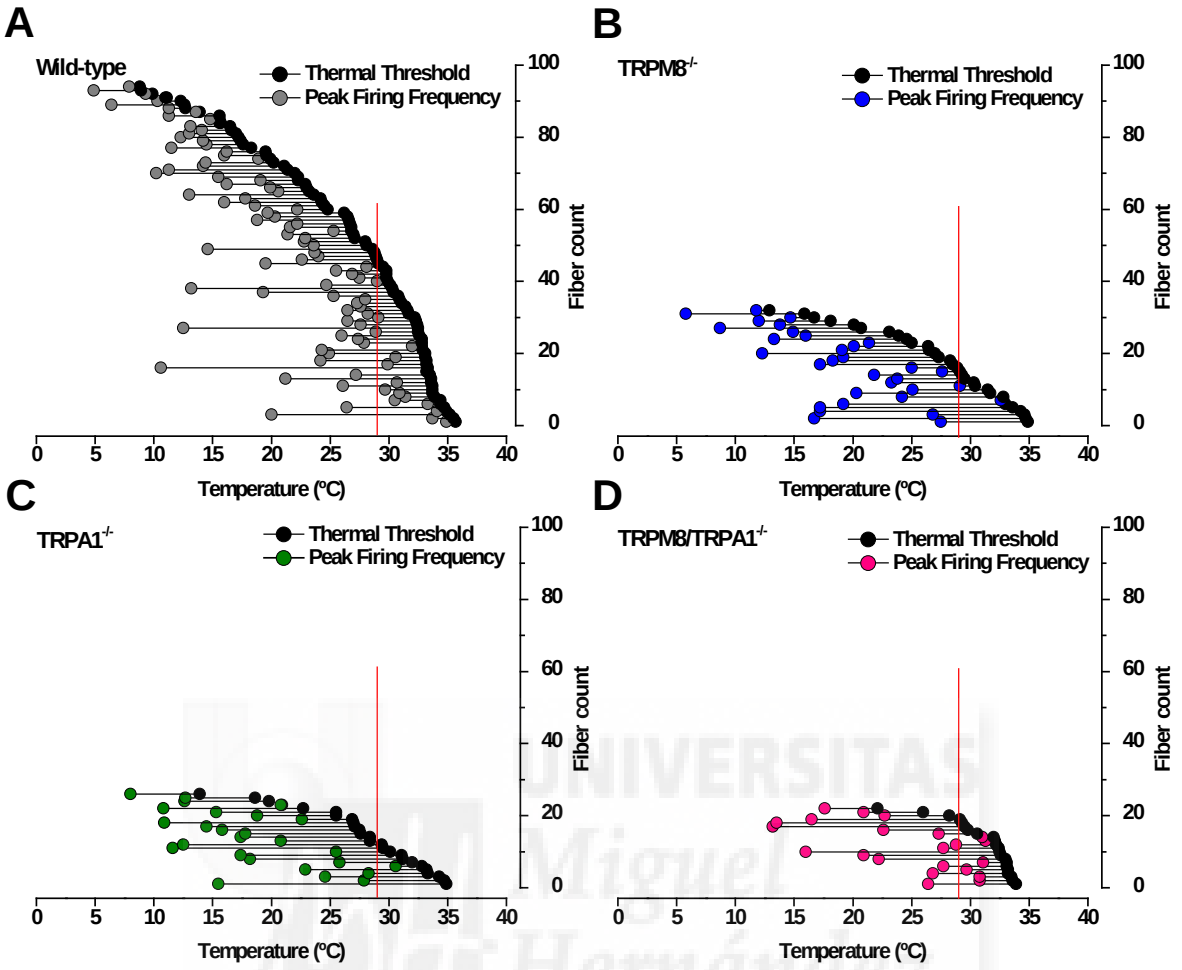

Figure 4.11. Threshold distributions in all groups of cold-sensitive fibers. Distribution of thermal thresholds of all the single-unit cold-sensitive fibers included in the study ranked from low to high threshold based on cell rank and connected by a line with their respective temperatures at peak firing frequency, for WT (A), TRPM8$^{-/-}$ (B), TRPA1$^{-/-}$ (C), and TRPM8$^{-/-}$/TRPA1$^{-/-}$ (D) single-unit cold-sensitive fibers. The red vertical line represents the division between low and high threshold at (29ºC).

Firing pattern

The sample recording shown in Figure 4.9 also evidences the striking differences in the firing pattern and duration of the responses to cold found among tongue nerve fibers responding to temperature decreases. Some fibers gave a brisk, high frequency impulse discharge when threshold was attained. This 'dynamic response' was often followed by a firing discharge ('static response') at lower frequency for variable times along the cooling pulse (Figure 4.12A, B) The contribution of the dynamic and static components to the overall response to the cooling pulse varied widely among units; in some of them the static discharge did not appear i.e. they were predominantly *phasic units* (Figure 4.12A,

large-amplitude unit) whereas others maintained a variable level of static firing even after reaching the lowest plateau temperature of the stimulating pulse and were considered *phasic + tonic units*, Figure 4.12A smaller amplitude unit and Figure 4.12B). In this last case, firing stopped abruptly when heating to recover basal temperature was initiated. Altogether, we classified these two subgroups of cold thermoreceptor fibers within the more general class of phasic-tonic cold thermoreceptor fibers. Another, functionally distinct type of unit was characterized by the development of a slow and gradual frequency increase parallel with the fall of temperature of the cooling pulse, lacking an initial phasic component. Rewarming slowly silenced this class of gradually-responding cold sensitive fibers. A typical example is the unit shown in the recording of Figure 4.12C.

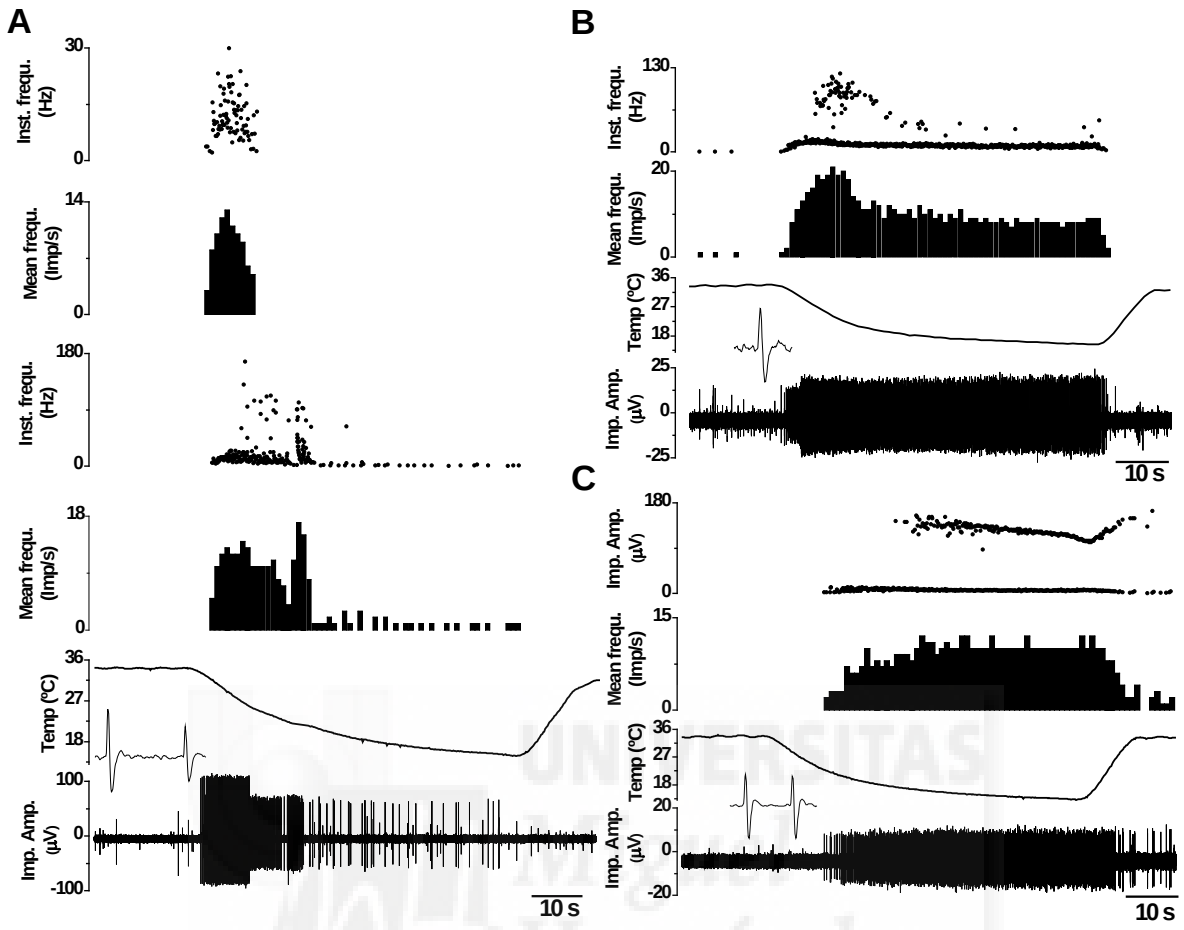

Figure 4.12. Response characteristics of WT cold-sensitive lingual nerve fibers in the mouse tongue. Impulse activity in response to a cooling pulse (A) in a recording containing two phasic-tonic cold-sensitive single-unit fibers one with a purely phasic response (*phasic fiber*) and the other with a weak tonic component of the response (*phasic + tonic fiber*). Traces from top to bottom: Instantaneous frequency (Hz) of the purely phasic fiber; Mean frequency (imp/s) of the phasic fiber; Instantaneous frequency (Hz) of the phasic + tonic fiber; Mean frequency (imp/s) of the phasic + tonic fiber; temperature recording of the bath solution and direct recording of impulse activity with an inset of an expanded view of the impulse discharge. (B) Recording of a phasic + tonic cold-sensitive fiber with a prominent tonic component. Traces from top to bottom: Instantaneous frequency (Hz); Mean frequency (imp/s); temperature recording of the bath solution; direct recording of impulse activity with an inset of an expanded view of the impulse discharge. (C) Impulse activity in a gradually-responding cold-sensitive fiber in response to a cooling pulse. Traces from top to bottom: Instantaneous frequency (Hz); Mean frequency (imp/s); temperature recording of the bath solution; direct recording of impulse activity with an inset of an expanded view of the impulse discharge.

An estimation of the incidence of each fiber class was obtained using the population of single units recorded in our experiments. 55% of them were phasic-tonic thermoreceptor fibers, with 37% responding only during the initial rapid fall of temperature of the cooling pulse (i.e., purely phasic units) and 18% exhibiting also a static component (phasic + tonic

units). Another 42% of the units corresponded to the distinct class of fibers characterized by their gradual response to the cooling pulse, the gradually-responding cold-sensitive fibers. Finally, 3% of the total number of cold fibers exhibited an erratic or irregular response to cooling and were not included in either group.

Among the two general classes of cold-sensitive fibers, phasic-tonic thermoreceptor fibers had a significantly lower threshold (30.1 ± 0.7 ºC) than the gradually-responding cold-sensitive fibers (21.4 ± 1.1ºC) ($p < 0.001$). Also, within the class of phasic-tonic fibers, threshold in the subgroup of purely phasic units was higher (29.4 ± 0.9ºC), though not significantly, than in units also responding tonically (31.6 ± 0.7ºC). Hence, the majority of phasic-tonic fibers belonged to the LT group (66% purely phasic and 82% of the phasic + tonic fibers), while most (85%) of the class of fibers responding gradually to cold were HT fibers.

Spontaneous activity

Twenty-six (28%) of the 94 total single units responding to cold had spontaneous activity at 35ºC (> 1 discharge in 10 s). This activity was usually composed of single nerve impulses fired more or less regularly (beating pattern) although in some fibers, impulses occurred in groups of two or more followed by a silent period (bursting pattern).

Of the two classes of cold-sensitive fibers distinguished according to their firing pattern, the highest incidence of spontaneous activity (38%) was found among the population of phasic-tonic thermoreceptor fibers, with a mean firing frequency of 1.1 ± 0.3 imp/s. Incidence of spontaneous activity and mean firing frequency values in the fiber subtypes within this class (purely phasic and phasic + tonic) were very similar to the values of the entire population. Altogether, phasic-tonic cold thermoreceptor units included in the LT group (> 29ºC) displayed spontaneous activity of a significantly higher mean frequency (1.4 ± 1.5 imp/s) than HT (≤ 29ºC) units (0.3 ± 0.2 imp/s; $p = 0.032$).

In the class of gradually responding cold-sensitive fibers, the incidence of spontaneous activity was comparatively low (10%). Moreover, spontaneously active fibers also exhibited a low firing rate (0.4 ± 0.2 imp/s). Again, in this class of cold-sensitive fibers, the incidence of the spontaneous activity was associated to their thermal threshold: LT fibers displayed a higher incidence of spontaneous activity (3/6) than HT fibers (1/33).

Considering the population of all cold-sensitive units showing spontaneous activity at 36ºC jointly, the mean firing frequency was 1.2 ± 0.4 imp/s. When cold sensitive fibers were grouped based on their thermal threshold, a higher percentage of LT cold-sensitive fibers (44%) exhibited spontaneous activity, at a higher mean firing frequency (1.8 ± 0.5 imp/s) than HT cold fibers, among which only 14% displayed ongoing activity at a significantly lower mean firing frequency (0.4 ± 0.1 imp/s, p = 0.041).

Response to cooling pulses

Bursting

During the cooling pulse a fraction of the fibers (22%) developed a bursting pattern of activity that evolved into a beating pattern at the plateau of the cooling pulse as is evidenced in the instantaneous frequency traces of Figures 4.12 and 4.13. 17% of the phasic-tonic fibers responded in bursts, which was only 9% of the purely phasic fibers and 35% of the phasic + tonic fibers. 32% of the gradually-responding cold-sensitive fibers showed bursting activity during cooling.

The change in firing pattern from beating to bursting is reflected in the distribution of interval durations between successive nerve impulses. Histograms of the impulse discharge evoked by the temperature change of the cooling pulse (Figure 4.14) evidence two clear distinct peaks of interval duration, corresponding to the short time intervals between the impulses within a burst, and the longer time intervals between the last impulse of a burst and the first impulse of the next (Figure 4.14A, B). In general, a beating pattern was evoked by the cooling pulse during the initial firing phase, which transitioned into a bursting pattern. In the purely phasic fibers this bursting again transitioned to beating during the final part of the cooling pulse where interval durations are close together, evidencing a rather regular firing pattern (Figure 4.14A). However, in the phasic + tonic and gradually-responding fibers, the bursting pattern generally remained through the entire cooling response (Figure 4.14B, C). The time course of the appearance of a bursting pattern in the impulse firing during cooling pulses is also apparent in the representation of instantaneous frequency values shown in the examples on the right in Figure 4.14. Difference in the bursting parameters for the different functional types of fibers can be found in Table 4.1.

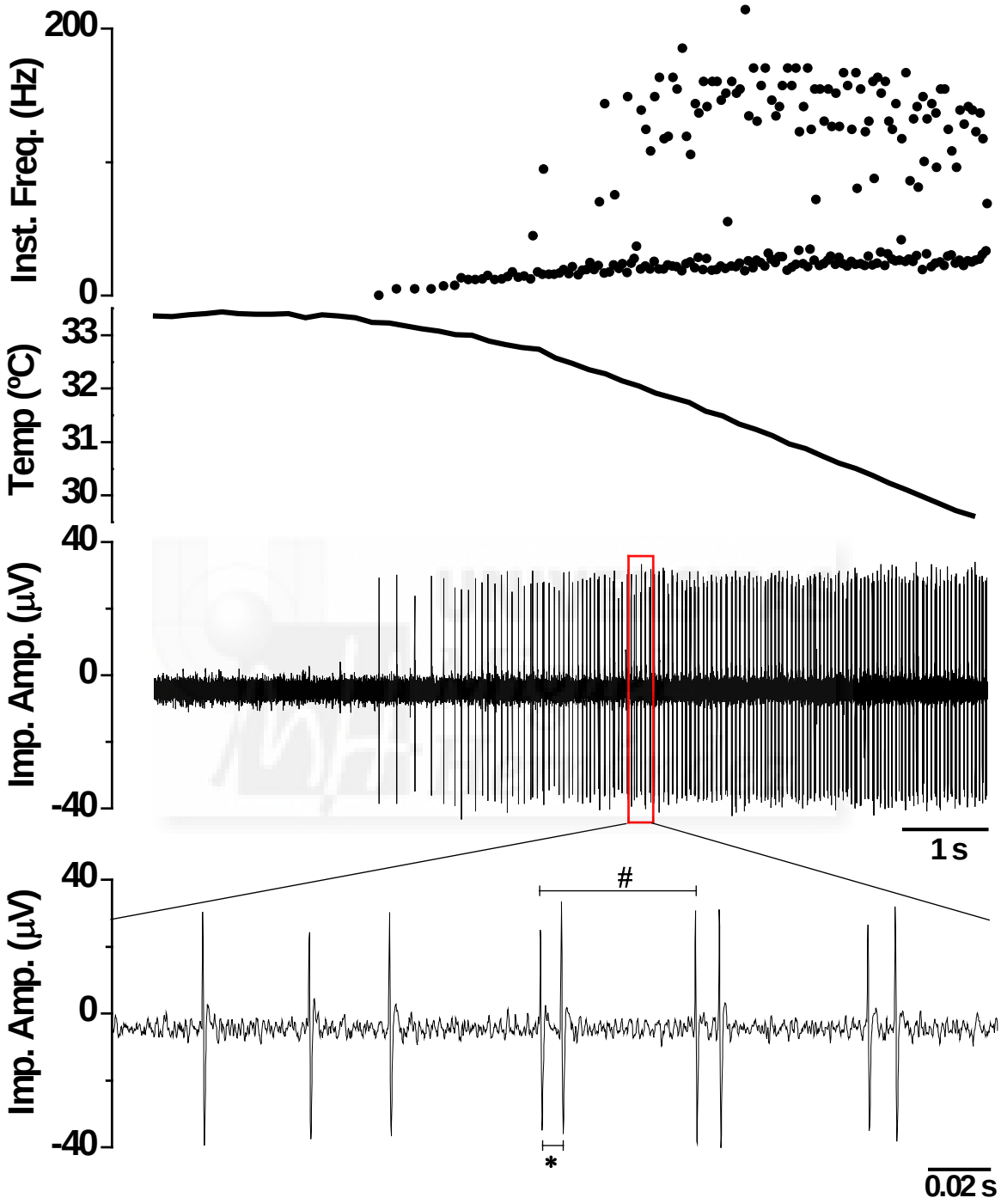

Figure 4.13. Change in firing pattern of a WT cold-sensitive fiber. Response of a LT purely phasic fiber where the temperature change initially evokes a beating firing pattern which gradually changes to a bursting pattern as the temperature decreases. Traces from top to bottom: Instantaneous frequency (Hz); temperature recording of the bath solution; direct recording of impulse activity. The red box indicates where an expanded view of the impulse discharge showing the beating to bursting pattern change can be observed. The asterisk (*) indicates the time period for the interspike interval (ISI), and the pound sign (#) indicates the cycle time.

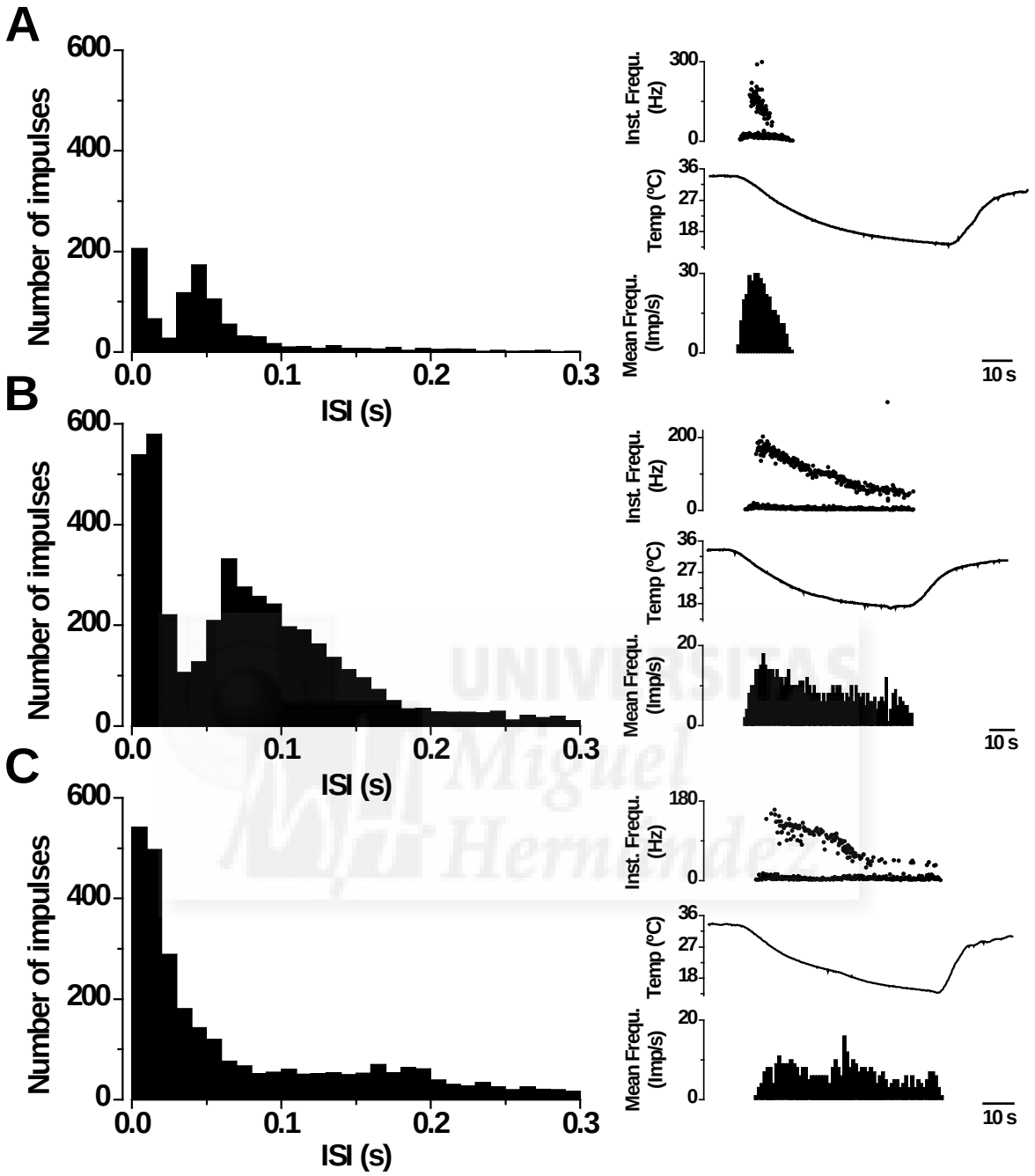

Figure 4.14. Changes in ISI firing pattern of WT cold-sensitive fibers during a cooling pulse. (A) Distribution of ISIs during a cooling pulse (left) for those purely phasic fibers with bursting activity, n = 3. An example of a purely phasic responding in bursts (right); traces from top to bottom: Instantaneous frequency (Hz), temperature of the bath solution, mean frequency (imp/s). (B) Distribution of ISIs during a cooling pulse (left) for the phasic + tonic fibers with bursting activity, n = 6. An example of a phasic + tonic fiber responding in bursts (right); traces from top to bottom: Instantaneous frequency (Hz), temperature of the bath solution, mean frequency (imp/s). (C) Distribution of ISIs during a cooling pulse (left) for those gradually-responding fibers with bursting activity, n = 11. An example of a gradually-responding fiber responding in bursts (right); traces from top to bottom: Instantaneous frequency (Hz), temperature of the bath solution, mean frequency (imp/s).

Class	ISI (ms)	Number of bursts/cooling pulse	Bursting pattern (%)	Cycle time (ms)	Impulses/ burst
Phasic-tonic					
Purely phasic	58.6 ± 2.5	88 ± 35.8	59	85.5 ± 3.3	2.1 ± 0.02
Phasic + tonic	96.6 ± 1.9	167.5 ± 45.8	54	139.1 ± 2.4	2.3 ± 0.05
Gradually-responding	156.4 ± 5.2	85.4 ± 27.4	68	259.6 ± 8.0	2.4 ± 0.03

Table 4.1. Cooling-induced changes in impulse firing pattern in WT mice. Data obtained from the 3 purely phasic, 6 phasic + tonic, and 11 gradually-responding cold-sensitive fibers with bursting activity. For each fiber, interspike interval (ISI), number of bursts per cooling cycle, percent of fibers firing with a bursting pattern, time between the onset of successive bursts (cycle time), and the mean number of impulses per burst were obtained during a cooling pulse. Data are mean ± SEM.

Firing frequency

The mean firing frequency of the entire population of single-unit cold-sensitive fibers during the 60 s cooling pulse was 3.6 ± 0.4 imp/s. When classified according to their cooling threshold, mean firing rate of the response for LT fibers (5.3 ± 0.7 imp/s) was significantly higher than that of HT fibers (2.1 ± 0.2 imp/s; $p = 0.001$). Bursting activity during cooling pulses was present in 20% of LT and 22% of HT fibers.

Mean impulse firing frequency was found to be the highest in the phasic-tonic thermoreceptor fibers with a mean rate during the complete duration of the cooling pulse of 6.7 ± 1.2 imp/s (excluding the group of purely phasic units that silenced when the cooling rate of temperature decrease falls). The gradually-responding cold sensitive fibers fired at a significantly lower average frequency (2.9 ± 0.6 imp/s; $p < 0.001$). Again, in each group LT fibers had the highest firing rate, first being the LT gradually-responding cold-sensitive fibers (7.9 ± 2.8 imp/s) and then the LT phasic + tonic cold-sensitive fibers (7.3 ± 1.4 imp/s).

The dynamic components of cold-evoked impulse activity in cold-sensitive fibers were evaluated measuring different parameters. The 'peak firing frequency' was first measured,

i.e. the maximal firing frequency/s value attained during the cooling pulse, and the 'temperature of peak firing frequency' which is the temperature value at which this maximal firing was attained. Among the whole population of cold-sensitive fibers there was a significant difference between the peak frequency of the LT (21.7 ± 1.9 imp/s) and HT (8.9 ± 0.7 imp/s, $p < 0.001$) groups as shown in Figure 4.15A. As expected, the population of phasic-tonic fibers that have lower thresholds also exhibit the highest peak frequency values (Figure 4.15B). The peak frequency value in the phasic-tonic thermoreceptors, 19.6 ± 1.6 imp/s, (17.7 ± 1.8 imp/s in the purely phasic and 23.4 ± 3.1 imp/s for phasic + tonic fibers) was also significantly higher than in gradually-responding fibers (8.7 ± 1.2 imp/s, $p < 0.001$). This is also true for the cooling threshold temperature required to reach peak frequency. Phasic--tonic thermoreceptors reached their peak firing during their cooling cycle at warmer temperatures (24.6 ± 1.1ºC for purely phasic, 27.3 ± 1.0ºC for phasic + tonic fibers) than gradually-responding cold-sensitive fibers (15.3 ± 0.9ºC), differences being significant ($p < 0.001$).

Figure 4.15C, D depicts the firing frequency change during the temperature fall taking place from the threshold temperature until the peak frequency was reached in all the fibers recorded. The slope of these lines provides a quantitative estimation of the sensitivity of the fibers and their ability to encode the dynamics of the temperature change. Average values of the slopes were significantly different based on thermal threshold: 6.2 ± 1.3 imp/s/ºC (LT) and 2.1 ± 0.4 imp/s/ºC (HT, $p = 0.001$). Based on firing pattern the average slope values were 4.7 ± 0.9 imp/s/ºC (purely phasic), 9.9 ± 4.3 imp/s/ºC (phasic + tonic), and 2.1 ± 0.5 imp/s/ºC (gradually-responding). The slopes of both the purely phasic and the phasic + tonic fibers were significantly greater than that of the gradually-responding fibers ($p = 0.001$). The data presented in the figure illustrate and confirm that low-threshold fibers are able to encode small changes in temperature with an increase in firing frequency, and that this capability is particularly associated to the phasic-tonic class of cold-thermosensitive fibers. A review of the firing properties of the different classes of WT cold-sensitive fibers can be found in Table 4.2.

In the phasic-tonic class of cold thermoreceptor fibers, cooling responses were also measured in terms of the mean firing frequency reached between the first and last action potential of the firing discharge given by that unit during the cooling pulse. When the

mean firing frequency values of the cold-evoked discharge were measured during this firing period, purely phasic fibers with their typical short, robust firing pattern exhibited the highest mean frequency value, 10.0 ± 1.2 imp/s, followed by the phasic + tonic group with an average frequency of 7.6 ± 1.0 imp/s. As could be expected, gradually-responding cold-sensitive fibers showed the lowest mean rate of firing between the first and the last nerve impulse of their response (3.6 ± 0.4 imp/s). Again, LT fibers within each respective group had higher frequency values than did the HT fibers within the same group.

As was evident in the sample records presented in Figure 4.12, cold-sensitive fibers in general tend to reduce or stop their firing rate near the end of the cooling pulse. Taken together, LT fibers were more likely to silence before the end of the cooling pulse, as was found in 73% of LT fibers when the pulse reached an average temperature of 19.8 ± 1.1ºC. Within the class of phasic-tonic cold thermoreceptor fibers, purely phasic units already silenced at a mean temperature of 19.5 ± 1.1ºC while among the phasic + tonic units, with a more prolonged discharge, 65% silenced when the cooling pulse reached a mean temperature of 14.4 ± 1.1ºC. In the phasic-tonic class as a whole, 88% silenced during cooling at a mean temperature of 18.2 ± 0.9ºC. The remaining 12% of fibers continued firing throughout the complete duration of the cooling pulse, silencing during rewarming when a mean temperature of 16.1 ± 0.5ºC was reached.

In contrast, only 41% of the gradually-responding cold-sensitive fibers silenced during the cooling pulse, at a mean temperature of 9.6 ± 1.1ºC, significantly lower ($p < 0.001$) than that for the phasic-tonic fibers. 49% of gradually-responding cold-sensitive fibers fired continuously during the cooling pulse and silenced during rewarming at a mean temperature of 21.0 ± 1.6ºC. The remaining 10% of fibers that did not silence during cooling or rewarming returned to their previous spontaneous firing rate at 36ºC

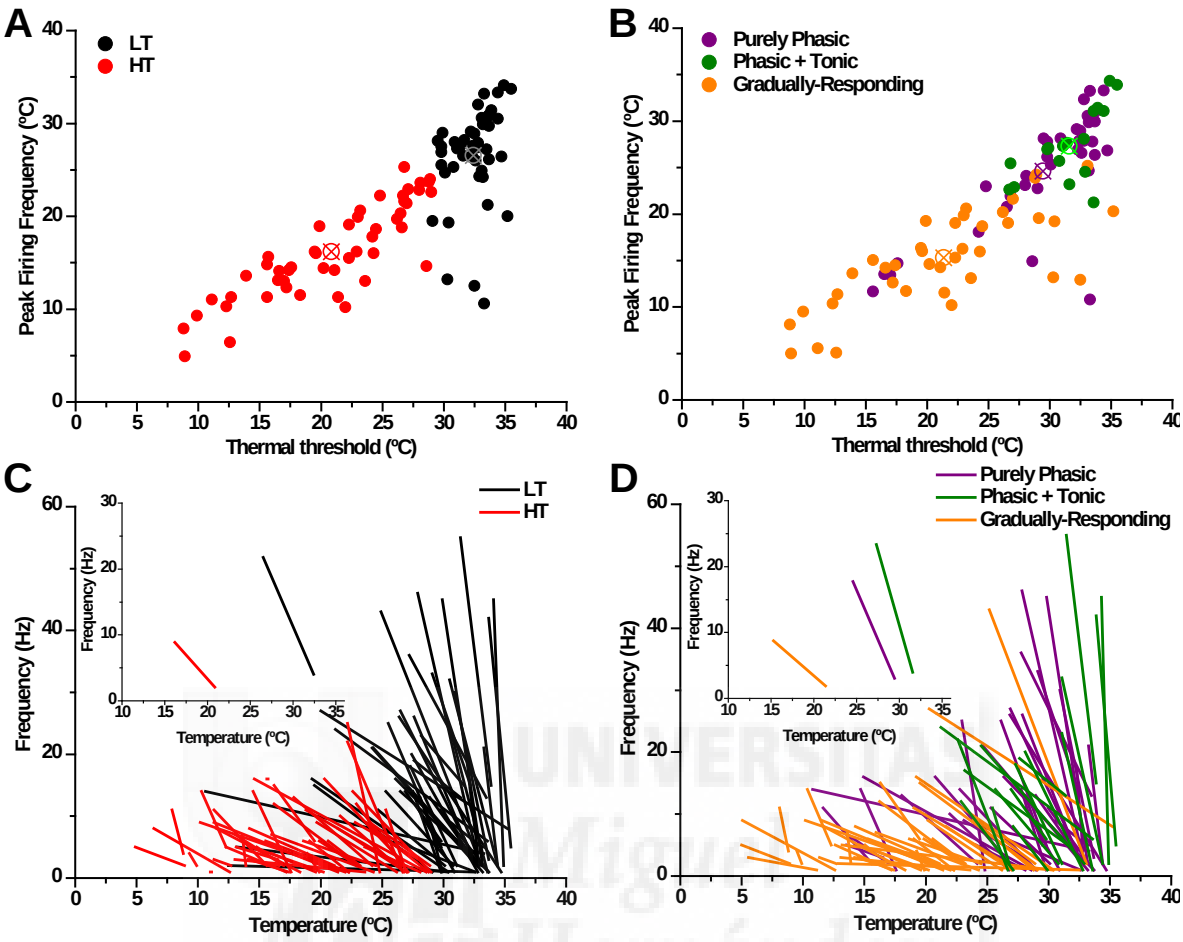

Figure 4.15. Distribution of WT cold-sensitive fiber responses to a cooling pulse. Distribution of thermal threshold versus the peak firing frequency for LT and HT fibers (A) and purely phasic, phasic + tonic, and gradually-responding fibers (B). Each dot represents an individual fiber. Average values are represented with an X symbol. Change in the mean impulse firing frequency versus temperature, plotted from the thermal threshold to the temperature of peak firing frequency was reached, separated based on thermal threshold (C) and firing pattern (D). The insets represent the average values for the LT and HT fibers (C) and the purely phasic, phasic + tonic, and gradually-responding fibers (D).

Class	Threshold (ºC)	Spont. Activity (Imp/s)	Mean Firing Frequency (Imp/s)	Peak Firing Frequency (ºC)	Duration to Peak Frequency (s)	Bursting (%)
Phasic-tonic						
Purely Phasic (n = 35)	29.4 ± 0.9	1.0 ± 0.4	2.7 ± 0.4	24.6 ± 1.1	6.8 ± 0.7	9%
Phasic + Tonic (n = 17)	31.6 ± 0.7	1.2 ± 0.3	6.7 ± 1.2	27.3 ± 1.0	7.6 ± 0.9	35%
Gradually-responding (n = 39)	21.4 ± 1.1	0.4 ± 0.2	2.9 ± 0.6	15.3 ± 0.8	18.3 ± 3.0	28%

Table 4.2. Functional properties of the different classes of WT cold-sensitive fibers. Average values of the main parameters associated to cooling of all WT single-unit cold-sensitive fibers studied are included. Values are represented as mean ± SEM.

Response to stepwise cooling

Successive temperature steps of 4 - 5ºC were performed from 34 - 35ºC down to 10ºC in 23 filaments of the lingual nerve of WT mice. All have been treated and measured as single-unit recordings, although the possibility that there was more than one unit in some of these recordings cannot be fully excluded. For the analysis of the cooling steps, the first 30 s after the onset of the temperature change was considered the dynamic part of the response and the last 30 s when temperature was stable, the static part of the response to the step (see Figure 4.16). The firing frequency of the ongoing activity at 35ºC was taken as the first value of static frequency at that temperature. Five temperature steps were then applied and mean frequency values during the dynamic and static responses to each step were measured.

Eighteen cold-sensitive units were classified as phasic-tonic or gradually-responding based on their response to rapid cooling pulses applied previously to the onset of the cooling steps. Ten were distinguished as phasic-tonic cold thermoreceptors (seven purely phasic and three phasic + tonic) and eight as gradually-responding cold-sensitive fibers. In five fibers, no previous cooling pulse was applied; however, based on the characteristics of their

impulse firing in response to the stepwise cooling (see below), three could tentatively be classified as phasic + tonic thermoreceptor units and two as gradually-responding units.

A typical example of the firing patterns obtained with stepwise cooling can be found in Figure 4.16. None of the phasic-tonic fibers however, could be defined as purely phasic based on their response to the cooling steps, as all of them maintained some impulse activity during the static portion of the step.

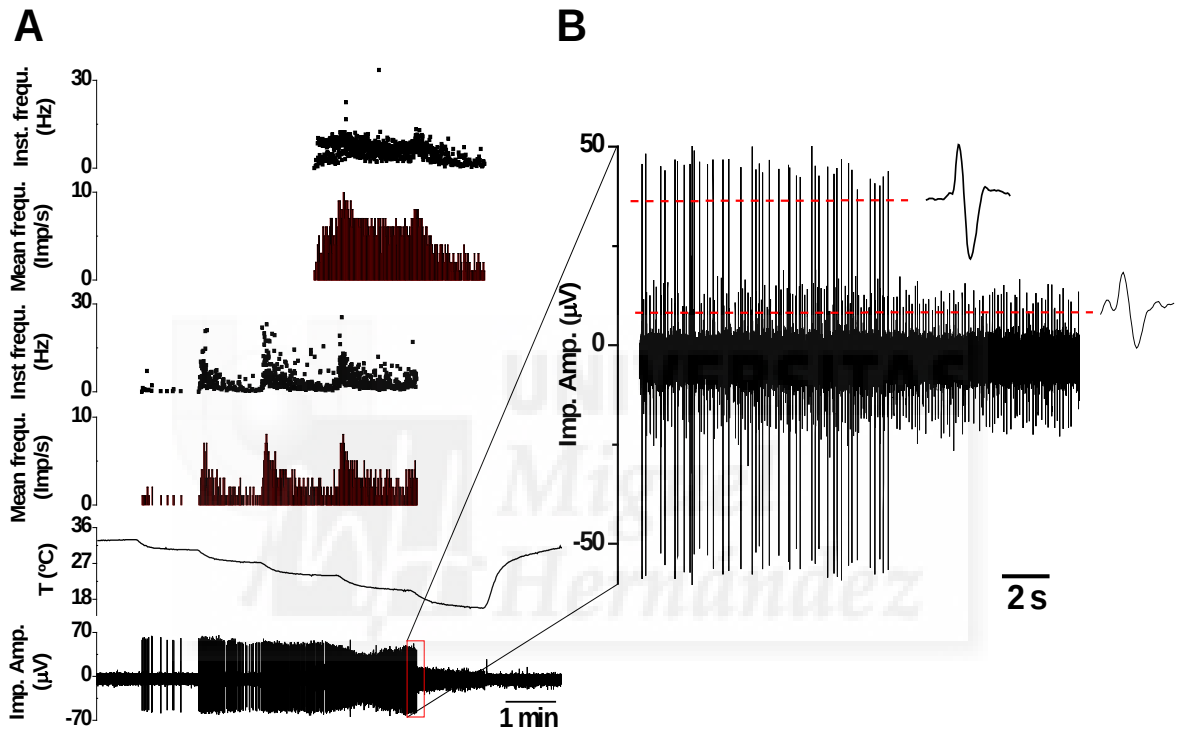

Figure 4.16. Response of cold fibers to stepwise cooling. Recording was performed in a filament containing two cold-sensitive nerve fibers of the WT mice tongue to stepwise cooling. (A) Traces from top to bottom: instantaneous frequency (Hz) of an HT gradually-responding fiber; mean firing rate (imp/s) of the HT gradually-responding fiber; instantaneous frequency (Hz) of a LT phasic + tonic fiber; mean firing frequency (imp/s) of the LT phasic + tonic fiber; temperature of the bath solution; and the direct recording of impulse activity. (B) Expanded recording of the indicated area in red showing the larger LT and smaller HT fiber. Red dotted lines indicate the impulse amplitude threshold used for unit discrimination.

In the 13 fibers classified as phasic-tonic, the impulse response evoked by the cooling step consisted in a brisk discharge of nerve impulses, reaching a peak and then decreasing exponentially during the dynamic portion of the cooling step to reach a lower frequency, stable firing during the second, static portion of the step (Figure 4.16A).

The mean firing frequency (imp/s) values during both the dynamic and the static portion of the cooling pulse were higher with successive temperature steps, reaching a peak value and then decreasing when steps to lower temperatures were applied (Figure 4.16). This is illustrated in the stimulus-response curve shown in Figure 4.17A, built with the data of all the phasic-tonic fibers together. It shows that the highest firing frequency was found in the second cooling step for the static portion and in the third cooling step for the dynamic portion. In the second step, with a mean static temperature of 26.5 ± 0.5ºC, the mean firing frequency was 6.0 ± 1.5 imp/s, not significantly different from the dynamic mean firing frequency (6.9 ± 1.9 imp/s). In the third step, at a mean static temperature of 23.1 ± 0.6ºC the mean firing frequency during the dynamic phase was 8.0 ± 1.5 imp/s, significantly higher than in the static phase, 5.5 ± 1.4 imp/s ($p = 0.037$). In the last two steps there were also significant differences between firing frequency during the dynamic and static phases of the steps. In the fourth step, from 23.1 ± 0.6ºC to 18.4 ± 0.7ºC, the mean frequency during the dynamic response was 5.7 ± 1.8 imp/s, and during the static response 3.9 ± 1.5 imp/s ($p = 0.001$). In the final step, from 18.4 ± 0.7ºC to 12.9 ± 0.9ºC, mean firing frequencies were 3.1 ± 1.0 imp/s (dynamic) and 1.8 ± 0.8 imp/s (static, $p = 0.003$). By the time the static phase of the fourth step was reached, three of the 13 fibers had silenced their impulse activity, and by the fifth step a total of five fibers had silenced.

For the 10 fibers previously identified as having a gradually-responding response to cold, the activity in the dynamic and static phases of the cooling steps had a much different trend than the phasic-tonic fibers (Figure 4.16A). The peak firing frequency was found in the fourth step with very similar dynamic and static activity, 5.0 ± 1.5 imp/s and 4.8 ± 1.6 imp/s, respectively (Figure 4.17B). The final step (with a total mean temperature of 13.8 ± 1.5ºC), showed the only significant difference in the mean firing frequency between the dynamic, 4.7 ± 1.4 imp/s, and the static, 2.1 ± 0.9 imp/s phases ($p = 0.004$).

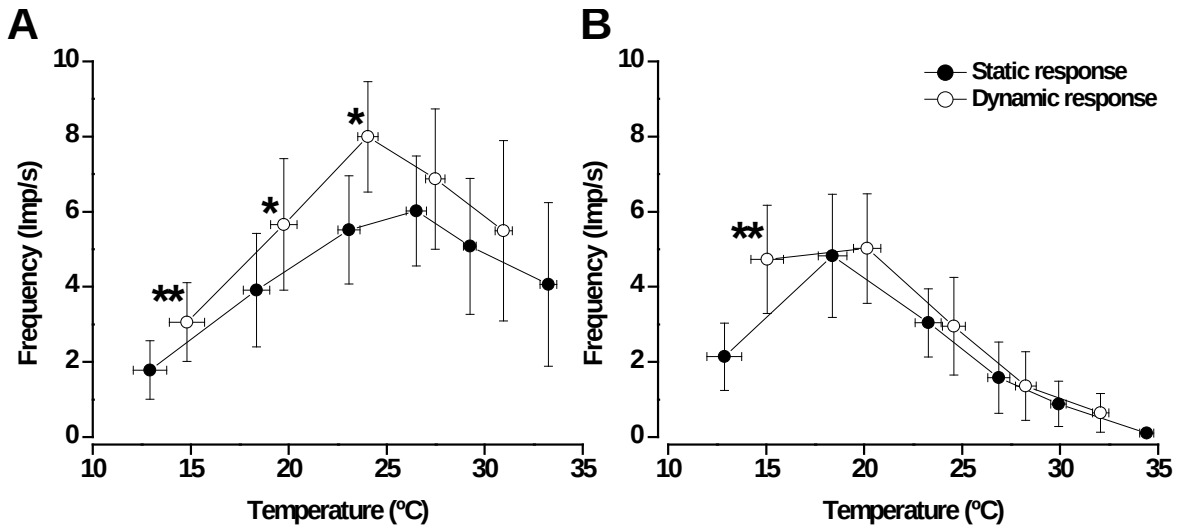

Figure 4.17. Mean firing frequency of static and dynamic responses for the different classes of cold-sensitive fibers. (A) Firing frequency of phasic-tonic fibers in response to temperature steps. Significant differences in dynamic and static phases, * $p \leq 0.05$ and ** $p = 0.003$. (B) Firing frequency of gradually-responding fibers in response to temperature steps. Significant differences in dynamic and static phases, ** $p = 0.004$.

The intensity-response curve of the whole population of cold-sensitive fibers innervating the tongue grouped irrespectively of their firing pattern characteristics provides information about the encoding capabilities of the total sensory input traveling to the central nervous system in response to cooling of the tongue. To obtain this curve, the data from the 23 fibers were pooled together and plotted in Figure 4.18 as the mean firing frequency during each entire cooling step (dynamic plus static portions of the cooling steps). Each temperature step was compared against the mean spontaneous activity at 33.7 ± 0.3ºC of 1.4 ± 0.8 imp/s. During the first three temperature steps, firing frequency gradually and significantly increased until the highest mean firing frequency of 5.7 ± 1.2 imp/s was reached, at a mean temperature of 22.0 ± 0.5ºC, significantly higher than that of the spontaneous firing frequency ($p < 0.001$). As seen in Figure 4.18, this mean firing frequency was 4.3 ± 1.1 imp/s greater than that of the control. After this peak value in the third step, the average firing frequency for lower temperatures decreased, while still remaining significantly higher than that of the control frequency ($p = 0.001$ fourth step and $p = 0.002$ fifth step).

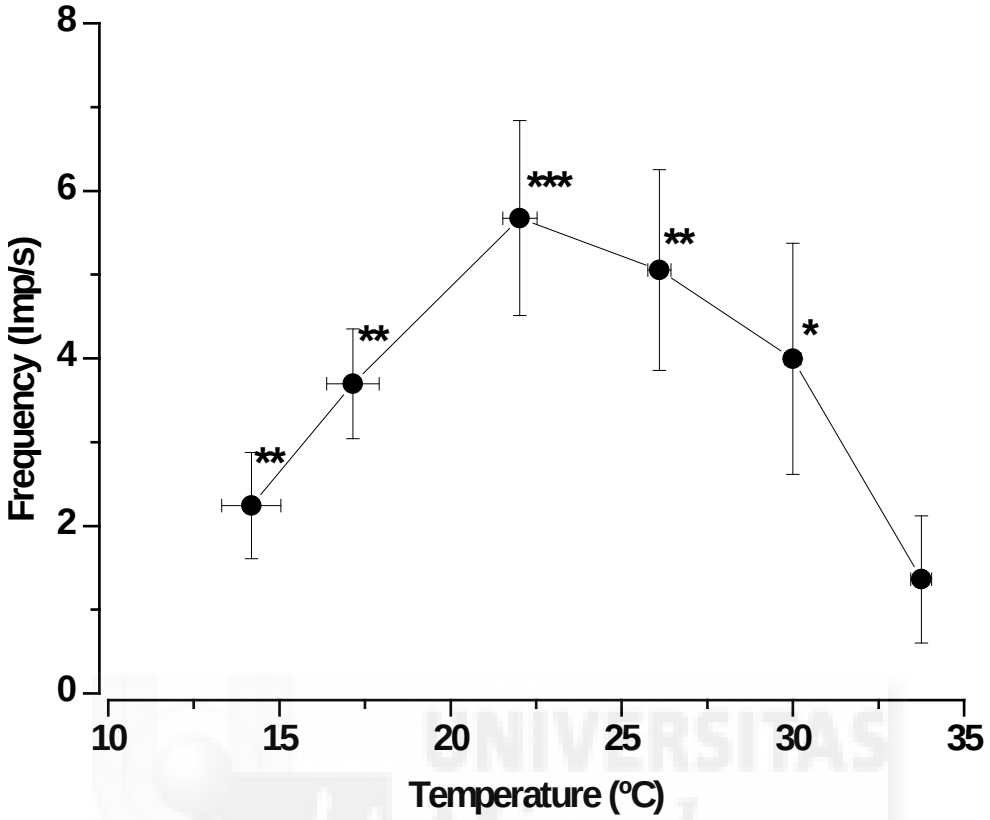

Figure 4.18. Intensity-response curve of the whole population of cold-sensitive fibers during cooling steps. (A) Mean firing frequency of the complete temperature steps, dynamic and static phases together, of the 23 WT cold-sensitive fibers. (* $P \leq 0.05$, ** $P \leq 0.01$, *** $P \leq 0.001$)

Bursting activity was also analyzed for all the fibers during the final 30 s of the static portion of each step measuring the distribution of ISIs between successive impulses as seen in Figure 4.19. However, as evidenced by the unimodal distribution of the ISIs, bursting activity in the 23 fibers studied was very sparse during the cooling steps, with 19/23 displaying no bursting activity whatsoever. Only four of the units exhibited some bursting activity, which was very limited and short-spanned during the whole of the response during the steps. In these fibers, a beating pattern of response was found during the cooling steps, which briefly transitioned into a bursting pattern between the third or fourth cooling steps (at mean temperatures of 23.2 ± 0.4ºC and 18.4 ± 0.5ºC, respectively), before transitioning again into a beating pattern for the remainder of the response.

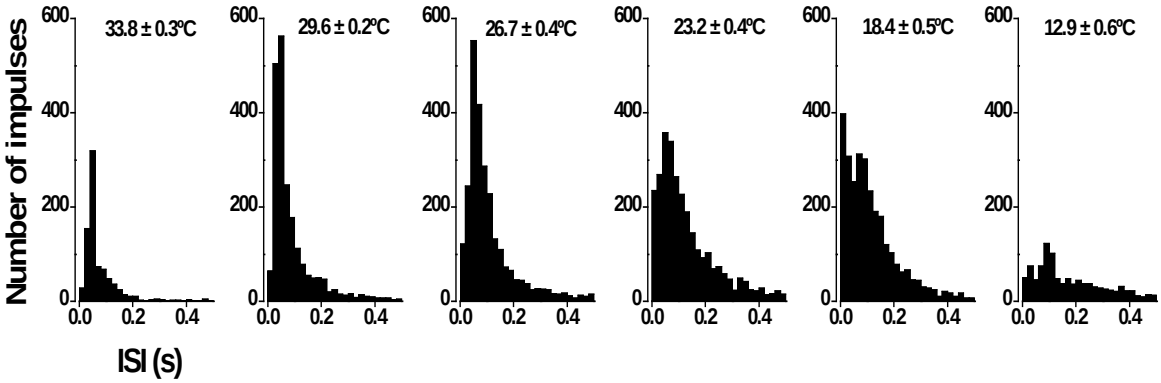

Figure 4.19. Change in ISI pattern of cold-sensitive fibers during cooling steps. Measurements were made during the last 30 s of the static portion of cooling steps n = 23. Graphs represent cooling steps starting from the spontaneous activity (left) and each following step (successive graphs left to right). Temperature of each step is represented as average ± SEM found at the top of each graph.

4.2.1.2. TRPM8$^{-/-}$ mice

A total of 61 cold-sensitive fibers were identified in the lingual nerve of TRPM8$^{-/-}$ mice. Of these, 32 were identified as single-unit recordings.

An estimation of the incidence of cold-evoked activity was also obtained by comparing the number of attempts to record a cold-sensitive fiber by placing different lingual nerve fibers on the recording electrode to the number of positive cold-sensitive responses found. In 18 separate experiments analyzed in the WT group, to record one cold-sensitive fiber a mean of 2.1 ± 0.3 attempts of recording from separate filaments were made. However, in the TRPM8$^{-/-}$ group, a mean of 8.3 ± 1.4 attempts needed to be made before a positive cold-sensitive response was found, a significantly higher ($p < 0.0001$) number of attempts testing different filaments than in the WT group (Figure 4.20). This result suggests that the number of cold-sensitive fibers is significantly reduced in TRPM8-/- animals.

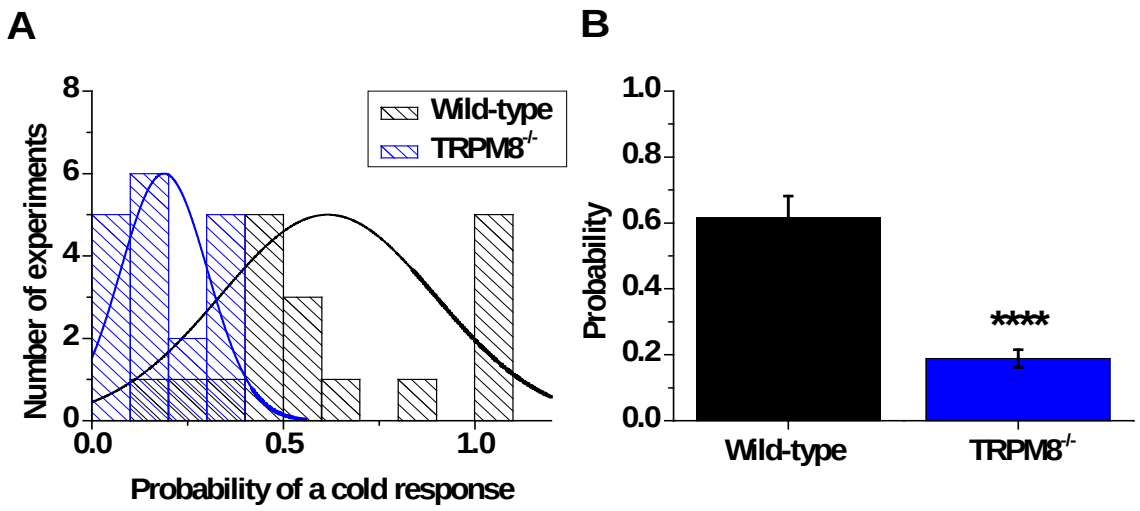

Figure 4.20. Probability of a cold response in WT versus TRPM8$^{-/-}$ lingual nerve filaments. (A) Probability curve of the incidence of a cold response in 18 separate experiments. (B) Probability of a cold response found in lingual nerve fibers is significantly lower in TRPM8$^{-/-}$ mice than in WT mice ($P < 0.0001$).

Temperature threshold

The mean threshold of all the 32 single-unit TRPM8$^{-/-}$ recording was 27.4 ± 1.0ºC. Using the same criteria as in the WT recordings, 47% were identified as LT, with a mean thermal threshold of 32.2 ± 0.5ºC while 53% were identified as HT cold-sensitive fibers, with a mean thermal threshold of 23.2 ± 1.2ºC. None of these values were significantly different from their corresponding WT mice values. The distribution of the thermal threshold of these fibers is found in Figure 4.21 and in Figure 4.11B where it can be compared with the WT distribution of fibers.

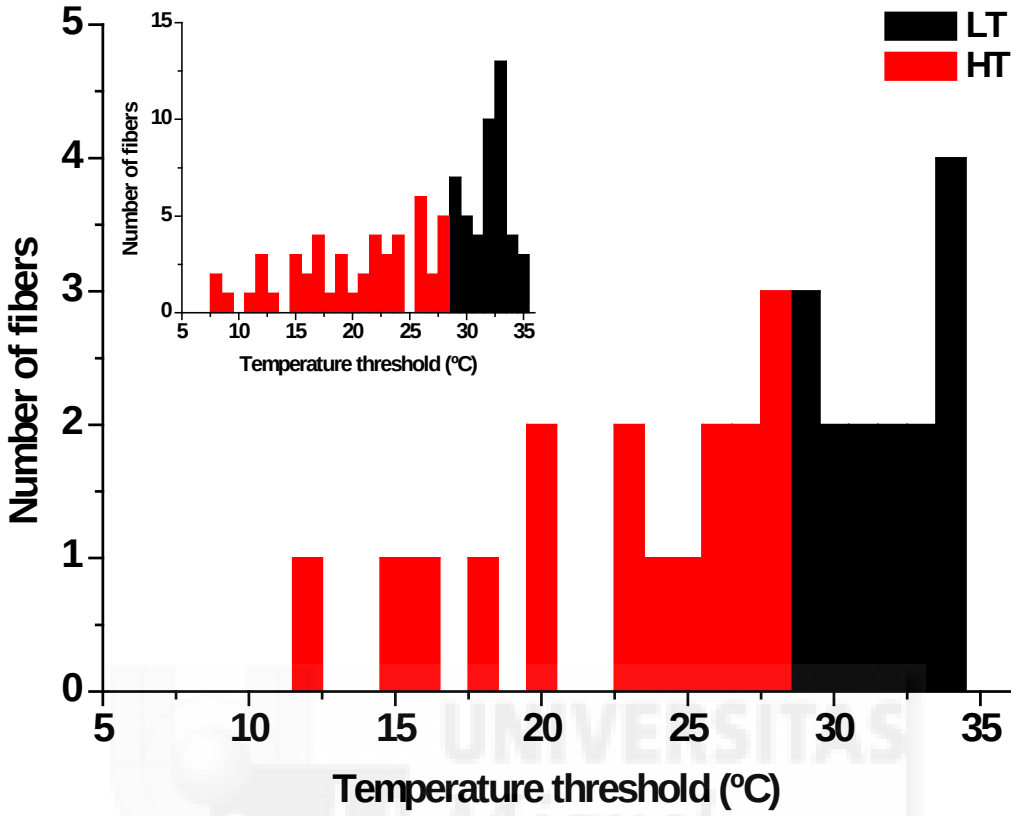

Figure 4.21. Cooling threshold distribution of TRPM8$^{-/-}$ cold-sensitive single units. Black bars represent LT fibers and red bars represent HT fibers (n = 32). The inset shows the cooling threshold distribution of WT cold-sensitive single units.

Firing pattern

Based on their firing pattern to a cooling pulse, single-unit TRPM8$^{-/-}$ fibers were identified as 31% phasic-tonic and 69% gradually-responding cold-sensitive fibers. Within the phasic-tonic group, only 2 were defined as being purely phasic fibers, while 80% were phasic + tonic cold-sensitive fibers, exhibiting a tonic component in the firing response to cooling pulses.

The phasic-tonic fibers had a slightly lower mean thermal threshold, 29.5 ± 1.6ºC, compared to the gradually-responding fibers, 26.4 ± 1.3ºC, though this difference was not significant. The thermal threshold of the gradually-responding fibers however, was significantly warmer in the TRPM8$^{-/-}$ fibers than compared to the WT gradually-responding fibers ($p = 0.011$). Within the phasic-tonic group of fibers, the phasic + tonic fibers had a significantly lower thermal threshold than the 2 fibers that were purely phasic (31.5 ± 0.9

ºC and 21.6 ± 4.9ºC, respectively; p = 0.044). All but one of the phasic + tonic fibers belong the LT group, while both of the purely phasic fibers were HT. 36% of the gradually-responding fibers were in the LT group as well.

Spontaneous activity

Spontaneous activity at a constant temperature of 35ºC was observed in 32% of the single unit recordings of cold-sensitive fibers. Those which had activity, had an average firing frequency of 0.3 ± 0.1 imp/s, which is significantly (p = 0.044) lower than in WT animals. While the highest incidence of spontaneous activity was found among the group of gradually-responding fibers, as 36% of them presented spontaneous activity, they also presented the lowest mean spontaneous firing frequency of 0.2 ± 0.1 imp/s, similar to the mean spontaneous firing frequency of WT gradually-responding fibers. The LT gradually-responding group had a higher incidence of spontaneous activity, 50%, as compared to the HT fibers, 29%. There was no difference however, in the mean firing frequency between LT and HT fibers (0.3 ± 0.1 imp/s and 0.2 ± 0.2 imp/s).

The phasic-tonic fibers had a significantly higher mean firing rate than the gradually-responding fibers, 0.6 ± 0.1 imp/s (p = 0.001), with 30% displaying spontaneous activity. This is a lower firing frequency than found in WT phasic-tonic fibers, but not significantly different. Within the phasic-tonic group of fibers, neither of the two purely phasic fibers displayed spontaneous activity, so those with activity were all phasic + tonic LT fibers.

When separated based on their thermal threshold, a higher percentage of LT fibers, 47%, had spontaneous activity compared with HT fibers, 24%. Those exhibiting activity had a mean firing frequency of 0.4 ± 0.1 imp/s (LT) and 0.2 ± 0.1 imp/s (HT). While WT LT and HT spontaneous firing frequency values were larger, there were no significant differences in the mean spontaneous firing frequency between the LT WT and TRPM8$^{-/-}$ groups or between HT WT and TRPM8$^{-/-}$ groups.

Response to cooling pulses

Bursting

During the cooling pulse a total of 66% of fibers exhibited a bursting pattern. Bursting activity was found in 80% of the LT fibers and 53% of the HT fibers. Based on firing

pattern, the group with the highest percentage of fibers responding in bursts came in the phasic + tonic group of fibers, with 75% exhibiting bursting; neither of the two purely phasic fibers responding to cooling in bursts. Of the gradually-responding group, 68% developed bursting activity. Histograms of the impulse discharge evoked by the cooling pulse for the phasic + tonic and gradually-responding fibers can be found in Figure 4.22, and the characteristics of the bursting parameters of these two groups is found in Table 4.3. While the WT phasic + tonic fibers, in general, maintained bursting activity throughout the entire cooling pulse, the majority of the TRPM8$^{-/-}$ phasic + tonic fibers with bursting activity exhibited a bursting pattern from the beginning of the cooling pulse which gradually transitioned to beating activity as the cooling intensified (Figure 4.22A). In the gradually-responding fibers with bursting activity, a bursting pattern in the impulse firing remained though the cooling pulse for the majority of the units (Figure 4.22B).

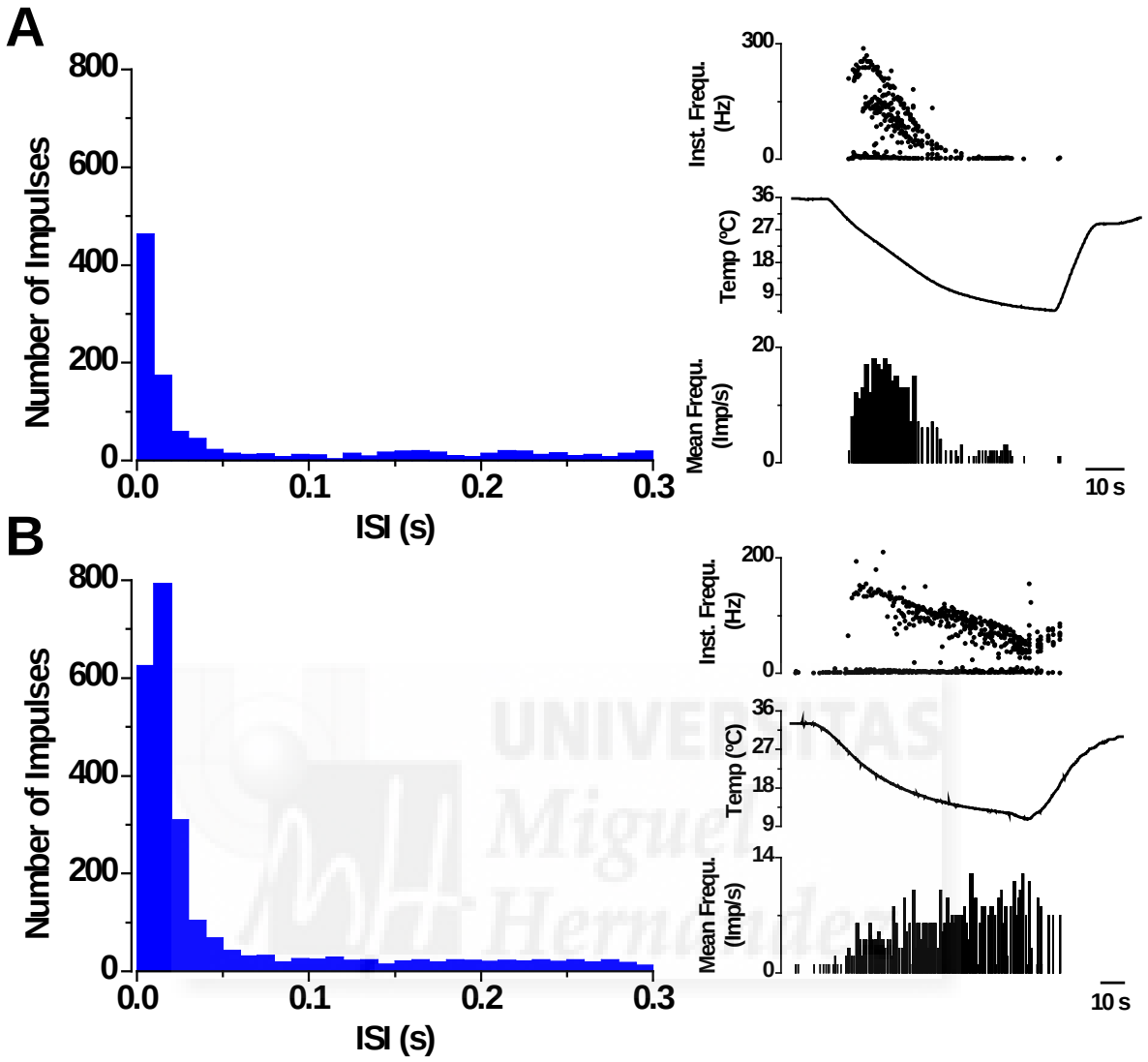

Figure 4.22. Firing pattern of TRPM8$^{-/-}$ cold-sensitive fibers during a cooling pulse. (A) Left, distribution of ISIs of phasic + tonic fibers showing bursting activity during a cooling pulse, n = 6. Right, an example of a phasic + tonic fiber responding in bursts Traces from top to bottom: Instantaneous frequency (Hz), temperature of the bath solution, mean frequency (imp/s). (B) Left, distribution of ISIs during a cooling pulse for those gradually-responding fibers with bursting activity, n = 15. Right, an example of a gradually-responding fiber firing in bursts. Traces from top to bottom: Instantaneous frequency (Hz), temperature of the bath solution, mean frequency (imp/s).

Class	ISI (ms)	Number of bursts/cycle	Bursting pattern (%)	Cycle time (ms)	Impulses/ burst
Phasic-tonic Phasic + Tonic	264.0 ± 17.5	63.3 ± 12.2	73	502.1 ± 66.2	2.8 ± 0.07
Gradually-responding	297.1 ± 11.6	54.5 ± 10.9	78	635.0 ± 22.2	3.1 ± 0.05

Table 4.3. Cooling-induced changes in impulse firing pattern in TRPM8$^{-/-}$ mice. Data obtained from the 6 phasic + tonic, and 15 gradually-responding cold-sensitive fibers with bursting activity. For each fiber, interstimulus interval (ISI), number of bursts per cooling cycle, percent of fibers firing with a bursting pattern, time between the onset of successive bursts (cycle time), and the mean number of impulses per burst were obtained during a cooling pulse. Data are mean ± SEM.

Firing frequency

The mean firing frequency response of all 32 single-unit fibers to the 60 s cooling pulse was 2.3 ± 0.3 imp/s in TRPM8$^{-/-}$ mice. The mean firing frequency to cooling of the LT fibers (2.9 ± 0.5 imp/s) was significantly higher than that of the HT fibers (1.8 ± 0.3 imp/s). Among the classes of cold thermosensitive fibers in TRPM8$^{-/-}$ mice, the highest mean firing frequency elicited by cooling pulses, was in the phasic-tonic fibers (excluding those with a purely phasic response) as found in the WT mice, with a mean firing frequency of 2.9 ± 0.7 imp/s. This response however, was significantly lower in than the WT phasic- tonic fibers ($p = 0.043$). The gradually-responding units mean firing frequency to the cooling pulse was 2.2 ± 0.3 imp/s, which was not significantly different from the phasic-tonic response or the WT gradually-responding unit response. As happened in WT mice, the TRPM8$^{-/-}$ LT fibers in each group exhibited the highest frequency rate in response to cooling pulses. LT gradually-responding fibers had a mean firing frequency of 2.8 ± 0.6 imp/s while the HT fibers this value was 1.9 ± 0.4 imp/s.

Peak frequency values of the whole population of TRPM8$^{-/-}$ cold sensitive fibers were inversely related to thermal threshold as occurred in WT mice (Figure 4.23A, B). The number of imp/s at the peak frequency was also higher, yet not significantly, in the LT group (9.6 ± 1.3 imp/s) than in the HT group (7.3 ± 1.0 imp/s), which is also what was observed in the WT response. However, comparing just the LT responses, the WT had a significantly higher ($p < 0.0001$) number of imp/s during the peak firing frequency than did

the TRPM8$^{-/-}$. Within fiber classes, peak frequency values for the phasic-tonic and gradually-responding fibers were 10.5 ± 1.6 imp/s and 7.4 ± 0.9 imp/s respectively (Figure 4.23B). Though these values are not significantly different among them, the phasic-tonic fibers of TRPM8$^{-/-}$ mice had peak frequency values significantly lower than those of the WT phasic-tonic fibers ($p = 0.012$).

Considering the temperature at which peak firing frequency was reached, the mean temperature at peak frequency for all TRPM8$^{-/-}$ fibers was 19.3 ± 1.1ºC (not significantly different from the WT fibers). Mean temperatures at peak firing frequency were 23.5 ± 1.2ºC in the LT group and 15.5 ± 1.2ºC in the HT group. The LT temperature at peak frequency was significantly lower in TRPM8$^{-/-}$ than in the WT mice ($p < 0.014$). There were no differences regarding the time between the thermal threshold and peak firing frequency (12.4 ± 2.3 s, LT and 16.9 ± 3.0 s, HT) or number of action potentials fired time between the thermal threshold and peak frequency (60.8 ± 13.7 imp, LT and 52.6 ± 15.1 imp, HT).

When this analysis was made for the two classes of cold-sensitive fibers, phasic-tonic fibers reached peak firing frequency at a significantly higher temperature, 23.8 ± 1.5ºC (16.9 ± 2.3ºC for purely phasic fibers and 25.5 ± 1.1ºC for phasic + tonic fibers), than did gradually responding fibers, 17.2 ± 1.2ºC ($p = 0.003$) as illustrated in Figure 4.23B. Neither of these values was significantly different from the corresponding WT peak firing frequency temperature values. A comparison of these and other values are shown in Table 4.4.

Figure 4.23C, D compares the change in frequency to the change in temperature between the thermal threshold and peak firing frequency for each group of fibers. Mean slope values for LT and HT fibers were not significantly different, 1.0 ± 0.2 imp/s/ºC and 0.7 ± 0.1 imp/s/ºC, respectively. However, these values were both significantly lower than their corresponding WT LT and HT slopes ($p = 0.001$). Mean slope values based on firing pattern were as follows: 1.0 ± 0.1 imp/s/ºC (purely phasic), 1.6 ± 0.3 imp/s/ºC (phasic + tonic), and 0.6 ± 0.1 imp/s/ºC (gradually-responding). Phasic + tonic and gradually-responding mean slope values were significantly different ($p = 0.004$), while both TRPM8$^{-/-}$ phasic + tonic and gradually-responding values were also significantly lower than

the WT phasic + tonic and gradually-responding mean slope values ($p = 0.007$ and $p = 0.001$, respectively).

When considering the mean firing frequency to a cooling pulse between the time of the first and last action potential fired, the highest activity was seen in the phasic-tonic group of fibers (3.6 ± 0.7 imp/s), followed by the gradually-responding fibers (2.6 ± 0.4 imp/s). The firing frequencies to cooling pulses of both the phasic-tonic and gradually-responding group were significantly lower than those of the WT groups ($p = 0.001$ and $p = 0.047$, respectively).

TRPM8$^{-/-}$ fibers were slightly more likely to stop firing during the duration of the cooling than after the onset of rewarming. Of the LT fibers, 73% ceased firing before the end of the cooling curve, at a mean temperature of 11.7 ± 0.9ºC, a significantly lower temperature than seen in the WT ($p = 0.001$). Among the phasic-tonic fibers, 70% silenced during the cooling curve at a mean temperature of 11.8 ± 1.7ºC, also significantly lower than the WT phasic-tonic silencing temperature ($p = 0.004$). 63% of the phasic + tonic fibers silenced during cooling at a mean temperature of 11.5 ± 2.2ºC. When considering just the fibers that continued to fire throughout the complete duration of the cooling pulse, 30% of phasic-tonic fibers kept firing, ultimately silencing during rewarming at a mean temperature of 11.2 ± 2.6ºC. All phasic-tonic fibers that silenced during rewarming belonged to the phasic + tonic group, as the two purely phasic fibers silenced during the cooling pulse.

Considering just the gradually-responding fibers, 55% silenced during cooling at a mean temperature of 10.0 ± 0.9ºC, similar to the WT value. The remaining 45% of the fibers continued to fire throughout the complete duration of the cooling pulse and silenced at the highest mean temperature among the groups of fibers, 16.7 ± 2.1ºC. This was slightly higher, yet not significantly so, than the temperature at which the phasic-tonic fibers silenced.

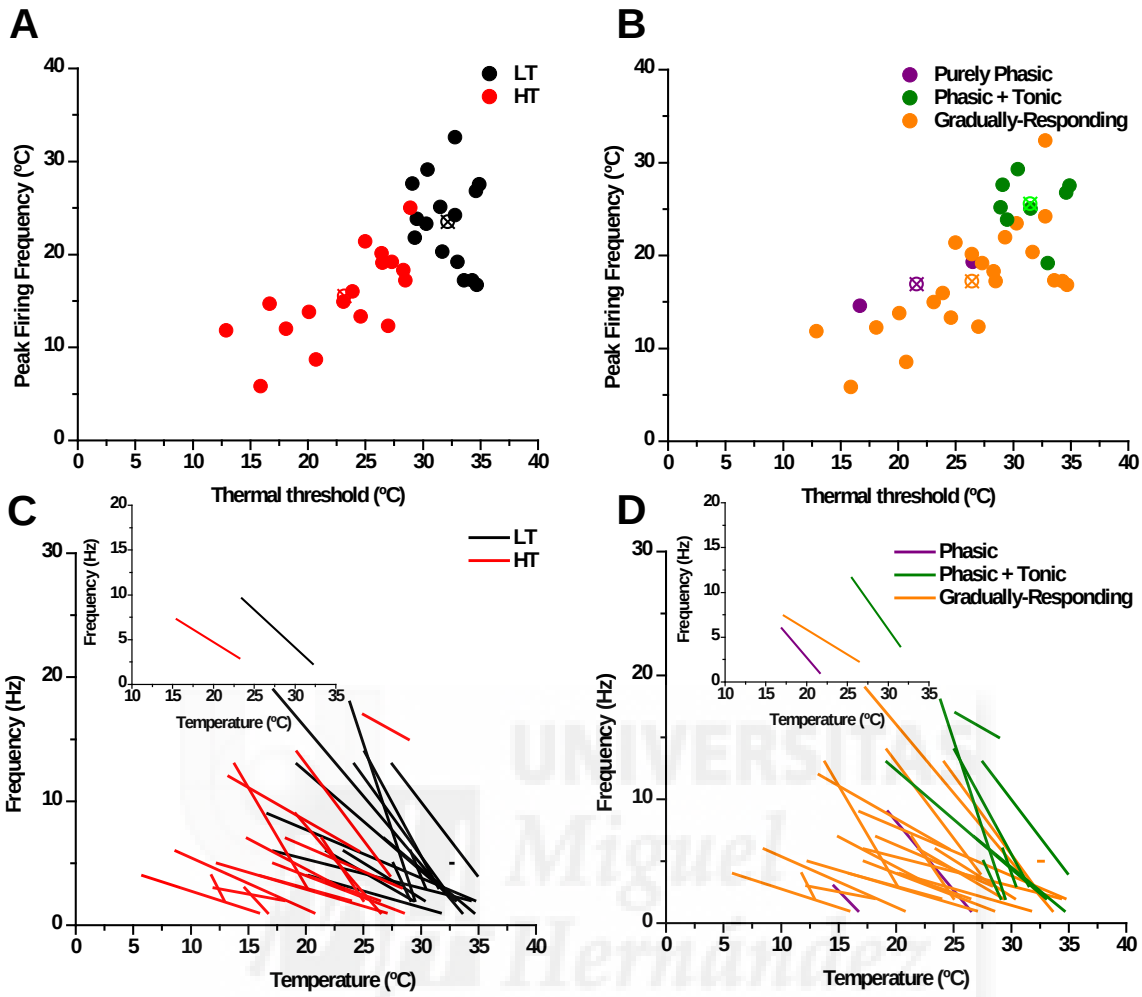

Figure 4.23. TRPM8$^{-/-}$ cold-sensitive fiber responses to a cooling pulse. A, B - Distribution of thermal threshold versus the peak firing frequency for LT and HT fibers (A) and purely phasic, phasic + tonic, and gradually-responding fibers (B). Each dot represents an individual fiber. Average values are represented with an X symbol. C, D - Change in the mean impulse firing frequency versus temperature, plotted from the thermal threshold to the temperature at which peak frequency was reached, separated based on thermal threshold (C) and firing pattern (D). The insets represent the average values for the LT and HT fibers (C) and the purely phasic, phasic + tonic, and gradually-responding fibers (D).

Class	Threshold (ºC)	Spont. Activity (Imp/s)	Mean Firing Frequency (Imp/s)	Peak Firing Frequency (ºC)	Duration to Peak Frequency (s)	Bursting (%)
Phasic-tonic						
Purely Phasic (n = 2)	21.6 ± 4.9		0.6 ± 0.2	16.9 ± 2.3	9.0 ± 1.3	0%
Phasic + Tonic (n = 8)	31.5 ± 0.9	0.2 ± 0.1	3.0 ± 0.7	25.5 ± 1.1	21.9 ± 2.2	75%
Gradually-responding (n = 22)	26.4 ± 1.3	0.1 ± 0.03	2.2 ± 0.3	17.2 ± 1.2	16.3 ± 1.2	68%

Table 4.4. **Properties of the different classes of cold-sensitive fibers in TRPM8$^{-/-}$ mice**. Average values of the different parameters analyzed in all the TRPM8$^{-/-}$ single-unit cold-sensitive fibers in each functional group. Values represented as the mean ± SEM.

Response to stepwise cooling

A total of 22 TRPM8$^{-/-}$ cold-sensitive fibers were tested using temperature steps, analyzing the dynamic and static phases of each step as done in the WT fibers. Based upon previously made cooling curves, nine cold-sensitive fibers were defined as phasic + tonic and 11 were defined as gradually-responding cold-sensitive fibers. In two fibers there was no previous cooling information available, however based on their impulse firing to the cooling steps they could tentatively be classified as gradually-responding cold-sensitive units.

In the nine phasic-tonic cold-sensitive fibers there was no increase in the dynamic portion of the cooling steps until the fourth step was reached (Figure 4.24A). In the first three steps, there was a steady increase in the average impulse activity with each step, but there were no differences in the dynamic and static firing frequencies. In the fourth step, at a mean temperature of 17.8 ± 0.1ºC, the dynamic firing frequency of 9.2 ± 2.5 imp/s was significantly higher than that of the static firing frequency, 7.0 ± 1.7 imp/s ($p = 0.004$). Additionally, in the fifth step at a mean temperature of 11.4 ± 0.6ºC, there was also a significantly higher firing frequency in the dynamic phase, 6.2 ± 1.0 imp/s, than the static phase, 3.2 ± 0.9 imp/s ($p = 0.011$). By the time of this last step, all of the nine fibers maintained impulse firing during the complete step.

In the 13 fibers defined as having a gradually-responding response to the cooling steps, the mean firing frequency to each step was comparatively lower than the corresponding phasic-tonic firing frequency to each step, as seen in Figure 4.24B. In the first four steps, there was no difference in the mean firing frequency between the dynamic and static phases of each step. The highest mean firing frequency for both step phases came during the fourth step at a mean temperature of 18.4 ± 0.3ºC with a mean firing frequency of 4.5 ± 1.9 imp/s (dynamic) and 3.9 ± 1.7 imp/s (static). The only significant difference between the two phases of the step came during the last step at a mean temperature of 13.2 ± 0.4ºC, with a mean dynamic firing frequency of 3.8 ± 1.3 imp/s and a mean static firing frequency of 2.6 ± 0.8 imp/s ($p = 0.011$).

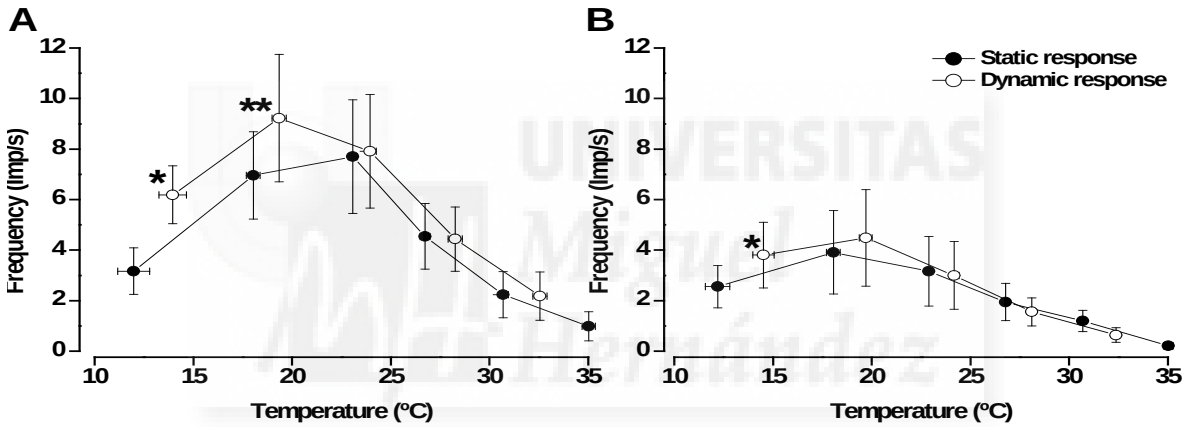

Figure 4.24. Mean firing frequency of static and dynamic responses during temperature steps in TRPM8$^{-/-}$ cold-sensitive fibers. A. Firing frequency of phasic-tonic fibers in response to temperature steps. Significant differences in dynamic and static phases, * $p = 0.011$ and ** $p = 0.004$. B. Firing frequency of gradually-responding fibers in response to temperature steps. Significant differences in dynamic and static phases, * $p = 0.011$.

The data from all the 22 fibers were analyzed together and plotted as the mean firing frequency during each entire cooling step, dynamic and static portions together (Figure 4.25). Each step was then compared against the mean spontaneous activity at 34.7 ± 0.3ºC of 0.5 ± 0.2 imp/s. After the first temperature step, where there was no significant increase in mean firing frequency compared to the spontaneous activity, the firing frequency significantly increased with each step, until the fourth step, at a mean temperature of 18.3 ± 0.2ºC, where the highest firing frequency was observed, 5.9 ± 1.4 imp/s ($p < 0.001$).

This peak in firing frequency appeared at cooler temperatures in the TRPM8$^{-/-}$ cold-sensitive fibers than in the WT fibers, which peaked during the third cooling step. During the fifth step (12.7 ± 0.4ºC), the mean firing frequency then started to drop, however still being significantly higher than the spontaneous activity (3.7 ± 0.7 imp/s, $p < 0.001$).

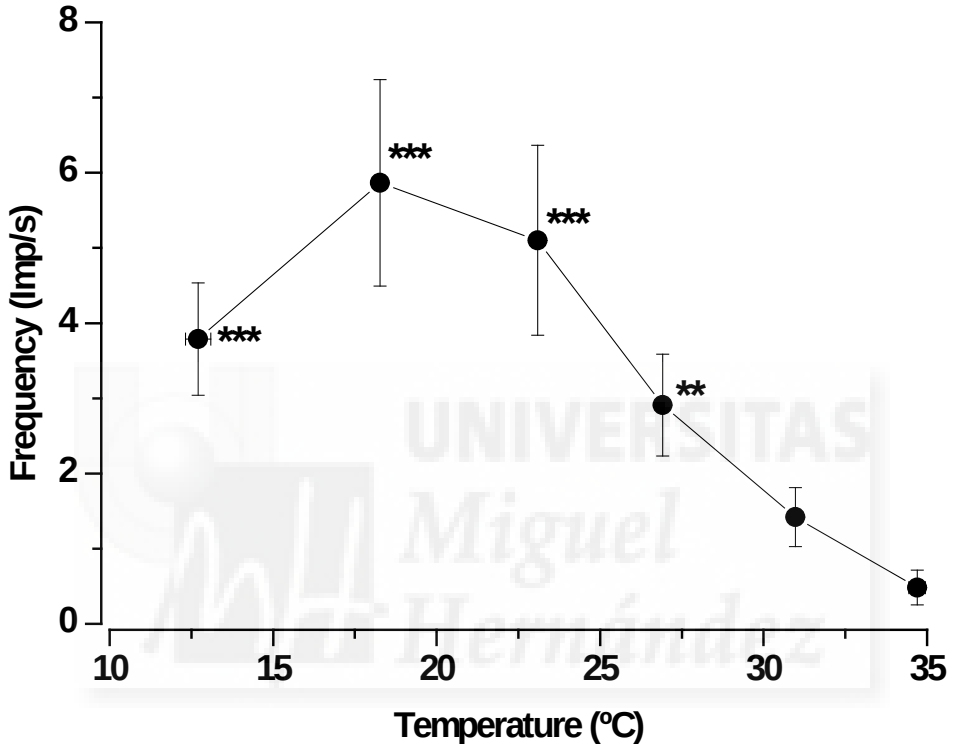

Figure 4.25. Mean firing frequency of TRPM8$^{-/-}$ in response to cooling steps. The data of 22 TRPM8$^{-/-}$ mice cold-sensitive fibers have been pooled together, irrespective of their firing pattern. (** $P \leq 0.01$, *** $P \leq 0.001$)

Additionally, bursting activity was analyzed for all the fibers during the final 30 s of the static portion of each step. Greatly different from the WT, only four of the 22 fibers did not show any bursting activity during the temperature steps. Of the 18 units exhibiting bursting activity, ten started firing directly with a bursting pattern with the onset of their thermal threshold, maintaining a bursting pattern throughout the remainder of their firing to cooling. The other eight fibers initiated their firing first in a beating pattern and then transitioning to a bursting pattern as cooler steps were reached, maintaining the bursting throughout the firing to cooling steps. The number of fibers firing with bursts increased with each

successive step, until the fourth step. Distributions of the ISI for each step are found in Figure 4.26.

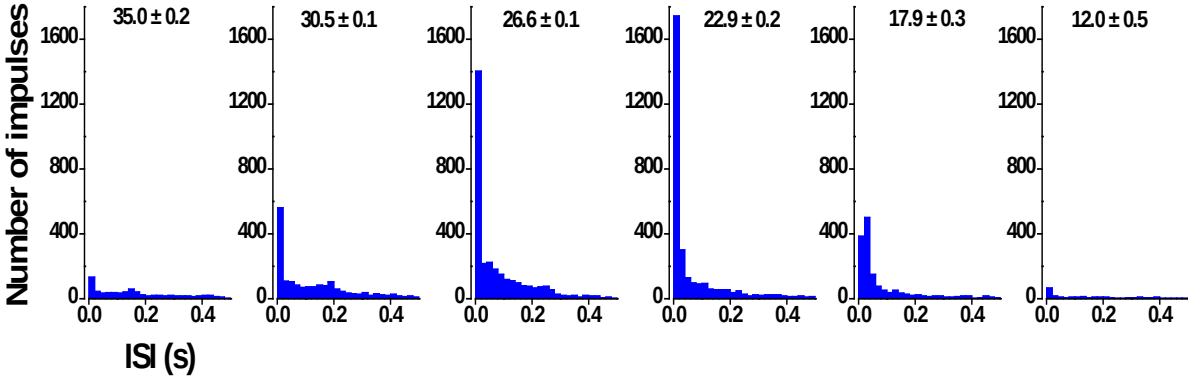

Figure 4.26. Changes in ISI pattern of TRPM8$^{-/-}$ cold-sensitive fibers. Measurements were made during the last 30 s of the static portion of cooling steps n = 22. Graphs represent cooling steps starting from the spontaneous activity (left) and each following step (successive graphs left to right). Temperature of each step is represented as mean ± SEM and is found at the top of each graph.

4.2.1.3. TRPA1$^{-/-}$ mice

A total of 51 cold-sensitive fibers were identified in the adult male TRPA1$^{-/-}$ mice, 26 of which were identified as single-unit fibers.

Temperature threshold

Of the 26 single units, 46% were found to be LT fibers, and 54% were found to be HT fibers. Based on the firing pattern of the single-unit fibers to the cooling pulse, 54% were defined as phasic-tonic fibers and 46% were defined as gradually-responding fibers. Of the phasic-tonic fibers, nine exhibited a purely phasic response while five had a phasic + tonic response.

Mean thermal threshold for all TRPA1$^{-/-}$ single-unit cold-sensitive fibers was 27.9 ± 1.0ºC. The mean thermal threshold of the 46% of LT fibers (32.2 ± 0.6ºC) was similar to that of the LT WT group. The 54% of fibers with a HT had a mean thermal threshold of 24.3 ± 1.2ºC, a significantly warmer temperature than the thermal threshold of the WT HT fibers ($p = 0.044$). Figure 4.27 shows the thermal threshold distribution of all single-unit cold-sensitive fibers. Figure 4.11C shows the thermal threshold distribution along with the

corresponding peak firing frequency for each fiber and where it can be compared to the WT.

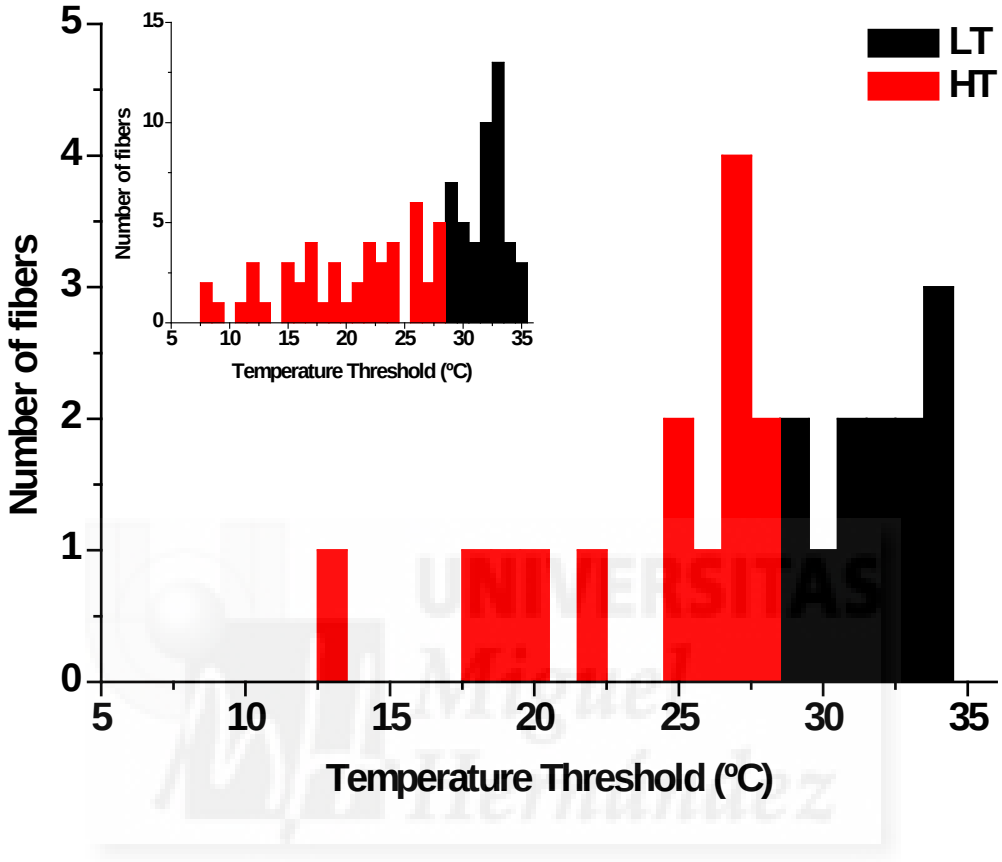

Figure 4.27. Cooling threshold distribution of TRPA1$^{-/-}$ cold-sensitive single units. Black bars represent LT fibers and red bars represent HT fibers (n = 26). The inset shows the cooling threshold distribution of WT cold-sensitive single units.

Firing pattern

TRPA1$^{-/-}$ single-unit cold-sensitive fibers were also divided based on their firing pattern to the cooling pulse. 54% were defined as phasic-tonic fibers, and of these 64% displayed a purely phasic response to cold while 36% had a phasic + tonic response. 46% of the single-unit fibers were defined as gradually-responding to cooling. Regarding the thermal threshold of these different groups, the phasic-tonic fibers had a significantly lower thermal threshold of 30.5 ± 1.1ºC than the gradually-responding fibers, with a threshold of 24.9 ± 1.4ºC ($p = 0.004$). Within the phasic-tonic group of fibers, the purely phasic had a threshold of 29.0 ± 1.4ºC while the phasic + tonic fibers had a threshold of 33.2 ± 0.9ºC.

Threshold values for these groups were similar to what was observed in the corresponding WT groups. All of the phasic + tonic fibers fell into the LT group of fibers, while five of the nine purely phasic fibers were LT. LT purely phasic fibers displayed a thermal threshold at 31.9 ± 0.8ºC, and HT purely phasic fibers had a significantly lower threshold at 25.4 ± 1.9ºC ($p = 0.011$). Of the gradually-responding fibers, 83% fell into the HT group.

Spontaneous activity

Of all the single-unit fibers, 50% exhibited spontaneous activity at 35ºC, at a mean of 1.3 ± 0.4 imp/s. The highest incidence of spontaneous activity was found in the LT cold-sensitive fibers, where 50% exhibited activity at a mean frequency of 1.1 ± 0.3 imp/s. Of the HT fibers, 43% had spontaneous activity and showed the highest mean frequency at 1.6 ± 0.8 imp/s.

When separated based on their firing pattern, a highest percentage of activity was found in the phasic-tonic fibers (57%) with a mean spontaneous activity of 1.4 ± 0.4 imp/s. Within this group of fibers, 56% of the purely phasic fibers fired at a mean frequency of 1.2 ± 0.6 imp/s while 60% of the phasic + tonic fibers fired at a mean frequency of 1.8 ± 0.5 imp/s. The majority of the spontaneous activity was found in the LT fibers as all of the phasic + tonic fibers and all but four of the purely phasic fibers were LT. However, two of the four HT purely phasic did exhibit spontaneous activity. Spontaneous activity in the $TRPA1^{-/-}$ phasic-tonic fibers was not significantly different from that of the WT phasic-tonic fibers.

When considering just the gradually-responding fibers, 42% exhibited spontaneous activity at a mean firing frequency of 1.2 ± 0.8 imp/s. This was a higher percentage than seen in the WT gradually-responding fibers but was not significantly different from the phasic-tonic fibers or the WT gradually-responding fibers. One of the two LT gradually-responding fibers exhibited spontaneous activity, and 40% of the HT gradually-responding fibers showed spontaneous activity at a mean firing frequency of 1.4 ± 1.0 imp/s.

Response to cooling pulses

Bursting

Bursting activity was only found in 3/26 single-unit fibers; two of the three fibers exhibiting bursting were HT, and all were gradually-responding units, resulting in 25% of

the total gradually-responding fibers responding in bursts. An example of this bursting activity can be found in Figure 4.28, along with the histogram of the impulse discharge evoked by the cooling pulse for these three gradually-responding fibers responding to cold in a bursting pattern. All three fibers started to initially exhibit activity to a cooling pulse in a beating pattern, which shortly transitioned into a bursting pattern. Two of the three units maintained this bursting pattern throughout the cooling pulse, while one transitioned back into a beating pattern before silencing with rewarming. Table 4.5 shows the bursting parameters measured for the gradually-responding fibers.

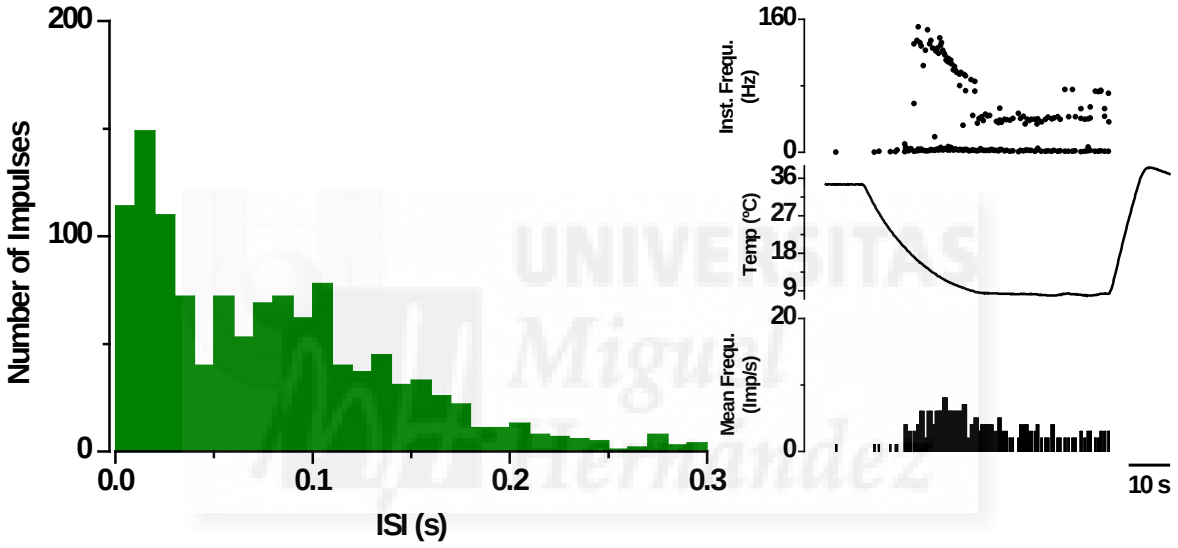

Figure 4.28. Changes in ISI pattern of TRPA1$^{-/-}$ cold-sensitive fibers during a cooling pulse. Distribution of ISIs during a cooling pulse (left) for those gradually-responding fibers with bursting activity, n = 3. An example of a gradually-responding responding in bursts (right). Traces from top to bottom: Instantaneous frequency (Hz), temperature of the bath solution, mean frequency (imp/s).

Class	ISI (ms)	Number of bursts/cycle	Bursting pattern (%)	Cycle time (ms)	Impulses/ burst
Gradually-responding	213.9 ± 5.7	104.7 ± 28.3	52	173.2 ± 7.7	2.2 ± 0.02

Table 4.5. Cooling-induced changes in impulse firing pattern in TRPA1$^{-/-}$ mice. Data obtained from the 3 gradually-responding cold-sensitive fibers with bursting activity. For each fiber, interspike interval (ISI), number of bursts per cooling cycle, percent of fibers firing with a bursting pattern, time between the onset of successive bursts (cycle time), and the mean number of impulses per burst were obtained during a cooling pulse. Data are mean ± SEM.

Firing frequency

The mean firing frequency of the whole population of TRPA1$^{-/-}$ single unit cold sensitive fibers was 5.2 ± 0.9 imp/s, significantly higher than the mean response of WT fibers ($p < 0.03$). The mean firing frequency for LT fibers was 6.2 ± 1.6 imp/s and lower, but not significantly so, for HT fibers, 4.3 ± 1.0 imp/s. The LT mean firing frequency was not significantly different than WT LT frequency, but the HT mean firing frequency was significantly higher than the WT HT frequency ($p = 0.03$).

When divided based on their firing pattern, the highest mean firing frequency during the complete cooling pulse was found in the phasic-tonic fibers, which fired at a mean of 6.1 ± 1.3 imp/s (4.5 ± 0.8 imp/s for the purely phasic and 9.0 ± 3.3 imp/s for the phasic + tonic fibers). Gradually-responding fibers had a mean firing frequency to cooling of 4.1 ± 1.2 imp/s lower, but not significantly so, than the phasic-tonic fibers. LT fibers within the purely phasic group had higher mean frequency than the HT fibers in the same group, but in the gradually-responding group of fibers, it was the HT fibers with a higher mean firing frequency to the cooling pulse.

For the LT fibers, the temperature at peak firing frequency was 21.7 ± 1.9ºC, significantly lower than that of the WT LT ($p = 0.013$), while the HT temperature at peak firing frequency, 15.6 ± 1.2ºC, was similar to the WT HT. TRPA1$^{-/-}$ peak firing frequency compared to their corresponding thermal threshold are shown in Figure 4.29A. The mean number of impulses fired during the peak firing frequency (Figure 4.29C) was higher in the LT than the HT fiber, but not significantly so, 21.6 ± 4.0 imp/s and 12.6 ± 2.0 imp/s, respectively.

The temperature at peak firing frequency in TRPA1$^{-/-}$ fibers was 18.4 ± 1.2ºC. Based on firing pattern (Figure 4.29B, D), the group with the highest temperature at peak firing frequency was the phasic-tonic group at 21.4 ± 1.6ºC (20.0 ± 2.1ºC purely phasic and 24.1 ± 2.4ºC phasic + tonic fibers). This was significantly higher than the gradually-responding fibers, whose temperature at peak firing frequency came at 14.9 ± 1.2ºC ($p = 0.005$). The temperature at peak firing frequency of TRPA1$^{-/-}$ phasic-tonic fibers was also significantly lower than that of the WT animals ($p = 0.006$), while the temperatures at peak frequency of gradually-responding fibers were similar in

TRPA1$^{-/-}$ and WT mice. In TRPA1$^{-/-}$ mice, the number of impulses during the peak firing frequency was also significantly higher in the phasic-tonic fibers (22.1 ± 3.3 imp/s) than in the gradually-responding fibers (10.5 ± 2.0 imp/s, $p = 0.004$). These values are similar to what was observed in the impulses during the peak firing frequency in the WT units. A comparison of various analysis parameters for the different classes of fibers is shown in Table 4.6.

When comparing the change in frequency to the change in temperature between the thermal threshold and peak firing frequency for each group of fibers (Figure 4.29C, D), mean slope values for LT and HT fibers were not significantly different, 2.1 ± 0.4 imp/s/ºC and 1.2 ± 0.3 imp/s/ºC, respectively. While the HT mean slope value was similar to the WT HT mean slope, the TRPA1$^{-/-}$ LT mean slope was significantly lower than the WT LT mean slope ($p = 0.035$). Mean slope values based on firing pattern were 2.1 ± 0.5 imp/s/ºC (purely phasic), 2.8 ± 0.5 imp/s/ºC (phasic + tonic), and 0.8 ± 0.2 imp/s/ºC (gradually-responding). Purely phasic and gradually-responding mean slope values were significantly different ($p = 0.008$), as well as phasic + tonic and gradually-responding mean slope values ($p < 0.001$). While mean slope values of TRPA1$^{-/-}$ purely phasic and phasic + tonic fibers were lower, yet not significantly different, than those of the WT, the TRPA1$^{-/-}$ gradually-responding fiber mean slope was significantly lower than the WT gradually-responding mean slope ($p = 0.018$).

Cold-evoked impulse activity measured as the average response between the first and last spike was also analyzed in TRPA1$^{-/-}$ cold-sensitive fibers. Based on this analysis, phasic-tonic fibers had a significantly higher firing frequency to cooling than did the gradually-responding fibers, 10.7 ± 1.7 imp/s and 4.9 ± 1.1 imp/s respectively ($p = 0.013$). The firing frequency of the purely phasic fibers (10.9 ± 1.8 imp/s) was very similar to that of the phasic + tonic fibers (10.3 ± 3.7 imp/s). LT purely phasic fibers also had a higher firing frequency, 12.4 ± 2.7 imp/s, than did the HT fibers, 9.0 ± 2.2 imp/s, though this difference was not significant.

When analyzing the temperature at which firing during the cooling pulse silences, similar percentage of LT (92%) and HT (71%) fibers silenced before the end of the cooling pulse at temperatures of 10.1 ± 0.9ºC (LT) and 8.2 ± 0.6ºC (HT). The temperature at which the LT TRPA1$^{-/-}$ fibers silenced during cooling is significantly lower than the temperature at which

LT WT fibers silenced ($p < 0.001$). Only 6/36 fibers maintained their firing throughout the whole cooling pulse, silencing during reheating. Of the phasic-tonic cold thermoreceptor fibers the purely phasic fibers silenced at the warmest mean temperature, 10.6 ± 0.6ºC, though significantly cooler than the WT purely phasic fiber ($p = 0.001$). Among those in the phasic + tonic group, all but one silenced during cooling, at a mean temperature of 8.2 ± 2.3ºC.

67% of the gradually-responding fiber silenced during the cooling pulse at a mean temperature of 8.1 ± 0.7ºC, significantly lower than the purely phasic fibers ($p = 0.015$). Of the fibers that maintained impulse activity for the duration of the cooling pulse, silencing during rewarming, all but one of these fibers fell into the gradually-responding fiber group. 33% of these fibers silenced during rewarming at a mean temperature of 22.1 ± 2.7ºC, similar to the WT response.

There was no difference seen in the difference in time between the thermal threshold and peak firing frequency between the LT fibers, 9.9 ± 1.9 s and the HT fibers, 10.0 ± 1.2 s. There was also no difference in the time when compared to the WT fibers. Additionally, the number of impulses fired between these two parameter was higher in the LT, 140.1 ± 62.0 impulses, than the HT fibers, 68.9 ± 12.3 impulses, but not significantly so.

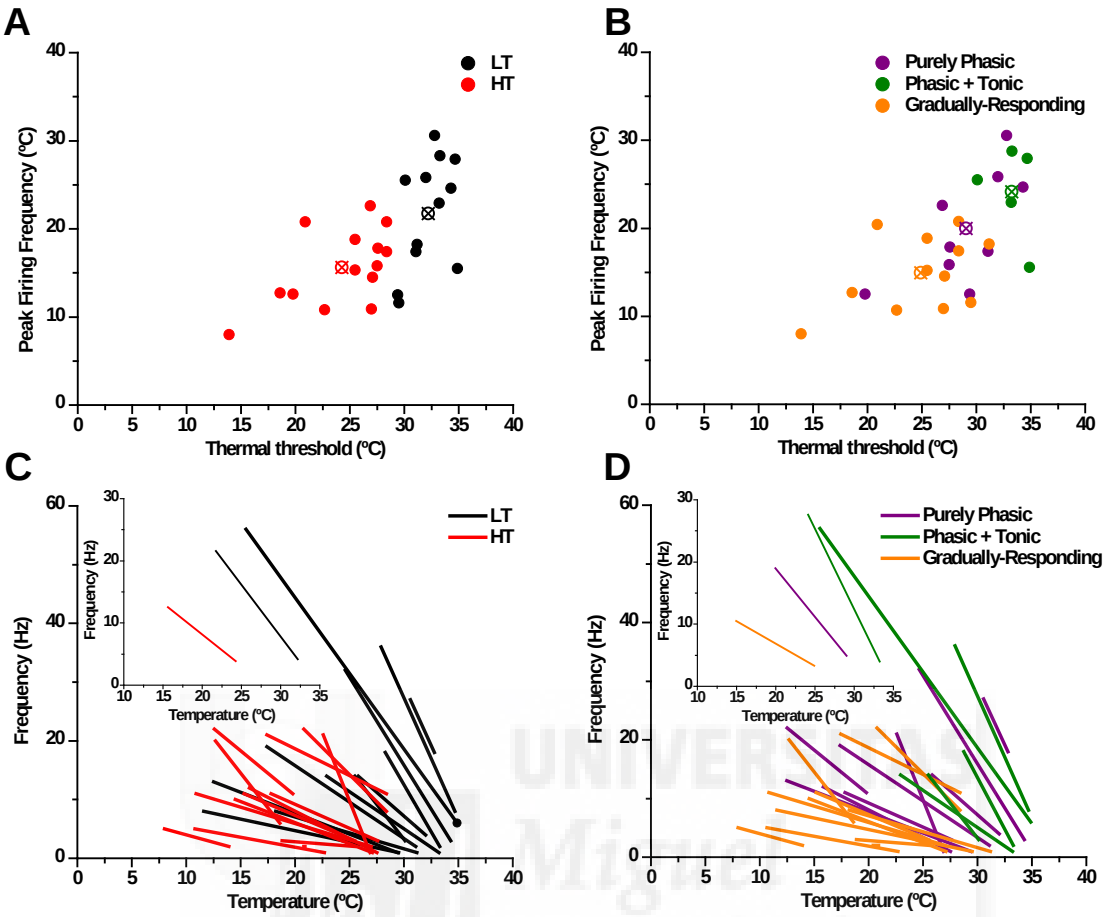

Figure 4.29. Distribution of TRPA1$^{-/-}$ cold-sensitive fiber responses to a cooling pulse. Distribution of thermal threshold versus the peak firing frequency for LT and HT fibers (A) and purely phasic, phasic + tonic, and gradually-responding fibers (B). Each dot represents an individual fiber. Average values are represented with an X symbol. Change in the mean impulse firing frequency versus temperature, plotted from the thermal threshold to the temperature at which peak frequency was reached, separated based on thermal threshold (C) and firing pattern (D). The insets represent the average values for the LT and HT fibers (C) and the purely phasic, phasic + tonic, and gradually-responding fibers (D).

Class	Threshold (ºC)	Spont. Activity (Imp/s)	Mean Firing Frequency (Imp/s)	Peak Firing Frequency (ºC)	Duration to Peak Frequency (s)	Bursting (%)
Phasic-tonic						
Purely Phasic (n = 9)	29.0 ± 1.4	1.2 ± 0.6	4.5 ± 0.8	20.0 ± 2.1	18.5 ± 1.1	0%
Phasic + Tonic (n = 5)	33.2 ± 0.9	1.8 ± 0.5	9.0 ± 3.3	24.1 ± 2.4	25.3 ± 2.2	0%
Gradually-responding (n = 12)	24.9 ± 1.4	1.2 ± 0.8	4.1 ± 1.2	14.9 ± 1.2	16.6 ± 1.2	25%

Table 4.6. Properties of the different classes of cold-sensitive fibers in TRPA1-/- mice. Average values of the different parameters analyzed in all the TRPA1$^{-/-}$ single-unit cold-sensitive fibers in each functional group. Values represented as mean ± SEM.

Response to stepwise cooling

The 14 TRPA1$^{-/-}$ units tested with cooling steps were defined with previously made cooling pulses as ten phasic-tonic (five purely phasic and five phasic + tonic) and two gradually-responding fibers. In the remaining two fibers no previous cooling information was available, however based on the impulse activity to the cooling steps they were tentatively defined as phasic + tonic fibers.

In the 12 fibers defined as having a phasic-tonic response to the cooling steps, the mean firing frequency in the dynamic phase of the steps continually increased until reaching peak mean firing frequency of 7.9 ± 2.7 imp/s during the fourth step (17.4 ± 0.5ºC), as seen in Figure 4.30. This was also significantly greater than the static response of the phasic-tonic fibers (5.4 ± 2.1 imp/s) during the same step ($p = 0.004$). During the fifth and final step (10.8 ± 0.5ºC) the mean firing frequency started to decline, while still remaining significantly greater than the static phase (6.0 ± 2.2 imp/s and 3.1 ± 1.5 imp/s, respectively, $p = 0.004$). During the static phase of the steps, there was an initial increase in the firing frequency, with the mean firing frequency during the static phase (3.3 ± 1.3 imp/s) being significantly higher than in the dynamic phase (2.4 ± 1.0 imp/s) during the first step (29.8 ± 0.2ºC, $p = 0.02$). The mean firing frequency during the static phase of the steps

reached its peak during the third step, at 5.4 ± 2.1 imp/s and a mean static temperature of 22.3 ± 0.6ºC. This was significantly lower than the mean firing frequency during the dynamic phase of the same step (7.1 ± 2.4 imp/s, p = 0.045).

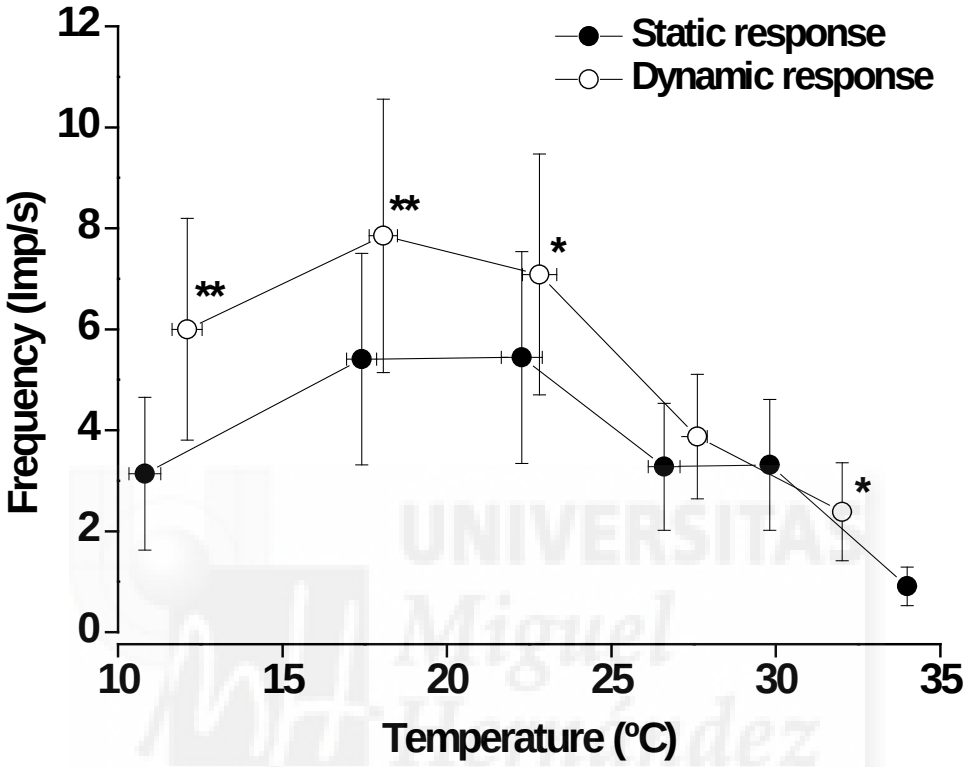

Figure 4.30. Mean firing frequency of static and dynamic responses during temperature steps in TRPA1$^{-/-}$ phasic-tonic cold-sensitive fibers. Significant differences between dynamic and static firing frequencies, * p ≤ 0.05 and ** p = 0.004.

The data from all 14 TRPA1$^{-/-}$ fibers were taken together and plotted in Figure 4.31 as the mean firing frequency during each cooling step, averaging the full dynamic and static phases together. Each of the five steps was then compared against the mean spontaneous activity of 1.9 ± 1.0 imp/s at a mean temperature of 34.0 ± 0.1ºC. During the first three temperature steps, the mean firing frequency gradually increased, however there was not a significant increase compared to the spontaneous activity until the second step (24.3 ± 0.4ºC) which reached a mean firing frequency of 9.5 ± 4.2 imp/s (p = 0.035). In the third step, at a mean temperature of 18.8 ± 0.5ºC, the highest mean firing frequency for all the steps was reached, with an average firing frequency of 10.6 ± 4.5 imp/s, significantly

greater than the spontaneous activity ($p = 0.001$). After the third step, the mean firing frequency started to decrease, while still remaining greater, just not significantly greater, than the mean spontaneous activity.

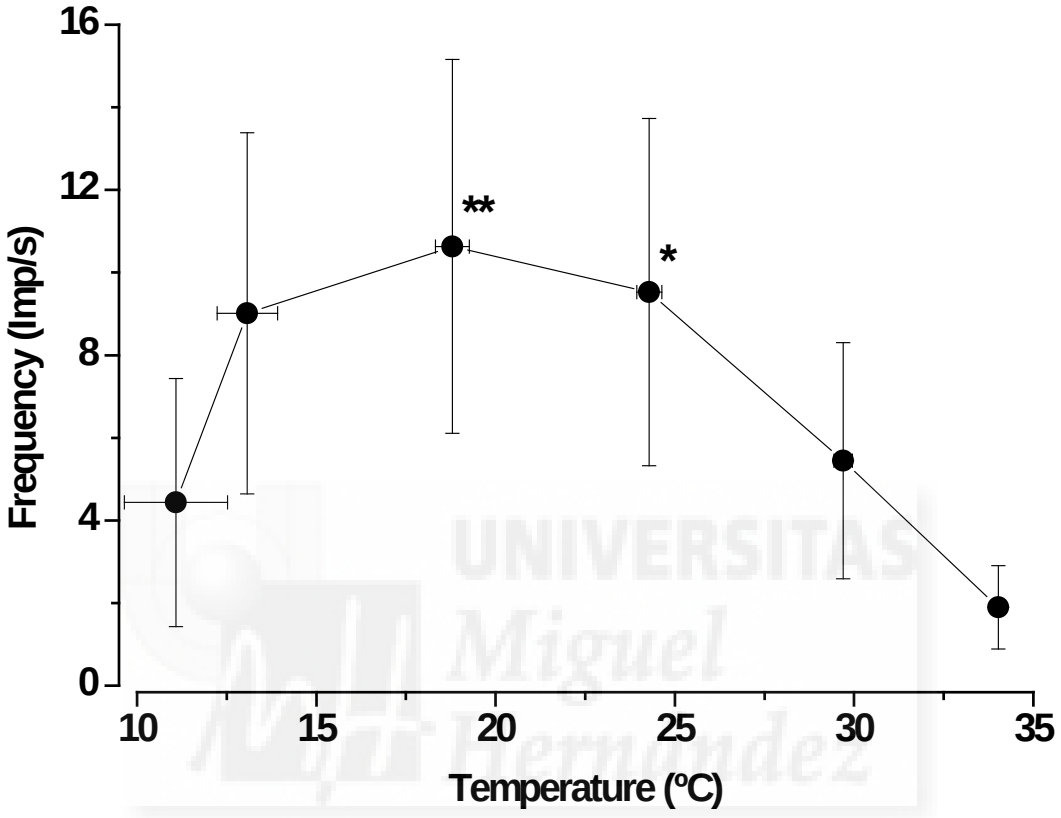

Figure 4.31. Mean firing frequency of TRPA1$^{-/-}$ cold-sensitive fibers to cooling steps. The data of 14 TRPA1$^{-/-}$ cold-sensitive fibers have been pooled together, irrespective of their firing pattern. p=0.035 and p=0.001

Finally, bursting activity was analyzed for the 14 units where cooling steps were applied, considering just the final 30 s of the static portion of each step, Figure 4.32. Six of the 14 units exhibited bursting activity during the cooling steps. Two of the units responding in bursts initiated the firing to cold directly with a bursting pattern of activity, maintaining the bursting throughout the remainder of their firing to the steps. The other four units responding in bursts first starting their firing with a beating pattern, transitioning into a bursting pattern as cooler steps were reached. These units also maintained a bursting pattern throughout the response to the cooling steps.

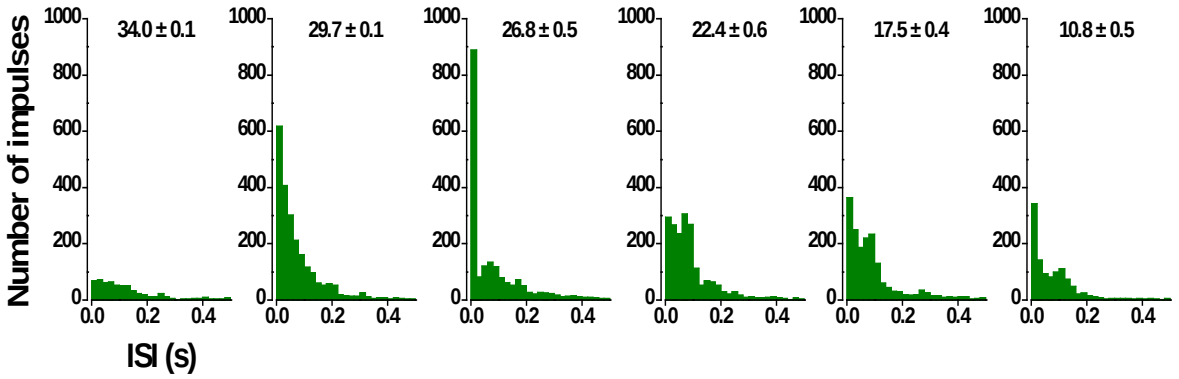

Figure 4.32. Changes in ISI pattern of TRPA1 cold-sensitive fibers. Measurements were made during the last 30 s of the static portion of cooling steps n = 14. Graphs represent cooling steps starting from the spontaneous activity (left) and each following step (successive graphs left to right). Temperature of each step is represented as mean ± SEM and is found at the top of each graph.

4.2.1.4. TRPM8$^{-/-}$/TRPA1$^{-/-}$ mice

In total, 27 cold-sensitive fibers were found in the TRPM8$^{-/-}$/TRPA1$^{-/-}$ adult male mice, 22 of which were characterized as single-unit fibers. Based on their thermal thresholds, all but three of the fibers fell into the LT range.

Temperature threshold

Average thermal threshold during cooling for all TRPM8$^{-/-}$/TRPA1$^{-/-}$ units was 31.1 ± 0.6ºC, significantly lower than the mean WT thermal threshold ($p = 0.013$). 79% of the fibers were found to have a LT. The mean thermal threshold of these LT fibers was 32.0 ± 0.4ºC, while the three HT fibers had a mean thermal threshold of 25.4 ± 1.8ºC. The distribution of all the thermal thresholds of the TRPM8$^{-/-}$/TRPA1$^{-/-}$ single-unit fibers is found in Figure 4.33 and also in Figure 4.11D. The average thermal threshold of the LT TRPM8$^{-/-}$/TRPA1$^{-/-}$ units and the LT WT units were not significantly different.

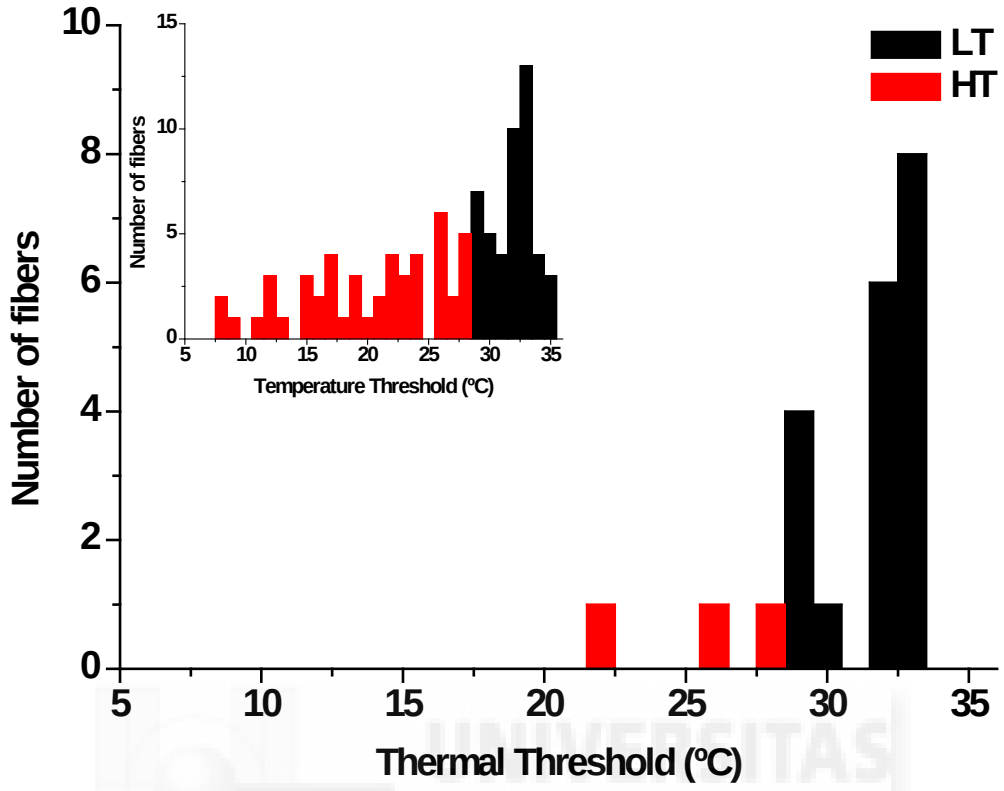

Figure 4.33. Cooling threshold distribution of TRPM8$^{-/-}$/TRPA1$^{-/-}$ cold-sensitive single units. Black bars represent LT fibers and red bars represent HT fibers (n = 22). The inset shows the cooling threshold distribution of WT cold-sensitive single units.

Firing pattern

Based on their firing pattern to the cooling pulse, 41% of the units were identified as having a phasic-tonic firing pattern and 59% had a gradually-responding firing pattern. Of the phasic-tonic fibers, only one fiber exhibited a purely phasic response to cooling. Of these two groups the phasic-tonic fibers showed a significantly lower thermal threshold of 32.8 ± 0.4ºC than the gradually-responding fibers with a threshold of 30.0 ± 0.9ºC ($p = 0.024$). The gradually-responding TRPM8$^{-/-}$/TRPA1$^{-/-}$ units responded at a significantly lower thermal threshold than did the gradually-responding WT units ($p = 0.001$), while the phasic-tonic values were similar in both animal groups. The phasic-tonic units were exclusively LT, while of the gradually-responding fibers 77% were LT.

Spontaneous activity

TRPM8$^{-/-}$/TRPA1$^{-/-}$ cold-sensitive fibers had the highest percentage of spontaneous activity of all the mice groups, 68%, with a mean firing frequency of 0.7 ± 0.3 imp/s. This is lower, but no significantly so, than the WT mean spontaneous activity firing frequency. With all but three fibers being LT, this is congruent with the fact that in the WT it was observed that most spontaneous activity is found in the LT fibers. The highest incidence of spontaneous activity was observed in the phasic-tonic population group. In that group, 89% of the fibers exhibited spontaneous activity at a mean firing frequency of 1.1 ± 0.5 imp/s. In the gradually-responding group of fibers, 54% showed spontaneous activity with a mean firing frequency of 0.3 ± 0.1 imp/s. While lower, this difference was not significant, and neither were they significantly different from their respective phasic-tonic and gradually-responding WT groups.

Response to cooling pulses

Bursting

59% of the fibers exhibited bursting activity, the highest percentage of any of the groups. When dividing these fibers bursting during cooling into the different classes, the one with the highest percentage was the phasic + tonic group of fibers with 75% of the fibers responding in bursts (Figure 4.34A). The one purely phasic fiber did not exhibit bursting. Also, 54% of the gradually-responding fibers showed bursting activity during a cooling pulse (Figure 4.34B). Table 4.7 shows a comparison of the bursting parameters measured for the phasic + tonic and gradually-responding fibers.

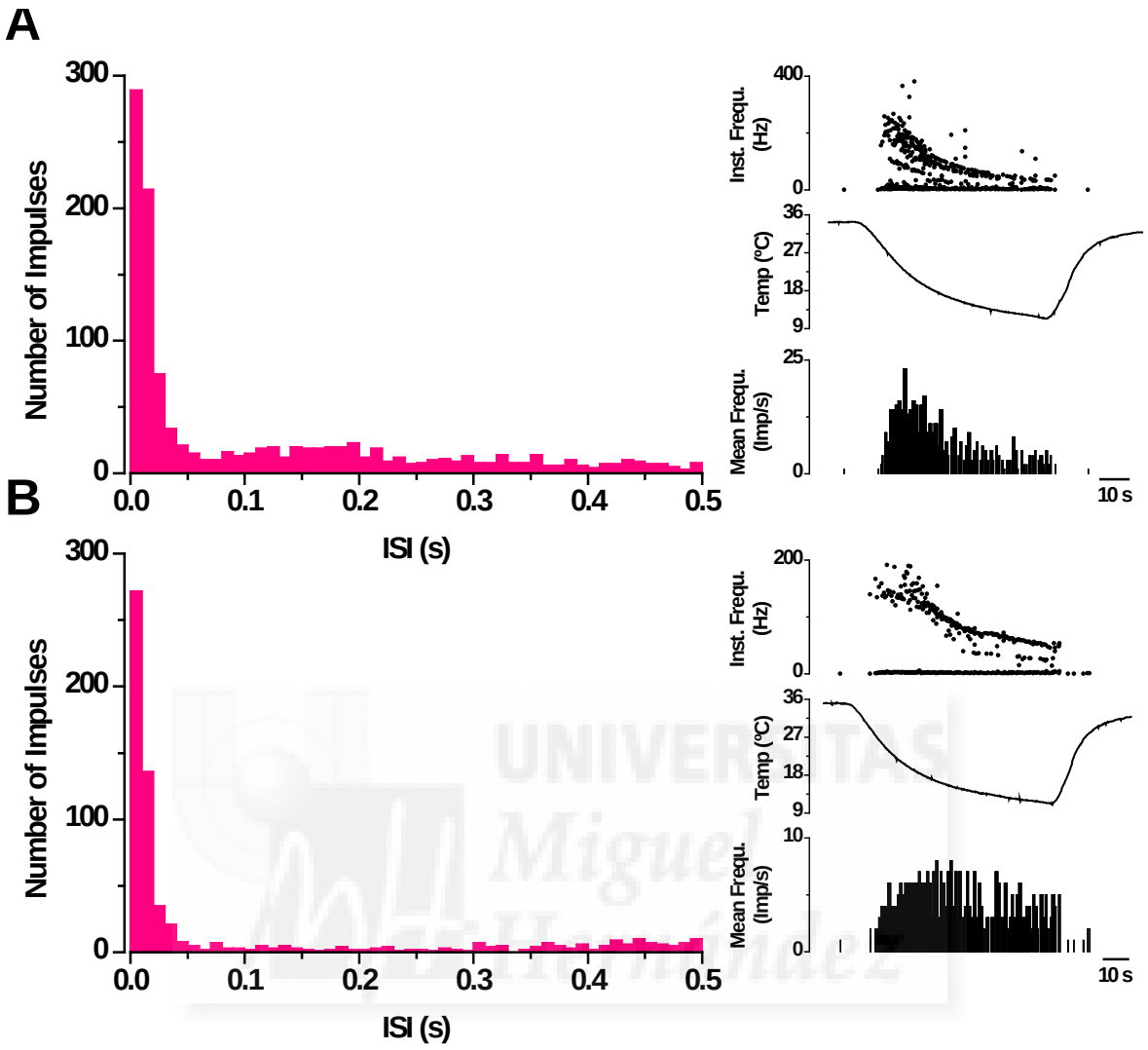

Figure 4.34. Firing pattern of TRPM8$^{-/-}$/TRPA1$^{-/-}$ cold-sensitive fibers during a cooling pulse. (A) Left. Distribution of ISIs during a cooling pulse (left) for the phasic-tonic fibers with bursting activity, n = 6. Right. An example of a tonic responding in bursts. Traces from top to bottom: Instantaneous frequency (Hz), temperature of the bath solution, mean frequency (imp/s). (B) Distribution of ISIs during a cooling pulse (left) for gradually-responding fibers with bursting activity, n = 7. Right. An example of a gradually-responding fiber firing in bursts. Traces from top to bottom: Instantaneous frequency (Hz), temperature of the bath solution, mean frequency (imp/s).

Class	ISI (ms)	Number of bursts/cycle	Bursting pattern (%)	Cycle time (ms)	Impulses/ burst
Phasic-tonic Phasic + Tonic	275.7 ± 13.3	56.7 ± 16.8	65	468.4 ± 20.2	2.7 ± 0.06
Gradually-responding	426.7 ± 20.1	55.7 ± 20.3	76	754.2 ± 29.2	2.3 ± 0.03

Table 4.7. Cooling-induced changes in impulse firing pattern in TRPM8$^{-/-}$/TRPA1$^{-/-}$ mice. Data obtained from the 6 phasic + tonic, and 7 gradually-responding cold-sensitive fibers with bursting activity. For each fiber, interstimulus interval (ISI), number of bursts per cooling cycle, percent of fibers firing with a bursting pattern, time between the onset of successive bursts (cycle time), and the mean number of impulses per burst were obtained during a cooling pulse. Data are mean ± SEM.

Firing frequency

The mean firing frequency in response to the cooling pulse was 2.3 ± 0.3 imp/s for all single-unit fibers and 2.5 ± 0.4 imp/s for the 19/22 LT fibers. This is similar to the WT mean firing frequency response, but significantly lower than what was observed in the WT LT fibers ($p = 0.039$).

When considering the different firing patterns, the highest mean firing frequency to a cooling pulse was found in the phasic-tonic group of fibers, responding at 3.4 ± 0.5 imp/s, similar to the WT phasic-tonic fibers. The gradually-responding cold-sensitive fibers had a significantly lower firing frequency to cooling at 1.5 ± 0.3 imp/s ($p = 0.004$). This value was also similar to the WT response.

Differences in the peak firing frequency compared to the thermal threshold for each fiber are found in Figure 4.35A, B. The value of the mean peak firing frequency for all single-unit fibers was significantly lower (8.3 ± 1.2 imp/s) than in the WT ($p = 0.003$). The mean number of impulses fired during the peak frequency was also significantly higher in the phasic-tonic fibers as compared to the gradually-responding fibers, with values of 13.1 ± 1.8 imp/s and 4.8 ± 0.5 imp/s, respectively ($p < 0.001$). This is represented, along with the mean number of impulses fired during the thermal threshold in Figure 4.35C, D.

The temperature of the peak firing frequency during cooling for the TRPM8$^{-/-}$/TRPA1$^{-/-}$ fibers was 24.3 ± 1.3ºC, higher, but no significantly so, than for the WT units. The highest mean temperature of peak firing frequency was found in the phasic-tonic fibers, responding

at 27.7 ± 1.1ºC. This was a significantly higher temperature than the gradually-responding fibers at 20.2 ± 1.8ºC ($p = 0.012$).

When comparing the change in frequency to the change in temperature between the thermal threshold and peak firing frequency for each group of fibers (Figure 4.35C, D), mean slope values for LT and HT fibers were not significantly different, 1.5 ± 0.4 imp/s/ºC and 0.4 ± 0.2 imp/s/ºC, respectively. Both, TRPM8$^{-/-}$/TRPA1$^{-/-}$ LT and HT mean slopes were significantly lower than the WT LT and HT mean slopes ($p < 0.001$ and $p = 0.047$). Based on firing pattern, the mean slope value of the phasic + tonic fibers (2.6 ± 0.8 imp/s/ºC) was significantly higher than the gradually-responding fibers (0.6 ± 0.1 imp/s/ºC, $p = 0.001$). While mean slope value of TRPM8$^{-/-}$/TRPA1$^{-/-}$ phasic + tonic fibers was lower, yet not significantly different, than those of the WT, the TRPM8$^{-/-}$/TRPA1$^{-/-}$ gradually-responding fiber mean slope was significantly lower than the WT gradually-responding mean slope ($p = 0.004$).

When the cooling activity was analyzed based on the average impulse activity from the first to the last action potential, the values were similar to what was observed in the firing frequency to cooling during the whole 60 s cooling curve. Again, the phasic-tonic fibers had the highest mean firing frequency at 3.6 ± 0.6 imp/s, significantly higher than the gradually-responding fiber firing frequency at 1.9 ± 0.3 imp/s ($p = 0.013$). There was no difference in the TRPM8$^{-/-}$/TRPA1$^{-/-}$ and the WT with respect to the time between the thermal threshold and the peak firing frequency or the total number of spikes occurring during this time.

When examining the time at which the fibers silenced during cooling or rewarming, 45% of the fibers silenced during the cooling curve at a mean temperature of 16.8 ± 1.2ºC. Only 33% of the phasic-tonic fibers silenced during the cooling pulse at a mean temperature of 17.3 ± 3.1ºC, which includes the one purely phasic unit. Of the fibers that continued firing throughout the cooling pulse, silencing during rewarming, the phasic + tonic group, at 75%, contained the highest percentage of units. The mean temperature at which they silenced was 15.8 ± 1.2ºC. Considering the gradually-responding group of fibers, this group contained the highest percentage of fibers which silenced during cooling (54%) at a mean temperature of 16.6 ± 1.3ºC. This included the three HT cold-sensitive fiber found in the TRPM8$^{-/-}$/TRPA1$^{-/-}$ units. Only 15% of the gradually-responding fibers silenced during

rewarming, at a higher temperature, 28.1 ± 0.01ºC, than the phasic + tonic fibers. The remaining fibers that did not silence during cooling or rewarming, maintained firing throughout the changes in temperature, exhibiting spontaneous activity at the return to 35ºC after cooling.

In review, a comparison of the responses to a cooling pulse of the primary analysis parameters for the different classes of fibers is found in Table 4.8.

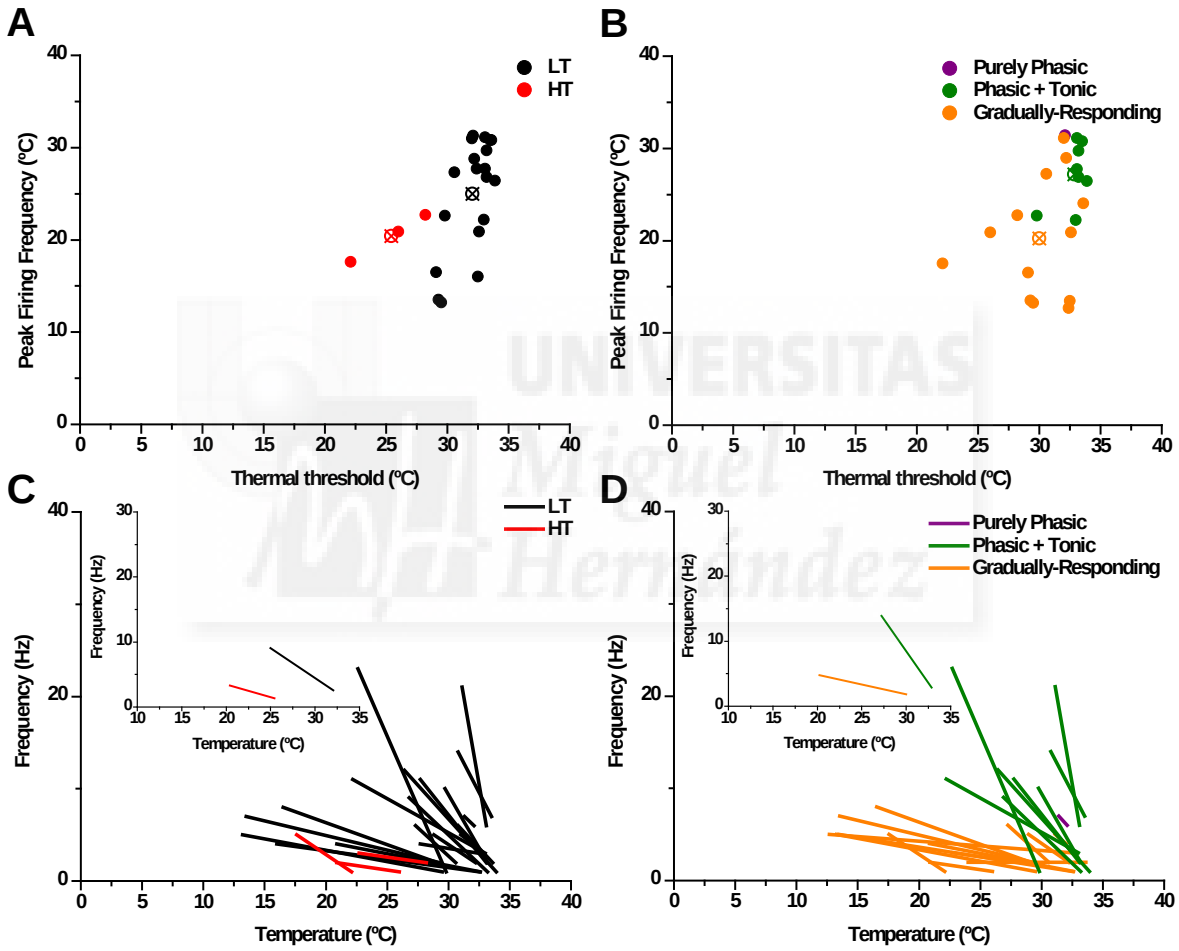

Figure 4.35. Distribution of TRPM8$^{-/-}$/TRPA1$^{-/-}$ cold-sensitive fiber responses to a cooling pulse. Distribution of thermal threshold versus the peak firing frequency for LT and HT fibers (A) and purely phasic, phasic + tonic, and gradually-responding fibers (B). Each dot represents an individual fiber. Average values are represented with an X symbol. Change in the mean impulse firing frequency versus temperature, plotted from the thermal threshold to the temperature at which peak frequency was reached, separated based on thermal threshold (C) and firing pattern (D). The insets represent the average values for the LT and HT fibers (C) and the purely phasic, phasic + tonic, and gradually-responding fibers (D).

Class	Threshold (ºC)	Spont. Activity (Imp/s)	Mean Firing Frequency (Imp/s)	Peak Firing Frequency (ºC)	Duration to Peak Frequency (s)	Bursting (%)
Phasic-tonic						
Purely Phasic (n = 1)	32.1	2.0	2.0	31.4	9.1	0%
Phasic + Tonic (n = 8)	32.9 ± 0.4	0.9 ± 0.6	3.5 ± 0.6	27.2 ± 1.2	18.4 ± 0.7	75%
Gradually-responding (n = 13)	30.0 ± 0.9	0.3 ± 0.2	1.5 ± 0.3	20.2 ± 1.8	14.9 ± 1.2	54%

Table 4.8. Properties of the different classes of cold-sensitive fibers in TRPM8$^{-/-}$/TRPA1$^{-/-}$ mice. Average values of the different parameters analyzed in all the TRPM8$^{-/-}$/TRPA1$^{-/-}$ single, cold-sensitive units in each functional group. Values represented as mean ± SEM.

Response to stepwise cooling

Successive temperature steps were performed in five TRPM8$^{-/-}$/TRPA1$^{-/-}$ cold-sensitive fibers. Six steps were made in these units, one more than in the other mice groups. Based on previously applied temperature pulses, the units were initially defined as four being gradually-responding fibers and one did not have previous cooling information available. After applying the cooling steps this fiber could tentatively be characterized as a gradually-responding unit based on its impulse firing to the steps.

Of these five gradually-responding fibers, the mean firing frequency in the dynamic and static portions of each step progressively increased with lower temperature until reaching the highest mean firing frequency during the fifth step (13.4 ± 0.1ºC). Dynamic and static mean firing frequencies during this step were 2.9 ± 1.1 imp/s and 3.2 ± 1.4 imp/s, respectively, as shown in Figure 4.36. No significant differences were observed between the mean firing frequencies of the dynamic and static phases during any of the six steps.

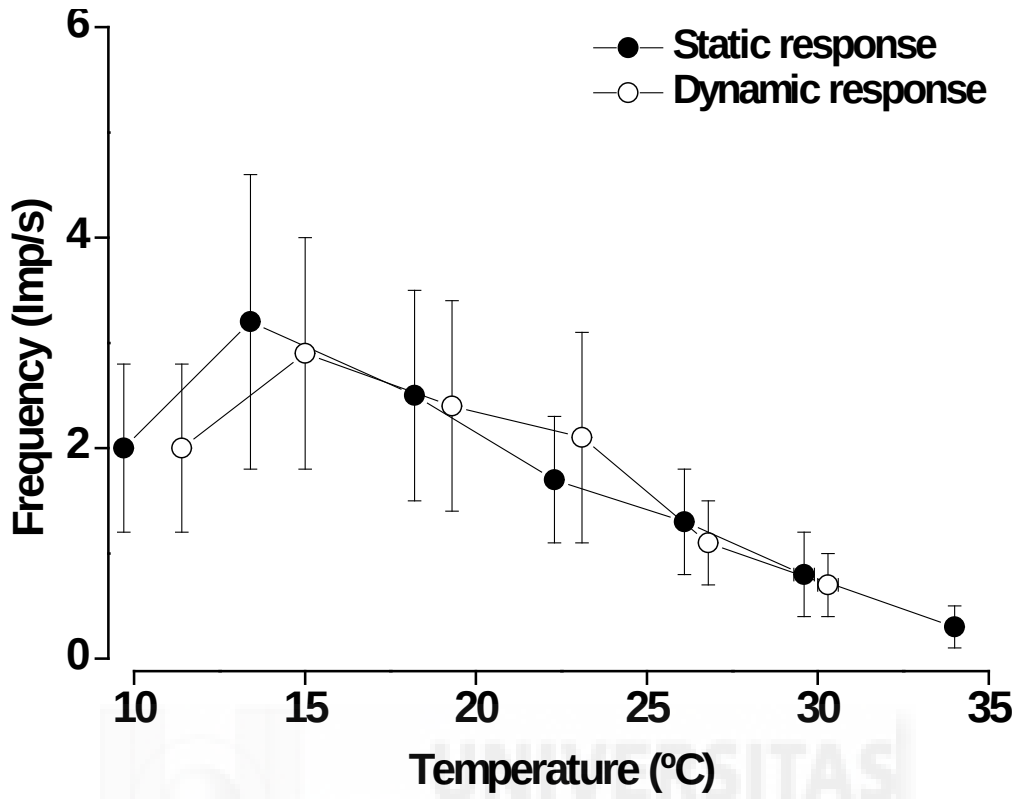

Figure 4.36. Mean firing frequency of static and dynamic responses during temperature steps in **TRPM8$^{-/-}$/TRPA1$^{-/-}$ cold-sensitive fibers.** Data of the five gradually-responding fibers have been represented. No significant differences between dynamic and static firing frequencies were observed.

The data from all five TRPM8$^{-/-}$/TRPA1$^{-/-}$ fibers were pooled and are plotted together in Figure 4.37, averaging the full dynamic and static portions of each step. Mean impulse frequency for each step was then compared to the mean spontaneous firing frequency of 0.3 ± 0.2 imp/s at 33.6ºC. Firing frequency to the cooling steps gradually increased until reaching the fifth step (14.2 ± 0.1ºC), which had the highest mean firing frequency (3.1 ± 1.2 imp/s). During the sixth and final step (10.5 ± 0.1ºC), the mean firing frequency activity then began to decrease (1.9 ± 0.6 imp/s). Only one of the five fibers silenced the firing frequency at the final static part of the step. As shown in Figure 4.37, while there was an increase in firing frequency from the average spontaneous activity during all the steps, none of the increases reached significance levels.

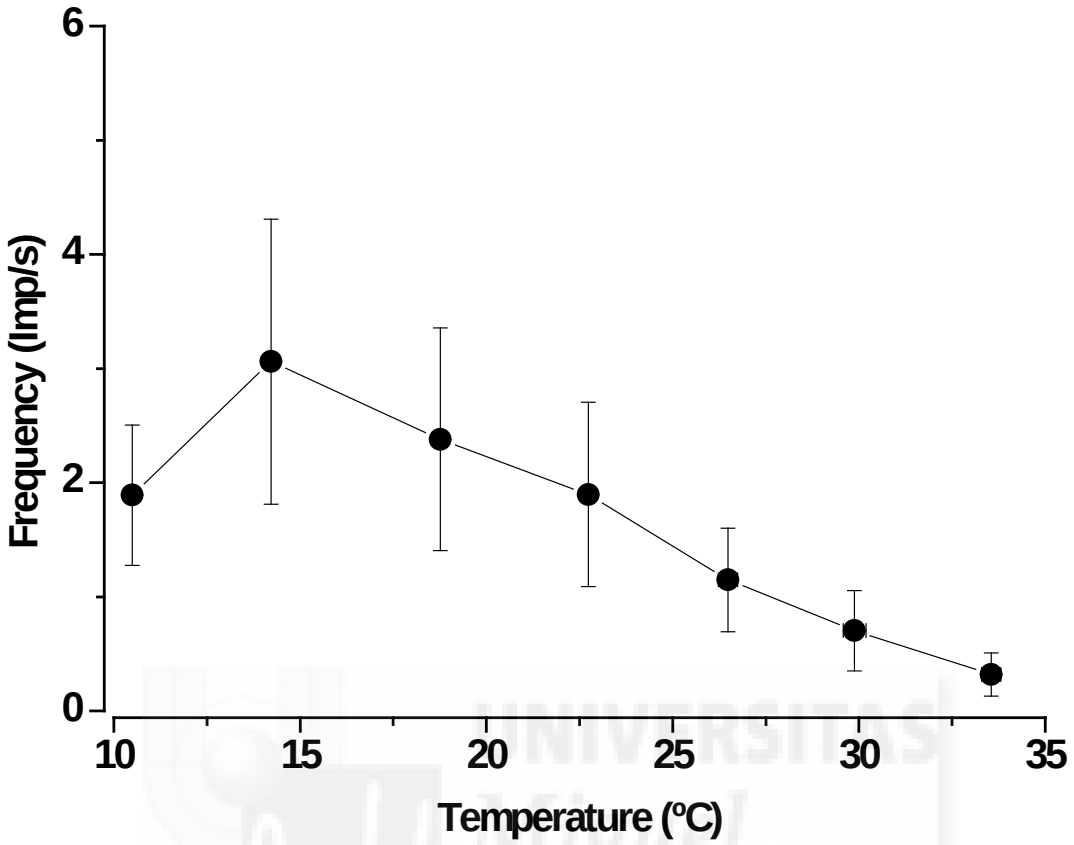

Figure 4.37. Mean firing frequency of TRPM8$^{-/-}$/TRPA1$^{-/-}$ in response to cooling steps. Data of the five cold-sensitive fibers have been pooled together. No significant differences in average firing frequency during the steps compared to the spontaneous activity were observed.

Lastly, bursting activity was analyzed in these same five units for the final 30 s of the static portion of each cooling step (Figure 4.38). Three of the five units exhibited bursting activity during the cooling steps, one of which initiated its response with a bursting pattern and continuing bursting throughout all the cooling steps. The other two fibers with bursting activity started to fire in a beating pattern and gradually transitioned into a bursting pattern with cooler temperatures. As cooler steps were reached more bursting activity was exhibited from those units responding in bursts.

A summary of the parameters analyzed for the WT, TRPM8$^{-/-}$, TRPA1$^{-/-}$, and TRPM8$^{-/-}$/TRPA1$^{-/-}$ purely phasic, phasic + tonic, and gradually-responding cold-sensitive fibers can be found in Table 4.9.

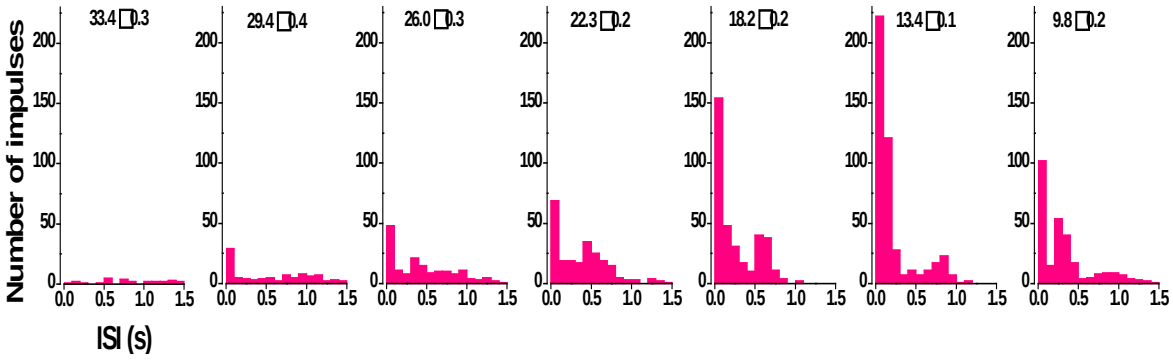

Figure 4.38. Changes in ISI pattern of TRPM8$^{-/-}$/TRPA1$^{-/-}$ cold-sensitive fibers. Measurements were made during the last 30 s of the static portion of cooling steps n = 5. Graphs represent cooling steps starting from the spontaneous activity (left) and each following step (successive graphs, left to right). Temperature of each step is represented as mean ± SEM and is found at the top of each graph.

	Wild-type			TRPM8$^{-/-}$			TRPA1$^{-/-}$			TRPM8$^{-/-}$/TRPA1$^{-/-}$		
	Purely Phasic	Phasic + Tonic	Gradually-Responding	Purely Phasic	Phasic + Tonic	Gradually-Responding	Purely Phasic	Phasic + Tonic	Gradually-Responding	Purely Phasic	Phasic + Tonic	Gradually-Responding
Number of fibers (%)	37%	18%	41%	6%	25%	69%	35%	19%	46%	5%	36%	59%
Spont. Act. (n)	13/35	7/17	4/39	0/2	3/8	8/22	5/9	3/5	5/12	1/1	7/8	7/13
(imp/s)	1.1±0.5	1.2±0.3	0.4±0.2		0.6±0.1	0.2±0.05	1.2±0.6	1.8±0.5	1.2±0.8	2.0	0.9±0.6	0.3±0.2
Thermal Threshold (ºC)	29.4±0.9	31.6±0.7	21.4±1.1	21.6±4.9	31.5±0.9	26.4±1.3	29.0±1.1	33.2±0.9	24.9±1.4	32.1	32.9±0.4	30.0±0.9
(Imp/s)	3.0±0.5	3.9±1.0	1.9±0.2	1.0±0.0	4.0±1.6	2.3±0.3	4.9±1.9	4.0±1.3	3.3±0.9	6.0	2.9±1.1	1.8±0.2
Peak Freq (ºC)	24.6±1.1	27.3±1.0	15.3±0.8	16.9±2.3	25.5±1.1	17.2±1.2	20.0±2.1	24.1±2.4	14.9±1.2	31.4	27.2±1.2	20.2±1.8
(Imp/s)	17.7±1.8	23.4±3.1	8.7±1.2	6.0±3.0	11.6±1.8	7.4±0.9	19.0±2.4	27.6±8.2	10.5±2.0	7.0	13.9±1.9	4.8±0.5
Mean Firing Freq (Imp/s)	2.7±0.4	6.7±1.2	2.9±0.6	0.6±0.2	3.0±0.7	2.2±0.3	4.5±0.8	9.0±3.4	4.1±1.2	2.0	3.5±0.6	1.5±0.3
Mean Freq – first to last (Imp/s)	10.0±1.2	7.6±1.0	3.6±0.4	3.3±1.6	3.7±0.8	2.6±0.4	10.9±1.8	10.3±3.7	4.9±1.1	5.6	3.3±0.6	1.9±0.3
Slope (Imp/s/ºC)	4.7±0.9	9.9±4.3	2.1±0.5	1.0±0.1	1.6±0.3	0.6±0.1	2.1±0.5	2.8±0.5	0.8±0.2	1.3	2.6±0.8	0.6±0.1
Bursting (n)	3/35	6/17	11/39	0/2	6/8	15/22	0/9	0/5	3/12	0/1	6/8	7/13
Silencing cooling (n)	35/35	11/17	16/39	2/2	5/8	12/22	9/9	4/5	8/12	1/1	2/8	7/13
(ºC)	19.5±1.1	14.4±1.1	9.6±1.1	12.6±3.6	11.5±2.2	10.0±0.9	10.6±0.6	8.2±2.3	8.1±0.7	23.0	14.4±1.9	16.6±1.3
Silencing rewarming (n)	0/35	6/17	19/39	0/2	3/8	10/22	0/9	1/5	4/12	0/1	6/8	2/13
(ºC)		16.1±0.5	21.0±1.6		11.2±2.6	16.7±2.1		8.6	22.1±2.7		15.8±1.2	28.1±0.01
Reheating (n)	4/35	5/17	4/39	0/2	4/8	3/22	0/9	0/5	0/12	1/1	4/8	3/13
(ºC)	29.0±3.7	27.6±2.3	19.1±4.9		30.6±1.4	19.7±5.8				26.8	29.4±2.2	21.3±3.7

Table 4.9. Summary of the firing properties of WT and KO purely phasic, phasic + tonic, and gradually-responding cold-sensitive fibers.

4.2.1.5. Effects of TRPM8, TRPA1 and TREK/TRAAK channel agonists

To establish the molecular phenotype of cold transducers expressed by individual lingual fibers, the TRPM8 agonist menthol (5µM; McKemy et al 2002), the TRPA1 agonist cinnamaldehyde (200 µM; Jordt et al., 2004) and the two-pore domain K+ channel modulator chloroform (20mM; de la Peña et al 2012), were applied to cold-sensitive fibers in combination with cooling. In 29 WT fibers analyzed, 65% did not display any increase in the ongoing or cold-evoked activity to any of the three substances studied.

Wild-type mice. A total of eight (28%) of the cold-sensitive units tested, increased their firing frequency in response to a cooling pulse in the presence of menthol (5 µM) as compared to the firing frequency during cooling under control conditions. An example recording to the effect of menthol (5 µM) on a WT cold-sensitive fiber can be found in Figure 4.39. Mean firing frequency during the complete cooling pulse increased in the presence of menthol (5 µM), from 4.0 ± 2.3 imp/s in control conditions to 7.5 ± 2.2 imp/s ($p = 0.04$, Figure 4.40). Of these eight fibers, there was also an increase, though not significant increase, in the spontaneous firing frequency at 35ºC from 0.3 ± 0.2 imp/s in control conditions to 4.1 ± 2.4 imp/s in the presence of menthol (5 µM). Also, five of the 29 studied fibers actually reduced their impulse activity during cooling in the presence of menthol 5µM.

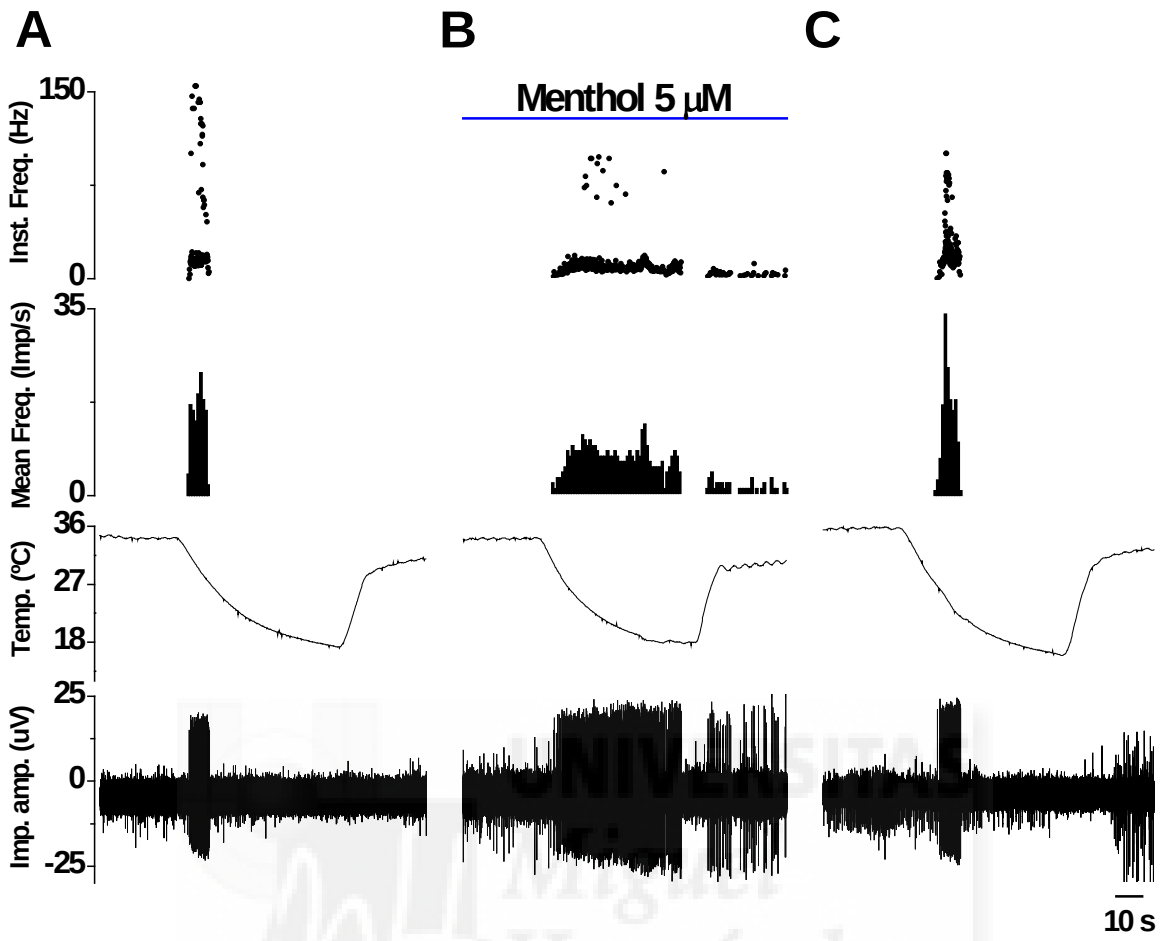

Figure 4.39. Example of the effect of menthol on a WT cold-sensitive fiber. A-C Sample recordings of the response of a WT fiber to cooling pulses in control conditions (A), in the presence of menthol (5 µM) (B), and three minutes after wash out (C). Traces from top to bottom: Instantaneous frequency (Hz), mean firing frequency (imp/s), temperature recording of the bath solution, direct recording of impulse activity. Duration of the perfusion with menthol (5 µM) is indicated by the horizontal red bar.

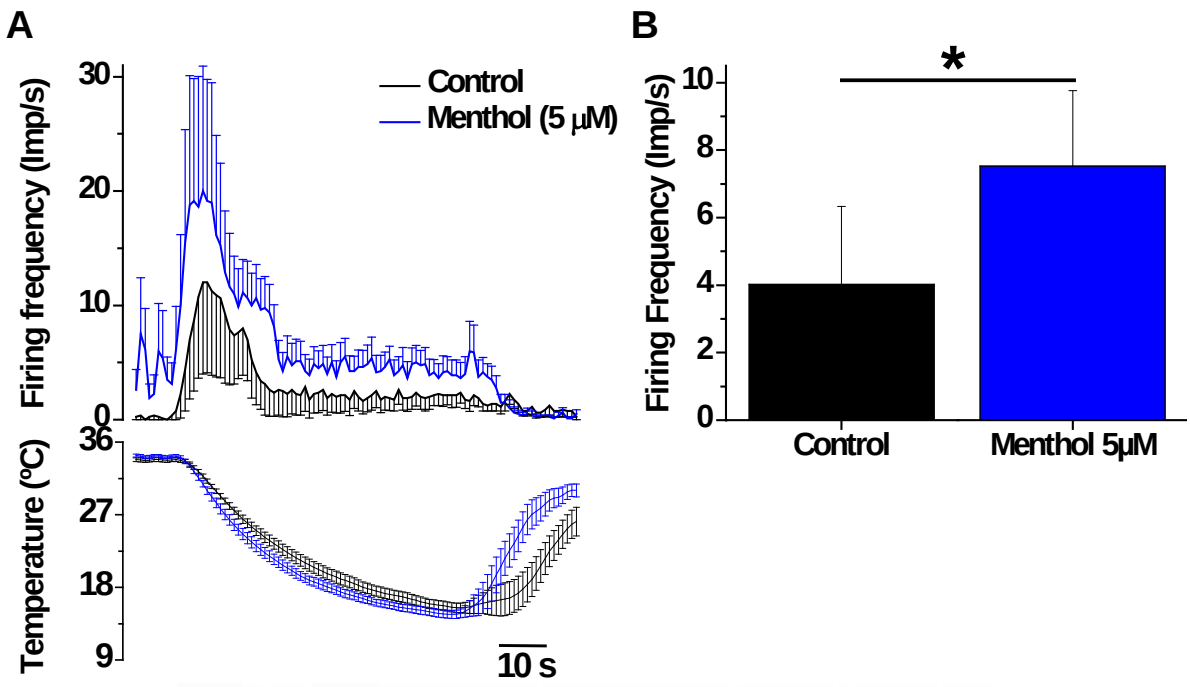

Figure 4.40. Effect of menthol on firing of WT cold-sensitive fibers. (A) Mean firing frequency in imp/s, (top traces) during a cooling curve (bottom) in the nine out of 29 WT cold-sensitive fibers where an increase in the mean firing frequency to cooling was observed under menthol (5 µM). (B) Magnitude of the mean firing frequency increase in the same units to a cooling pulse without (black column) and during the perfusion with of menthol (5 µM) (blue column). Mean firing frequency during menthol (5 µM) application was significantly higher than in control conditions ($p = 0.04$).

None of the fibers tested showed in increase in firing frequency in response to a cooling pulse in the presence of cinnamaldehyde (200 µM); in 41% of fibers there was a reduction or complete silence in the firing frequency during cooling. An example of this silencing effect produced by cinnamaldehyde (200 µM) is shown in Figure 4.41. On average, the spontaneous activity significantly fell from a mean of 1.2 ± 0.5 imp/s in control conditions to 0.1 ± 0.1 imp/s in the presence of cinnamaldehyde (200 µM, $p = 0.031$). Additionally, the mean firing frequency in response to a cooling pulse also significantly decreased with cinnamaldehyde (200 µM) from 7.3 ± 1.7 imp/s in control conditions to 1.2 ± 0.6 imp/s ($p = 0.001$). 42% of those fibers showed a complete silence to cooling in the presence of cinnamaldehyde (200 µM).

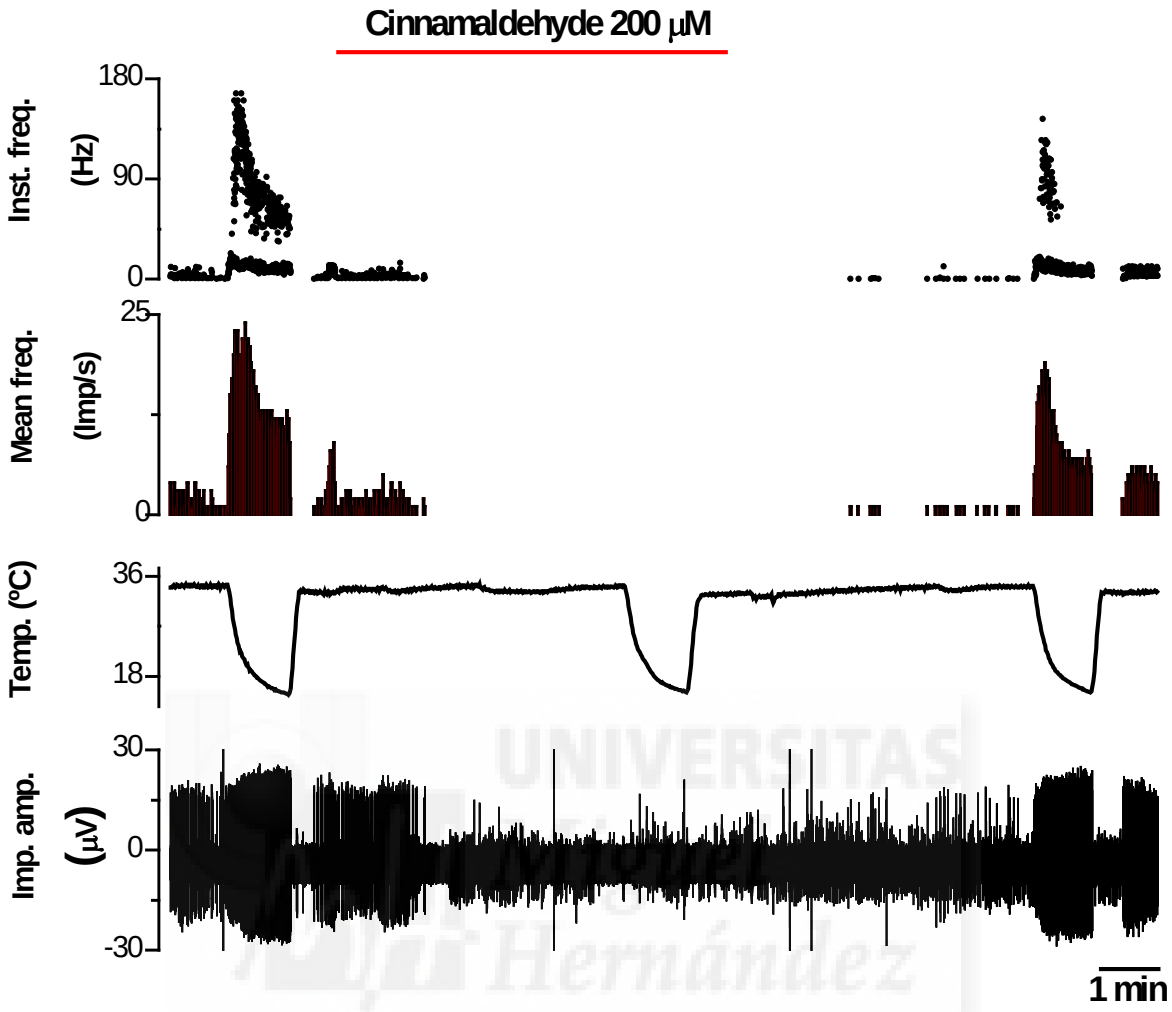

Figure 4.41. Example of the effect of cinnamaldehyde on a WT cold-sensitive fiber. Traces from top to bottom: instantaneous frequency (Hz), mean firing frequency (imp/s), temperature recording of the bath solution, direct recording of impulse activity. Duration of the perfusion with cinnamaldehyde (200 µM) is indicated by the horizontal red bar.

Just two of the 29 fibers showed in increase in the mean firing frequency in response to a cooling pulse in the presence of chloroform (20 mM), while five showed a decrease in firing frequency during a cooling pulse in the presence of chloroform (20 mM). While not significant, for those which showed a decrease their impulse activity, the spontaneous firing frequency dropped from 2.1 ± 1.7 imp/s in control conditions to 1.2 ± 1.2 imp/s in the presence of chloroform (20 mM), and the mean firing frequency during a cooling pulse dropped from 5.2 ± 2.1 imp/s (control) to 0.7 ± 0.6 imp/s (chloroform (20 mM)). Three of

these five fibers exhibited a complete silence in their firing frequency in response to a cooling pulse in the presence of chloroform (20 mM).

TRPM8$^{-/-}$. The same protocol as used in the WT cold-sensitive fibers was used in the cold-sensitive fibers from TRPM8$^{-/-}$ mice. Seventeen TRPM8$^{-/-}$ cold-sensitive fibers were analyzed using menthol (5 µM), chloroform (20 mM), and cinnamaldehyde (100 µM and 200 µM). There were a large proportion of fibers (64%) that did not show an increase in the firing frequency to a cooling pulse in the presence of any of the agonists tested, similar to the proportion found in the WT fibers, as seen in Figure 4.42. Additionally, 3/17 (17.6%) fibers showed an increase in the firing frequency to menthol (5 µM) as the mean increase in the firing frequency of spontaneous activity of 2.0 ± 2.0imp/s, and a mean increase in the firing frequency to the cooling pulse of 6.6 ± 4.5imp/s compared to control conditions, although neither of these values were significant. Only two fibers showed an increase in the firing frequency to a cooling pulse in the presence of cinnamaldehyde (100 µM and 200 µM) and only one fiber showed an increase in the firing frequency to the cooling pulse in the presence of chloroform (20 mM).

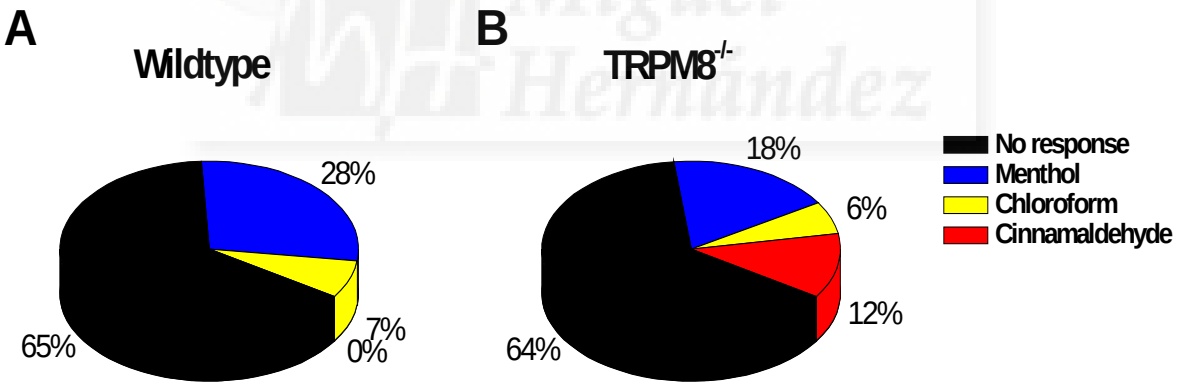

Figure 4.42. Enhancement by various chemical agonists of the firing response to a cooling pulse in WT and TRPM8$^{-/-}$ cold-sensitive fibers; the percentage of cold-sensitive fibers responding to menthol (5 µM), chloroform (20 mM), and cinnamaldehyde (100 or 200 µM) in 29 WT (A) and 17 TRPM8$^{-/-}$ (B) cold-sensitive fibers has been represented. 'No response' indicates that none of the applied substances increased the mean firing frequency evoked by the cooling pulse.

As in the WT mice, 41% of the cold-sensitive TRPM8$^{-/-}$ fibers also exhibited a decrease in their firing frequency to a cooling pulse in the presence of chloroform (20 mM), a higher

percentage than found in the WT fibers. Also, a higher percentage of fibers showed an increase in firing frequency to chloroform (20 mM). In the units showing a decrease in spontaneous activity firing frequency went from 1.1 ± 0.4 imp/s in control conditions to 0.4 ± 0.2 imp/s in the presence of chloroform (20 mM); the difference is not significant. Also, under chloroform (20 mM, the increase in firing frequency induced by a cooling pulse was less pronounced, going from 4.4 ± 2.2 imp/s in control conditions to 0.2 ± 0.1 imp/s in the presence of chloroform (20 mM, $p = 0.016$). Additionally, similar to the WT response, 35% of the cold-sensitive TRPM8$^{-/-}$ fibers exhibited a decrease in their firing frequency in the presence of cinnamaldehyde (100 µM and 200 µM). In just those six fibers which showed a decrease, the spontaneous activity remained the same, as only one fiber exhibited spontaneous activity, while the mean firing frequency to the cooling pulse decreased significantly from 1.7 ± 0.4 imp/s in control conditions to 0.1 ± 0.03 imp/s in the presence of cinnamaldehyde (100 µM and 200 µM, $p = 0.013$).

In 14 TRPM8$^{-/-}$/TRPA1$^{-/-}$ cold-sensitive fibers, chloroform (20 mM) was applied to observe its effect on cold evoked impulse activity. In control conditions the firing frequency to the cooling pulse was 2.4 ± 0.4 imp/s, and this value decreased significantly in the presence of chloroform (20 mM) to 0.3 ± 0.1 imp/s ($p < 0.001$). The difference in the mean firing frequency to cooling in control conditions compared to in the presence of chloroform (20 mM) was -2.1 ± 0.4 imp/s. In eight of the 14 fibers tested there was a complete silencing after chloroform application with firing frequency to cold returning in control conditions. These effects are illustrated in Figure 4.43.

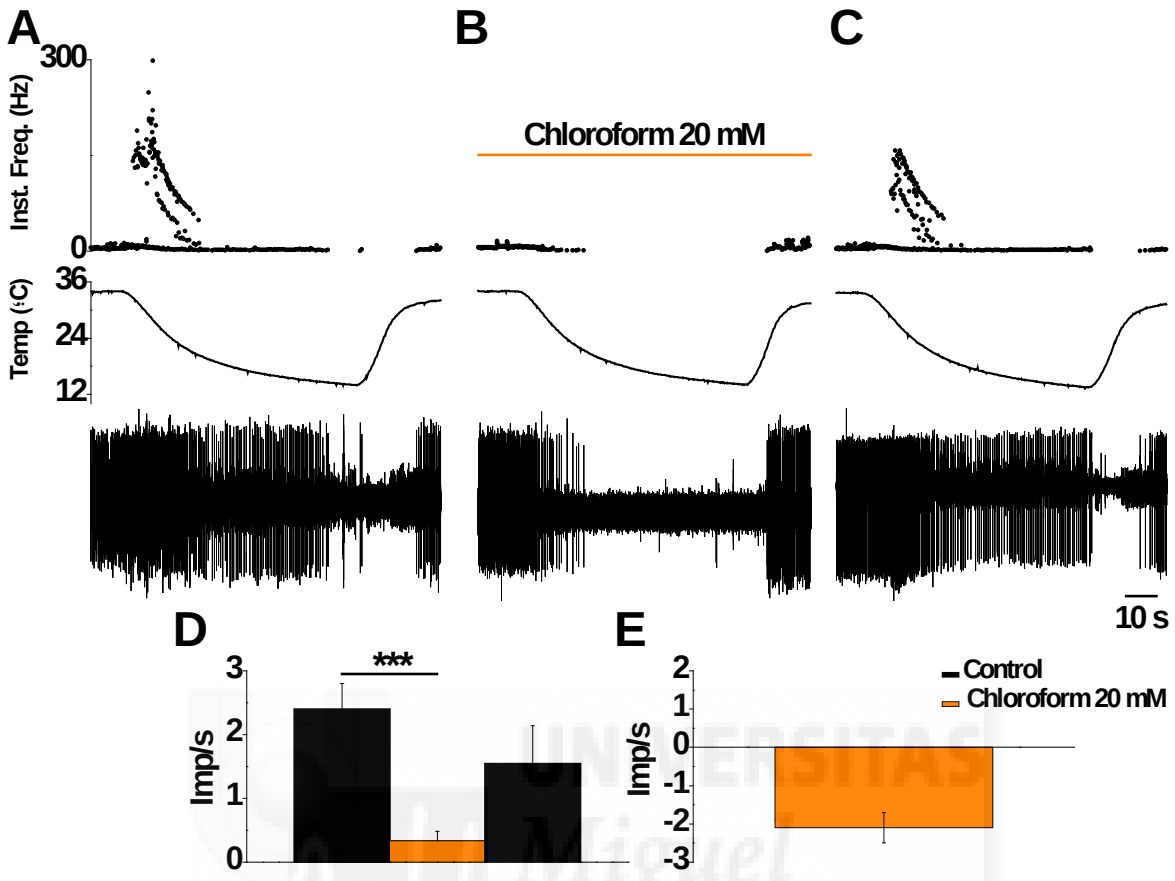

Figure 4.43. Response of TRPM8$^{-/-}$/TRPA1$^{-/-}$ cold-sensitive fibers to chloroform. A-C Sample recordings of the response of a TRPM8$^{-/-}$/TRPA1$^{-/-}$ fiber to cooling pulses in control conditions (A), in the presence of chloroform (20 mM) (B), and three minutes after wash out (C). Traces from top to bottom: Instantaneous frequency (Hz), temperature recording of the bath solution, direct recording of impulse activity. (D) Change in mean firing frequency per second during the cooling curve. There is a significant decrease in activity in the presence of chloroform (20 mM, $p < 0.001$) (E) Change in firing mean frequency during the cooling curve with chloroform (20 mM) as compared to control conditions.

4.2.1.6. Inflammation

In order to determine whether responsiveness of cold-sensitive fibers is altered by inflammation, in a series of experiments carrageenan (2% in saline) was injected into the mouse tongue (see Methods). The injection of carrageenan caused a rapid edema in the tongue tissue at the site of the injection, which continued to develop during the two hours before the mice were sacrificed. Initial swelling due to the injection of the fluid into the tissue was exacerbated by the carrageenan during this time. Figure 4.44 shows the cumulative sum of firing in single-unit cold-sensitive to a cooling pulse. The integral of

firing as a function of temperature was half-activated at 31.6 ± 1.09 ºC in control fibers as compared to 25.4 ± 0.81°C in inflamed fibers.

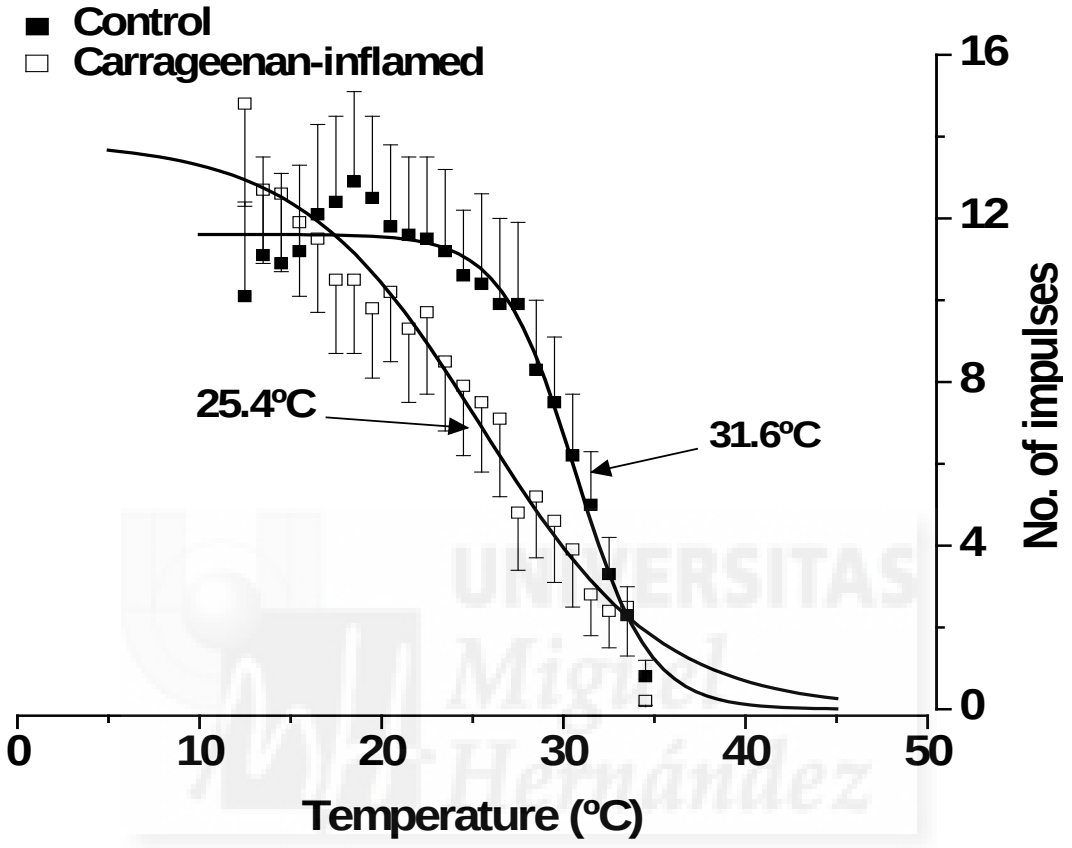

Figure 4.44. Effect of inflammation on cold-sensitive fiber activity. Cumulative firing during a cold ramp of single-unit nerve fibers in the tongue. Black square are in control conditions (n = 40) and open squares are values for the tongue injected with carrageenan (n = 32).

4.2.2. Response characteristics of lingual TG cell bodies

Adult male TRPM8-YFP and TRPM8$^{-/-}$ mice were used to explore the effects of temperature and certain ion channel agonists on trigeminal neurons innervating the tongue using the intracellular calcium fluorometric imaging technique. The fluorescent probe fura-2 was used to measure the effects on the intracellular calcium concentration $[Ca^{2+}]_i$ of cooling, menthol (100 µM), hypotonic solution (217 mOsm), AITC (100 µM), and

capsaicin (0.5 µM) as described in Methods. Figure 4.45 shows typical responses to these different stimuli from three different WT TG neurons.

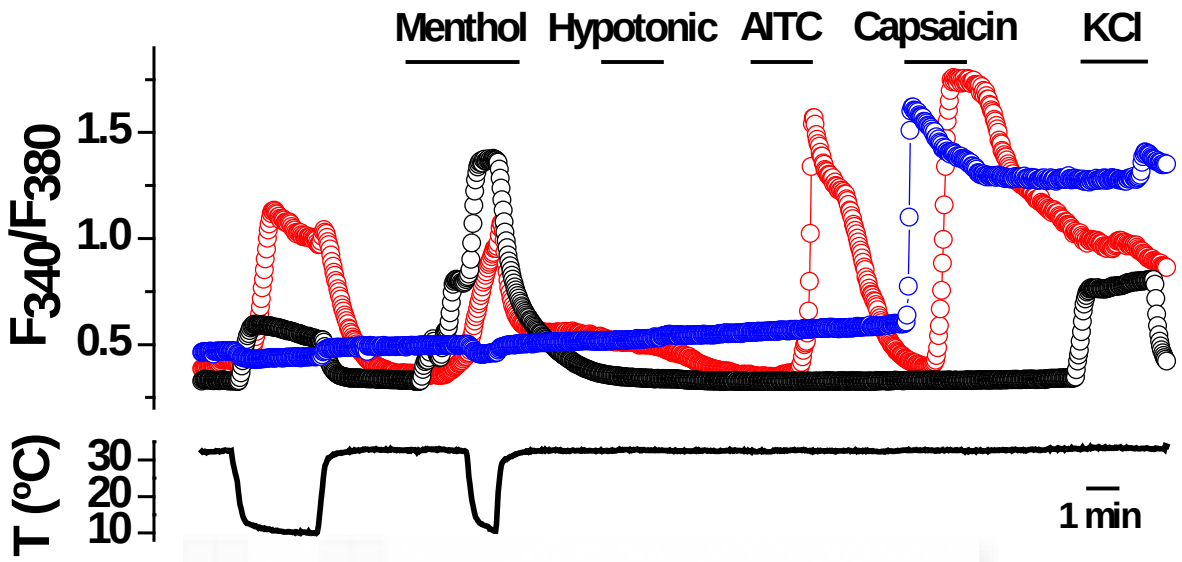

Figure 4.45. Response characteristics of DiI+ TG neurons to various stimuli in wild-type mice. Calcium imaging experiment showing response characteristics of DiI+ labeled TG neurons originating in the tongue from WT mice to various stimuli: menthol (100 µM), hypotonic solution (217 mOsm), AITC (100 µM), capsaicin (0.5µM), and KCl (30 mM). Traces from top to bottom: change in $[Ca^{2+}]_i$ of the neurons; temperature recording of the bath solution.

4.2.2.1. Wild-type neurons

TRPM8-YFP mice were used to clearly identify the neurons expressing TRPM8 channels; DiI positively identified the neurons in the TG originating from the lingual nerve in the tongue. Firstly, DiI+ neurons were identified on the coverslip, and the area with the largest number was selected. TRPM8+ neurons were then identified in the same field by their YFP fluorescence. In the experiments with WT mice, 390 neurons were analyzed, 43 of which were DiI+ neurons. 55 of the 390 neurons were TRPM8+. Of the 43 DiI+ neurons, seven were doubly labeled with DiI and YFP. In the 43 neurons projecting to the tongue, intracellular calcium responses to cooling pulses (34ºC to 10ºC, at a cooling rate of 1.2ºC/s evaluated as the change in the F_{340}/F_{380} ratio were measured.

Response to cold and menthol (100 µM)

Of the 43 DiI+ WT TG neurons, a three minute cooling pulse with control solution activated a total of eight neurons, 19%. Figure 4.46 shows an example of the $[Ca^{2+}]_i$ response in two cold-sensitive neurons. Of the eight putative lingual neurons (i.e. DiI+) responding to cold, six were also labeled with YFP and thus considered TRPM8+ lingual neurons. The mean thermal threshold for these eight neurons was 19.7 ± 7.2ºC, ranging from 26.6ºC to 11.87ºC. The response to a cooling pulse of the neuron with the lowest thermal threshold is shown in the black trace of Figure R44a. This was the only that could be considered a LT neuron accordingly with the criterion adopted for the classification of cold-sensitive lingual nerve fibers. It is necessary to indicate that the rapid cooling rate of the stimulating pulse (1.2ºC/s) made it difficult to accurately determine the threshold value. The mean F_{340}/F_{380} ratio difference during cooling was 0.26 ± 0.07.

When menthol (100 µM), was perfused at 35ºC a total of 12 lingual neurons responded with a $[Ca^{2+}]_i$ rise of variable amplitude as evidenced in the sample traces of Figure 4.46A. All lingual neurons initially responding to a cooling pulse were also activated by menthol (100 µM) at 35ºC. When a rapid cooling pulse was applied during perfusion with menthol (100 µM) five lingual neurons that had not been recruited by the first cooling pulse now showed a $[Ca^{2+}]_i$ increase in response to the second cooling pulse. Hence, 30% of the lingual neurons, and 86% of the lingual neurons that were TRPM8+ responded positively to cold and menthol (100 µM). The mean F_{340}/F_{380} ratio difference of $[Ca^{2+}]_i$ evoked by the cooling pulse under menthol (100 µM) was 0.62 ± 0.12, significantly higher than the increase caused by just a cooling pulse alone ($p = 0.015$, Figure 4.46B). For those neurons that responded to a cooling pulse and also to a cooling pulse during the application of menthol (100 µM, $n = 7$) the F_{340}/F_{380} ratio difference during a cooling pulse in the presence menthol (100 µM) showed a mean response 3.9 times greater than that of the ratio difference during a cooling pulse with control solution.

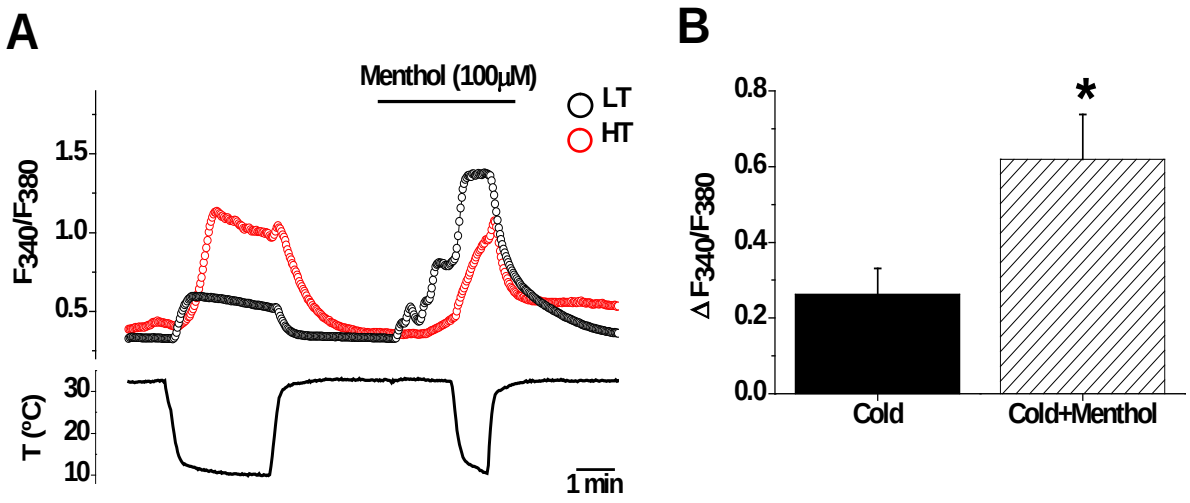

Figure 4.46. Effect of menthol on WT DiI+ TG neurons. Calcium imaging experiment showing response characteristics of two DiI+ labeled TG neurons originating in the tongue from WT mice to a cold and menthol (100 µM) application. (A) A three minute cooling pulse from 34 to 10ºC in control condition was followed by menthol (100 µM) which included an additional one minute cooling pulse. Responses of a LT TRPM8+ neuron shown in black and a HT TRPM8- neuron shown in red. Traces from top to bottom: change in $[Ca^{2+}]_i$ of the neurons; temperature recording of the bath solution. (B) Bar graphs summarizing the effect of cold and menthol (100 µM) on responses in WT DiI+ TG neurons. (* $p \leq 0.05$)

Response to hypotonic solution (217 mOsm)

Of the 43 lingual TG neurons just two (5%) showed a $[Ca^{2+}]_i$ increase to a hypotonic solution (217 mOsm, ~30% osmolality decrease). An example of one of these $[Ca^{2+}]_i$ increases can be seen in Figure 4.47A.

The two neurons that exhibited a $[Ca^{2+}]_i$ increase to hypotonic solution (30%) were cold insensitive and did not show a positive $[Ca^{2+}]_i$ increase to any of the other chemical compounds tested, apart from KCl (30 mM). The mean F_{340}/F_{380} ratio of $[Ca^{2+}]_i$ was 0.13 ± 0.05.

Response to AITC (100 µM)

Of the 43 lingual TG neurons just four different neurons (9%) showed a $[Ca^{2+}]_i$ increase to AITC. Examples of these $[Ca^{2+}]_i$ increases can be seen in Figure 4.47A.

The four neurons with a $[Ca^{2+}]_i$ increase to AITC (100 µM) gave a mean F_{340}/F_{380} ratio value of 0.67 ± 0.2 (Figure R45b). Two of these neurons also had a $[Ca^{2+}]_i$ increase to a cooling pulse, where one responded to the cooling pulse and the cooling pulse plus menthol (100 µM) but not to menthol (100 µM) alone and the other had a $[Ca^{2+}]_i$ increase to the

cooling pulse, menthol (100 µM), and the cooling plus menthol (100 µM), (this neuron can be found in Figure 4.47A). The $[Ca^{2+}]_i$ increase to AITC (100 µM) was significantly greater than the $[Ca^{2+}]_i$ increase to a cooling pulse alone ($p = 0.035$, Figure 4.47B). All four neurons showing an increase in $[Ca^{2+}]_i$ to AITC (100 µM) also showed a $[Ca^{2+}]_i$ increase to capsaicin (0.5 µM).

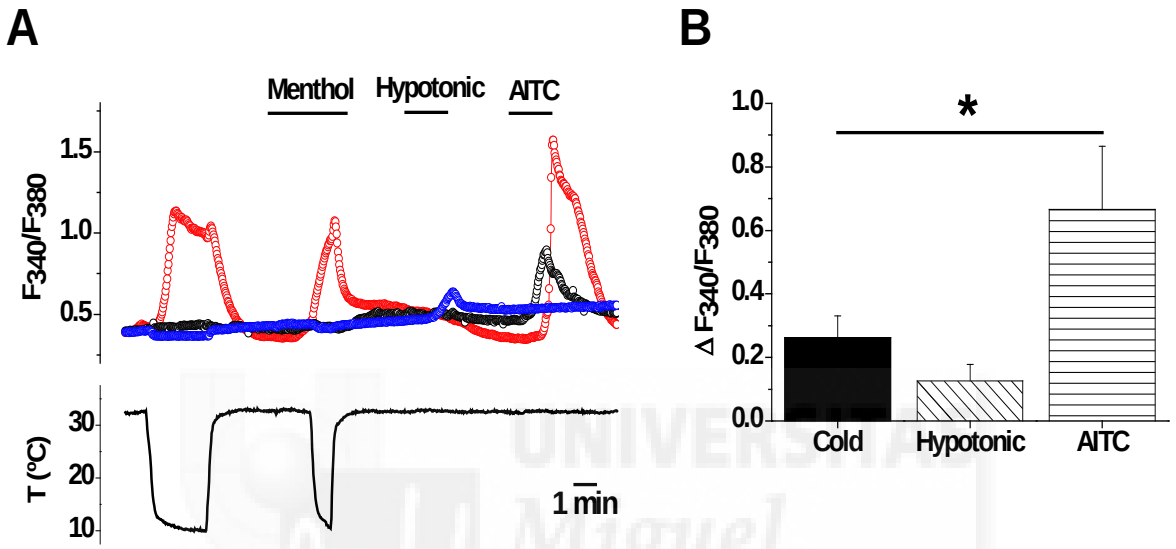

Figure 4.47. Effect of hypotonic solution and AITC on WT DiI+ TG neurons. Calcium imaging experiment showing (A) response characteristics of three DiI labeled TG neurons originating in the tongue from WT mice to a cold, menthol (100 µM), hypotonic solution (217 mOsm), and AITC (100 µM) application. Traces from top to bottom: change in $[Ca^{2+}]_i$ of the neurons; temperature recording of the bath solution. (B) Bar graphs summarizing the effect of cold, menthol (100 µM, n = 8), hypotonic solution (217 mOsm, n = 2), and AITC (100 µM, n = 4) on responses in WT DiI+ TG neurons. (* $p \leq 0.05$)

Response to capsaicin (0.5 µM)

A total of nine lingual neurons (21%) displayed an increase in $[Ca^{2+}]_i$ in response to capsaicin (0.5 µM), with a mean F_{340}/F_{380} ratio of 0.8 ± 0.2. This was significantly greater than the mean $[Ca^{2+}]_i$ increase to a cooling pulse alone ($p = 0.049$, Figure 4.48B). Of these nine neurons, four also displayed an increase in $[Ca^{2+}]_i$ to the cooling pulse. As stated above, four of the neurons with an increase in $[Ca^{2+}]_i$ to capsaicin (0.5 µM) also had a $[Ca^{2+}]_i$ increase to AITC (100 µM), with two of them having a $[Ca^{2+}]_i$ increase to the cooling pulse plus menthol (100 µM) as well. Two of the neurons had a $[Ca^{2+}]_i$ increase exclusively to capsaicin (0.5 µM). Examples of these types of responses can be seen in Figure 4.48A.

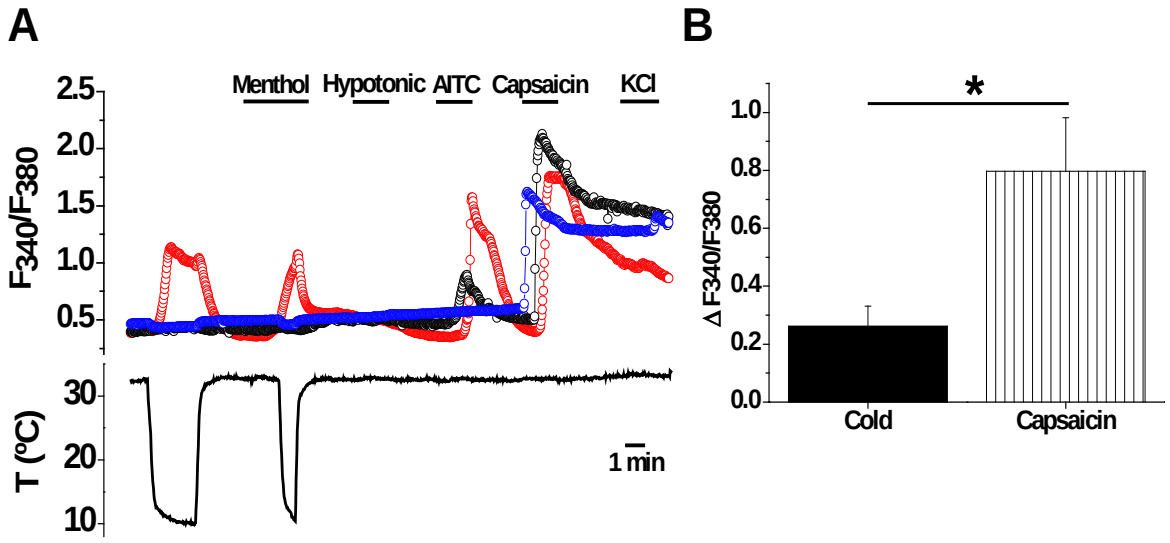

Figure 4.48. Effect of capsaicin on WT DiI+ TG neurons. Calcium imaging experiment showing (A) response characteristics of three DiI labeled TG neurons originating in the tongue from WT mice to a cold, menthol (100 µM), hypotonic solution (217 mOsm), AITC (100 µM), capsaicin (0.5 µM), and KCl (30 mM) application. Traces from top to bottom: change in $[Ca^{2+}]_i$ of the neurons; temperature recording of the bath solution. (B) Bar graphs summarizing the effect of cold, menthol (100 µM), hypotonic solution (217 mOsm), AITC (100 µM), capsaicin (0.5 µM), and KCl (30 mM) on responses in WT DiI+ TG neurons. (* $p \leq 0.05$)

4.2.2.2. TRPM8$^{-/-}$ neurons

TRPM8$^{-/-}$ mice labeled in the tongue with DiI were used to clearly identify the TG neurons with axons traveling in the lingual nerve. As with the WT neurons, DiI+ neurons were first identified on the coverslip, and the area with the largest number was selected. In the experiments with TRPM8$^{-/-}$ mice, 277 neurons were analyzed, 37 of which were DiI+ neurons. In these 37 neurons the F_{340}/F_{380} ratio change in $[Ca^{2+}]_i$ to different agonists was measured.

<u>Response to cold and menthol (100µM)</u>

In DiI+ TG neurons from TRPM8$^{-/-}$ mice a three minute cooling pulse with control solution alone did not increase the $[Ca^{2+}]_i$ in any of the neurons tested. When menthol (100 µM) was applied at 35ºC a modest increase in $[Ca^{2+}]_i$ was seen in two of the 37 neurons. When the cooling pulse was applied in the presence of menthol (100 µM) one of these neurons with an $[Ca^{2+}]_i$ increase to menthol (100 µM) at 35ºC did not show an increased in $[Ca^{2+}]_i$, while the other with an $[Ca^{2+}]_i$ increase to menthol (100 µM) did increase its $[Ca^{2+}]_i$ during

a cooling pulse. A sluggish $[Ca^{2+}]_i$ response was evoked in one other neuron by the cooling pulse applied during exposure to menthol (100 µM; Figure 4.49).

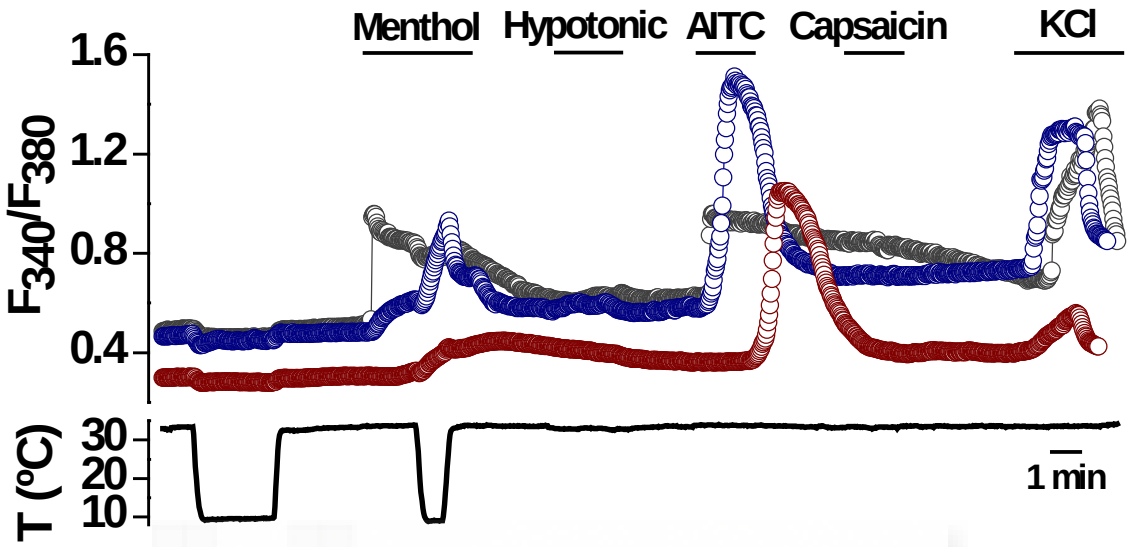

Figure 4.49. Effect of menthol on TRPM8$^{-/-}$ DiI+ TG neurons. Calcium imaging experiment showing response characteristics of three DiI labeled TG neurons originating in the tongue from TRPM8$^{-/-}$ mice to a cold, menthol (100 µM), hypotonic solution (217 mOsm), AITC (100 µM), capsaicin (0.5 µM), and KCl (30 mM) application. Traces from top to bottom: change in $[Ca^{2+}]_i$ of the neurons; temperature recording of the bath solution.

Response to hypotonic solution (217 mOsm)

Of the 37 DiI+ neurons a total of four (11%) showed an increase in $[Ca^{2+}]_i$ to a hypotonic solution (217 mOsm). An example can be seen in Figure 4.50. The mean F_{340}/F_{380} ratio difference for the four neurons with increase in $[Ca^{2+}]_i$ to hypotonic solution (217 mOsm) was 0.12 ± 0.04. Of these four, one also had an increase in $[Ca^{2+}]_i$ to AITC (100 µM).

Response to AITC (100 µM)

Six neurons, i.e. 15% of the total number of lingual neurons found in TRPM8$^{-/-}$ mice showed an increase in $[Ca^{2+}]_i$ to AITC (100 µM) with a mean F_{340}/F_{380} ratio difference of 0.55 ± 0.13. One of them had an increase in $[Ca^{2+}]_i$ to menthol (100 µM) and menthol (100 µM) plus a cooling pulse (Figure 4.50), and one neuron showed an increase in $[Ca^{2+}]_i$ to cold only during exposure to menthol (100 µM,). Of the other three neurons with an

increase in $[Ca^{2+}]_i$ to AITC (100 µM), one of them, as mentioned above, also showed an increase in $[Ca^{2+}]_i$ to hypotonic solution (217 mOsm).

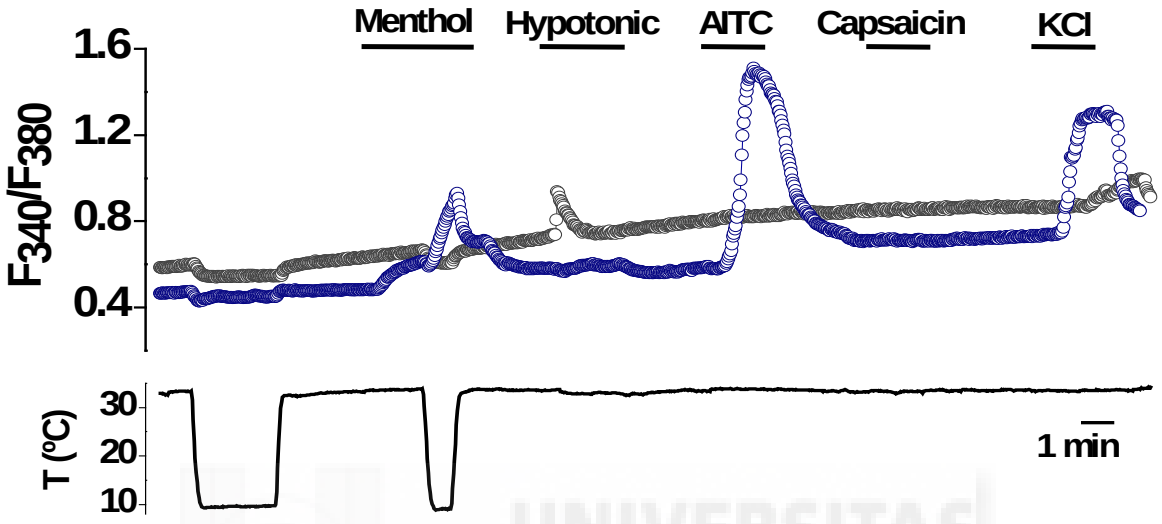

Figure 4.50. Effect of hypotonic solution and AITC on TRPM8$^{-/-}$ DiI+ TG neurons. Calcium imaging experiment showing (A) response characteristics of two DiI labeled TG neurons originating in the tongue from TRPM8$^{-/-}$ mice to a cold, menthol (100 µM), hypotonic solution (217 mOsm), and AITC (100 µM), capsaicin (0.5 µM), and KCl (30 mM) application. Traces from top to bottom: change in $[Ca^{2+}]_i$ of the neurons; temperature recording of the bath solution. (B) Bar graphs summarizing the effect of cold, menthol (100 µM), hypotonic solution (217 mOsm), and AITC (100 µM) on responses in TRPM8$^{-/-}$ DiI+ TG neurons.

Response to capsaicin (0.5 µM)

Of all the 37 DiI+ TRPM8$^{-/-}$ TG neurons only one exhibited an increase in $[Ca^{2+}]_i$ to capsaicin (0.5 µM). This neuron had a mean F_{340}/F_{380} ratio difference of 0.96. It did not show an increase in $[Ca^{2+}]_i$ to any of the other substances applied.

4.2.2.3. Comparison of WT and TRPM8$^{-/-}$ lingual neurons responsiveness

Figure 4.51 shows the change in the F_{340}/F_{380} ratio difference in the WT and TRPM8$^{-/-}$ DiI+ TG neurons to a cooling pulse and all of the applied substances, while Figure 4.52 shows the total percentage of WT and TRPM8$^{-/-}$ neurons that responded to each of the applied substances and the percentages of neurons responding to cold. None of the DiI+ neurons in

the TRPM8$^{-/-}$ mice showed an increase in $[Ca^{2+}]_i$ to a cooling pulse alone, only having an increase in $[Ca^{2+}]_i$ when menthol (100 µM) was present during the cooling pulse.

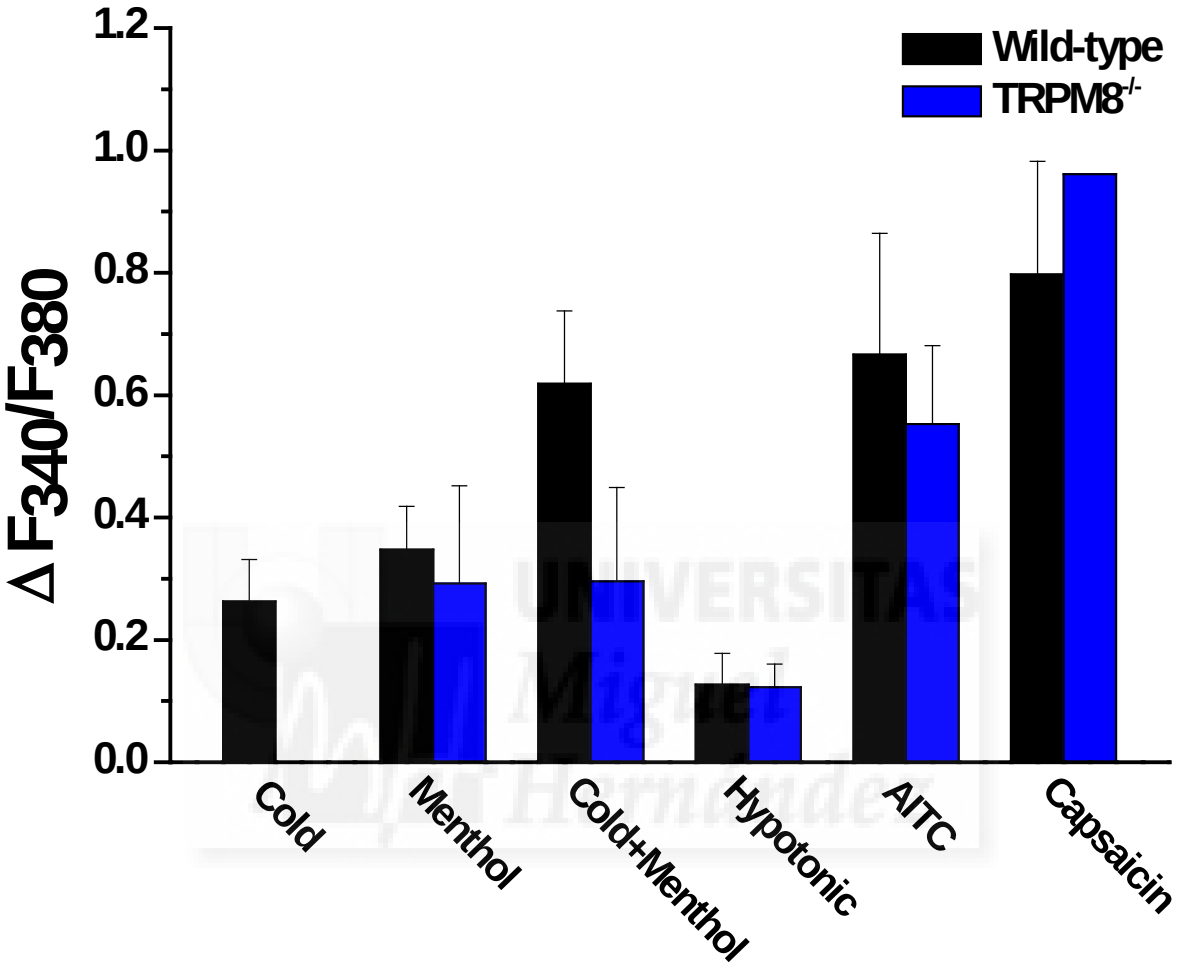

Figure 4.51. F_{340}/F_{380} ratio differences in WT and TRPM8$^{-/-}$ DiI+ neurons. Mean change in F_{340}/F_{380} ratio difference during cold, menthol (100 µM), cold + menthol (100 µM), hypotonic (217 mOsm), AITC (100 µM), and capsaicin (0.5 µM) application in WT and TRPM8$^{-/-}$ TG neurons.

The percentage of neurons with an increase in $[Ca^{2+}]_i$ to cold, menthol (100 µM), hypotonic solution (217 mOsm), AITC (100 µM), and capsaicin (0.5 µM) is represented in Figure 4.52A. The positive cold response here includes neurons with an increase in $[Ca^{2+}]_i$ to a cooling pulse and a cooling pulse during the presence of menthol (100 µM) together. The percentage of neurons with an increase in $[Ca^{2+}]_i$ to a cooling pulse as well as menthol (100 µM) greatly reduced in the TRPM8$^{-/-}$ neurons. The group of cold-sensitive neurons

that only showed an increase in $[Ca^{2+}]_i$ to menthol (100 µM), without an increase in $[Ca^{2+}]_i$ to AITC (100 µM), was completely absent in the TRPM8$^{-/-}$ neurons (25% of the WT DiI+ TG neurons and 0% of the TRPM8$^{-/-}$ DiI+ TG neurons), as shown in Figure 4.52B. All the cold-sensitive TRPM8$^{-/-}$ DiI+ TG neurons also had an increase in $[Ca^{2+}]_i$ to AITC (100 µM).

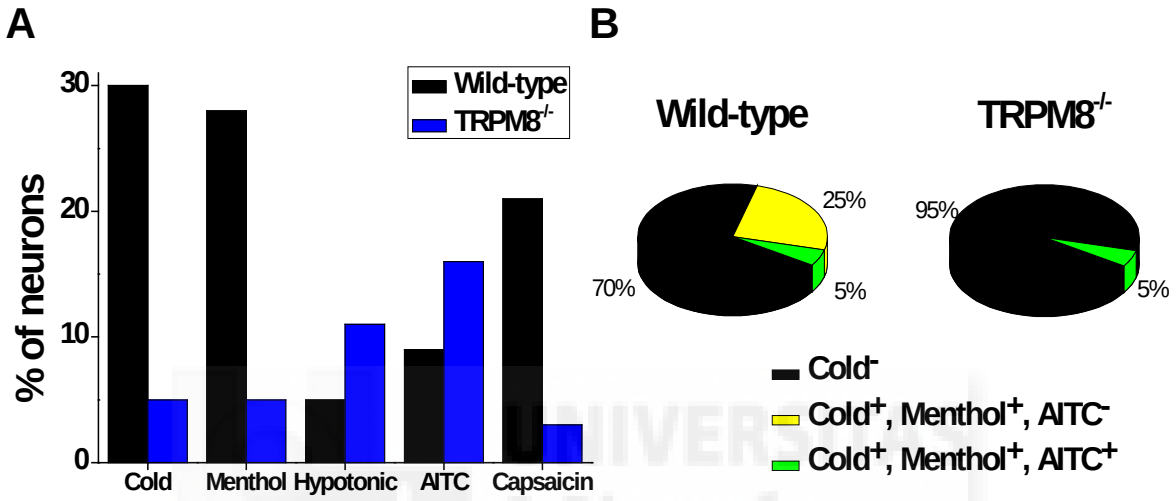

Figure 4.52. Responses in DiI+ labeled TG neurons. (A) Comparison of the neurons responding to cold, menthol (100 µM), hypotonic solution (217 mOsm), AITC (100 µM), and capsaicin (0.5 µM) in WT and TRPM8$^{-/-}$ mice. (B) Charts showing the percentages of cold-insensitive and two types of cold-sensitive responses in WT and TRPM8$^{-/-}$ DiI+ labeled neurons.

4.3. Water intake

The contribution of the various classes of cold-sensitive fibers of the tongue and their various transducing mechanisms to the regulation of water intake was analyzed in WT and TRPM8$^{-/-}$ and/or TRPA1$^{-/-}$ mice. An experimental cage was designed to allow the adjustment of the temperature of the mouse's drinking water to the desired temperature value. In the group of No-Choice Water Temperature experiments, a single bottle containing water at a given temperature was offered to the animal. In the group of Water Temperature Preference experiments, a control bottle with water at room temperature, 22ºC, was tested against a second bottle at varying temperatures (40º, 30º, 15º, 10º, and 5ºC). Animals were water-deprived 24 hours before the test, which was performed during a one hour period. Number of entries to drink, total time spent drinking (s), and volume of water drunk (ml) were all recorded during the experiments (see METHODS).

4.3.1. Drinking during No-Choice Water Temperature experiments.

In these experiments, no temperature alternative for the water was offered obligating the mice to drink the water at the temperature provided (40º, 30º, 22º, 15º, 10º, and 5ºC). The same parameters were measured for the WT (n = 9) and KO (TRPM8$^{-/-}$ n = 6, TRPA1$^{-/-}$ n = 10, TRPM8$^{-/-}$/TRPA1$^{-/-}$ n = 8) groups of mice.

4.3.1.1. Wild-type mice

At room temperature (22ºC) during the one-hour test performed after the 24h-water deprivation period, WT mice entered to drink a mean of 16 ± 1.3 times/hr and spent a mean of 124.6 ± 12.6 s/hr drinking, with a mean of 7.9 ± 0.6 s/entry. Also, at 22ºC, mice drank a mean of 1.2 ± 0.1 ml/hr, as seen in Figure 4.53. The fewest number of entries for all the temperature tested was the control temperature of 22ºC. When the water was heated or cooled from 22ºC, mice entered increasingly more times to drink, entering significantly

more when the water temperature was set at 40º, 30º, 10º, and 5ºC. The largest difference from 22ºC was found at 5ºC where mice entered a mean of 27.7 ± 2.1 entries/hr, $p < 0.001$). A similar trend was seen in the amount of time spent drinking, where mice spent increasingly more time as the water was heated or cooled from 22ºC. However, the amount of time spent drinking became significant at 5ºC, where mice drank for a mean of 194.6 ± 11.8 s/hr ($p < 0.001$) which represent 156% more time devoted to drinking than at room temperature. While WT mice entered more times to drink and spent more time drinking as temperatures were changed from room temperature, there was no significant difference in the amount of total water consumed between the different temperatures.

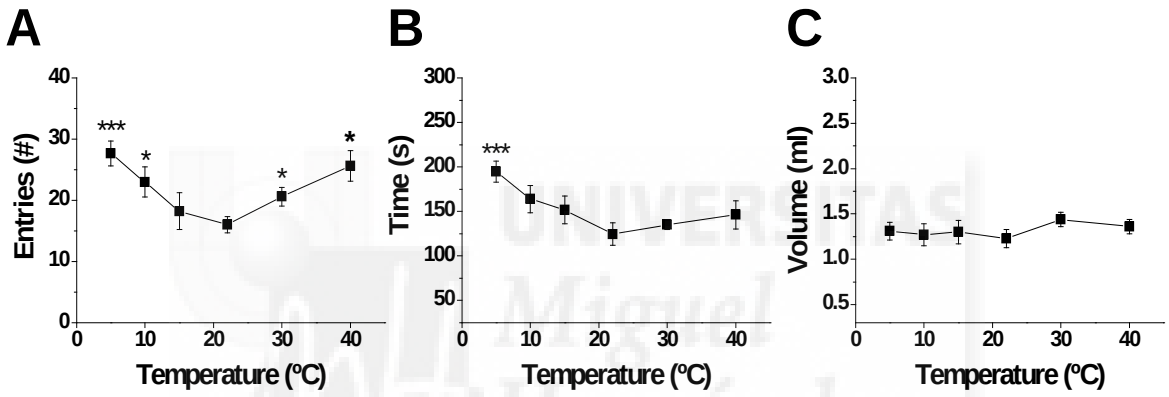

Figure 4.53. No-choice drinking behavior of WT mice during different temperatures. Mean numbers of (A) entries made to drink, (B) time spent drinking, and (C) volume of water consumed over the different temperature trials. Values are compared to the control temperature at 22ºC (* $p \leq 0.05$ and *** $p \leq 0.001$).

4.3.1.2. TRPM8$^{-/-}$ mice

At room temperature, TRPM8$^{-/-}$ mice entered to drink a mean of 13.3 ± 1.6 entries/hr, and they spent a mean time drinking of 74.7 ± 11.1 s/hr, with a mean of 5.7 ± 0.8 s/entry. They drank at 22ºC a mean volume of 0.75 ± 0.1 ml/hr. While the number of entries made to drink was similar to the WT mice at 22ºC, the mean time spent drinking and the total volume ingested were significantly lower than in the WT ($p = 0.016$ and $p = 0.008$, respectively). When considering the number of entries made to drink at the various temperatures, TRPM8$^{-/-}$ mice did not enter significantly more times as temperature rose or fell, as observed in the WT mice. At cooler temperatures, there was a slight increase in the

entries made, but these values were not significant for any of the temperatures. Also in the amount of time spent drinking, there were no significant differences across any of the temperatures tested, with all the values being lower than their corresponding WT temperature values. The total amount of water drunk for all temperatures was also lower for the TRPM8$^{-/-}$ mice when compared to the total at the same temperatures in the WT. The mean volume of water however, within the TRPM8$^{-/-}$ temperature groups did not significantly change for any temperature except for when the water was the coldest. At 5ºC mice drank a significantly less volume of water compared to when the water was at room temperature ($p = 0.01$). Overall, TRPM8$^{-/-}$ mice showed a striking reduction of total drinking resulting of shorter and more infrequent entries to drink (Figure 4.54). This effect appeared to be rather independent of the drinking water temperature.

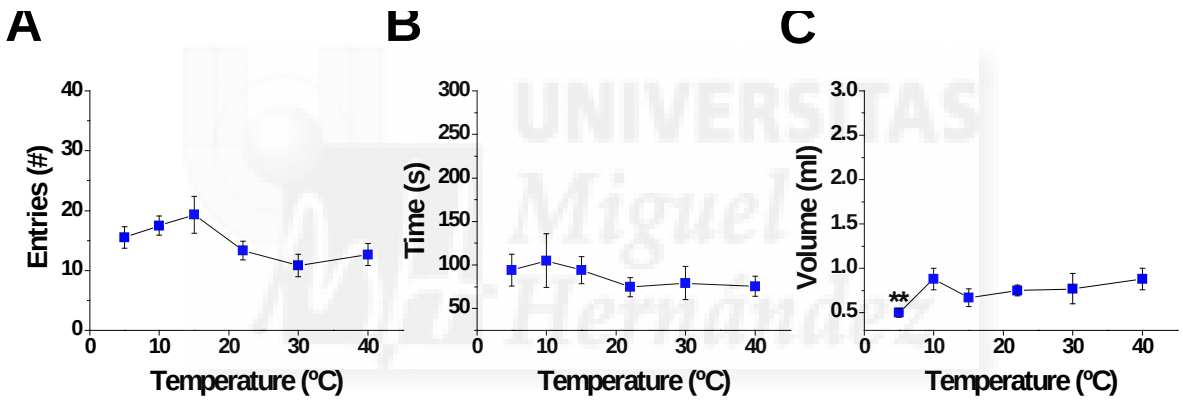

Figure 4.54. No-choice drinking behavior of TRPM8$^{-/-}$ mice during different temperatures. Mean numbers of (A) entries made to drink, (B) time spent drinking, and (C) volume of water consumed over the different temperature trials. Values are compared to the control temperature at 22ºC (** $p \leq 0.01$).

4.3.1.3. TRPA1$^{-/-}$ mice

At room temperature TRPA1$^{-/-}$ mice had a mean of 16.6 ± 1.7 entries/hr and spent a mean of 159.8 ± 22.7 s/hr drinking, with a mean of 9.8 ± 0.9 s/entry. They also drank a mean volume of 1.55 ± 0.1 ml/hr of water (Figure 4.55). All of these control values were similar to what was found in the WT mice at room temperature. In regards to the average number of entries, TRPA1$^{-/-}$ mice showed the same trend as did the WT mice; as the temperature was warmed or cooled from 22ºC more entries to drink were made. These values were

significant at 40º, 10º, and 5ºC. The largest difference was seen at 5ºC were the mean number of entries made was 29.8 ± 4.3 entries/hr ($p = 0.01$). When considering the mean amount of time spent drinking at the different temperatures, while all the means for the different temperatures were higher in the TRPA1$^{-/-}$ mice than in the WT, as in the WT, there was not a significant increase in the amount of time when the water was heated above room temperature. However, as the water was cooled, mice spent a significantly longer amount of time drinking compared to when the water was at 22ºC. Here the largest difference was observed at 10ºC, with a mean amount of time spent drinking of 259 ± 30.1 s/hr ($p = 0.017$).

The mean volume of water consumed at the different temperatures for the TRPA1$^{-/-}$ mice, was similar to the amount consumed at room temperature, except at two of the temperatures, 30ºC and 15ºC where the mice drank significantly more than at room temperature. At both 30 and 15ºC mice drank a mean of 2.0 ± 0.2 ml/hr ($p = 0.038$ and $p = 0.039$, respectively). Also, the mean volume of water consumed was higher for every temperature tested compared to the amount of water consumed in the WT mice. Overall, the TRPA1$^{-/-}$ mice drank a significantly larger amount of water and spent more time drinking than the WT mice.

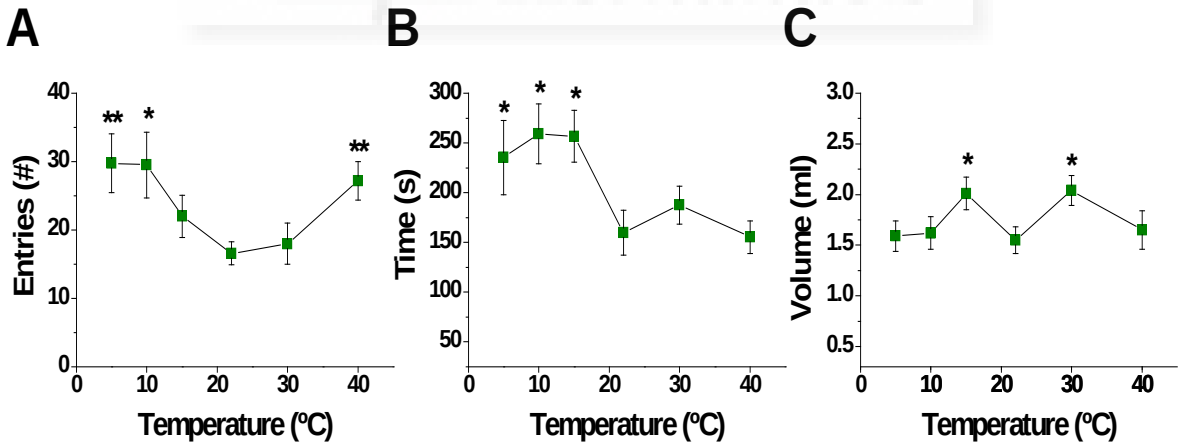

Figure 4.55. No-choice drinking behavior of TRPA1$^{-/-}$ mice during different temperatures. Mean numbers of (A) entries made to drink, (B) time spent drinking, and (C) volume of water consumed over the different temperature trials. Values are compared to the control temperature at 22ºC (* $p \leq 0.05$ and ** $p \leq 0.01$).

4.3.1.4. TRPM8$^{-/-}$/TRPA1$^{-/-}$ mice

At room temperature TRPM8$^{-/-}$/TRPA1$^{-/-}$ mice entered to drink a mean of 6.4 ± 0.6 times/hr and spent a mean of 107.4 ± 9.7 s/hr drinking, with a mean of 19.0 ± 3.5 s/entry. Also, at 22ºC, mice drank a mean of 1.0 ± 0.1 ml/hr, as seen in Figure 4.56. While the mean amount of time spent drinking and mean amount of volume drunk were lower than the WT value, they were not significantly lower. However, the mean number of entries to drink was significantly higher than in the WT ($p < 0.001$) also making the mean amount of time per entry significantly higher as well ($p = 0.002$).

Considering the number of entries made to drink, a significantly higher number of entries was made when the water was at 30ºC ($p = 0.019$), 15ºC ($p = 0.002$), and 5ºC ($p = 0.039$). The highest difference was found at 15ºC were mice entered to drink at a mean of 10.4 ± 0.8 entries/hr. The amount of time spent drinking was relatively consistent despite the temperature of the drinking water, expect at 40ºC were mice drank for a significantly less amount of time, 78.9 ± 5.1 s/hr, than at room temperature ($p = 0.028$). Again, as seen in the WT, the total volume of water consumed was not affected based on the temperature of the water, with no significant differences among the various temperature tests

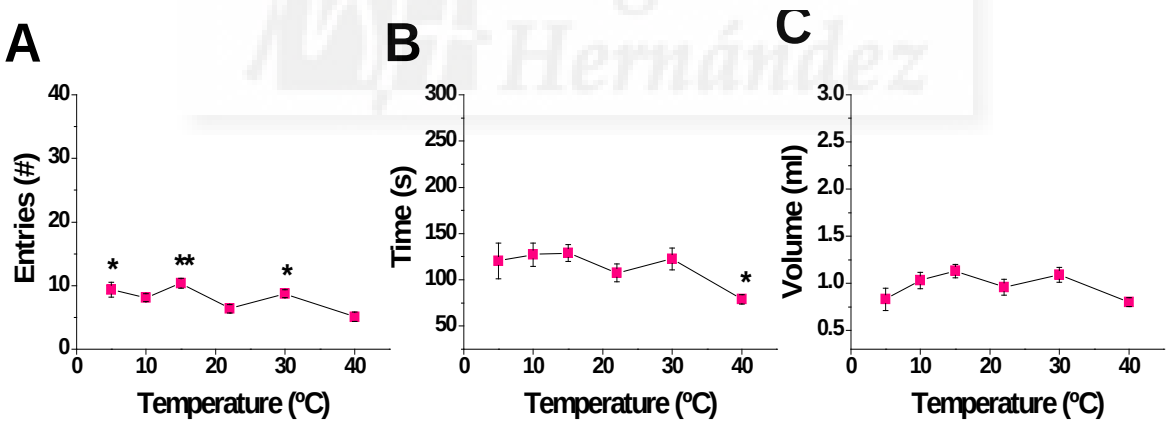

Figure 4.56. No-choice drinking behavior of TRPM8$^{-/-}$/TRPA1$^{-/-}$ mice during different temperatures. Mean numbers of (A) entries made to drink, (B) time spent drinking, and (C) volume of water consumed over the different temperature trials. Values are compared to the control temperature at 22ºC (* $p \leq 0.05$ and ** $p \leq 0.01$).

4.3.2. Drinking during Water Temperature Preference experiments

As explained above, in these experiments the animal was free to choose to drink during the 1-hour test period from one of the two bottles of water available. One of them was at 22ºC in all the experiments whereas the other was at 40º, 30º, 22º, 15º, 10º, or 5ºC in each experiment.

4.3.2.1. Wild-type mice

When both drinking bottles were at room temperature (22ºC), the mice drank from both bottles equally in respect to the mean number of entries to drink (10.5 ± 1.6 entries/hr and 8.3 ± 1.5 entries/hr, $p = 0.326$, $n = 15$), total time spent drinking (42.1 ± 4.0 s/hr and 37.6 ± 5.5 s/hr, $p = 0.513$, $n = 15$), and also in total water volume drunk (0.5 ± 0.1 ml/hr and 0.3 ± 0.1 ml/hr, $p = 0.213$, $n = 6$). Since the mice were previously trained to drink from the water bottles as placed in the experimental cage, within the first minute of starting the experiment the majority of mice went directly to the area of the water bottles. Mice would explore the bottles, initially drinking from both bottles. If no preference was made based on the water temperature, mice alternated drinking from both bottles. When the temperature of one of the bottles was lowered or raised, particularly if the temperature was extreme, the mice approached the bottle to explore with the snout, and at times would avoid it all together. In most cases initial entries were made to drink in both bottles before the preferred temperature was decided. Altogether, as seen in Figure 4.57, as the water temperature was increasingly warmer or cooler around 22ºC, mice drank increasingly less and spent less time drinking from these bottles, clearly preferring the bottle at 22ºC.

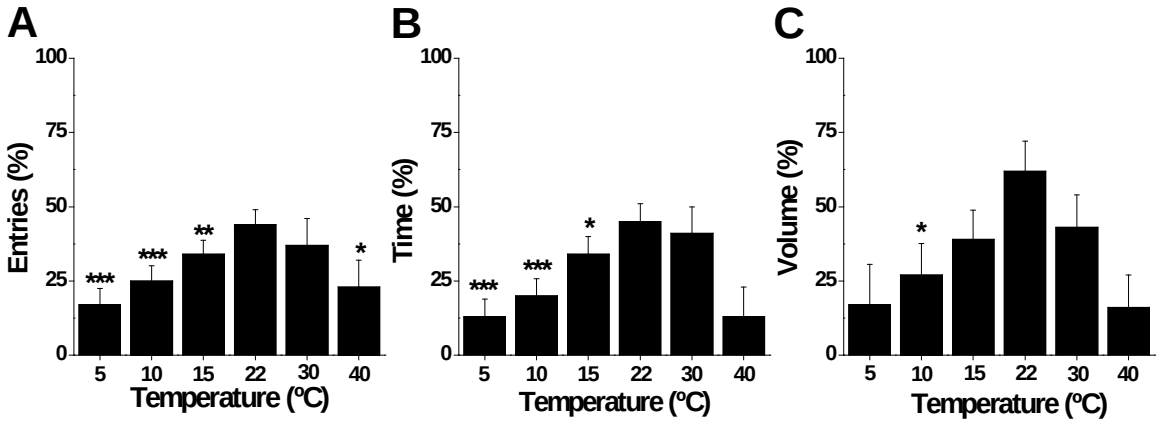

Figure 4.57. Drinking water temperature preference in WT mice. (A) Entries, (B) drinking time, and (C) volume drunk at the bottle where temperature was varied expressed as percent of entries, time, or volume of an additional control bottle at room temperature, 22ºC. (* $p \leq 0.05$, ** $p \leq 0.01$, *** $p \leq 0.001$)

There was a general tendency of WT mice to reduce the percentage of entries made, time spent drinking, and volume ingested to the bottle at warmer temperatures, preferring room temperature water, although the only significant difference was seen in the percentage of entries made when the drinking water was at 40ºC over room temperature ($p = 0.033$). The mean number of entries made at 40ºC was 4.0 ± 1.5 entries/hr, as compared to 18.2 ± 4.4 entries/hr at 22ºC. At cooler temperatures a significant decrease in the percentage of entries and the percentage of time spent drinking was found in the 22/15ºC, 22/10ºC, and 22/5ºC experiments. The largest difference in percentage was seen during the 22/5ºC experiment ($p < 0.001$, entries and $p = 0.001$, time). The mean number of entries dropped from 13.9 ± 1.4 entries/hr at room temperature to 2.9 ± 1.0 entries/hr at 5ºC. The mean time spent drinking dropped from 61.5 ± 6.1 s/hr at 22ºC to 10.2 ± 5.3 s/hr at 5ºC. When considering the percentage of water volume drank, while the trend showed a preference for water at 22ºC over all other temperatures, the only significant difference was observed in the 22/10ºC where mice drank a significantly higher percentage of water at 22ºC over water at 10ºC ($p = 0.03$). Mean volumes were 0.4 ± 0.1 ml/hr at room temperature and 0.2 ± 0.1 ml/hr at 10ºC.

Additionally, when considering the total volume of water that was drunk when adding the volume of the two bottles together during the one hour period (as seen in Figure 4.58), with the option 40/22ºC and 30/22ºC, mice drank a significantly greater total volume of water

(1.3 ± 0.2 ml and 1.1 ± 0.1 ml respectively) than with both bottles at room temperature (0.8 ± 0.04 ml, p = 0.031 and p = 0.015 respectively). Contrarily, when bottles were set at 22/10ºC mice drank a significantly lower total volume of water (0.6 ± 0.1 ml, p = 0.021).

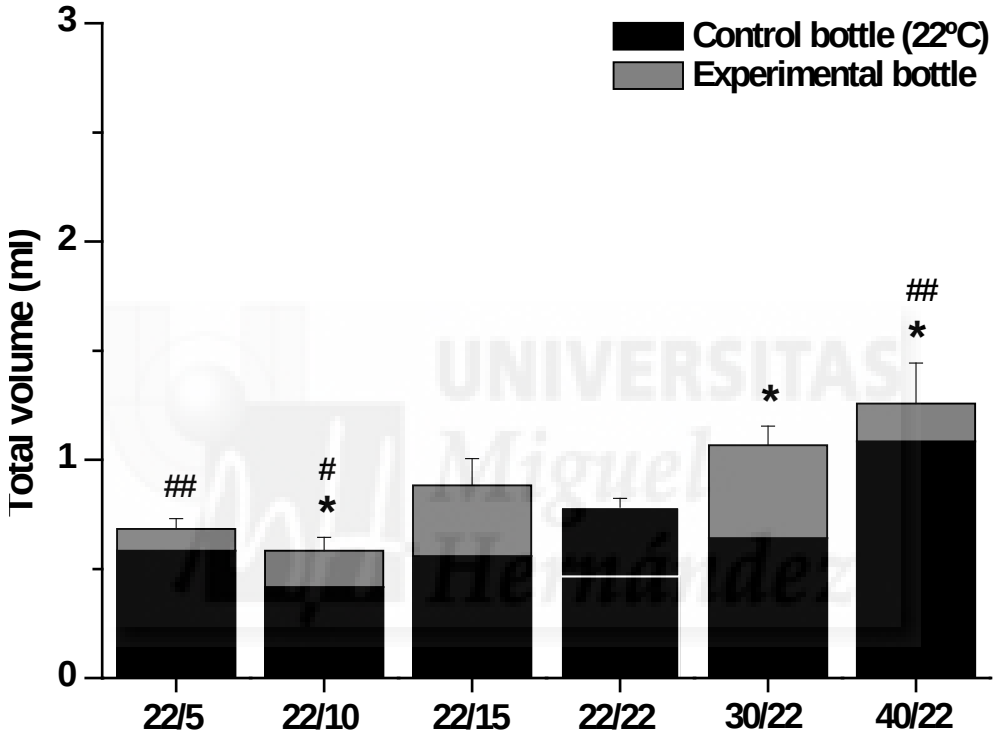

Figure 4.58. Water volume ingested at different temperature in WT mice. Total volume of water drunk between the experimental and control bottles over the one hour test period compared to the control group of 22/22ºC (* $p \leq 0.05$). Mean volume of water drunk from the control bottle compared to the experimental bottle during each temperature trial (# = 0.047, ## ≤ 0.01).

The overall conclusion of these experiments is that when presented with a choice of water temperatures in the preference experiments, WT mice avoided water that was below 15ºC and also water at 40ºC. Also, thirst following deprivation appears to be satiated with a lower volume of water when its temperature was low.

4.3.2.2. TRPM8$^{-/-}$ mice

TRPM8$^{-/-}$ mice showed a very different water temperature preference profile compared to WT mice. As expected, with both drinking bottles at room temperature they drank equally from both with regards to the mean number of entries to drink (7.4 ± 1.6 entries/hr and 7.3 ± 1.1 entries/hr, $p = 0.933$, $n = 12$), mean time spent drinking (68.5 ± 14.2 s/hr and 92.3 ± 19.4 s/hr, $p = 0.488$, $n = 12$), and also in mean water volume drunk (0.7 ± 0.1 ml/hr and 0.8 ± 0.2 ml/ hr, $p = 0.558$, $n = 9$).

As occurred with WT mice, TRPM8$^{-/-}$ mice avoided the 40ºC water and also preferred room temperature (22ºC) water over 30ºC water. As seen in Figure 4.59, values were significantly lower in terms of percentage of entries made to drink, percentage of time spent drinking, and percent of volume drunk. There was a clear preference for room temperature water over 40ºC and 30ºC. In contrast, with the cooler water however, the preference trend observed in the TRPM8$^{-/-}$ mice was much different from that of the WT mice. TRPM8$^{-/-}$ mice did not avoid the cooler water, even preferring it over 22ºC in some instances. In the 22/10ºC experiment, when compared to the 22ºC bottle (4.8 ± 1.4 entries/hr, $p = 0.012$) mice showed a significant increase in the percentage of entries made at 10ºC bottle (12.3 ± 2.2 entries/hr). The same was true in the 22/5ºC experiment (6.5 ± 2.0 entries/hr, 22ºC and 17.1 ± 3.2 entries/hr, 5ºC), where the percentage of entries was significantly higher in the 5ºC water bottle ($p = 0.049$). Regarding the percentage of time, there was also a significant increase in the 22/10ºC experiment where the mean amount of time was 29.5 ± 7.7 s/hr for the bottle at room temperature compared to 113.0 ± 19.8 s/hr for the bottle at 10ºC ($p = 0.014$). While the percentage of volume drunk was not significantly greater in the cooler water compared to the room temperature water, there was still a general trend to the preference of the cooler water, remarkably different from the avoidance observed in the WT mice.

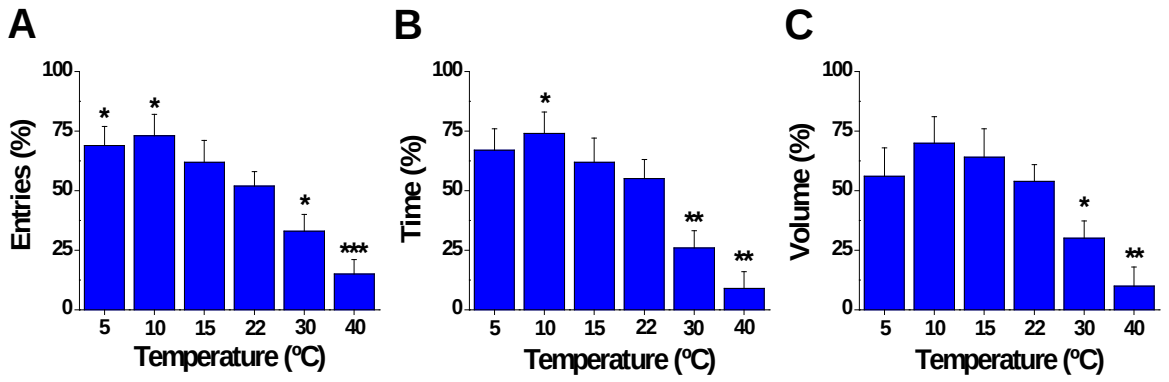

Figure 4.59. Drinking water temperature preferences in TRPM8$^{-/-}$ mice. Percentage of the total average (A) entries, (B) time, and (C) volume drunk at the bottle at the given temperature, compared to the percentage of entries, time, or volume of an additional control bottle at room temperature, 22ºC. (* $p \leq 0.05$, ** $p \leq 0.01$, *** $p \leq 0.001$)

In regards to the total amount of water drunk, in ml, of the two bottles together, there was no significant difference in any of the temperature groups compared to the total in the 22/22ºC experiment (Figure 4.60). The total volume at 22/22ºC, 1.4 ± 0.2 ml/hr, was significantly higher than the total volume drunk at 22/22ºC in the WT mice ($p = 0.015$). The total volumes drank at 22/10ºC (1.2 ± 0.1 ml/hr) and at 22/5ºC (1.2 ± 0.1 ml/hr) were also significantly higher than the total volume drank in the WT at the same temperatures.

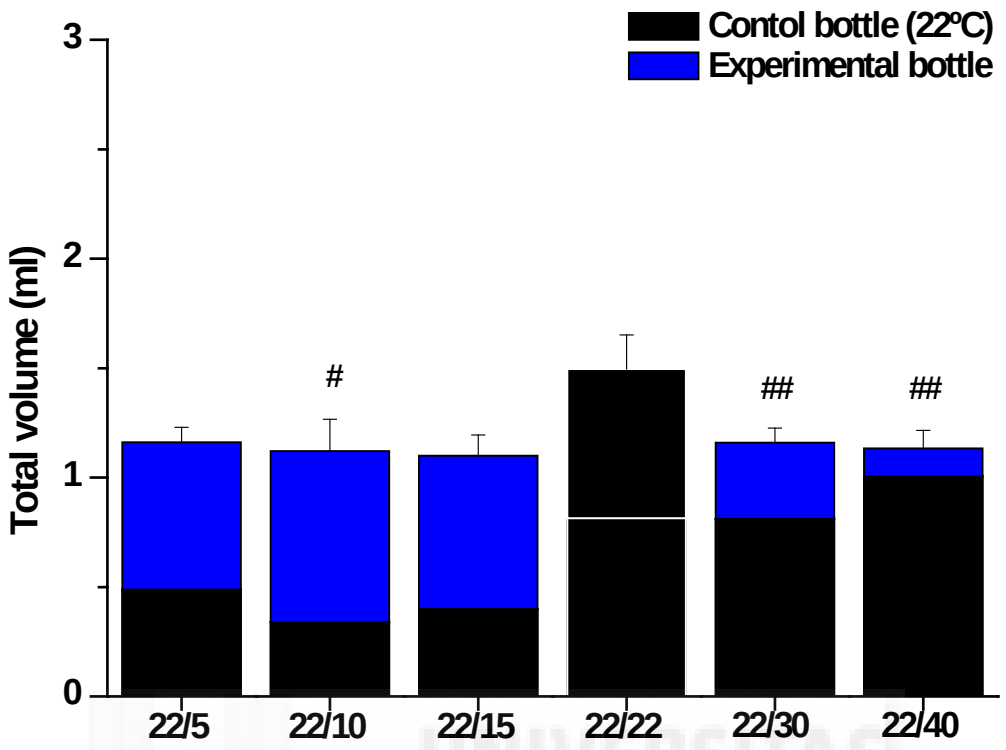

Figure 4.60. Total volume of water drunk by TRPM8$^{-/-}$ mice. Water volumes consumed from the experimental and control bottles over the one hour test period were added. Comparison between values at 22º/22ºC and the rest did not show significant differences. Mean volume of water drunk from the control bottle compared to the experimental bottle during each temperature trial (# = 0.037, ## ≤ 0.01).

4.3.2.3. TRPA1$^{-/-}$ mice

In TRPA1$^{-/-}$ mice, with both drinking bottles at room temperature, mice drank equally from both bottles with regards to the mean number of entries to drink (12.8 ± 1.4 entries/hr and 10.4 ± 1.9 entries/hr, p = 0.186, n = 10), mean time spent drinking (103.3 ± 7.6 s/hr and 93.4 ± 16.3 s/hr, p = 0.588, n = 10), and also in mean water volume drunk (0.9 ± 0.1 ml/hr and 0.9 ± 0.1 ml/hr, p = 0.841, n = 10). Similar to the WT preferences, TRPA1$^{-/-}$ mice also avoided water at high and low temperatures (Figure 4.61).

In all three of the parameters studied, mice avoided drinking water at 40ºC when presented with a choice over water at 22ºC. Percentages of entries, time, and volume were all significantly lower at 40ºC. Drinking water at 30ºC was preferred over room temperature water, significantly so when considering the percent of water volume consumed

($p = 0.039$). Mean consumption at these temperatures was 1.2 ± 0.2 ml/hr at 30ºC and 0.5 ± 0.2 ml/hr at 22ºC.

When choosing between water at low temperature and water at room temperature, TRPA1$^{-/-}$ mice showed a clear preference for water at 22ºC over cooler water. As seen in Figure 4.61, for all three temperature experiments, 22/15ºC, 22/10ºC, and 22/5ºC, there was a significant decrease in the percentage of entries made to drink, time spent drinking, and volume of water ingested. The largest difference was observed in the 22/5ºC with a significant decrease in the percentage of entries ($p < 0.001$) where the mean number of entries dropped from 19.6 ± 2.6 entries/hr (22ºC) to 6.1 ± 1.3 entries/hr (5ºC), a significant decrease in the percentage of time spent drinking ($p = 0.002$) where mean amount of time decreased from 179.8 ± 11.9 s/hr (22ºC) to 33.1 ± 15.3 s/hr (5ºC), and a significant decrease in the percentage of volume ingested ($p = 0.002$) where mean amount of water volume dropped from 1.7 ± 0.1 ml/hr (22ºC) to 0.2 ± 0.1 ml/hr (5ºC).

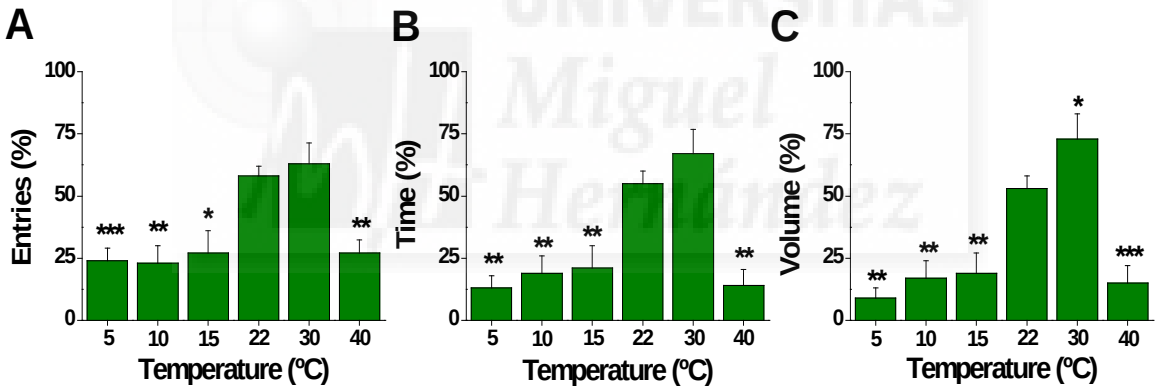

Figure 4.61. Drinking water temperature preferences in TRPA1$^{-/-}$ mice. Percentage of the mean (A) entries, (B) time, and (C) volume drunk at the bottle at the given temperature, compared to the percentage of entries, time, or volume of an additional control bottle at room temperature, 22ºC. (* $p \leq 0.05$, ** $p \leq 0.01$, *** $p \leq 0.001$)

There were no differences in the total amount of water ingested in ml between any of the temperature preference groups compared to the total of water ingested during the control 22/22ºC experiment (Figure 4.62). However the total amount of water drank during each temperature preference experiment was significantly greater than the same temperature preference experiment in the WT: 40/22ºC, 2.2 ± 0.2 ml/hr ($p = 0.012$); 30/22ºC,

1.8 ± 0.2 ml/hr (p = 0.026); 22/22ºC, 1.8 ± 0.2 ml/hr (p = 0.001); 22/15ºC, 1.7 ± 0.2 ml/hr (p = 0.016); 22/10ºC, 1.6 ± 0.2 (p = 0.001); and 22/5ºC, 1.9 ± 0.1 ml/hr (p < 0.001).

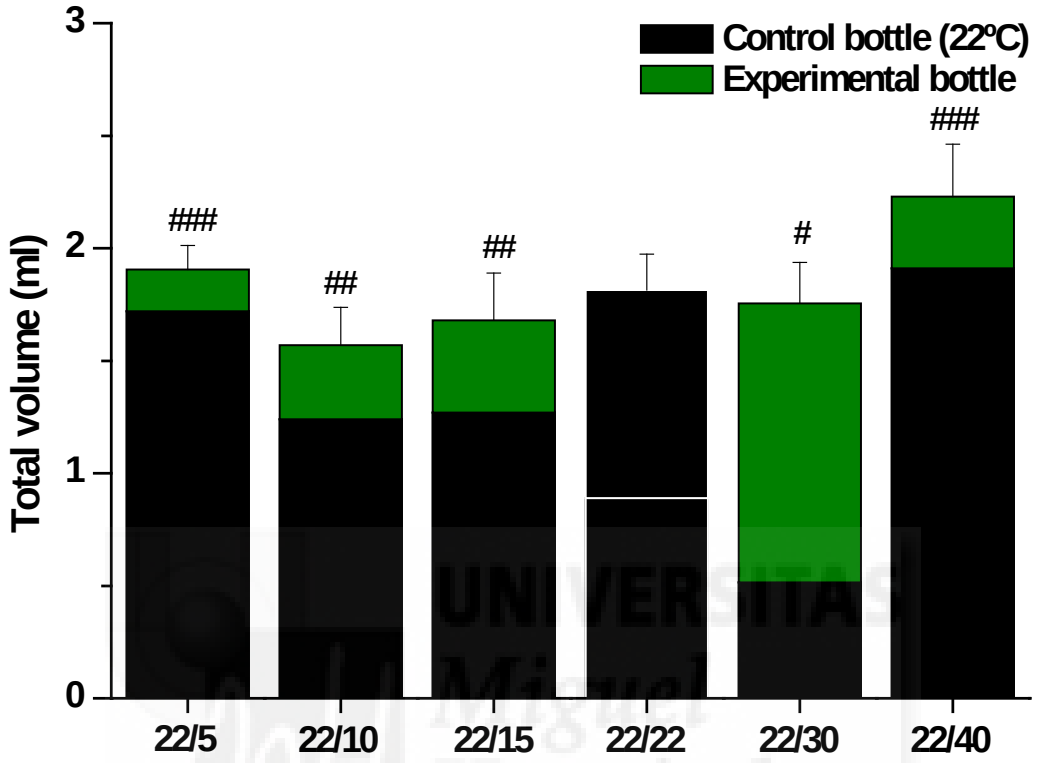

Figure 4.62. Total volume of water drunk by TRPA1$^{-/-}$ mice. Water volumes consumed from the experimental and control bottles over the one hour test period were added. Comparison between values at 22º/22ºC and the rest did not show significant differences. Mean volume of water drunk from the control bottle compared to the experimental bottle during each temperature trial (# = 0.028, ## ≤ 0.01, ### < 0.001).

4.3.2.4. TRPM8$^{-/-}$/TRPA1$^{-/-}$ mice

In TRPM8$^{-/-}$/TRPA1$^{-/-}$ mice, mice drank equally from both bottles at 22ºC with regards to the mean number of entries to drink (5.9 ± 0.8 entries/hr and 5.5 ± 1.1 entries/hr, p = 0.781, n = 16), mean time spent drinking (70.0 ± 14.7 s/hr and 50.1 ± 12.0 s/hr, p = 0.303, n = 16), and also in mean water volume drunk (0.6 ± 0.2 ml/hr and 0.5 ± 0.2 ml/hr, p = 0.901, n = 6). TRPM8$^{-/-}$/TRPA1$^{-/-}$ mice showed a clear temperature preference to the cooler water over room temperature water, as seen in Figure 4.63. When water was set at warmer temperatures, 40ºC and 30ºC, while there was a slightly lower value of all three parameters

to these temperatures over drinking water at 22ºC, none of them were significantly different. Regarding the percentage of entries made to drink and the percentage of time spent drinking, their values were significantly higher for water at 15ºC, 10ºC, and 5ºC. The largest percentage difference came during the 22/5ºC experiment ($p = 0.001$, entries and time), where the mean number of entries was only 2.9 ± 0.7 entries/hr at 22ºC and 11.6 ± 1.7 entries/hr at 5ºC, and the mean amount of time spent drinking was 29.1 ± 11.2 s/hr (22ºC) and 136.9 ± 18.8 s/hr (5ºC). Regarding the volume of water consumed during the different temperature experiments, the only significant difference was seen in the 22/10ºC experiment, where mice drank a significantly larger percentage of volume of water at 10ºC as compared to 22ºC ($p = 0.004$). The mean amount of water consumed at room temperature was 0.3 ± 0.1 ml/hr and increased to a mean of 1.1 ± 0.2 ml/hr at 10ºC.

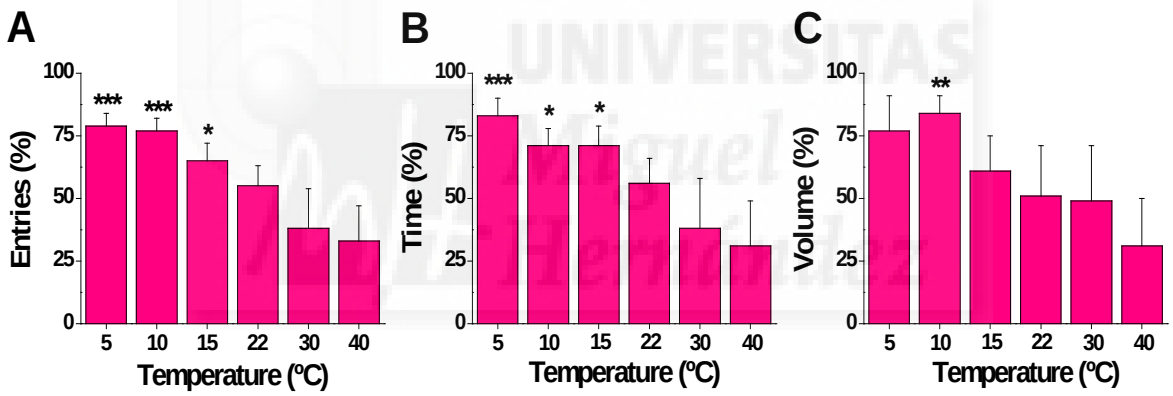

Figure 4.63. Drinking water temperature preferences in TRPM8$^{-/-}$/TRPA1$^{-/-}$ mice. Percentage of the mean (A) entries, (B) time, and (C) volume drunk at the bottle at the given temperature, compared to the percentage of entries, time, or volume of an additional control bottle at room temperature, 22ºC. (* $p \leq 0.05$, ** $p \leq 0.01$, *** $p \leq 0.001$)

When considering the total volume of water drunk between the two bottles in the different trials, TRPM8$^{-/-}$/TRPA1$^{-/-}$ mice drank a mean of 1.1 ± 0.1 ml/hr when both bottles were at room temperature. This is a significantly larger amount of water consumed than the WT at room temperature ($p = 0.018$). As seen in Figure 4.64, the largest mean amount of water consumed came during the 22/10ºC trials, 1.6 ± 0.1 ml/hr, which was significantly higher than control trial at room temperature ($p = 0.009$). Additionally, during the temperature

preference tests at lower temperatures (22/15ºC, 22/10ºC, and 22/5ºC) mice drank significantly more water than the WT mice at the same temperatures (1.4 ± 0.1 ml/hr, p = 0.009; 1.6 ± 0.1 ml/hr, p = 0.002; and 1.3 ± 0.2 ml/hr, p = 0.003, respectively).

A summary of drinking patterns during the drinking temperature preference tests of the WT, TRPM8$^{-/-}$, TRPA1$^{-/-}$, and TRPM8$^{-/-}$/TRPA1$^{-/-}$ mice can be found in Table 4.10.

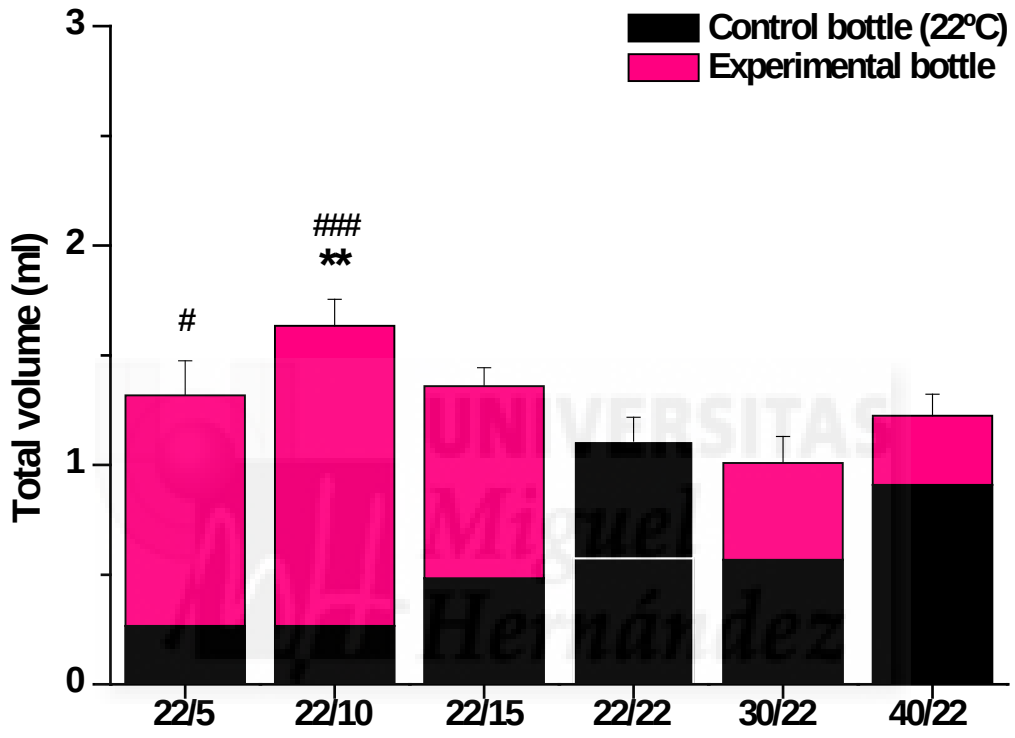

Figure 4.64. Total volume of water drunk TRPM8$^{-/-}$/TRPA1$^{-/-}$ mice. Total volume ingested between the experimental and control bottles over the one hour test period. (** p = 0.009). Mean volume of water drunk from the control bottle compared to the experimental bottle during each temperature trial (# ≤ 0.017, ### < 0.001).

Temp (ºC)		WT				TRPM8$^{-/-}$			
		% Entries	% Time	% Volume	Total Volume	% Entries	% Time	% Volume	Total Volume
40	22	–*/ +	–/ +	–/ +	+ *	–***/ +	–**/ +	–**/ +	–
30	22	–/ +	–/ +	–/ +	+ *	–*/ +	–**/ +	–*/ +	–
22	22	=	=	=		=	=	=	
15	22	–**/ +	–*/ +	–/ +	+	+ /–	+ /–	+ /–	–
10	22	–***/ +	–***/ +	–*/ +	–*	+ */–	+ */–	+ /–	–
5	22	–***/ +	–***/ +	–/ +	–	+ */–	+ /–	=	–

Temp (ºC)		TRPA1$^{-/-}$				TRPM8$^{-/-}$/TRPA1$^{-/-}$			
		% Entries	% Time	% Volume	Total Volume	% Entries	% Time	% Volume	Total Volume
40	22	–**/ +	–**/ +	–***/ +	+	–/ +	–/ +	–/ +	=
30	22	+ /–	+ /–	–*/ +	=	–/ +	–/ +	=	=
22	22	=	=	=		=	=	=	
15	22	–*/ +	–**/ +	–**/ +	=	+ */–	+ */–	+ /–	+
10	22	–**/ +	–**/ +	–**/ +	–	+ ***/–	+ */–	+ **/–	+ **
5	22	–***/ +	–**/ +	–**/ +	=	+ ***/–	+ ***/–	+ /–	+

Table 4.10. Drinking patterns of WT and KO mice during the drinking water temperature preferences experiments. Temperature 22/22 was used as the control. The – symbol indicates a decrease in the trend of the response, while –* indicates a significant decrease in the response. In the same way, + indicates an increase in the trend of the response, while +* indicates a significant increase. The = symbol indicates that there was no change in the response. The responses of each parameter to the different temperatures shown on the left are separated by the / symbol. The column 'total volume' considers the sum of the total volume of water drunk between the two bottles, comparing the total volume of each experimental temperature against total volume of water drank in control conditions, 22/22. (* $p \leq 0.05$, ** $p \leq 0.01$, *** $p \leq 0.001$)

5. DISCUSSION

The tongue and its sensory innervation has been repeatedly used in *'in vivo'* experiments to analyze the functional properties of sensory receptor fibers, in particular cold thermoreceptors (Hensel et al 1960, Hensel & Zotterman 1951b, Lundy & Contreras 1995, Pittman & Contreras 1998). The present work shows that the excised tongue of the mouse superfused *ex vivo* is also a useful experimental model to record the impulse activity of single fibers of the lingual nerve under well-controlled experimental conditions. It allowed us to unambiguously identify and characterize the functional classes of cold-sensitive fibers innervating the tongue, the ionic mechanisms underlying their functional properties, and the contribution of the thermosensitive innervation of the tongue and oropharyngeal mucosa to shape water drinking behavior. The most salient conclusions of this study are that cold thermoreceptor fibers of the tongue are functionally heterogeneous, exhibiting a wide range of thermal thresholds and temperature coding patterns that are linked to the different expression of various types of thermosensitive channels. Moreover, the populations of cold-sensitive lingual nerve fibers appear to contribute importantly to the definition of preferred water temperature, behavioral drinking patterns and final volume of water ingested by healthy animals, thus emerging as an important peripheral mechanism for the maintenance of body fluid homeostasis in mammals.

5.1. Sensory innervation of the mouse tongue by cold-sensitive TG sensory neurons

The degree of success in picking up a cold-sensitive fiber in the recording experiments was used in the present experiments to roughly estimate the relative proportion of each of the functionally different fiber subclasses within the total number of lingual cold-sensitive afferents. According to the differences in recording success between WT and TRPM8$^{-/-}$ mice (where the activity of TRPM8-expressing neurons, possibly phasic-tonic fibers, see below was silenced) (Parra et al 2010), we estimated that TRPM8-contaning fibers

represent 2/3 of the total number of lingual nerve cold-sensitive fibers. These fibers are the peripheral axons of the green fluorescent cell bodies visualized in the TG of TRPM8-YFP mice, whose average number for the tongue was around 36 per TG ganglion. Although the possibility of a loss of certain neuron types during culture makes the extrapolation of figures obtained in tissue culture to the in *vivo* situation risky, we tentatively estimate that, in total, a minimum of about 50 TG cold-sensitive fibers innervate the mouse tongue. This number looks modest in terms of providing spatial discrimination capacities for the detection of cold stimuli. This fact, together with the observed accumulation of cold-sensitive fiber terminals into the tip of the tongue supports the interpretation that the sensory inflow supplied to the CNS by cold-sensitive afferents of the tongue primarily supplies general information on the temperature of food and liquids.

Most TRPM8+ cold nerve terminals were associated to the fungiform papillae, where they innervate the surrounding epithelial cells, without reaching taste bud cells (Abe et al 2005). In mice, the fungiform papillae form a specific patterned array (Jung et al 1999) maintaining a minimum distance between repetitive neighboring elements (Mbiene et al 1997, Wolpert 1998) whose spatial distribution is possibly directed by signaling molecules such as BDNF (Brain derived neurotrophic factor), NT4 (Neurotrophin-4), E cadherin and laminin (Barlow et al 1996, Mbiene & Mistretta 1997). TRPM8+ ramified terminals follow a similar distribution pattern, suggesting that the same signaling molecules that determine the stereotyped spatial array of fungiform papillae also govern cold sensory innervation of the tongue.

5.2. Functional diversity of cold-sensitive fibers of the tongue

The responsiveness of peripheral sensory fibers innervating the skin, exposed mucosa, and internal organs to cold stimulation has been explored in early studies, which defined the existence of a set of specific receptor fibers responding to cold thermal stimuli with a large increase in activity, inhibited upon warming (Hensel 1953, Hensel & Zotterman 1951a, Iggo 1959, Iggo & Young 1975, Kenshalo & Duclaux 1977, Poulos 1971, Poulos 1975). Such specific cold thermoreceptors were distinguished by the presence of background

ongoing activity at the basal temperature of the supporting tissues of variable frequencies depending on the species, often characterized by beating at higher temperatures and bursting at lower temperatures around this value (Bade et al 1979, Carr et al 2003, Dykes 1975, Gallar et al 1993, Iggo & Young 1975, Parra et al 2010, Poulos & Molt 1976, Schafer et al 1986). Rapid cooling shifts of 1-10ºC produced an initial high-frequency firing (dynamic response), the discharge rate thereafter relaxing to a level of activity appropriate for the steady temperature level (static response) (Dubner et al 1975, Iggo 1969). The impulse firing characteristics of this canonical population of cold thermoreceptor fibers were further defined by examining the response to small temperature steps over a range of steady temperatures (Gallar et al 1993, Parra et al 2010, Spray 1986). Dynamic bursting was usually induced only within a mild temperature range of cold receptor activity, whereas at lower and higher temperatures, the dynamic response mainly consisted of a repetitive beating discharge of high frequency (Schafer et al 1986). Detailed analysis of the intensity-response curves to dynamic and static temperature changes showed differences among individual fibers within this population of cold-specific thermoreceptor fibers, in their thermal threshold and coding capabilities.

The present work confirms that this population of specific cold thermoreceptors represents a significant portion of the cold-sensitive nerve fibers innervating the tongue, which corresponds in our study to the class of phasic-tonic cold thermoreceptor fibers. Measurement of thermal threshold values in this population of phasic-tonic fibers reinforces the observation already made by Hensel (Hensel et al 1960), that thermal threshold among the canonical cold thermoreceptor lingual nerve fibers vary in quite a large range. Threshold differences could be attributed in part to the accessibility of the stimulus to nerve endings, so that temperature changes would reach deeply located nerve terminals more slowly. However, TRPM8+ cold sensory fibers innervating the tongue are found at a relatively homogeneous deepness within the mucosa. Therefore, it could be expected that the change in temperature caused by the fast-flowing cold saline takes place rapidly and homogeneously throughout tongue's mucosal surface. Hence, it seems more likely to assume that threshold variability reflects real differences in the transducing/encoding properties among cold receptor fibers. This interpretation is further supported by the electrophysiological information obtained in cultured TG neurons

responding to cold, the vast majority of which exhibit active and passive membrane properties characteristic of cold-specific sensory neurons (Madrid et al 2009, Viana et al 2002) in spite of their wide range of thresholds, a difference explained by subtle differences in the expression of other non-TRP ion channels like K_v1, K2P or HCN channels (Madrid et al 2009, Madrid et al 2006, Orio et al 2012, Thut et al 2003, Viana et al 2002).

In addition to the clear segregation of cold-sensitive fibers of the tongue according to their threshold, these exhibit significant differences in other response characteristics, reaffirming the idea that distinct functional populations of sensory afferents activated by temperature reductions within non-noxious levels clearly exist, with very different thresholds and a capacity for dynamic detection and encoding of temperature decreases. Representations of typical cold-sensitive responses for each firing pattern group for the WT and KO mice can be found in Figure 5.1.

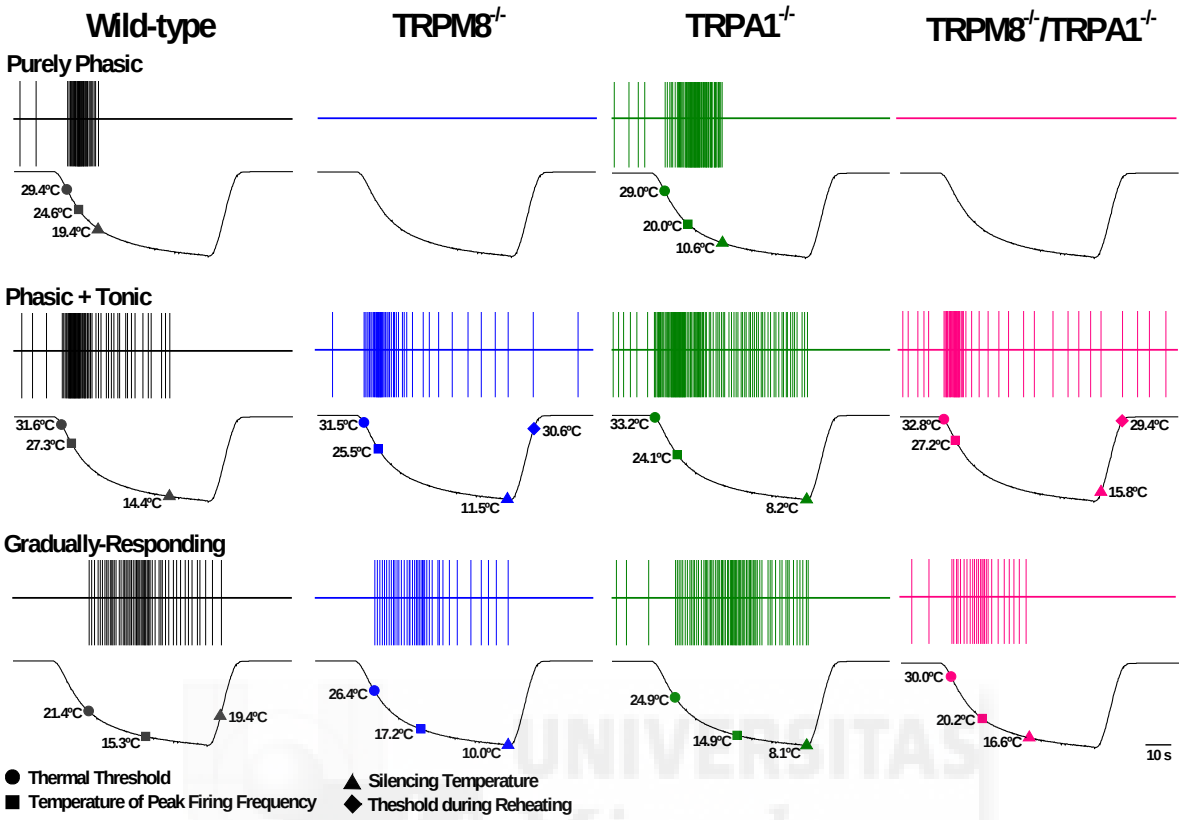

Figure 5.1. Representative traces of cold-evoked activity during a cooling pulse. Traces representing the typical response pattern of wild-type, TRPM8$^{-/-}$, TRPA1$^{-/-}$, and TRPM8$^{-/-}$/TRPA1$^{-/-}$ purely phasic, phasic + tonic, and gradually-responding fibers. Mean values for the thermal threshold (●), temperature of peak firing frequency (■), silencing temperature (▲), and threshold during reheating (♦) are included in the temperature traces for each group.

Thermal threshold was an initial criterion applied to differentiate two populations, the phasic-tonic and the gradually-responding cold-sensitive fibers; 29ºC was chosen in this study as the cutoff for the thermal threshold between the two populations because a large majority of fibers classified as phasic-tonic based on a number of common characteristics of their firing pattern have a threshold over this value (see Figure 4.15 and Table 4.9). In addition to their lower threshold, phasic-tonic fibers exhibited in comparison with gradually responding fibers a higher incidence of spontaneous activity, a much higher peak frequency in response to cooling pulses which was reached at warmer temperatures, larger capacity to encode the temperature decrease in significant changes in firing frequency, and narrower temperature margins for firing so that almost all of the phasic thermoreceptor fibers

silenced when temperature drops overpassed 20ºC. In the chart of Table 5.1, these differences are summarized schematically.

	Phasic-Tonic	Gradually-responding
Spontaneous activity (35ºC)	High incidence (38%) High frequency value (~ 1.1 imp/s)	Low incidence (10%) Low frequency value (~ 0.4 imp/s)
Thermal threshold	Low (~ 30ºC)	High (~ 21ºC)
Peak response		
Temperature	Small ΔT(ºC) to cooling (-8ºC to -10ºC)	Large ΔT(ºC) to cooling (-20ºC)
Peak firing	High (~ 20 imp/s)	Low (~ 9 imp/s)
Dynamic response to cooling	Sharp	Sluggish
Slope	~ 6.4 imp/s/ºC	~ 2.1 imp/s/ºC
Silencing with extreme cooling	Higher incidence (88%) Warmer temp. (~ 18ºC)	Lower incidence (40%) Cooler temp. (~ 10ºC)
Bursting	17%	28%

Table 5.1. Summary of the firing properties of phasic-tonic and gradually-responding cold-sensitive fibers.

5.3. Correspondence between the tongue's phasic-tonic fibers and canonical low-threshold cold thermoreceptors

Threshold, impulse firing characteristics, and sensitivity to menthol of phasic-tonic lingual nerve fibers make them comparable to conventional low-threshold cold thermoreceptors previously described for many tissues including the tongue '*in vivo*'. In the present study, external temperature was homogeneous and tightly controlled, allowing the comparison between fibers under very similar environmental conditions. We distinguished within this class of fibers the purely phasic and the phasic + tonic fiber subtypes. Although differences

between both groups are small and a subdivision risks to be somewhat artificial, they seem to reflect subtle differences in the blend of ionic mechanisms underlying the transducing and stimulus coding capacities within the population of specific cold thermoreceptors.

Purely phasic fibers fired for a short amount of time during the cooling pulse, starting at a higher threshold (i.e., lower temperature, around 29ºC), rarely exhibited a bursting pattern and stopped their firing when the temperature fell to about 10ºC. Altogether, their overall sensitivity to temperature reductions is smaller than in the group of phasic + tonic fibers, as reflected by their smaller peak frequency value which additionally required a larger temperature fall to be reached, and the slower slope of their temperature-firing frequency curve. This subpopulation of cold thermoreceptor fibers seems to mainly provide a brisk, short and vigorous signal from the presence of a cold stimulus; in that sense, the phasic cold thermoreceptor afferents could play a sensory role for temperature detection somewhat equivalent to the contribution to rapid detection of mechanical stimuli made by low-threshold phasic mechanoreceptors of the skin, although this speculation needs to be tested experimentally.

For the group of phasic + tonic fibers, the threshold values, background mean activity and characteristics of the dynamic response to cooling pulses (transition to bursting pattern, peak frequency values, slope of temperature-frequency curves, and silencing temperature) are very similar to those reported in specific cold thermoreceptors previously described in other tissues, with a few small differences, possibly attributable to the experimental conditions and the architecture and characteristics of the various tissues rather than to qualitative differences in neuronal properties. It is worth noting that when compared in terms of their response to stepwise cooling, it was difficult to distinguish between purely phasic and phasic + tonic fibers, reinforcing the view that differences among these two fiber subtypes are mainly associated to large and rapid temperature changes.

The intensity-response curves obtained with the entire population of phasic-tonic cold thermoreceptor fibers, illustrated in Figure 4.24A, reflects the overall encoding capacity of temperature values both during dynamic changes and under static conditions and is rather similar to those obtained in the cold thermoreceptor population in other tissues. The curves showed that the dynamic sensitivity of thermoreceptors is temperature dependent with maximal sensitivity at or slightly above the static maximum. It is worth noting that the

largest discrimination capacity moves around temperature reductions of 10ºC, being maximal between 30ºC and 24ºC for both static and dynamic responses, which appear to be in the range of temperature oscillations in the mouth. Lingual thermoreceptors are therefore tuned to respond maximally somewhere in the mid-range of their sensitive range, as already noticed by Iggo (Iggo 1969).

5.4. Functional heterogeneity of gradually-responding cold-sensitive fibers

Hensel & Zotterman noticed in their pioneering electrophysiological studies of specific cold thermoreceptor fibers in the lingual nerve (Hensel & Zotterman 1951b) the additional presence of a reduced number of sensory fibers with the properties of low threshold mechanoreceptors that also exhibited thermal sensitivity to cold. Since then, a variable responsiveness to cold has been reported in sensory receptors of different modalities (Georgopoulos 1977, Hunt & McIntyre 1960). In the skin, slowly adapting mechanoreceptors associated with vibrissae are particularly sensitive to small temperature reductions (Cahusac & Noyce 2007, Tapper 1965). Duclaux and Kensahlo (Duclaux & Kenshalo 1972) analyzed cold sensitivity of type I slowly adapting mechanoreceptors (Merkel receptors) of the skin of cats and monkeys, confirming that in many of them their background activity at a skin temperature of 30ºC increased during the application of a 2ºC cooling step, stabilizing afterwards at a higher static firing frequency value, and silencing by reheating. In contrast to specific cold thermoreceptors, the steady-state activity in these mechanosensory fibers increased with the adapting temperature of the skin. Although these authors did not record the activity in cutaneous low-threshold cold thermoreceptors in parallel, they concluded by comparing their data with those obtained by previous authors, that the temperature-coding capacity of mechanosensory fibers with cold sensitivity is very different, as evidenced also in the intensity response curves built with the peak frequency values in mechanosensory fibers evoked by cooling pulses of increasing magnitude. It is of note that these curves are very similar to those obtained for the gradually-responding fibers of the tongue here (see Figure 4.24B).

Cold sensitivity has also been described for polymodal nociceptors of different tissues and in different animal species, including man (Arndt & Klement 1991, Beitel & Dubner 1976, Campero et al 1996, Croze et al 1976, Georgopoulos 1976, Georgopoulos 1977, LaMotte & Thalhammer 1982). Although the population of gradually-responding fibers was identified *a posteriori* in this study, and no special effort was made to explore a possible polymodality, heating was occasionally tested without evoking the typical heat responses seen in polymodal nociceptors.

The functional significance in terms of detection of cold temperatures, of the population of gradually-responding cold-sensitive fibers is open to discussion. Although they represent a relatively large fraction of the tongue cold-sensitive innervation, their low sensitivity and limited capacity to code the amplitude and changing rate of thermal stimuli suggests that they contribute modestly to sensing small temperature oscillations in the tongue or mouth. However, when comparing the intensity response curve of the full population of lingual cold-sensitive fibers (Figure 4.18) with the one representing only data from phasic-tonic fibers (Figure 4.17A), it becomes evident that the thermal range and the sensitivity to detect temperature differences are clearly larger when the joint information provided by the two functional classes of cold-sensitive fibers is taken in consideration together. Therefore, it seems legitimate to conclude that both fiber classes contribute to build the total sensory inflow sent to the brain to inform about temperature reductions in the tip of the tongue caused by stimuli of very different origin (evaporative cooling, cold liquids or foods, cold objects explored with the tongue).

5.5. Contribution of TRP channels to responsiveness of the various classes of cold-sensitive fibers

5.5.1. TRPM8$^{-/-}$

The TRPM8 channel is generally accepted as the main transducer for cold in specific cold thermoreceptor fibers (Bautista et al 2007, Colburn et al 2007, Dhaka et al 2007). In agreement with this, genetically-induced expression of TRPM8 channels in hippocampal neurons originally lacking native TRPM8 channels develop cold sensitivity (de la Pena et al

2012) while low-threshold cold thermoreceptor fibers of the cornea of the eye became silent and unresponsive to cold in TRPM8-null mice (Parra et al 2010).

In recording experiments in the lingual nerve of TRPM8$^{-/-}$ mice, a sharp reduction in the probability of finding sensory fibers displaying sensitivity to cooling pulses was noticed, suggesting that the number of specific cold thermoreceptor fibers firing spontaneously and responding with an impulse discharge to temperature reduction was sharply reduced. Still, impulse activity associated to cooling with a vast range of thermal thresholds was found in TRPM8$^{-/-}$ mice lingual nerve fibers, even though the probability of locating such cold-sensitive fibers descended to 20% in comparison with experiments performed in WT animals. The most striking difference with control mice was the virtual absence of purely phasic fibers, reinforcing the impression that phasic fibers of the tongue resemble low-threshold cold thermoreceptors described in the mouse cornea, which apparently have TRPM8 as the main if not the sole mechanism for sensing temperature decreases (Parra et al 2010). Applying the classification criteria for cold-sensitive fibers established for WT animals to TRPM8$^{-/-}$ mice, it can be concluded that the proportion of phasic-tonic fibers remaining in TRPM8$^{-/-}$ mice decreased from 60% to 30%, with the remaining 70% of the cold-sensitive fibers belonging to the gradually-responding group. It is noteworthy that in both groups of fibers, the spontaneous activity firing frequency at 35ºC was significantly reduced, suggesting that TRPM8 channels generally contribute to a more depolarized background membrane potential in all types cold-sensitive nerve terminals. In TRPM8$^{-/-}$ mice the response to cooling pulses of the remaining phasic-tonic cold thermoreceptor fibers was altered, as witnessed by the reduction of the peak frequency value and the flatter slope of the curve representing firing frequency increases versus temperature decreases. Moreover, the appearance of a bursting pattern during dynamic cooling was disturbed, changing to a beating pattern shortly after the onset of the cooling pulse. Altogether these results confirm the idea that sensitivity to cold in the population of phasic-tonic cold thermoreceptor endings is determined by a variable expression of TRPM8 and of other cold-sensitive channels, including background potassium channels contributing to cold-induced depolarization and Kv1 channels behaving as a break against cold-induced depolarization (Belmonte et al 2009, Belmonte & Viana 2008, Madrid et al 2009, Viana et al 2002). TRPM8 appears to be critical in a fraction of the endings, while in the rest,

cold-induced depolarization is sustained in a variable degree by other classes of thermosensitive potassium channels (Madrid et al 2006). It is tempting to speculate that in the cooling-induced gating of channels, the architecture and surface-volume ratio of the nerve terminals play a critical role in their effective capacity to evoke the level of depolarization required for the generation of propagated action potentials. The absence of cold thermal responses in DiI labelled TG neurons of TRPM8$^{-/-}$ mice speaks in this direction, although the possibility that the number of neurons explored in this work was insufficient or that culture conditions may alter channel expression of TG neurons has to be considered.

When considering just the gradually-responding fibers that remain in the TRPM8$^{-/-}$, it was found that their thermal threshold was significantly lower than in WT gradually-responding fibers. The mean firing frequency, when measured from the first to the last spike fired, as well as the slope were also significantly lower in the TRPM8$^{-/-}$ gradually-responding fibers than in the WT ones. This suggests that TRPM8 channels confer some degree of cold-sensitivity to gradually-responding fibers.

5.5.2. TRPA1$^{-/-}$

The role of TRPA1 channels in somatosensory cold transduction is controversial. Many studies support that TRPA1 is indeed involved in sensing noxious cold (Bandell et al 2004, del Camino et al 2010, Fajardo et al 2008, Karashima et al 2009, Kwan et al 2006, Story et al 2003), while others do not attribute a significant functional role to the effects of cold on TRPA1 gating observed in cellular models (Bautista et al 2006, Jordt et al 2004, Knowlton et al 2010, Nagata et al 2005).

Here, it was found that the response characteristics to cooling in the TRPA1$^{-/-}$ lingual nerve sensory fibers of mice resemble those of the WT mice, although some slight differences were apparent. A clear difference was that the thermal threshold of the high threshold cold fibers in TRPA1-null mice shifted to warmer values, suggesting that the presence of TRPA1 channels in this population of cold-sensitive fibers, whose sensitivity to vigorous cooling is well established, contributes decisively to their sensitivity to cooling below the level at which other less specific cold thermosensitive channels are already activated. The distribution of fibers based on their thermal threshold and firing pattern characteristics was

rather similar to that of WT mice and suggests that all fibers in which TRPM8 played a determinant role in the development of cold sensitivity do not express TRPA1 at least at a level capable of influencing their thermal threshold. However, certain differences were noticed particularly within the gradually-responding fiber type as could be predicted from the shift of threshold in HT fibers. In WT mice only a small percentage of these fibers displayed spontaneous activity at 35ºC and at very low mean firing frequency. However, in TRPA1$^{-/-}$ mice the percentage of gradually-responding fibers displaying spontaneous activity was higher and their mean firing frequency significantly higher. Moreover, the mean frequency increase in response to a cooling pulse was of a higher mean frequency and established more gradually as reflected by smaller slope of the temperature decrease-firing frequency curve. It can be speculated that the expression of TRPA1 determines that gradually-responding fibers respond more vigorously to intense cold than when their thermosensitivity depends only on non-selective voltage-gated channels. This contribution of TRPA1 thermosensitive fibers to confer a sharper and more vigorous capacity to discriminate cooling is reflected in the stimulus-response curve obtained with small cooling steps, that was flatter than in WT mice, so that only strong cooling was able to significantly increase the firing rate of the overall population of cold thermosensitive fibers allowing significant quantitative differences in the sensory inflow signaling the cooling of the tongue.

5.5.3. TRPM8$^{-/-}$/TRPA1$^{-/-}$

In these animals, like in the TRPM8$^{-/-}$ mice there was an absence of purely phasic fibers, supporting the argument that TRPM8 mediates the cooling activity in this specific group of cold-sensitive fibers activated by temperature changes within moderate ranges.

Additionally, there were significant differences between the remaining cold-sensitive fibers found falling into the phasic-tonic group and the gradually-responding fibers in these animals in several of the parameters studied, including thermal threshold, peak firing frequency, temperature at peak firing frequency, mean firing frequency, and slope. All the fibers had a significantly lower thermal threshold and peak firing frequency than the WT fibers and in general were overall less responsive with a lower mean firing frequency and lower slopes.

It is worth noting that the probability of finding cold-sensitive fibers in this population of mice was rather low, indicating that the determinant elements conferring fine sensitivity to temperature reductions to many of the peripheral cold-sensitive sensory fibers are TRPM8, and in a lesser degree, TRPA1 channels. Nonetheless, our data with TRPM8$^{-/-}$/TRPA1$^{-/-}$ mice provide new evidence that temperature variations within a non-noxious range, i.e., not acting indirectly on peripheral receptor terminals through chemical or mechanical stimuli, affect the impulse activity of a number of sensory receptor fibers.

The possibility that temperature is acting not only on peripheral endings but also on their parent axons cannot be directly excluded in our experimental model, because a part of the trajectory of the recorded axons is exposed to the temperature stimuli applied to the tongue. However, it is long known that cold decreases axonal ion currents (Keynes & Rojas 1974) thereby reducing axonal excitability (threshold, latency, refractoriness, supernormality, strength-duration time constant, and rheobase) (Burke et al 1999), leading ultimately to a blockade of conduction of impulses in mammalian nerve fibers (Douglas & Malcolm 1955, Franz & Iggo 1968). Moreover, in a preparation of baro- and chemoreceptors superfused *in vitro* the stimulus-evoked nerve impulse activity decreased proportionally to temperature reductions from 40ºC to 30ºC (Gallego et al 1979). Hence, if anything, the effects of cold on parent axons in our experimental conditions would tend to decrease rather than to increase impulse firing.

As mentioned above, in addition to the inward currents activated by cold and mediated by TRPs, other ion currents carried by different types of potassium channels which are inhibited by cold, have been associated to cold transduction and coding, including TREK-1, TREK-2, and TRAAK, Kv1 (most likely Kv1.1/2) and Kv7.2/3 channels (Belmonte & Viana 2008, Madrid et al 2009, Noel et al 2009, Reid & Flonta 2001, Vetter et al 2013, Viana et al 2002). Here we did not explore which of these mechanisms are responsible for the residual thermosensitivity seen in our different TRP-null mice. Nonetheless, in all cold-sensitive fibers where chloroform was tested during the cooling pulse, there was a reduction or silence in the firing frequency to cooling. Since chloroform is a known activator of thermosensitive TREK-1 potassium channels, its attenuating or blocking effect on cold responses supports the idea that this and presumably other background potassium

channels are involved in the excitation by cold of the presumably heterogeneous population of sensory receptor types other than specific cold thermoreceptos, affected by cold.

This study shows the complete absence of an intracellular calcium response to cooling in the somas of TRPM8$^{-/-}$ TG neurons innervating the tongue, confirming previous studies using cell bodies of cultured sensory ganglion neurons of TRPM8$^{-/-}$ animals. Still, in the lingual nerve of the same animals used to obtain these cell bodies, it was possible to record the cold-sensitive fiber activity described above. This confirms the existence of overlapping functional thermosensitive mechanisms in the nerve terminals (Madrid et al 2009, Madrid et al 2006) and the importance that the architecture and size of peripheral sensory terminals possibly play in the efficacy of obtaining membrane depolarizations leading to propagated action potentials with a presumably limited density of thermosensitive ion channels.

5.6. Contribution of cold-sensitive fibers to water intake

Indirect experimental evidence suggests that oropharyngeal mucosal hydration is detected by sensory receptors and serves to regulate thirst and water intake (Eccles 2000). The modality of sensory receptors involved in the detection of wetness levels of the oral mucosa and the mechanism(s) involved in their excitation are largely ignored. It has been proposed (Eccles 2000) that some still unidentified peripheral sensory fibers act as 'osmoreceptors', or alternatively that drying of the mucosa is sensed by mechanoreceptors which detect the sheer forces as the mucosal surfaces slide over each other during swallowing or with tongue movements. Saliva acts as a lubricant in the oral cavity and any reduction in salivation would increase the friction between the mucosal surfaces in the oropharynx. Sensory discharges in these sensory receptors would represent neural signals triggering behavioral responses for water intake. However, as pointed out by Eccles (Eccles 2000) "hydration and lubrication of the oral cavity may not be the only physical factors involved in the satiety of thirst as there is some evidence to indicate that fluid temperature may also play a role in satiety." Recently, it was shown that peripheral cold thermoreceptors of the ocular surface expressing TRPM8 are activated indirectly by reductions of ocular surface wetness and contribute to the regulation of tear secretion (Hirata & Oshinsky 2012, Kurose & Meng

2013, Orio et al 2012, Parra et al 2010). Hence, the possibility that a similar mechanism is contributing to the maintenance of mouth wetness both to evoke conscious sensations leading to water drinking and to modulate salivary secretion (Brunstrom 2002) appears to be an interesting hypothesis to explore.

As described in the Introduction section, the original theory that mouth dryness is critical for the regulation of drinking was soon contradicted by the observation that sham drinking has little effect on future drinking (Bellows 1939) and superseded by the discovery of osmoreceptors and a role for the lateral hypothalamus, showing that thirst appears to be mediated by at least two processes: osmometric thirst, associated with a change in the solute concentration of the interstitial fluid (Verney 1947) and volumetric thirst, associated with depletion of intravascular volume (hypovolemia), arising from vomiting, diarrhea, or a hemorrhage (Fitzsimons & Moore-Gillon 1980). Integration of signals from osmometric and volumetric thirst appears to be governed by the median preoptic nucleus (Thrasher 1989). Despite this, it is unclear whether or not these models can account for much of the fluid intake that is observed in humans. This is because most drinking behaviors are non-homeostatic, and do not occur in response to a specific deficit. When human subjects were given free access to water over a 24-hour period (Phillips et al 1984) they felt thirsty and drank mainly in association with eating. This was the case despite the fact that they remained hydrated throughout. There were no concomitant changes in body fluid variables. Thus, these authors hypothesized that when water is readily available, humans experience thirst in order to anticipate a future fluid deficit. It is noteworthy that the subjects in this study attributed part, if not all, of their thirst to oral sensations, such as a dry unpleasant taste or to viscid saliva in the mouth. This is important because it implies that while mouth dryness is not exclusively the 'seat' of thirst it may still influence aspects of normal everyday drinking behavior (Brunstrom 2002).

In that context, the present behavioral experiments in mice explored the role that modulating water intake played by the information provided by the various classes of cold thermoreceptors of the tongue, oropharyngeal mucosa, esophagus, and stomach in the contribution of the various molecular sensors involved in the definition of their signaling properties to the modulation of water drinking behavior.

The first conclusion that can be drawn from behavioral experiments is that WT mice are able to discriminate differences in the temperature of the drinking water in the range used in this study. In the experiments in which no choice in the temperature of the drinking water was offered, water-deprived mice could drink only at the provided water temperatures. In WT mice, the volume of water finally consumed did not significantly change over the various experimental temperatures. However, control water temperature (22ºC) was shown to be the one at which mice entered to drink the fewest number of times and spent the least time actively drinking as compared to the other experimental temperatures. As the water was warmed and cooled from 22ºC there was an overall trend to enter more and spend more time drinking although the final volume of water ingested was the same as at 22ºC. Humans, immediately after drinking, experience a reduction of thirst that is more pronounced with cold (5ºC) water (Brunstrom & Macrae 1997). When they are offered a very short period (10–15 seconds) to rehydrate, cold (0°C) water is liked as much as, but is ingested less than, 10°C water (Boulze et al 1983). If this drinking pattern is extrapolated to the no-choice cold water drinking seen in mice it could be inferred that here also, cold water more efficiently suppresses thirst sensation, but being a transitory effect, thirst still drives the animal to repeat drinking attempts more frequently. However, a similar behavior was also observed in mice with warm water. On another hand, temperature preference experiments in intact, healthy animals show that mice preferred water at 22ºC over cooler water thus favoring the opposite alternative, and that the tendency to increase the number of entries and to spent longer times in the process of drinking when the bottle is below this temperatures is not associated with a pleasant or refreshing sensation of the cooler water, as previously described (Eccles 2000, Eccles et al 2013, Labbe et al 2009, Zellner & Durlach 2002) but rather to a certain level of aversion and/or unpleasant sensation evoked by cold water. If so, this feeling would be dominated by the drive of water-deprived mice to seek out and consume water for rehydration, thus leading them ultimately to drink the same amount of water regardless of temperature. Unlike the first hypothesis, this interpretation could also be applied to hot temperatures. Accordingly, it is proposed that the relative unpleasantness of cold or hot water prevents the animals from spending much time drinking during each entry, and forces them to enter more times and spend more time drinking to consume the same final volume. Such behavior also

agrees with the observation of Steiner (Steiner et al 1986) that albino rats display a preference towards a drinking water closer in temperature to that of the body (30ºC) over a markedly cooler drinking water (12ºC).

Selective deletion of TRP channels linked to cold transduction provided information about the role in water drinking behavior of the different classes of cold thermoreceptors identified in this study and the hypothetical mechanism whereby they become activated by water intake. Sensory innervation relevant to the initiation of behavioral responses associated to water drinking originates at the lateral and anterior parts of the mouth and tongue mucosal membranes, innervated by TG somatosensory neurons, and at the posterior part of the tongue, vallate papillae, tonsils and lateral and posterior oropharyngeal walls, innervated by branches of the IX (glossopharyngeal) and X (vagus) nerves, whose neurons are respectively located in the petrosal and nodose ganglia (Mu & Sanders 2000). Down from the epiglottis, the pharyngeal and laryngeal mucosa are supplied by nodose ganglion visceral neurons through branches of the superior laryngeal nerve and the vagus which also provides sensory innervation to the lower esophagus and stomach, as well as by DRG somatosensory neurons that provide these viscera only low and high threshold mechanosensory and nociceptive afferents implicated in motility and pain (Kondo et al 2010, Zhong et al 2008). A part of the axons of nodose neurons innervating the lower esophagus and stomach respond rather selectively to cold (El Ouazzani & Mei 1982), and their firing has been functionally linked to the coordination of digestive activity and thermoregulation. In contrast with TG and DRG cold thermoreceptor neurons that express TRPM8 and TRPA1 channels, vagal neurons sensitivity to cold appears to depend primarily on the expression of TRPA1 channels (Fajardo et al 2008).

Deletion of TRPM8 channels markedly changed water drinking behavior in mice, supporting the general proposition that thermal information provided by oropharyngeal cold thermoreceptors contributes to shape the behavior patterns for thirst satiation (Brunstrom & Macrae 1997). In no-choice experiments, the volume of water ingested by TRPM8$^{-/-}$ mice was as a whole lower than the in WT and similar at the control temperature of 22ºC and with higher or lower water temperatures, except when the temperature dropped to 5ºC where a significantly lower volume of water was consumed. This suggests that TRPM8$^{-/-}$ mice retain the capacity to distinguish differences in temperature when very cold values are

reached. Otherwise, in these animals the number of entries made to drink or the amount of time spent drinking was analogous across each of the water temperatures and as a whole more infrequent and shorter than in WT animals. Electrophysiological recordings of cold thermoreceptors of the tongue indicated that a significant proportion of phasic-tonic fibers was unresponsive to low threshold cold stimuli. Behavioral data suggest that silencing this fraction of specific cold thermoreceptors eliminates an important cue to define temperature-based drinking behavior.

The no-choice drinking behavior of TRPA1$^{-/-}$ mice was, in general, rather similar to that of the WT mice. It is noteworthy that the volume of water drank by TRPA1$^{-/-}$ mice was larger than that by WT mice, and across the different temperatures TRPA1$^{-/-}$ mice consumed significantly more at temperatures of 30ºC and 15ºC. This surprising difference may be explained considering that in addition to oropharyngeal thermoreceptors, vagal sensory fibers innervating the lower esophagus and stomach also appear to modulate water intake. As stomach filling terminates water drinking in dehydrated rats even in the presence of systemic thirst stimuli for thirst (increased plasma osmolality, decreased plasma volume) suggesting that neural signals related to the cumulative volume of ingested fluid in the stomach and small intestine inhibit drinking behavior (Stricker & Hoffmann 2006). In humans, thirst is more effectively suppressed by the accumulative effect of larger volumes and cooler water ingested (Brunstrom & Macrae 1997). The majority of vagal afferents are polymodal, responding to physical stimuli (mechanical and thermal) and chemical irritants (Carr & Undem 2003, Higashi 1986, Lennerz et al 2007). In mice, around 18% of nodose ganglion neurons are cold-sensitive and express TRPA1 and TRPV1 (Fajardo et al 2008). When water enters the lower esophagus and the stomach, the peripheral axons of these neurons are likely stimulated both by water temperature and by mechanical distension contributing to the termination of water ingestion (Stricker & Hoffmann 2006). In TRPA1$^{-/-}$ mice these signals are absent in a large extent, thereby suppressing their inhibitory effect on water intake and explaining the larger volume of water ingested by TRPA1$^{-/-}$ mice. This excessive drinking was also confirmed in the water temperature preference experiments when the volume of water drunk from the control and the experimental bottles were summated in each of the temperature preference tests. On another hand as occurred in WT animals, TRPA1$^{-/-}$ mice entered a significantly greater number of times when offered

hot and cold water than when water was at 22ºC, and spent a significantly greater time drinking when water temperature was cold. This similar behavior was also noticed in the temperature preference experiments where the avoidance of hot water and of some cold temperatures was even more vigorous than in WT animals. Hence TRPA1-null mice appear to conserve the temperature discriminating capacity, primarily dependent on the expression of TRPM8 but not the feeling of fullness or stomach distention.

TRPM8$^{-/-}$/TRPA1$^{-/-}$ mice largely lose their ability to discriminate water temperatures, particularly those below warm values, as reflected by the scarce differences in drinking behavior parameters when exposed either to one or two water bottles at different temperatures. TRPM8$^{-/-}$/TRPA1$^{-/-}$ mice drank a similar mean volume of water across the different temperatures, but an overall lower amount than WT mice, suggesting that the positive drinking drive provided by TRPM8+ low threshold cold thermoreceptors of the oropharyngeal area is more potent than the inhibitory influence of TRPA1 vagal fibers of the stomach. A representation of the percentage of entries, time, and volume of each animal group for the different temperatures is shown in Figure 5.2.

The variety of thermal threshold and electrophysiological response characteristics observed in the population of cold-sensitive fibers of the tongue also possibly extends to the thermal receptor fibers innervating the rest of the mouth mucosa. Collectively, these thermal sensory afferents, together with the oral mechanoreceptors and the mechano- and cold-sensitive fibers innervating the upper segment of the gastrointestinal tract appear to provide a sensory inflow that encodes the desiccation level of the mouth, its wetting during water drinking, and the degree of stomach filling by cool water, thereby regulating the ingestion of a final water volume and preventing the risk of an excessive dilution of internal body fluids.

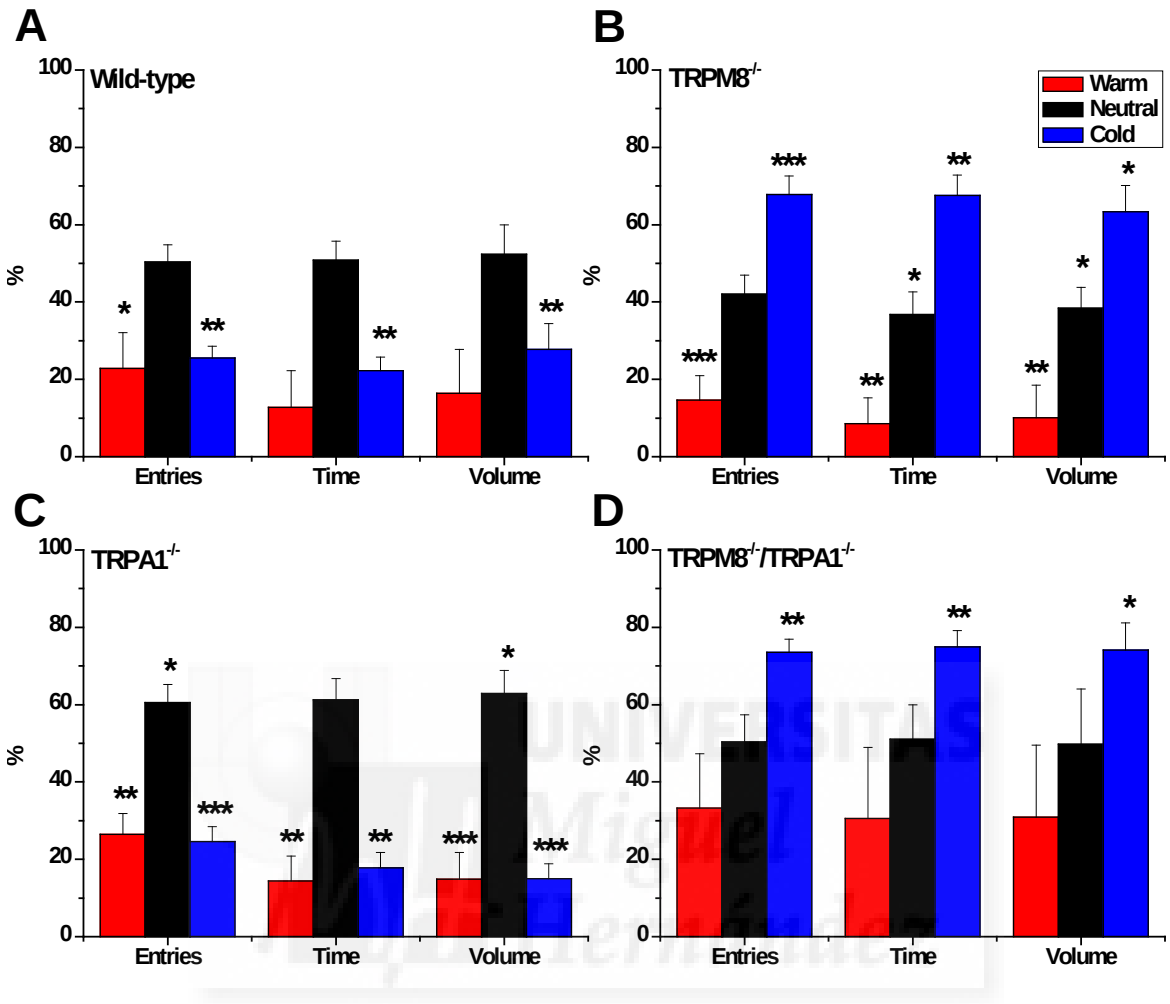

Figure 5.2. Drinking water temperature preference in all mice groups. Water temperature was grouped as warm (40ºC), neutral (30 and 22ºC), and cold (15, 10, and 5ºC) and compared against the control bottle at 22ºC at each of the temperatures. The mean percentage of entries, time, and volume were measured for these three temperature groups for the WT (A), TRPM8$^{-/-}$ (B), TRPA1$^{-/-}$ (C), and TRPM8$^{-/-}$/TRPA1$^{-/-}$ (D) mice. (* $p \leq 0.05$, ** $p \leq 0.01$, *** $p \leq 0.001$)

6. CONCLUSIONS

1. Single nerve impulse activity recorded from cold thermoreceptor fibers in the mouse tongue *in vitro* permits the study of thermosensitive fibers in well-controlled experimental conditions and their classification according to their firing pattern and sensitivity to cold.
2. Cold-sensitive fibers of the tongue are functionally heterogeneous. Phasic-tonic and gradually-responding fiber classes have been identified. Together they appear to contribute to sensory inflow, signaling temperature reductions of the tongue within a wide range of cooling stimuli.
3. The persistence of cold-sensitive fibers in TRPM8$^{-/-}$ mice indicates that a fraction of the cold-sensitive fibers in the lingual nerve possess additional transducing mechanisms for cold. The absence of purely phasic fibers in TRPM8$^{-/-}$ mice suggests that phasic fibers fully rely on TRPM8 for their cold-transducing capacity.
4. The absence of cold sensory fibers recruited by temperatures below 25ºC in TRPA1$^{-/-}$ mice suggests that cold transduction in the population of cold-sensitive fibers with a high threshold depends largely on TRPA1.
5. Persistence of cold-sensitive fibers in TRPM8$^{-/-}$/TRPA1$^{-/-}$ mice suggests that other channels are involved in cold detection, possibly TREK-1 potassium channels since there is a reduction in cold evoked activity in the presence of chloroform.
6. WT mice are able to discriminate differences in the temperature of the drinking water ranging from very warm (~40ºC) to very cold (~10ºC) temperatures. In the absence of choice, they ingest the same volume of water despite its temperature, yet clearly prefer neutral temperature water when given the choice between warmer or colder temperatures.
7. TRPM8 plays a role in the temperature preference of the water consumed as well as in the voluntary drive to drink. In the absence of TRPM8 channels, mice drank less overall water than the wild-type and showed no aversion to cold temperatures.
8. TRPA1 channels help control the total volume of water drunk and contribute to prevent overdrinking. This effect seems to be mediated through the

TRPA1-expressing vagal sensory fibers that innervate the lower esophagus and stomach thereby modulating water intake.

9. The drinking pattern of TRPM8$^{-/-}$/TRPA1$^{-/-}$ mice suggests that the positive drive to drink provided by TRPM8 cold thermoreceptors of the oropharyngeal area is stronger than the inhibitory influence of TRPA1 vagal fibers of the lower esophagus and stomach since TRPM8$^{-/-}$/TRPA1$^{-/-}$ mice showed a low volume of consumed water with a preference for water at colder temperatures.

CONCLUCIONES

1. Los impulsos nerviosos registrados en fibras unitarias de termorreceptores de frío en la lengua de ratón *in vitro,* permite el estudio de fibras termosensibles en condiciones experimentales bien controladas y su clasificación de acuerdo a su patrón de disparo y la sensibilidad al frío.
2. Las fibras sensibles al frío de la lengua son funcionalmente heterogéneas. Se han identificado dos clases diferentes: fibras fásico-tónicas y fibras de respuesta gradual. Juntas parecen contribuir a la entrada sensorial, enviando información sobre la reducción de la temperatura en la lengua, dentro de un gran rango de temperatura.
3. La presencia de fibras sensibles a fríos en ratones TRPM8$^{-/-}$ indica que una fracción de las fibras sensibles a frío, en el nervio lingual, poseen mecanismos de transducción adicionales. La ausencia de fibras con descarga puramente fásica en ratones TRPM8$^{-/-}$ sugiere que estas fibras basan totalmente su capacidad de transducción del frío a TRPM8.
4. La ausencia de fibras sensoriales de frío reclutadas por temperaturas inferiores a 25ºC en ratones TRPA1$^{-/-}$ sugiere que la transducción de frío en la población de fibras sensibles al frío con un alto umbral depende en gran medida de TRPA1.
5. La persistencia de fibras sensibles a frío en ratones TRPM8$^{-/-}$/TRPA1$^{-/-}$ sugiere que otros canales están involucrados en la detección del frío, posiblemente el canal de potasio TREK-1 ya que hay una reducción en la actividad de frío evocada en presencia de cloroformo.
6. Los ratones silvestres son capaces de discriminar diferencias en la temperatura del agua que beben, en un rango de temperaturas desde muy caliente (~ 40ºC) hasta muy frío (~ 10ºC). Cuando no tienen elección, ingieren la misma cantidad de agua a pesar de la temperatura, sin embargo, cuando se les da la posibilidad de elegir entre agua a temperatura más cálida o más fría claramente prefieren agua a temperatura neutra.
7. TRPM8 juega un papel en la preferencia de la temperatura del agua consumida y también en el impulso para beber. En la ausencia de canales TRPM8, los ratones

bebieron menos agua que los ratones silvestres y no mostraron aversión a las temperaturas bajas.

8. Los canales TRPA1 ayudan a controlar el volumen total de agua ingerida y contribuyen a evitar beber en exceso. Este efecto parece estar mediado a través de fibras sensoriales vagales que expresan estos canales e inervan la parte inferior del esófago y el estómago, modulando de esta manera la ingesta de agua.
9. El patrón de consumo de los ratones TRPM8$^{-/-}$/TRPA1$^{-/-}$ sugiere que el impulso positivo para beber proporcionada por los termorreceptores de frío que expresan TRPM8 en la zona orofaríngea es más fuerte que la influencia inhibidora de las fibras vagales TRPA1 de la parte inferior del esófago y del estómago, ya que ratones TRPM8$^{-/-}$/TRPA1$^{-/-}$ mostraron un consumo menor de agua y una preferencia por el agua a temperaturas más frías.

7. REFERENCES

Abe J, Hosokawa H, Okazawa M, Kandachi M, Sawada Y, et al. 2005. TRPM8 protein localization in trigeminal ganglion and taste papillae. *Brain research. Molecular brain research* 136: 91-8

Adrian ED. 1926. The impulses produced by sensory nerve endings: Part I. *The Journal of physiology* 61: 49-72

Alberts B. 2002. *Molecular biology of the cell*. New York: Garland Science. xxxiv, 1548 p. pp.

Almaraz L, Manenschijn JA, de la Pena E, Viana F. 2014. Trpm8. *Handbook of experimental pharmacology* 222: 547-79

Arndt JO, Klement W. 1991. Pain evoked by polymodal stimulation of hand veins in humans. *The Journal of physiology* 440: 467-78

Atoyan R, Shander D, Botchkareva NV. 2009. Non-neuronal expression of transient receptor potential type A1 (TRPA1) in human skin. *The Journal of investigative dermatology* 129: 2312-5

Axelsson HE, Minde JK, Sonesson A, Toolanen G, Hogestatt ED, Zygmunt PM. 2009. Transient receptor potential vanilloid 1, vanilloid 2 and melastatin 8 immunoreactive nerve fibers in human skin from individuals with and without Norrbottnian congenital insensitivity to pain. *Neuroscience* 162: 1322-32

Babes A, Zorzon D, Reid G. 2004. Two populations of cold-sensitive neurons in rat dorsal root ganglia and their modulation by nerve growth factor. *The European journal of neuroscience* 20: 2276-82

Bade H, Braun HA, Hensel H. 1979. Parameters of the static burst discharge of lingual cold receptors in the cat. *Pflugers Archiv : European journal of physiology* 382: 1-5

Bandell M, Macpherson LJ, Patapoutian A. 2007. From chills to chilis: mechanisms for thermosensation and chemesthesis via thermoTRPs. *Current opinion in neurobiology* 17: 490-7

Bandell M, Story GM, Hwang SW, Viswanath V, Eid SR, et al. 2004. Noxious cold ion channel TRPA1 is activated by pungent compounds and bradykinin. *Neuron* 41: 849-57

Barlow HB, Mollon JD. 1982. *The Senses*. Cambridge Cambridgeshire ; New York: Cambridge University Press. xii, 490 p. pp.

Barlow LA, Chien CB, Northcutt RG. 1996. Embryonic taste buds develop in the absence of innervation. *Development* 122: 1103-11

Basbaum AI, Bautista DM, Scherrer G, Julius D. 2009. Cellular and molecular mechanisms of pain. *Cell* 139: 267-84

Bautista DM, Jordt SE, Nikai T, Tsuruda PR, Read AJ, et al. 2006. TRPA1 mediates the inflammatory actions of environmental irritants and proalgesic agents. *Cell* 124: 1269-82

Bautista DM, Movahed P, Hinman A, Axelsson HE, Sterner O, et al. 2005. Pungent products from garlic activate the sensory ion channel TRPA1. *Proceedings of the National Academy of Sciences of the United States of America* 102: 12248-52

Bautista DM, Siemens J, Glazer JM, Tsuruda PR, Basbaum AI, et al. 2007. The menthol receptor TRPM8 is the principal detector of environmental cold. *Nature* 448: 204-8

Bean BP. 2007. The action potential in mammalian central neurons. *Nature reviews. Neuroscience* 8: 451-65

Behrendt HJ, Germann T, Gillen C, Hatt H, Jostock R. 2004. Characterization of the mouse cold-menthol receptor TRPM8 and vanilloid receptor type-1 VR1 using a fluorometric imaging plate reader (FLIPR) assay. *British journal of pharmacology* 141: 737-45

Beitel RE, Dubner R. 1976. Response of unmyelinated (C) polymodal nociceptors to thermal stimuli applied to monkey's face. *Journal of neurophysiology* 39: 1160-75

Bellows RT. 1939. Time factors in water drinking in dogs. *Amer J Physiol* 125: 87-97

Belmonte C. 1996. Signal transduction in nociceptors: general principles In *Neurobiology of Nociceptors*, ed. C Belmonte, F Cervero, pp. 243-57. New York, USA: Oxford University Press Inc.

Belmonte C, Brock JA, Viana F. 2009. Converting cold into pain. *Experimental brain research. Experimentelle Hirnforschung. Experimentation cerebrale* 196: 13-30

Belmonte C, De la Pena E. 2013. Thermosensation In *Neurosciences - From Molecule to Behavior: a university textbook*, ed. CG Galizia, P-M Lledo, pp. 303-19. Berlin Heidelberg: Springer

Belmonte C, Viana F. 2008. Molecular and cellular limits to somatosensory specificity. *Molecular pain* 4: 14

Benzing H, Hensel H, Wurster R. 1969. Integrated static acitivity of lingual cold receptors. *Pflugers Archiv : European journal of physiology* 311: 50-4

Bernard C. 1855. Lecons de Physiologie Exérimentale Appliquée a la Médecine. *Bailliere* 2: 510

Bessac BF, Sivula M, von Hehn CA, Caceres AI, Escalera J, Jordt SE. 2009. Transient receptor potential ankyrin 1 antagonists block the noxious effects of toxic industrial isocyanates and tear gases. *FASEB journal : official publication of the Federation of American Societies for Experimental Biology* 23: 1102-14

Bessou P, Perl ER. 1969. Response of cutaneous sensory units with unmyelinated fibers to noxious stimuli. *Journal of neurophysiology* 32: 1025-43

Blix M. 1882. Experimental bidrag till losning af fragan om hudnervernas specifika energi. *Upsala lak*: 87-102

Block SM. 1992. Biophysical principles of sensory transduction. *Society of General Physiologists series* 47: 1-17

Boulze D, Montastruc P, Cabanac M. 1983. Water intake, pleasure and water temperature in humans. *Physiology & behavior* 30: 97-102

Brunstrom JM. 2002. Effects of mouth dryness on drinking behavior and beverage acceptability. *Physiology & behavior* 76: 423-9

Brunstrom JM, Macrae AW. 1997. Effects of temperature and volume on measures of mouth dryness, thirst and stomach fullness in males and females. *Appetite* 29: 31-42

Buggy J, Jonhson AK. 1977. Preoptic-hypothalamic periventricular lesions: thirst deficits and hypernatremia. *The American journal of physiology* 233: R44-52

Burke D, Mogyoros I, Vagg R, Kiernan MC. 1999. Temperature dependence of excitability indices of human cutaneous afferents. *Muscle & nerve* 22: 51-60

Burton H, Terashima SI, Clark J. 1972. Response properties of slowly adapting mechanoreceptors to temperature stimulation in cats. *Brain research* 45: 401-16

Cahusac PM, Noyce R. 2007. A pharmacological study of slowly adapting mechanoreceptors responsive to cold thermal stimulation. *Neuroscience* 148: 489-500

Cain DM, Khasabov SG, Simone DA. 2001. Response properties of mechanoreceptors and nociceptors in mouse glabrous skin: an in vivo study. *Journal of neurophysiology* 85: 1561-74

Campero M, Serra J, Ochoa JL. 1996. C-polymodal nociceptors activated by noxious low temperature in human skin. *The Journal of physiology* 497 (Pt 2): 565-72

Cannon WB. 1918. Croonian Lecture: The Physiological Basis of Thirst. *Proc R Soc Lond B* 90: 283-301

Carpenter MB, Sutin J. 1983. *Human neuroanatomy*. Baltimore: Williams & Wilkins. xiv, 872 p. pp.

Carr MJ, Undem BJ. 2003. Pharmacology of vagal afferent nerve activity in guinea pig airways. *Pulmonary pharmacology & therapeutics* 16: 45-52

Carr RW, Pianova S, Fernandez J, Fallon JB, Belmonte C, Brock JA. 2003. Effects of heating and cooling on nerve terminal impulses recorded from cold-sensitive receptors in the guinea-pig cornea. *The Journal of general physiology* 121: 427-39

Caterina MJ, Rosen TA, Tominaga M, Brake AJ, Julius D. 1999. A capsaicin-receptor homologue with a high threshold for noxious heat. *Nature* 398: 436-41

Caterina MJ, Schumacher MA, Tominaga M, Rosen TA, Levine JD, Julius D. 1997. The capsaicin receptor: a heat-activated ion channel in the pain pathway. *Nature* 389: 816-24

Cechetto DF. 1987. Central representation of visceral function. *Federation proceedings* 46: 17-23

Cesare P, McNaughton P. 1996. A novel heat-activated current in nociceptive neurons and its sensitization by bradykinin. *Proceedings of the National Academy of Sciences of the United States of America* 93: 15435-9

Clapham DE. 2003. TRP channels as cellular sensors. *Nature* 426: 517-24

Colburn RW, Lubin ML, Stone DJ, Jr., Wang Y, Lawrence D, et al. 2007. Attenuated cold sensitivity in TRPM8 null mice. *Neuron* 54: 379-86

Corey DP, Garcia-Anoveros J, Holt JR, Kwan KY, Lin SY, et al. 2004. TRPA1 is a candidate for the mechanosensitive transduction channel of vertebrate hair cells. *Nature* 432: 723-30

Cosens DJ, Manning A. 1969. Abnormal electroretinogram from a Drosophila mutant. *Nature* 224: 285-7

Croze S, Duclaux R, Kenshalo DR. 1976. The thermal sensitivity of the polymodal nociceptors in the monkey. *The Journal of physiology* 263: 539-62

Daniels RL, McKemy DD. 2007. Mice left out in the cold: commentary on the phenotype of TRPM8-nulls. *Molecular pain* 3: 23

Darian-Smith I, Johnson KO, LaMotte C, Shigenaga Y, Kenins P, Champness P. 1979. Warm fibers innervating palmar and digital skin of the monkey: responses to thermal stimuli. *Journal of neurophysiology* 42: 1297-315

Davies A, Lumsden A. 1984. Relation of target encounter and neuronal death to nerve growth factor responsiveness in the developing mouse trigeminal ganglion. *The Journal of comparative neurology* 223: 124-37

de la Pena E, Malkia A, Cabedo H, Belmonte C, Viana F. 2005. The contribution of TRPM8 channels to cold sensing in mammalian neurones. *The Journal of physiology* 567: 415-26

de la Pena E, Malkia A, Vara H, Caires R, Ballesta JJ, et al. 2012. The influence of cold temperature on cellular excitability of hippocampal networks. *PloS one* 7: e52475

Deaux E. 1973. Thirst satiation and the temperature of ingested water. *Science* 181: 1166-7

del Camino D, Murphy S, Heiry M, Barrett LB, Earley TJ, et al. 2010. TRPA1 contributes to cold hypersensitivity. *The Journal of neuroscience : the official journal of the Society for Neuroscience* 30: 15165-74

Denton D, Shade R, Zamarippa F, Egan G, Blair-West J, et al. 1999. Correlation of regional cerebral blood flow and change of plasma sodium concentration during genesis and satiation of thirst. *Proceedings of the National Academy of Sciences of the United States of America* 96: 2532-7

Denton DA. 1982. *The hunger for salt : an anthropological, physiological, and medical analysis*. Berlin ; New York: Springer-Verlag. xix, 650 p. pp.

Dhaka A, Earley TJ, Watson J, Patapoutian A. 2008. Visualizing cold spots: TRPM8-expressing sensory neurons and their projections. *The Journal of neuroscience : the official journal of the Society for Neuroscience* 28: 566-75

Dhaka A, Murray AN, Mathur J, Earley TJ, Petrus MJ, Patapoutian A. 2007. TRPM8 is required for cold sensation in mice. *Neuron* 54: 371-8

Dhaka A, Viswanath V, Patapoutian A. 2006. Trp ion channels and temperature sensation. *Annual review of neuroscience* 29: 135-61

Dodt E, Zotterman Y. 1952. The discharge of specific cold fibres at high temperatures; the paradoxical cold. *Acta physiologica Scandinavica* 26: 358-65

Douglas WW, Malcolm JL. 1955. The effect of localized cooling on conduction in cat nerves. *The Journal of physiology* 130: 53-71

Dubin AE, Patapoutian A. 2010. Nociceptors: the sensors of the pain pathway. *The Journal of clinical investigation* 120: 3760-72

Dubner R, Sumino R, Wood WI. 1975. A peripheral "cold" fiber population responsive to innocuous and noxious thermal stimuli applied to monkey's face. *Journal of neurophysiology* 38: 1373-89

Duclaux R, Kenshalo DR. 1972. The temperature sensitivity of the type I slowly adapting mechanoreceptors in cats and monkeys. *The Journal of physiology* 224: 647-64

Duncan LM, Deeds J, Hunter J, Shao J, Holmgren LM, et al. 1998. Down-regulation of the novel gene melastatin correlates with potential for melanoma metastasis. *Cancer research* 58: 1515-20

Dykes RW. 1975. Coding of steady and transient temperatures by cutaneous "cold" fibers serving the hand of monkeys. *Brain research* 98: 485-500

Eccles R. 1994. Menthol and related cooling compounds. *The Journal of pharmacy and pharmacology* 46: 618-30

Eccles R. 2000. Role of cold receptors and menthol in thirst, the drive to breathe and arousal. *Appetite* 34: 29-35

Eccles R, Du-Plessis L, Dommels Y, Wilkinson JE. 2013. Cold pleasure. Why we like ice drinks, ice-lollies and ice cream. *Appetite* 71: 357-60

El Ouazzani T, Mei N. 1982. Electrophysiologic properties and role of the vagal thermoreceptors of lower esophagus and stomach of cat. *Gastroenterology* 83: 995-1001

Enyedi P, Czirjak G. 2010. Molecular background of leak K+ currents: two-pore domain potassium channels. *Physiological reviews* 90: 559-605

Epstein AN. 1960. Water intake without the act of drinking. *Science* 131: 497-8

Fain GL. 2003. *Sensory transduction*. Sunderland, Mass.: Sinauer Associates. xi, 340 p. pp.

Fajardo O, Meseguer V, Belmonte C, Viana F. 2008. TRPA1 channels mediate cold temperature sensing in mammalian vagal sensory neurons: pharmacological and genetic evidence. *The Journal of neuroscience : the official journal of the Society for Neuroscience* 28: 7863-75

Finger TE. 1993. What's so special about special visceral? *Acta anatomica* 148: 132-8

Fink M, Duprat F, Lesage F, Reyes R, Romey G, et al. 1996. Cloning, functional expression and brain localization of a novel unconventional outward rectifier K+ channel. *The EMBO journal* 15: 6854-62

Fink M, Lesage F, Duprat F, Heurteaux C, Reyes R, et al. 1998. A neuronal two P domain K+ channel stimulated by arachidonic acid and polyunsaturated fatty acids. *The EMBO journal* 17: 3297-308

Fitzsimons JT. 1963. The effects of slow infusions of hypertonic solutions on drinking and drinking thresholds in rats. *The Journal of physiology* 167: 344-54

Fitzsimons JT. 1976. The physiological basis of thirst. *Kidney international* 10: 3-11

Fitzsimons JT. 1979. *The physiology of thirst and sodium appetite*. Great Britian: Cambridge University Press. 1-572 pp.

Fitzsimons JT, Moore-Gillon MJ. 1980. Drinking and antidiuresis in response to reductions in venous return in the dog: neural and endocrine mechanisms. *The Journal of physiology* 308: 403-16

Fonfria E, Murdock PR, Cusdin FS, Benham CD, Kelsell RE, McNulty S. 2006. Tissue distribution profiles of the human TRPM cation channel family. *Journal of receptor and signal transduction research* 26: 159-78

Franz DN, Iggo A. 1968. Conduction failure in myelinated and non-myelinated axons at low temperatures. *The Journal of physiology* 199: 319-45

Gallar J, Acosta MC, Belmonte C. 2003. Activation of scleral cold thermoreceptors by temperature and blood flow changes. *Investigative ophthalmology & visual science* 44: 697-705

Gallar J, Pozo MA, Tuckett RP, Belmonte C. 1993. Response of sensory units with unmyelinated fibres to mechanical, thermal and chemical stimulation of the cat's cornea. *The Journal of physiology* 468: 609-22

Gallego R, Eyzaguirre C, Monti-Bloch L. 1979. Thermal and osmotic responses of arterial receptors. *Journal of neurophysiology* 42: 665-80

Gaudet R. 2007. Structural Insights into the Function of TRP Channels In *TRP Ion Channel Function in Sensory Transduction and Cellular Signaling Cascades*, ed. WB Liedtke, S Heller. Boca Raton (FL)

Gaudet R. 2008. TRP channels entering the structural era. *The Journal of physiology* 586: 3565-75

Gees M, Owsianik G, Nilius B, Voets T. 2012. TRP channels. *Comprehensive Physiology* 2: 563-608

Georgopoulos AP. 1976. Functional properties of primary afferent units probably related to pain mechanisms in primate glabrous skin. *Journal of neurophysiology* 39: 71-83

Georgopoulos AP. 1977. Stimulus-response relations in high-threshold mechanothermal fibers innervating primate glabrous skin. *Brain research* 128: 547-52

Gray H, Lewis WH. 1918. *Anatomy of the human body*. Philadelphia and New York,: Lea & Febiger.

Gross JB, Gottlieb AA, Barlow LA. 2003. Gustatory neurons derived from epibranchial placodes are attracted to, and trophically supported by, taste bud-bearing endoderm in vitro. *Developmental biology* 264: 467-81

Hallin RG, Wiesenfeld Z. 1981. A standardized electrode for percutaneous recording of A and C fibre units in conscious man. *Acta physiologica Scandinavica* 113: 561-3

Hao J, Padilla F, Dandonneau M, Lavebratt C, Lesage F, et al. 2013. Kv1.1 channels act as mechanical brake in the senses of touch and pain. *Neuron* 77: 899-914

Hardie RC, Minke B. 1992. The trp gene is essential for a light-activated Ca2+ channel in Drosophila photoreceptors. *Neuron* 8: 643-51

Harlow DE, Barlow LA. 2007. Embryonic origin of gustatory cranial sensory neurons. *Developmental biology* 310: 317-28

Hensel H. 1953. The time factor in thermoreceptor excitation. *Acta physiologica Scandinavica* 29: 109-16

Hensel H. 1973. Cutaneous thermoreceptors In *Somatosensory system*, ed. A Iggo, pp. 79-110. Berlin, New York: Springer-Verlag

Hensel H, Iggo A, Witt I. 1960. A quantitative study of sensitive cutaneous thermoreceptors with C afferent fibres. *The Journal of physiology* 153: 113-26

Hensel H, Kenshalo DR. 1969. Warm receptors in the nasal region of cats. *The Journal of physiology* 204: 99-112

Hensel H, Zotterman Y. 1951a. The effect of menthol on the thermoreceptors. *Acta physiologica Scandinavica* 24: 27-34

Hensel H, Zotterman Y. 1951b. The response of mechanoreceptors to thermal stimulation. *The Journal of physiology* 115: 16-24

Herrick CJ. 1944. The fasciculus solitarius and its connections in amphibians and fishes. *The Journal of comparative neurology* 81: 307-31

Higashi H. 1986. Pharmacological aspects of visceral sensory receptors. *Progress in brain research* 67: 149-62

Hille B. 2001. *Ion channels of excitable membranes*. Sunderland, Mass.: Sinauer. xviii, 814 p. pp.

Hirata H, Oshinsky ML. 2012. Ocular dryness excites two classes of corneal afferent neurons implicated in basal tearing in rats: involvement of transient receptor potential channels. *Journal of neurophysiology* 107: 1199-209

Ho K, Nichols CG, Lederer WJ, Lytton J, Vassilev PM, et al. 1993. Cloning and expression of an inwardly rectifying ATP-regulated potassium channel. *Nature* 362: 31-8

Holmes JH, Gregersen MI. 1950. Observations on drinking induced by hypertonic solutions. *The American journal of physiology* 162: 326-37

Howard J, Bechstedt S. 2004. Hypothesis: a helix of ankyrin repeats of the NOMPC-TRP ion channel is the gating spring of mechanoreceptors. *Current biology : CB* 14: R224-6

Huang W, Sved AF, Stricker EM. 2000. Water ingestion provides an early signal inhibiting osmotically stimulated vasopressin secretion in rats. *American journal of physiology. Regulatory, integrative and comparative physiology* 279: R756-60

Hunt CC, McIntyre AK. 1960. Properties of cutaneous touch receptors in cat. *The Journal of physiology* 153: 88-98

Iggo A. 1959. Cutaneous heat and cold receptors with slowly conducting (C) afferent fibres. *Quarterly journal of experimental physiology and cognate medical sciences* 44: 362-70

Iggo A. 1969. Cutaneous thermoreceptors in primates and sub-primates. *The Journal of physiology* 200: 403-30

Iggo A, Muir AR. 1969. The structure and function of a slowly adapting touch corpuscle in hairy skin. *The Journal of physiology* 200: 763-96

Iggo A, Young DW. 1975. Cutaneous thermoreceptors and thermal nociceptors In *The somatosensory systems*, ed. HH Kornhuber, pp. 5-22. Stuttgart: Thieme

Jan LY, Jan YN. 2012. Voltage-gated potassium channels and the diversity of electrical signalling. *The Journal of physiology* 590: 2591-9

Jaquemar D, Schenker T, Trueb B. 1999. An ankyrin-like protein with transmembrane domains is specifically lost after oncogenic transformation of human fibroblasts. *The Journal of biological chemistry* 274: 7325-33

Johnson AK, Cunningham JT, Thunhorst RL. 1996. Integrative role of the lamina terminalis in the regulation of cardiovascular and body fluid homeostasis. *Clinical and experimental pharmacology & physiology* 23: 183-91

Johnson KO, Darian-Smith I, LaMotte C. 1973. Peripheral neural determinants of temperature discrimination in man: a correlative study of responses to cooling skin. *Journal of neurophysiology* 36: 347-70

Johnson KO, Darian-Smith I, LaMotte C, Johnson B, Oldfield S. 1979. Coding of incremental changes in skin temperature by a population of warm fibers in the monkey: correlation with intensity discrimination in man. *Journal of neurophysiology* 42: 1332-53

Jordt SE, Bautista DM, Chuang HH, McKemy DD, Zygmunt PM, et al. 2004. Mustard oils and cannabinoids excite sensory nerve fibres through the TRP channel ANKTM1. *Nature* 427: 260-5

Julius D. 2013. TRP channels and pain. *Annual review of cell and developmental biology* 29: 355-84

Julius D, Nathans J. 2012. Signaling by sensory receptors. *Cold Spring Harbor perspectives in biology* 4: a005991

Jung HS, Oropeza V, Thesleff I. 1999. Shh, Bmp-2, Bmp-4 and Fgf-8 are associated with initiation and patterning of mouse tongue papillae. *Mechanisms of development* 81: 179-82

Kandel ER. 2012. *Principles of neural science*. New York: McGraw-Hill. p. pp.

Kang D, Choe C, Kim D. 2005. Thermosensitivity of the two-pore domain K+ channels TREK-2 and TRAAK. *The Journal of physiology* 564: 103-16

Kapatos G, Gold RM. 1972. Tongue cooling during drinking: a regulator of water intake in rats. *Science* 176: 685-6

Karashima Y, Damann N, Prenen J, Talavera K, Segal A, et al. 2007. Bimodal action of menthol on the transient receptor potential channel TRPA1. *The Journal of neuroscience : the official journal of the Society for Neuroscience* 27: 9874-84

Karashima Y, Talavera K, Everaerts W, Janssens A, Kwan KY, et al. 2009. TRPA1 acts as a cold sensor in vitro and in vivo. *Proceedings of the National Academy of Sciences of the United States of America* 106: 1273-8

Katsura H, Tsuzuki K, Noguchi K, Sakagami M. 2006. Differential expression of capsaicin-, menthol-, and mustard oil-sensitive receptors in naive rat geniculate ganglion neurons. *Chemical senses* 31: 681-8

Kenshalo DR, Duclaux R. 1977. Response characteristics of cutaneous cold receptors in the monkey. *Journal of neurophysiology* 40: 319-32

Kenshalo DR, Hall EC. 1974. Thermal thresholds of the rhesus monkey (Macaca mulatta). *Journal of comparative and physiological psychology* 86: 902-10

Keynes RD, Rojas E. 1974. Kinetics and steady-state properties of the charged system controlling sodium conductance in the squid giant axon. *The Journal of physiology* 239: 393-434

Knowlton WM, Bifolck-Fisher A, Bautista DM, McKemy DD. 2010. TRPM8, but not TRPA1, is required for neural and behavioral responses to acute noxious cold temperatures and cold-mimetics in vivo. *Pain* 150: 340-50

Kobayashi K, Fukuoka T, Obata K, Yamanaka H, Dai Y, et al. 2005. Distinct expression of TRPM8, TRPA1, and TRPV1 mRNAs in rat primary afferent neurons with adelta/c-fibers and colocalization with trk receptors. *The Journal of comparative neurology* 493: 596-606

Kondo T, Oshima T, Obata K, Sakurai J, Knowles CH, et al. 2010. Role of transient receptor potential A1 in gastric nociception. *Digestion* 82: 150-5

Konietzny F, Hensel H. 1977. The dynamic response of warm units in human skin nerves. *Pflugers Archiv : European journal of physiology* 370: 111-4

Kumazawa T. 1996. The polymodal receptor: bio-warning and defense system. *Progress in brain research* 113: 3-18

Kurose M, Meng ID. 2013. Dry eye modifies the thermal and menthol responses in rat corneal primary afferent cool cells. *Journal of neurophysiology* 110: 495-504

Kwan KY, Allchorne AJ, Vollrath MA, Christensen AP, Zhang DS, et al. 2006. TRPA1 contributes to cold, mechanical, and chemical nociception but is not essential for hair-cell transduction. *Neuron* 50: 277-89

Kwan KY, Glazer JM, Corey DP, Rice FL, Stucky CL. 2009. TRPA1 modulates mechanotransduction in cutaneous sensory neurons. *The Journal of neuroscience : the official journal of the Society for Neuroscience* 29: 4808-19

Labbe D, Almiron-Roig E, Hudry J, Leathwood P, Schifferstein HN, Martin N. 2009. Sensory basis of refreshing perception: role of psychophysiological factors and food experience. *Physiology & behavior* 98: 1-9

Lamb TD. 2013. Evolution of phototransduction, vertebrate photoreceptors and retina. *Progress in retinal and eye research* 36: 52-119

LaMotte RH, Campbell JN. 1978. Comparison of responses of warm and nociceptive C-fiber afferents in monkey with human judgments of thermal pain. *Journal of neurophysiology* 41: 509-28

LaMotte RH, Thalhammer JG. 1982. Response properties of high-threshold cutaneous cold receptors in the primate. *Brain research* 244: 279-87

Lennerz JK, Dentsch C, Bernardini N, Hummel T, Neuhuber WL, Reeh PW. 2007. Electrophysiological characterization of vagal afferents relevant to mucosal nociception in the rat upper oesophagus. *The Journal of physiology* 582: 229-42

Lishko PV, Procko E, Jin X, Phelps CB, Gaudet R. 2007. The ankyrin repeats of TRPV1 bind multiple ligands and modulate channel sensitivity. *Neuron* 54: 905-18

Llinas RR. 1988. The Intrinsic Electrophysiological Properties of Mammalian Neurons: Insights into Central Nervous System Function. *Science* 242: 1654

Lundy RF, Jr., Contreras RJ. 1995. Tongue adaptation temperature influences lingual nerve responses to thermal and menthol stimulation. *Brain research* 676: 169-77

Macpherson LJ, Geierstanger BH, Viswanath V, Bandell M, Eid SR, et al. 2005. The pungency of garlic: activation of TRPA1 and TRPV1 in response to allicin. *Current biology : CB* 15: 929-34

Macpherson LJ, Hwang SW, Miyamoto T, Dubin AE, Patapoutian A, Story GM. 2006. More than cool: promiscuous relationships of menthol and other sensory compounds. *Molecular and cellular neurosciences* 32: 335-43

Madrid R, de la Pena E, Donovan-Rodriguez T, Belmonte C, Viana F. 2009. Variable threshold of trigeminal cold-thermosensitive neurons is determined by a balance between TRPM8 and Kv1 potassium channels. *The Journal of neuroscience : the official journal of the Society for Neuroscience* 29: 3120-31

Madrid R, Donovan-Rodriguez T, Meseguer V, Acosta MC, Belmonte C, Viana F. 2006. Contribution of TRPM8 channels to cold transduction in primary sensory neurons and peripheral nerve terminals. *The Journal of neuroscience : the official journal of the Society for Neuroscience* 26: 12512-25

Maingret F, Fosset M, Lesage F, Lazdunski M, Honore E. 1999. TRAAK is a mammalian neuronal mechano-gated K+ channel. *The Journal of biological chemistry* 274: 1381-7

Maingret F, Lauritzen I, Patel AJ, Heurteaux C, Reyes R, et al. 2000. TREK-1 is a heat-activated background K(+) channel. *The EMBO journal* 19: 2483-91

Malkia A, Madrid R, Meseguer V, de la Pena E, Valero M, et al. 2007. Bidirectional shifts of TRPM8 channel gating by temperature and chemical agents modulate the cold sensitivity of mammalian thermoreceptors. *The Journal of physiology* 581: 155-74

Mangiapane ML, Thrasher TN, Keil LC, Simpson JB, Ganong WF. 1983. Deficits in drinking and vasopressin secretion after lesions of the nucleus medianus. *Neuroendocrinology* 37: 73-7

Martin MR, Mason CA. 1977. The seventh cranial nerve of the rat. Visualization of efferent and afferent pathways by cobalt precipitation. *Brain research* 121: 21-41

Mbiene JP, Maccallum DK, Mistretta CM. 1997. Organ cultures of embryonic rat tongue support tongue and gustatory papilla morphogenesis in vitro without intact sensory ganglia. *The Journal of comparative neurology* 377: 324-40

Mbiene JP, Mistretta CM. 1997. Initial innervation of embryonic rat tongue and developing taste papillae: nerves follow distinctive and spatially restricted pathways. *Acta anatomica* 160: 139-58

McKemy DD, Neuhausser WM, Julius D. 2002. Identification of a cold receptor reveals a general role for TRP channels in thermosensation. *Nature* 416: 52-8

McKinley MJ, Bicknell RJ, Hards D, McAllen RM, Vivas L, et al. 1992. Efferent neural pathways of the lamina terminalis subserving osmoregulation. *Progress in brain research* 91: 395-402

Meseguer V, Karashima Y, Talavera K, D'Hoedt D, Donovan-Rodriguez T, et al. 2008. Transient receptor potential channels in sensory neurons are targets of the antimycotic agent clotrimazole. *The Journal of neuroscience : the official journal of the Society for Neuroscience* 28: 576-86

Meyer RA, Campbell JN. 1981. Evidence for two distinct classes of unmyelinated nociceptive afferents in monkey. *Brain research* 224: 149-52

Mochizuki T, Wu G, Hayashi T, Xenophontos SL, Veldhuisen B, et al. 1996. PKD2, a gene for polycystic kidney disease that encodes an integral membrane protein. *Science* 272: 1339-42

Montell C. 2003. Thermosensation: hot findings make TRPNs very cool. *Current biology : CB* 13: R476-8

Montell C, Birnbaumer L, Flockerzi V, Bindels RJ, Bruford EA, et al. 2002. A unified nomenclature for the superfamily of TRP cation channels. *Molecular cell* 9: 229-31

Montell C, Rubin GM. 1989. Molecular characterization of the Drosophila trp locus: a putative integral membrane protein required for phototransduction. *Neuron* 2: 1313-23

Mountcastle VB, Bard P. 1968. *Medical physiology*. Saint Louis,: C. V. Mosby.

Mu L, Sanders I. 2000. Sensory nerve supply of the human oro- and laryngopharynx: a preliminary study. *The Anatomical record* 258: 406-20

Nadel JA, Davis B, Phipps RJ. 1979. Control of mucus secretion and ion transport in airways. *Annual review of physiology* 41: 369-81

Nagata K, Duggan A, Kumar G, Garcia-Anoveros J. 2005. Nociceptor and hair cell transducer properties of TRPA1, a channel for pain and hearing. *The Journal of neuroscience : the official journal of the Society for Neuroscience* 25: 4052-61

Noel J, Zimmermann K, Busserolles J, Deval E, Alloui A, et al. 2009. The mechano-activated K+ channels TRAAK and TREK-1 control both warm and cold perception. *The EMBO journal* 28: 1308-18

Oldfield BJ, Badoer E, Hards DK, McKinley MJ. 1994. Fos production in retrogradely labelled neurons of the lamina terminalis following intravenous infusion of either hypertonic saline or angiotensin II. *Neuroscience* 60: 255-62

Orio P, Parra A, Madrid R, Gonzalez O, Belmonte C, Viana F. 2012. Role of Ih in the firing pattern of mammalian cold thermoreceptor endings. *Journal of neurophysiology* 108: 3009-23

Pangborn MP, Chrisp RB, Bertolero LL. 1970. Gustatory, salivary, and oral thermal responses to solutions of sodium chloride at four temperatures. *Perception and Psychophysics* 8: 69-75

Papazian DM, Schwarz TL, Tempel BL, Jan YN, Jan LY. 1987. Cloning of genomic and complementary DNA from Shaker, a putative potassium channel gene from Drosophila. *Science* 237: 749-53

Parra A, Madrid R, Echevarria D, del Olmo S, Morenilla-Palao C, et al. 2010. Ocular surface wetness is regulated by TRPM8-dependent cold thermoreceptors of the cornea. *Nature medicine* 16: 1396-9

Patel AJ, Honore E, Maingret F, Lesage F, Fink M, et al. 1998. A mammalian two pore domain mechano-gated S-like K+ channel. *The EMBO journal* 17: 4283-90

Peier AM, Moqrich A, Hergarden AC, Reeve AJ, Andersson DA, et al. 2002. A TRP channel that senses cold stimuli and menthol. *Cell* 108: 705-15

Perl ER. 1996. Cutaneous polymodal receptors: characteristics and plasticity. *Progress in brain research* 113: 21-37

Petho G, Reeh PW. 2012. Sensory and signaling mechanisms of bradykinin, eicosanoids, platelet-activating factor, and nitric oxide in peripheral nociceptors. *Physiological reviews* 92: 1699-775

Phelan KD, Falls WM. 1991. The spinotrigeminal pathway and its spatial relationship to the origin of trigeminospinal projections in the rat. *Neuroscience* 40: 477-96

Phelps CB, Gaudet R. 2007. The role of the N terminus and transmembrane domain of TRPM8 in channel localization and tetramerization. *The Journal of biological chemistry* 282: 36474-80

Phillips PA, Rolls BJ, Ledingham JG, Morton JJ. 1984. Body fluid changes, thirst and drinking in man during free access to water. *Physiology & behavior* 33: 357-63

Pierau FK, Wurster RD. 1981. Primary afferent input from cutaneous thermoreceptors. *Federation proceedings* 40: 2819-24

Pittman DW, Contreras RJ. 1998. Responses of single lingual nerve fibers to thermal and chemical stimulation. *Brain research* 790: 224-35

Pongs O, Kecskemethy N, Muller R, Krah-Jentgens I, Baumann A, et al. 1988. Shaker encodes a family of putative potassium channel proteins in the nervous system of Drosophila. *The EMBO journal* 7: 1087-96

Pongs O, Leicher T, Berger M, Roeper J, Bahring R, et al. 1999. Functional and molecular aspects of voltage-gated K+ channel beta subunits. *Annals of the New York Academy of Sciences* 868: 344-55

Poulos DA. 1971. Trigeminal temperature mechanisms. In *Oral and facial sensory and motor functions*, ed. R Dubner, Y Kawamura. New York: Appleton-Century-Crofts

Poulos DA. 1975. Central processing of peripheral temperature information In *The somatosensory system*, ed. HH Kornhuber, pp. 78-93. Stuttgart: Thieme

Poulos DA, Molt JT. 1976. Response of central trigeminal neurons to cutaneous thermal stimulation In *Sensory function of the skin of primates*, ed. Y Zotterman, pp. 263-83. Oxford: Pergamon Press

Ramsey IS, Delling M, Clapham DE. 2006. An introduction to TRP channels. *Annual review of physiology* 68: 619-47

Reid G, Flonta M. 2001. Cold transduction by inhibition of a background potassium conductance in rat primary sensory neurones. *Neuroscience letters* 297: 171-4

Rhodes KJ, Monaghan MM, Barrezueta NX, Nawoschik S, Bekele-Arcuri Z, et al. 1996. Voltage-gated K+ channel beta subunits: expression and distribution of Kv beta 1 and Kv beta 2 in adult rat brain. *The Journal of neuroscience : the official journal of the Society for Neuroscience* 16: 4846-60

Ringkamp M, Tal M, Hartke TV, Wooten M, McKelvy A, et al. 2012. Local loperamide injection reduces mechanosensitivity of rat cutaneous, nociceptive C-fibers. *PloS one* 7: e42105

Robertson GL, Shelton RL, Athar S. 1976. The osmoregulation of vasopressin. *Kidney international* 10: 25-37

Rong W, Burnstock G, Spyer KM. 2000. P2X purinoceptor-mediated excitation of trigeminal lingual nerve terminals in an in vitro intra-arterially perfused rat tongue preparation. *The Journal of physiology* 524 Pt 3: 891-902

Rusu MC, Nimigean V, Podoleanu L, Ivascu RV, Niculescu MC. 2008. Details of the intralingual topography and morphology of the lingual nerve. *International journal of oral and maxillofacial surgery* 37: 835-9

Sant'Ambrogio G, Brambilla-Sant'Ambrogio F, Mathew OP. 1986. Effect of cold air on laryngeal mechanoreceptors in the dog. *Respiration physiology* 64: 45-56

Schafer K, Braun HA, Isenberg C. 1986. Effect of menthol on cold receptor activity. Analysis of receptor processes. *The Journal of general physiology* 88: 757-76

Schaible HG, Schmidt RF. 1988. Excitation and sensitization of fine articular afferents from cat's knee joint by prostaglandin E2. *The Journal of physiology* 403: 91-104

Schepers RJ, Ringkamp M. 2010. Thermoreceptors and thermosensitive afferents. *Neuroscience and biobehavioral reviews* 34: 177-84

Schmidt RF. 1986. Thirst and hunger: general sensations In *Fundamentals of Sensory Physiology*, ed. RF Schmidt, pp. 256-71: Springer Berlin Heidelberg

Schulz DJ, Temporal S, Barry DM, Garcia ML. 2008. Mechanisms of voltage-gated ion channel regulation: from gene expression to localization. *Cellular and molecular life sciences : CMLS* 65: 2215-31

Sherrington CS. 1903. Qualitative difference of spinal reflex corresponding with qualitative difference of cutaneous stimulus. *The Journal of physiology* 30: 39-46

Smith DV, Davis BJ. 2000. Neural Representation of Taste In *The neurobiology of taste and smell*, ed. TE Finger, WL Silver, D Restrepo, pp. 353-92. New York: Wiley-Liss

Soeira G, Abd el-Bary TH, Dujovny M, Slavin KV, Ausman JI. 1994. Microsurgical anatomy of the trigeminal nerve. *Neurological research* 16: 273-83

Spray DC. 1986. Cutaneous temperature receptors. *Annual review of physiology* 48: 625-38

Stein RJ, Santos S, Nagatomi J, Hayashi Y, Minnery BS, et al. 2004. Cool (TRPM8) and hot (TRPV1) receptors in the bladder and male genital tract. *The Journal of urology* 172: 1175-8

Steiner JE, Voss C, Galili D. 1986. Temperature preference of drinking water in rats. *Physiology & behavior* 37: 583-5

Stolwijk JA, Wexler I. 1971. Peripheral nerve activity in response to heating the cat's skin. *The Journal of physiology* 214: 377-92

Story GM, Peier AM, Reeve AJ, Eid SR, Mosbacher J, et al. 2003. ANKTM1, a TRP-like channel expressed in nociceptive neurons, is activated by cold temperatures. *Cell* 112: 819-29

Stricker EM, Hoffmann ML. 2006. Control of thirst and salt appetite in rats: early inhibition of water and NaCl ingestion. *Appetite* 46: 234-7

Stucky CL, Dubin AE, Jeske NA, Malin SA, McKemy DD, Story GM. 2009. Roles of transient receptor potential channels in pain. *Brain research reviews* 60: 2-23

Takashima Y, Daniels RL, Knowlton W, Teng J, Liman ER, McKemy DD. 2007. Diversity in the neural circuitry of cold sensing revealed by genetic axonal labeling of transient receptor potential melastatin 8 neurons. *The Journal of neuroscience : the official journal of the Society for Neuroscience* 27: 14147-57

Talavera K, Gees M, Karashima Y, Meseguer VM, Vanoirbeek JA, et al. 2009. Nicotine activates the chemosensory cation channel TRPA1. *Nature neuroscience* 12: 1293-9

Tapper DN. 1965. Stimulus-response relationships in the cutaneous slowly-adapting mechanoreceptor in hairy skin of the cat. *Experimental neurology* 13: 364-85

Thornton SN. 2010. Thirst and hydration: physiology and consequences of dysfunction. *Physiology & behavior* 100: 15-21

Thrasher TN. 1989. Role of forebrain circumventricular organs in body fluid balance. *Acta physiologica Scandinavica. Supplementum* 583: 141-50

Thrasher TN, Nistal-Herrera JF, Keil LC, Ramsay DJ. 1981. Satiety and inhibition of vasopressin secretion after drinking in dehydrated dogs. *The American journal of physiology* 240: E394-401

Thut PD, Wrigley D, Gold MS. 2003. Cold transduction in rat trigeminal ganglia neurons in vitro. *Neuroscience* 119: 1071-83

Treede RD. 1995. Peripheral acute pain mechanisms. *Annals of medicine* 27: 213-6

Tsavaler L, Shapero MH, Morkowski S, Laus R. 2001. Trp-p8, a novel prostate-specific gene, is up-regulated in prostate cancer and other malignancies and shares high homology with transient receptor potential calcium channel proteins. *Cancer research* 61: 3760-9

Venkatachalam K, Montell C. 2007. TRP channels. *Annual review of biochemistry* 76: 387-417

Verney EB. 1947. The antidiuretic hormone and the factors which determine its release. *Proc R Soc Lond B Biol Sci* 135: 25-106

Vetter I, Hein A, Sattler S, Hessler S, Touska F, et al. 2013. Amplified cold transduction in native nociceptors by M-channel inhibition. *The Journal of neuroscience : the official journal of the Society for Neuroscience* 33: 16627-41

Viana F. 2011. Chemosensory properties of the trigeminal system. *ACS chemical neuroscience* 2: 38-50

Viana F, de la Pena E, Belmonte C. 2002. Specificity of cold thermotransduction is determined by differential ionic channel expression. *Nature neuroscience* 5: 254-60

Viana F, Ferrer-Montiel A. 2009. TRPA1 modulators in preclinical development. *Expert opinion on therapeutic patents* 19: 1787-99

Voets T, Droogmans G, Wissenbach U, Janssens A, Flockerzi V, Nilius B. 2004. The principle of temperature-dependent gating in cold- and heat-sensitive TRP channels. *Nature* 430: 748-54

Walker RG, Willingham AT, Zuker CS. 2000. A Drosophila mechanosensory transduction channel. *Science* 287: 2229-34

Wang Y, Erickson RP, Simon SA. 1993. Selectivity of lingual nerve fibers to chemical stimuli. *The Journal of general physiology* 101: 843-66

Weil A, Moore SE, Waite NJ, Randall A, Gunthorpe MJ. 2005. Conservation of functional and pharmacological properties in the distantly related temperature sensors TRVP1 and TRPM8. *Molecular pharmacology* 68: 518-27

Wes PD, Chevesich J, Jeromin A, Rosenberg C, Stetten G, Montell C. 1995. TRPC1, a human homolog of a Drosophila store-operated channel. *Proceedings of the National Academy of Sciences of the United States of America* 92: 9652-6

Whitehead MC, Frank ME. 1983. Anatomy of the gustatory system in the hamster: central projections of the chorda tympani and the lingual nerve. *The Journal of comparative neurology* 220: 378-95

Widmaier EP, Raff H, Strang KT. 2006. *Vander's human physiology : the mechanisms of body function*. Boston: McGraw-Hill. xxxi, 827 p. pp.

Williams LS, Schmalfuss IM, Sistrom CL, Inoue T, Tanaka R, et al. 2003. MR imaging of the trigeminal ganglion, nerve, and the perineural vascular plexus: normal appearance and variants with correlation to cadaver specimens. *AJNR. American journal of neuroradiology* 24: 1317-23

Winter CA, Risley EA, Nuss GW. 1962. Carrageenin-induced edema in hind paw of the rat as an assay for antiiflammatory drugs. *Proc Soc Exp Biol Med* 111: 544-7

Wolpert L. 1998. Pattern formation in epithelial development: the vertebrate limb and feather bud spacing. *Philosophical transactions of the Royal Society of London. Series B, Biological sciences* 353: 871-5

Xing H, Ling J, Chen M, Gu JG. 2006. Chemical and cold sensitivity of two distinct populations of TRPM8-expressing somatosensory neurons. *Journal of neurophysiology* 95: 1221-30

Xing H, Ling JX, Chen M, Johnson RD, Tominaga M, et al. 2008. TRPM8 mechanism of autonomic nerve response to cold in respiratory airway. *Molecular pain* 4: 22

Zellner DA, Durlach P. 2002. What is refreshing? An investigation of the color and other sensory attributes of refreshing foods and beverages. *Appetite* 39: 185-6

Zhang L, Jones S, Brody K, Costa M, Brookes SJ. 2004. Thermosensitive transient receptor potential channels in vagal afferent neurons of the mouse. *American journal of physiology. Gastrointestinal and liver physiology* 286: G983-91

Zhang X, McNaughton PA. 2006. Why pain gets worse: the mechanism of heat hyperalgesia. *The Journal of general physiology* 128: 491-3

Zhong F, Christianson JA, Davis BM, Bielefeldt K. 2008. Dichotomizing axons in spinal and vagal afferents of the mouse stomach. *Digestive diseases and sciences* 53: 194-203

Zhu X, Chu PB, Peyton M, Birnbaumer L. 1995. Molecular cloning of a widely expressed human homologue for the Drosophila trp gene. *FEBS letters* 373: 193-8

Zotterman Y. 1935. Action potentials in the glossopharyngeal nerve and in the chorda tympani. *Skand Arch Physiol* 72: 73-75

Zotterman Y. 1936. Specific action potentials from the lingual nerve of the cat. *Skand Arch Physiol* 75: 105-19